Hereditary Peripheral Neuropathies : from Molecular Genetics to a cellular model of hiPSC-derived motor neurons

Federica Miressi

Ph.D. Thesis

Université de Limoges

University of Limoges

ED 615 - Sciences Biologiques et Santé (SBS)

EA6309 Maintenance Myélinique et Neuropathies Périphériques

A thesis submitted to University of Limoges
in partial fulfillment of the requirements of the degree of

Doctor of Philosophy

Neuroscience

Presented and defensed by

Federica Miressi

On December 11, 2020

Hereditary Peripheral Neuropathies: from Molecular Genetics to a cellular model of hiPSC-derived motor neurons

Thesis supervisors: Dr Anne-Sophie **LIA** and Dr Pierre-Antoine **FAYE**

JURY:

Reporters

M. Cyril **GOIZET**, PU-PH,
Service Génétique Médicale, INSERM U1211, CHU Bordeaux

M. Pascal **REYNIER**, PU-PH,
Dpt Biochimie et Génétique, CHU Angers; UMR CNRS 6015-INSERM 1083, Université Angers

Examiners

M. Laurent **MAGY**, PU-PH,
Service Neurologie, CHU Limoges; EA6309, Université Limoges

M. Frédéric **FAVREAU**, PU-PH,
Service Biochimie et Génétique Moléculaire, CHU Limoges; EA6309 Université Limoges

M. Julien **CASSEREAU**, MCU-PH,
Dpt Neurologie, CHU Angers; UMR CNRS 6015-INSERM 1083, Université Angers

M. Fabrice **LEJEUNE**, CR1 INSERM,
UMR9020 CNRS - UMR-S1277 Inserm, Institut de Biologie Lille

A mio padre…

Acknowledgements

Remerciements

Ces trois ans et cet intense travail de thèse n'auraient pas pu être possibles sans la participation de toutes les personnes qui m'ont guidée, aidée, soutenue, d'un point de vue professionnel et personnel. J'espère que ces quelques lignes pourront, en quelque sorte, vous montrer à quel point je vous suis reconnaissante.

Je tiens à remercier, tout d'abord, le **Pr. Franck Sturtz**, pour m'avoir accueillie au sein de son équipe de recherche. Je vous remercie pour vos questions, toujours riches de nouvelles pistes de réflexion, et pour vos conseils, précis et intéressants. Je remercie aussi le co-directeur de l'équipe, le **Pr. Alexis Desmoulière**, pour son soutien dans ce parcours.

Je remercie, tout particulièrement, mes directeurs de thèse, les **Docteurs Anne-Sophie Lia et Pierre-Antoine Faye**. Merci, Anne-Sophie, pour avoir toujours suivi mon travail au cours de ces quatre années, pour avoir été présente, pour les bons et les mauvais résultats, pour m'avoir encouragée à me perfectionner, chaque fois. Merci pour ton support scientifique mais surtout personnel. Merci de m'avoir fait confiance, ce jour lointain, il y a cinq ans, et avoir continué dans ces années de thèse. Merci, Pierre-Antoine, pour m'avoir appris une bonne partie de tout ce que je sais faire aujourd'hui. Je te remercie pour m'avoir transmis ta précision et ta rigueur, mais surtout ta passion pour la recherche, et pour ce thème, en particulier. Merci pour m'avoir appris à être autonome, mais pour avoir été aussi présent quand j'avais un doute ou une question. Et merci aussi pour avoir répondu à mes mails à minuit, et pour ne jamais m'avoir appelé avant 9h30 du matin.

Je remercie le **Pr. Frédéric Favreau**, pour avoir suivi mon travail, avec attention et intérêt, pour ses conseils pertinents, et ses paroles, toujours gentilles et d'encouragement. Je vous remercie, aussi, d'avoir accepté de participer au jury de ma thèse, et d'évaluer ce manuscrit.

Je tiens à remercier tous les membres de mon jury de thèse: les **Professeurs Cyril Goizet et Pascal Reynier**, pour avoir voulu me faire l'honneur d'évaluer et juger ce travail, en qualité de Rapporteurs, ainsi que les **Docteurs Julien Cassereau et Fabrice Lejeune**, pour avoir accepté le rôle d'examinateurs.

Je remercie le **Pr. Laurent Magy** pour avoir accepté, également, de faire partie de ce jury, mais aussi pour toute sa disponibilité et aide dans ce travail.

Je remercie tout le personnel du **Service de Neurologie** du CHU de Limoges. Je remercie le **Pr. Jean-Michel Vallat**, pour son expertise scientifique. Un grand merci au **Dr. Laurence Richard**, pour toute son aide, sa patience, et la disponibilité démontrée pendant ces trois ans. Merci aussi à **Fanny** et tout le personnel technique.

Je remercie le **Service de Biochimie et Génétique Moléculaire** du CHU de Limoges, pour m'avoir accueillie et formée depuis le début de ce parcours, et pour tout le support technique apporté à ce travail de thèse.

Je remercie le **Service de Cytogénétique**, et, en particulier, le **Dr. Sylvie Bourthoumieu**, pour sa gentillesse et son expertise, mais aussi pour m'avoir formée à différentes techniques.

Je remercie tous les membres de l'EA6309, présents et passés.

Je remercie **les Docteurs Claire Demiot, Fabrice Billet, Justine Lerat, Mathilde Duchesne, Quentin Ballouhey, et le Pr. Laurent Fourcade**, pour leur aide et leurs conseils.

Un gros merci à mon PhD-mate, **Hichem** (ou Docteur Hichem, ou Prof Bouchenaki), qui a été toujours là pour moi, juste de l'autre coté de l'armoire. Il y a trois ans, on parlait de tout abandonner, on a commencé à concevoir notre business du "Pharma-pizza-kebab", et notre tour des Marchés de Noel. Ces trois ans sont passés super rapidement (et, en même temps, super lentement, comme on dit toujours), avec nos animaux volants, nos sports extrêmes, nos longues discussions en Salle des Prot, et beaucoup de "FEDEEE !! " (et de "DEDEEE" dans le bus, bien sûr). Merci pour ton amitié, ton support constant, et pour m'avoir fait rire et avancer, parce que "l'important c'est qu'on termine". Et nous avons terminé, ensemble. Je te souhaite de trouver ton chemin, et de le suivre toujours avec succès.

Merci **Marion**, ma "technicienne personnelle". Merci pour l'énorme travail que tu as fait pendant ma deuxième année de thèse. Merci pour avoir appris rapidement, pour m'avoir aidée et encouragée dans les grosses journée de manip, pour m'avoir permise de prendre, de temps en temps, un samedi ou un dimanche de repos. Mais surtout je te remercie pour notre amitié, nos gossip "sous-hotte", nos soirées karaoké, et tous les moments de fou rire dans ces 10 m^2. Ce fameux octobre 2018, je n'aurais pas pu faire un meilleur choix !

Je remercie **Nesrine**, l'héritière de ce travail. Cette année a été plus difficile de ce qu'on avait pu imaginer, mais nous avons avancé. Merci pour avoir été toujours là, pour avoir trouvé le temps, même quand les obligations étaient nombreuses et importantes. Merci pour avoir toujours continué ton travail, de manière professionnelle et responsable. Merci pour avoir accepté mes crises d'angoisse, pour avoir fait 16 comptages en une heure, pour avoir couru avec moi pour la Cyto (toujours en retard!). Mais surtout merci d'être une personne gentille, joueuse, altruiste, qui met toujours les autres avant elle (et qui me prépare les repas quand je travaille trop!). Bon courage pour tout ce qui reste à faire, je te confie mes cellules et tout le matériel que j'ai pu "récupérer". Je suis sûre tu feras un très bon travail!

Je remercie **Aurore**, notre grande sœur, toujours prête à aider les doctorants désespérés. Merci pour ta positivité, ton bonheur, et ton humour (toujours au bon moment!), mais aussi pour tous les conseils et les réponses que tu as pu me donner pendant ces trois ans! Merci pour notre voyage à Gênes, pour ton calme à l'arrêt de la navette, à Paris, à écouter la vie de l'espagnol, pour la nuit à l'aéroport, et les coupes de prosecco avec les pieds dans la piscine.

Merci à **Paco**. J'ai compris que tu allais souvent me sauver la vie, quand tu es venu à l'aéroport pour récupérer moi et mes quatre valises, il y a quatre ans déjà. Merci pour ton support informatique et statistique, mais surtout pour tous les repas et les soirées hors du labo, à Limoges et à Paris !

Merci **Angélique**, pour ta gentillesse, ta patiente, ton aide précieux dans toutes les taches administratives. Merci pour toutes les commandes que tu as fait partir dans l'urgence, et qui ont toujours sauvé mon travail!

Merci à la nouvelle génération de doctorantes, "les filles", **Amandine, Ioanna et Zeina**. Merci pour les soirées ensemble, la patinoire, et le mölkky! Merci pour avoir accepté mes idées géniales de fêtes déguisées (et poilues!). Continuez à bien travailler et rappelez vous que vous pouvez toujours compter les unes sur les autres. J'attends vos mails dans deux et trois ans !

Je remercie tous les anciens membres de l'EA6309. Un gros merci au Dr. **Martial** Caillaud, pour m'avoir guidé pendant les premiers mois de ce parcours. Mais, surtout, merci pour les soirées ensemble, et pour une belle collection de souvenirs et anecdotes, que je ne mentionne pas ici, dans le respect mutuel! Merci pour ne pas m'avoir réveillé, quand les discussions de fin soirée étaient longues et ton fauteuil très confortable. Je te souhaite le meilleur pour la suite! Je tiens à remercier aussi **Dorothée, Max, Betty, et Claire Cécile**, pour les moments passés ensemble pendant mes premiers mois à Limoges.

Je remercie **Nicolas**, pour tout son aide au début et au cours de ma thèse, pour sa patiente, sa disponibilité, et, bien sur, toutes ses chansons.

Je remercie **Claire Carrion et Catherine Ouk**, pour tout leur aide et leurs conseils, en microscopie et cytometrie.

Un gros merci à tous les doctorants et tout le personnel des autres équipes de recherche, pour le support technique et scientifique.

Je remercie mes amis, dispersés dans le monde.

Merci à **Giulia**, ma Sarah, ma Cassandra, ma Phoebe (avec le meilleures caractéristiques de chacune). Merci pour ces 18 ans d'amitié, pour tout ton intérêt pour ce que je fais, pour tes encouragements, pour tes messages (oui, les messages vocaux dans la voiture aussi). Je te remercie parce que je sais que tu es là, et tu seras toujours là pour moi, même quand nous serons éloignées, même si tu ne me serres pas (trop) fort pour quatre mois. Merci pour avoir supporté cette distance, sans jamais la rendre absence.

Je remercie **Maria**, ma confidente quotidienne, ma petite Masterchef. Merci parce qu'on peut parler de tout, de la pure science et les problèmes aux labo, aux cheveux et les jeans mom. Merci pour ton support, ton aide, et tes belles paroles. Et merci pour tes silences, parce que certaines choses n'ont pas besoin d'être dites. Merci pour cette amitié qui n'est jamais affectée par la distance. J'espère toujours qu'un jour nous serons à nouveau collègues, pour recommencer nos pauses de midi ensemble.

Merci à **Genia et Marco**, la raison de mon étape incontournable à Bari. Merci pour votre support et vos messages fou. Je vous souhaite le meilleur pour votre avenir, vous êtes mes scientifiques spéciaux (coeur violet). Je remercie **Annarita**, pour son amitié et sa compréhension, pour sa disponibilité malgré toutes les nouvelles importantes de ces dernières années.

Je remercie **Viviana**, mon irremplaçable copine d'aventures professionnelles. Cette expérience nous l'avons commencé ensemble, loin, mais en parallèle. Comme la première fois, tu as été présente, dans les moments des bons résultats, et ceux de crise, quand les journées commençaient tôt, et quand les journées ne finissaient plus. Malgré tout a changé, le bruit du vent et celui de la petite cuillère de café sont restés des constantes dans nos vies. Encore une dernière année, et l'aventure se terminera pour toi aussi, surement au mieux, comme tu le mérites.

Je remercie **Silvia, Teresa et Anna**, mes copines du lycée, toujours prêtes à m'accueillir avec une soirée ensemble et un verre de vin. Merci à **Kevin**, pour prendre soin de deux des mes choses plus précieuses : ma meilleure amie et mon pc.

Je remercie de tout mon cœur **Sylvie, Jacques, Laura, Nico, et Ernestine**, ma famille d'adoption. Je vous remercie pour m'avoir accueille et traitée toujours avec amour et gentillesse. Merci pour les moments passés ensemble qui m'ont permis de me sentir plus "chez moi".

Je remercie ma tante **Anna** et mon oncle **Gino**, mes cousins **Nicola et Ruggiero**, pour être toujours là.

Je remercie **Flavien**, mille (et encore mille) fois. Aucune phrase pourrait faire comprendre à quel point je te suis reconnaissante pour ce que tu as fait pendant ces trois ans. Merci pour avoir renoncé à tous tes weekend, tous tes samedi et dimanche, tous les jours fériés, tous les anniversaires, parce que "Je dois aller au labo". Merci pour avoir supporté toutes mes mauvaises journées, les horaires décalées, les nuits de travail, le stress avant chaque présentation. Merci pour n'avoir jamais vu ça comme un problème, pour avoir compris, pour avoir mis ma thèse même avant toi-même. Merci pour avoir pris ma main quand je ne pouvais pas dormir. Tout ça a commencé grâce à toi, quand tu m'as fait croire que j'aurais pu l'affronter. Mais, si j'ai pu l'affronter, c'était seulement grâce à ton soutien, a ta patiente, et à ta force, qui est devenue la mienne.

Merci à **ma sœur**, parce que je sais à quel point cette épreuve a été dure pour toi. Merci parce que des fois les journées étaient longues, et tu le comprenais sans même en parler. Merci parce que (trop) souvent rentrer était impossible, et tu as choisi de l'accepter, de faire semblant que se voir deux fois par an pouvait nous suffire. Merci pour ta patiente, pour m'avoir supporté à distance, pour m'avoir encouragé à chaque obstacle. Parce que les obstacles on les a toujours affrontés ensemble. Merci pour être mon ancre, mon soutien, parce que si nous sommes debout c'est parce que nous nous tenons l'une à l'autre. "Sempre e per sempre".

Je remercie **mes parents**, parce qu'ils ont fait de moi ce que je suis aujourd'hui, parce que je suis leur image, le réflexe de leurs enseignements. Je les remercie parce qu'ils ont renoncé à ma présence pour ma réussite, parce qu'ils ont su être à mes cotés, sans envahir mon espace, parce qu'ils n'arrêteront d'éclairer mon chemin, quelle que soit la distance qui nous sépare. Tout ce travail, comme chaque objectif atteint de ma vie, est pour eux.

Ringraziamenti

Questi tre anni e questo impegnativo lavoro di tesi non sarebbero mai stati possibili senza la partecipazione di tutte quelle persone che mi hanno guidata, aiutata, sostenuta, da un punto di vista lavorativo e personale. Spero che queste poche righe possano, in qualche modo, dimostrarvi quanto io vi sia riconoscente.

Ci tengo a ringraziare, in primo luogo, il **Prof. Franck Sturtz**, per avermi accolto nella sua equipe di ricerca. La ringrazio per le sue domande, sempre ricchi di nuovi spunti di riflessione, e i suoi consigli, sempre attenti e precisi, per migliorare il mio lavoro. Ringrazio ugualmente il **Prof. Alexis Desmoulière**, co-direttore dell'equipe, per il suo sostegno nel mio percorso.

Ringrazio, in modo particolare, i miei direttori di tesi, i **Dottori Anne-Sophie Lia e Pierre-Antoine Faye**, perché tutto questo non sarebbe stato possibile senza di loro. Grazie, Anne-Sophie, per aver sempre seguito il mio lavoro in questi quattro anni, per essere stata sempre presente, per i buoni e i cattivi risultati, per avermi spronata a perfezionarmi, ogni volta. Grazie per il tuo supporto scientifico, ma soprattutto personale. Grazie per avermi dato fiducia, quel lontano giorno di 5 anni fa, e aver continuato in questi anni di tesi. Grazie, Pierre-Antoine, per avermi insegnato tutto quello che posso dire, oggi, di saper fare. Grazie per avermi trasmesso la tua precisione e il tuo rigore, ma soprattutto la tua passione per la ricerca, e per questo tema, in particolare. Grazie per avermi insegnato ad essere autonoma, ma essere stato presente ogni qualvolta avessi un dubbio o bisogno di aiuto. Grazie anche per aver risposto alle mie e-mail a mezzanotte, e per non avermi mai telefonata prima delle 9 e mezza di mattina.

Ringrazio il Prof. **Frédéric Favreau**, per aver seguito il mio lavoro, con attenzione e interesse, per i suoi consigli pertinenti, e le sue parole, sempre gentili e di sprono. Lo ringrazio, inoltre, di aver accettato di far parte della mia commissione di tesi e di valutare questo manoscritto.

Ci tengo particolarmente a ringraziare tutti i membri della mia commissione di dottorato: i **Prof. Cyril Goizet e Pascal Reynier** per avermi fatto l'onore di valutare e giudicare questo lavoro, nelle vesti di Rapportatori, come anche i **Dr. Julien Cassereau e Fabrice Lejeune**, per aver accettato il ruolo di esaminatori.

Ringrazio il **Prof. Laurent Magy**, per aver accettato di far parte anch'egli di questa commissione, ma anche per tutta la sua disponibilità e aiuto dimostrato.

Ringrazio anche tutto il personale del **Servizio di Neurologia** del CHU di Limoges. Ringrazio il **Prof. Jean-Michel Vallat**, per la sua competenza scientifica. Un enorme grazie va ovviamente al **Dr. Laurence Richard**, per tutto il suo aiuto, la sua pazienza e la disponibilità dimostrata in questi anni. Grazie anche a **Fanny** e a tutto il personale tecnico.

Ringrazio il **Servizio di Biochimica e Genetica Molecolare** del CHU di Limoges, per avermi accolta e formata fin dall'inizio di questo percorso, e per il supporto tecnico fornito a questo lavoro di tesi.

Ringrazio il **Servizio di Citogenetica** e, in particolar modo, il **Dr. Sylvie Bourthoumieu** per la sua gentilezza e le sue competenze, ma anche per avermi formata a tecniche diverse.

Ringrazio tutti i membri dell'EA6309, i vecchi e i nuovi, chi ci è sempre stato e chi è stato solo di passaggio.
Ringrazio i **Dr. Claire Demiot, Fabrice Billet, Justine Lerat, Mathilde Duchesne, Quentin Ballouhey, e il Prof. Laurent Fourcade**, per il loro aiuto e i loro consigli sempre pertinenti.

Un grazie particolare va al mio PhD-mate, **Hichem** (o Docteur Hichem, o Pr. Bouchenaki), che è sempre stato lì per me, giusto dall'altro lato dell'armadio. Sono passati tre anni da quando parlavamo di voler abbandonare tutto, da quando abbiamo progettato il business del "Pharma-pizza-kebab", da quando mi hai accompagnato all'azoto per la prima volta perché avevo paura di bruciarmi. Tre anni sono passati velocissimi (e lentissimi al tempo stesso, come diciamo sempre) tra animali volanti, sport estremi, lunghe conversazioni nella sala delle Proteine, e molti "FEDEEEE!!". Grazie per la tua amicizia, per il tuo supporto costante, per avermi fatto sorridere e tirare aventi perché "l'importante è che finiamo". E abbiamo finito, insieme. Ti auguro di trovare la tua strada, e di seguirla sempre con successo.

Grazie a **Marion**, la "mia tecnica personale". Grazie per il lavoro enorme svolto durante il mio secondo anno di tesi. Grazie per aver imparato rapidamente, per avermi aiutata e incoraggiata nelle grosse giornate in laboratorio, per avermi permesso di avere, ogni tanto, un sabato o una domenica di riposo. Ma soprattutto ti ringrazio per la nostra amicizia, i gossip sotto cappa, le serate karaoke, e tutte le risate che ci siamo fatte in quei $10m^2$. Quell'ottobre 2018 non avrei potuto scegliere collega migliore!

Ringrazio **Nesrine**, l'erede di questo lavoro. È stato un anno più difficile di quanto avemmo mai potuto prevedere, ma siamo andate avanti. Grazie per esserci sempre stata, per aver sempre trovato il tempo, anche quando gli impegni erano tanti e importanti. Grazie per aver sempre portato avanti il tuo lavoro, con serietà e professionalità, lasciando il resto al di fuori della sala. Grazie per aver accettato i miei attacchi di ansia, per aver fatto 16 conteggi in un'ora, per aver corso con me per la Cyto (sempre in ritardo!). Ma soprattutto grazie per essere una persona buona, solare, altruista, che mette sempre gli altri davanti se stessa (e mi prepara i pasti quando lavoro troppo!). Buona fortuna per quello che resta da fare, ti affido le mie cellule e tutto il materiale recuperato con fatica! Sono sicura farai un ottimo lavoro!

Ringrazio **Aurore**, la nostra sorella maggiore, sempre pronta ad aiutare noi dottorandi disperati. Grazie per la tua positività, la tua allegria, il tuo humour (sempre al momento giusto!), ma anche per tutti i consigli e le risposte che hai potuto darmi in questi tre anni. Grazie il nostro viaggio a Genova, la tua calma alla fermata della navetta, a Parigi, a conversare con il ragazzo spagnolo, la nottata in aeroporto, e le coppe di prosecco con i piedi in piscina.

Grazie a **Paco**, che ho capito mi avrebbe spesso salvato la vita, quando recuperò me e le mie 4 valigie in aeroporto, ben 4 anni fa. Grazie per il tuo supporto informatico e statistico, oltre che per le pause-pranzo e le serate fuori dal labo, a Limoges e a Parigi!

Ringrazio **Angélique**, per la sua gentilezza, la sua pazienza, e il suo aiuto prezioso in tutte le faccende amministrative e burocratiche. Grazie per tutti gli ordini che hai fatto partire all'ultimo minuto e che hanno sempre salvato il mio lavoro!

Grazie alla nuova generazione di dottorande, le "ragazze", **Amandine, Ioanna e Zeina**. Grazie per le serate insieme, il pattinaggio su ghiaccio, e il mölkky! E grazie per aver accettato le miei idee

geniali di feste in maschera (feste pelose!)! Continuate a dare del vostro meglio, lavorate sodo, e ricordatevi che potrete sempre contare l'una sull'altra. Aspetto le vostre mail tra due e tre anni!

Grazie a tutti gli ex membri dell'EA6309. Un grazie speciale al Dr. **Martial** Caillaud, per avermi guidato nei primi mesi di questo percorso. Ma soprattutto grazie per le serate insieme, e per una bella collezione di aneddoti che qui non cito, per rispetto reciproco! Grazie per non avermi svegliata quando le conversazioni di fine serata diventavano lunghe e la tua poltrona troppo comoda. Ti auguro il meglio, in ogni parte del mondo che sceglierai. Ci tengo anche a ringraziare **Dorothée, Max, Betty, e Claire Cécile**, per i momenti trascorsi insieme nei miei primi mesi a Limoges.

Ringrazio **Nicolas**, per tutto il suo aiuto all'inizio e durante la tesi, per la sua pazienza, la sua disponibilità, e ovviamente tutte le sue canzoni.

Ringrazio **Claire Carrion e Catherine Ouk**, per tutto il loro aiuto tecnico e i loro consigli, in microscopia e citometria.

Un grazie a tutti i dottorandi e tutto il personale delle altre équipe di ricerca , per il loro supporto tecnico e scientifico.

Ringrazio i miei amici, lontani e sparpagliati per il mondo.

Grazie a **Giulia**, la mia Sarah, la mia Cassandra, e la mia Phoebe (con le più belle caratteristiche di ognuna di loro). Grazie per questi 18 anni di amicizia, per il tuo interesse in tutto quello che faccio, per i tuoi incoraggiamenti, per i tuoi messaggi (sì, anche i vocali in macchina, contro i pedoni). Ti ringrazio perché so che ci sei, e ci saresti, sempre, anche quando siamo lontane, anche quando non ci abbracciamo per sei mesi, anche quando non ci sentiamo per ben 24 ore. Grazie per aver sopportato questa distanza, senza mai farmi pesare l'assenza.

Ringrazio **Mari**, la mia confidente quotidiana, la mia Masterchef. Grazie perché possiamo parlare di tutto, dalla scienza pura e i problemi di laboratorio, ai capelli e i jeans mom. Grazie per il tuo supporto, il tuo aiuto, le tue belle parole. E grazie anche per i tuoi silenzi, perché certe cose non abbiamo bisogno di dircele. Grazie per questa amicizia che non sente la distanza. Spero sempre che un giorno ridiventeremo colleghe, per poter ricominciare insieme le nostre pause pranzo.

Grazie a **Genia e Marco**, la ragione della mia tappa obbligata a Bari. Grazie per tutte le risate, per il vostro sostegno e i vostri messaggi. Vi auguro il meglio per il vostro futuro, siete i miei scienziati speciali (cuore viola). Ringrazio **Annarita**, per la sua amicizia e la sua comprensione, la sua disponibilità nonostante tutte le novità di questi ultimi anni!

Ringrazio **Viviana**, la mia insostituibile compagna di "avventure lavorative". Questa esperienza l'abbiamo iniziata insieme, lontane, ma in parallelo. Come la prima volta sei stata presente, nei momenti dei buoni risultati, in quelli di crisi, quando le giornate iniziavano presto, e quando le giornate non finivano mai. Nonostante tutto sia cambiato, il rumore del vento e quello del cucchiaino di caffè sono rimaste delle costanti nelle nostre vite. Ancora un anno e l'avventura si concluderà anche per te, e sono sicura nel migliore dei modi, come meriti.

Ringrazio **Silvia, Teresa e Anna**, le amiche del liceo, sempre pronte ad accogliermi con una serata insieme e un calice di vino. Grazie a Kevin, per accudire e proteggere due delle cose che ho più a cuore: la mia migliore amica, e il mio pc.

Ringrazio con tutto il cuore **Sylvie, Jacques, Laura, Nico, e Ernestine**, la mia famiglia di adozione. Vi ringrazio per avermi accolta, ospitata, trattata con amore e gentilezza. Grazie per tutti i momenti passati insieme che mi hanno permesso di sentirmi più vicina a "casa".

Ringrazio i miei zii, **Anna e Gino**, e i miei cugini, **Nicola e Ruggiero**, per esserci stati ed esserci sempre.

Ringrazio **Flavien**, mille e ancora mille volte. Nessuna frase potrà far comprendere quanto io ti sia grata, per tutto quello che hai fatto in questi tre anni. Grazie per aver rinunciato a tutti i tuoi weekend, tutti i sabato e domeniche, tutti i giorni di festa, tutti i compleanni, perché "Devo andare in laboratorio". Grazie per aver sopportato tutti i giorni no, gli orari scombussolati, le nottate di lavoro, lo stress prima di ogni presentazione. Grazie per non averne mai fatto un problema, per aver capito, per aver messo la mia tesi anche prima di te stesso. Grazie per avermi tenuto la mano quando non potevo dormire. Tutto questo è cominciato grazie a te, quando mi hai fatto credere che avrei potuto affrontarlo. Ma, se ho potuto affrontarlo, è stato solo grazie al tuo sostegno, alla tua pazienza, alla tua forza che è stata anche la mia.

Grazie a **mia sorella**, perché so quanto per lei sia stata una prova difficile. Grazie perché a volte le giornate erano lunghe, e lo capivi senza neanche parlarne. Grazie perché a volte non era possibile tornare, e hai scelto di non farmelo pesare, di fingere che vederci due volte all'anno potesse bastarci. Grazie per la tua pazienza (che con me ce ne vuole tanta), per avermi sopportata a distanza, per avermi spronata ad ogni ostacolo. Perché gli ostacoli li abbiamo sempre affrontati insieme. Grazie per essere la mia speranza, la mia ancora, il mio sostegno, perché se siamo in piedi è perché ci reggiamo a vicenda. Sempre e per sempre.

Ringrazio **i miei genitori**, perché mi hanno resa quella che sono oggi, perché sono la loro immagine, il riflesso dei loro insegnamenti. Li ringrazio perché hanno rinunciato alla mia presenza per la mia realizzazione, perché hanno saputo essermi vicino senza mai invadere i miei spazi, perché non smetteranno di illuminare la mia strada, per quanto lontani possano essere. Tutto questo lavoro, come ogni mio traguardo, è per loro.

Rights

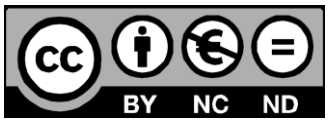

Table of Contents

List of Figures

List of Tables

List of abbreviations

$^1O_2$: Singlet oxygen
3D: Three dimensions
AARS1: Alanine-tRNA synthetase
aCGH: array Comparative Genomic Hybridization
AD-CMT2: Autosomal Dominant Charcot-Marie-Tooth type 2
ADOA: Autosomal Dominant Optic Atrophy
ADP: Adenosine Diphosphate
ALB: Albumin
AMPK: AMP-activated Protein Kinase
ANS: Autonomic Nervous System
ANT: Adenine Nucleotide Transporter
AO: Antioxidant
AP: Anteroposterior
AR-CMT: Autosomal Recessive Charcot-Marie-Tooth type 2
ARS: Aminoacyl-tRNA-synthetase
ASO: Antisense Oligonucleotide
ATP: Adenosine Triphosphate
BDNF: Brain-Derived Neurotrophic Factor
BMP: Bone Morphogenetic Protein
BSA: Bovine Serum Albumin
CACT: Carnitine Acylcarnitine Translocase
CANVAS: Cerebellar Ataxia, Neuropathy, Vestibular Areflexia Syndrome
Caspr: Contactin-associated protein
CAT: Catalase
CGH: Comparative Genomic Hybridization
ChAT: Cholyne Acetyltransferase
CL: Cardiolipin
CMAP: Compound Muscle Action Potential
CMT: Charcot-Marie-Tooth
CMTX: X-linked Charcot-Marie-Tooth
CNS: Central Nervous System
CNV: Copy Number Variation
CoQ: Coenzyme Q
CoQ: Coenzyme Q
CPT: Carnitine Palmitoyltransferase or Carnitine Acyltransferase
Cx32: Connexin-32
Cyp26: cytochrome P450 family 26
DAB: 3,3'-Diaminobenzidine
DAPI: 4',6-Diamidino-2-phenylindole
dHMN: distal Hereditary Motor Neuropathy
DI-CMT: Dominant Intermediate Charcot-Marie-Tooth
DNM2: Dynamin-2
DNTB: 5,5-dithio-bis-(2-nitrobenzoic acid
DPBS: Dulbecco's Phosphate-Buffered Saline
DRP1: Dynamin-Related Protein 1
DV: Dorsovental
DYNC1H1: Dynein, cytoplasmic 1, heavy chain 1
EB: Embryonic Body
EMG: Electromyography
ER: Endoplasmic Reticulum
ETC: Electron Transport Chain
ETS: Electron Transport System
$FADH_2$: Flavin Adenine Dinucleotide
FB: Fibroblast
FBS: Fetal Bovine Serum
FF: Feeder-Free
FGF: Fibroblast Growth Factor
Fis1: mitochondria, Fission protein 1
FMN: Flavin Mononucleotide
GARS1: Glycyl-tRNA synthetase
GDAP1: Ganglioside-induced Differentiation-Associated Protein 1
GDAP1L1: Ganglioside-induced Differentiation-Associated Protein 1-Like 1
GDNF: Glial cell-Derived Neurotrophic Factor
GED: GTPase Effector Domain
GPx: Glutathione Peroxidase
GSH: Glutathione/reduced Glutathione
GSR: Glutathione Reductase
GSSG: oxidized Glutathione
GST: Glutathione S-Transferase
GTP: Guanosine Triphosphate
H_2O_2: Hydrogen peroxide
HARS1: Histidyl-tRNA synthetase
HB9: Homeobox gene HB9
HD: Hydrophobic Domain
hESC: human Embryonic Stem Cell
hiPSC: human induced-Pluripotent Stem Cell
HIV: Human Immunodeficiency Virus

HMN: Hereditary Motor Neuropathy
HR: Heptad Repeat
HSAN: Hereditary Sensory and Autonomic Neuropathy
HSN: Hereditary Sensory Neuropathy
ICC: Immunocytochemistry
IF: Intermediate filament
IGF: Insulin-like Growth Factor
IMM: Inner Mitochondrial Membrane
INF2: Inverted Formin 2
JC-1: 5,5',6,6'-Tetrachloro-1,1',3,3'-tetraethylbenzimidazolocarbocyanine iodide
KARS1: Lysine-tRNA synthetase
KIF5A: Kinesin family member 5a
KO: Knock-Out
KSR: KnockOut Serum Replacement
LD: Lipid Droplet
LMNA: LAMIN A/C
L-OPA1: Long-OPA1
MAG: Myelin Associated Glycoprotein
MAM: Mitochondrial-Associated Membrane
MAP2: Microtubule-Associated Protein 2
MARS1: Methionyl-tRNA synthetase
MBP: Metal-Binding Proteins (MBPs)
MBP: Myelin Basic Protein
MCS: Motor Conduction Study
MEF: Mouse Embryonic Fibroblast
MES: 2-(N-morpholino)ethanesulphonic acid
MF: Microfilament
Mff: Mitochondrial Fission Factor
MFN: Mitofusin
MiD: Mitochondrial dynamics protein
MN: Motor Neuron
MN: Motor Neuron
MNCV: Motor Nerve Conduction Velocity
MORC2: Microrchidia family CW-type zinc-finger 2
MPA: Metaphosphoric Acid
MPP: Matrix Processing Protease
MPT: Mitochondrial Permeability Transition
MPZ: Myelin Protein Zero
MT: Microtubule
mtDNA: Mitochondrial DNA
MTS: Mitochondrial Targeting Sequence
MTT: 3-[4,5-dimethylthiazol-2-yl]-2,5-diphenyl tetrazolium bromide
NADH: Nicotinamide Adenine Dinucleotide
NCS: Nerve Conduction Study
nDNA: nuclear DNA
NEFL: Neurofilament protein, light polypeptide
NF: Neurofilament
NGF: Nerve Growth Factor
NGS: Next Generation Sequencing
NMD: Nonsense-mediated mRNA Decay
nmDMD : nonsense mutation Duchenne Muscular Dystrophy
NO or NO•: Nitric Oxide Radical
$NO^{\bullet}_2$: Nitrogen Dioxide Radical
NO_2^-: Nitrite
NOX: NADPH oxidase
NP: Neural Progenitor
$O_2^{\bullet-}$: Superoxide or superoxide anion
O_2^{2-}: Peroxide
OCT 3/4: Octamer binding transcription factor 3/4
OH•: Hydroxyl radical
OMM: Outer Mitochondrial Membrane
$ONOO^-$: Peroxynitrite
OPA1: Optic Atrophy 1
OXPHOS: Oxidative Phosphorylation
P4HB: Prolyl 4-Hydroxylase Subunit β
PAX6: Paired box 6
PCR: Polymerase Chain Reaction
PD: Parkinson's Disease
PDH: Pyruvate Dehydrogenase
PFA: Paraformaldehyde
PGP 9.5: Protein Gene Product 9.5
PINK1: PTEN-Induced putative Kinase 1
PLP: Proteolipid Protein
PMP2: Peripheral Myelin Protein 2
PMP22: Peripheral Myelin Protein 22
PNS: Peripheral Nervous System
PTC: Premature Termination Codon
PUFA: Polyunsaturated Fatty Acid
qPCR: quantitative PCR
RA: Retinoic Acid
RAB7: Ras-associated protein
RC: Rostrocaudal

RER: Rough Endoplasmic Reticulum
RI-CMT: Recessive Intermediate Charcot-Marie-Tooth
RIN: RNA Integrity Number
RNS: Reactive Nitrogen Species
ROS: Reactive Oxidative Species
rRNA: ribosomal RNA
RT: Room Temperature
RT-PCR: Reverse-Transcription Polymerase Chain Reaction
SACS: Sacsin Molecular Chaperone
SC: Schwann Cell
SEM: Standard Error of the Mean
SFN: Small Fibers Neuropathy
Shh: Sonic Hedgehog
SNS: Somatic Nervous System
SOCE: Store-Operated Ca^{2+} Entry
SOD: Superoxide Dismutase
S-OPA1: Short OPA1
SOX: SRY-Box Transcription Factor
SV: Structural Variant
TA: Tail-Anchored
TBP: TATA Binding Protein
TCA: Tricarboxylic Acid
TEAM: Triethanolamine
TGF-β: Transforming Growth Factor-β
TIM: Translocases of the Inner Membrane
TM: Transmembrane
TMD: Transmembrane Domain
TOM: Tranlocases of the Outer Membrane
tRNA: transfer RNA
Tuj1: class III β-tubulin
UPR: Unfolded Protein Response
VDAC: Voltage-Dependent Anion Channels
VNS: Vegetative Nervous System
WES: Whole Exome Sequencing
WGS: Whole Genome Sequencing
Wnt: Wingless-type MMTV integration site
WT: Wild-Type
YARS1: Tyrosyl-tRNA synthetase
α-SMA: α-Smooth Muscle Actin
ΔpH: H^+ ion concentration gradient
ΔΨm: mitochondrial membrane potential

Introduction

Chapter I. The peripheral nervous system

I.1. Overview

The nervous system is the complex organization which enables the interaction of human body with the external world. It consists in two parts: the central nervous system (CNS) and the peripheral nervous system (PNS) (Figure1).

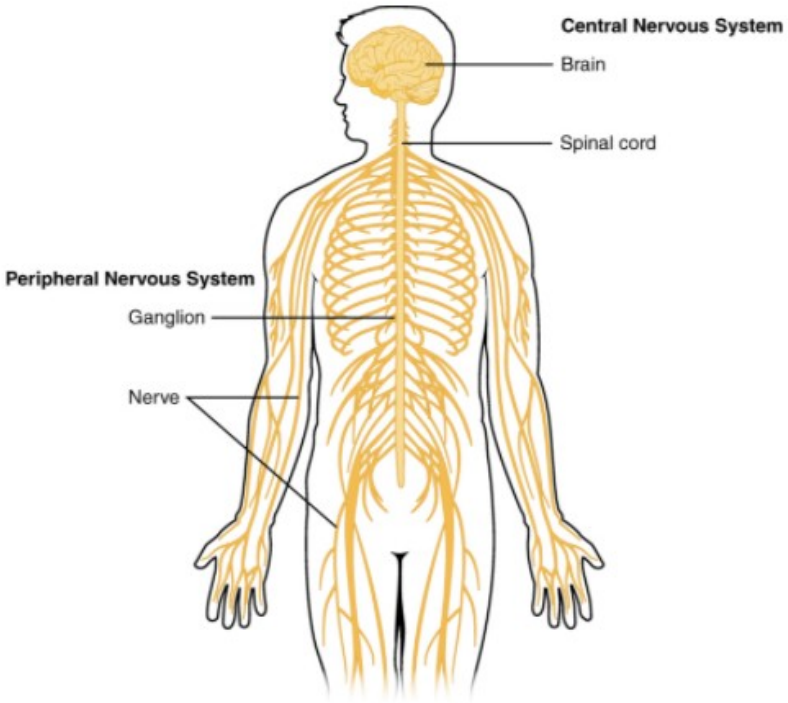

Figure 1 Human Central and Peripheral Nervous Systems [From: (OpenStax College 2013)].

The central nervous system is composed of the brain and the spinal cord, protected by the cranium and the vertebral column, respectively. It receives and integrates stimuli coming from the outer and the inner space and elaborates an appropriated response. The peripheral nervous system is made up of nerve fibers and ganglia. Anatomically, it is organized in an afferent arm, or sensory division, which conducts the information from receptors to CNS, and an efferent arm, or motor division, transferring

the central orders to the effector organs. Afferent neural cell bodies are located in dorsal root ganglia and afferent nerve fibers enter into spinal cord through dorsal roots. On the contrary ventral roots consist predominantly of efferent motor fibers, whose cell bodies are located in grey matter of spinal cord. Dorsal and ventral roots form spinal nerves which carry sensory and motor information between the spinal cord and the body. In the human body, there are 31 pairs of spinal nerves: eight cervical, twelve thoracic, five lumbar, five sacral nerves and one coccygeal nerve pair.

Moreover, peripheral nervous system, can be functionally divided in somatic nervous system and autonomic nervous system (Figure 2).

Somatic nervous system (SNS) represents the voluntary division. It is composed by a motor and a sensory component. The somatic sensory neurons are involved in mechanoreception, thermoception and nociception at skin, glands, or internal organs' level (Manivannan and Suresh 2012). The somatic motor arm controls skeletal muscles contraction through motor neurons.

Autonomic or vegetative nervous system (ANS or VNS) supplies smooth muscles, cardiac muscle and glands. It represents the unconscious control of internal organs' functions like digestion, body temperature, heart rate or respiratory rate. The ANS is organized in sympathetic, parasympathetic and enteric nervous system. Sympathetic nervous system usually elaborates "fight or flight" responses, since it is activated in stressful and emergency conditions. The parasympathetic nervous system controls the "rest and digest" responses, in ordinary situations when the human body is relaxed and at rest. These two components of the ANS are complementary in their functions, rather than opposite. If sympathetic nervous system increases heart rate and force of contraction, blood pressure, bronchodilatation and pupil dilatation, the parasympathetic nervous system reduces heart rate and blood pressure, and it stimulates salivation, digestive secretions and peristalsis. The third ANS division is represented by the enteric nervous system, even if it often considered an independent section of the nervous system. It consists in a neural network within the gut wall, which controls intestinal motility, secretory glands and blood flow of the gastrointestinal tract (Furness 2012).

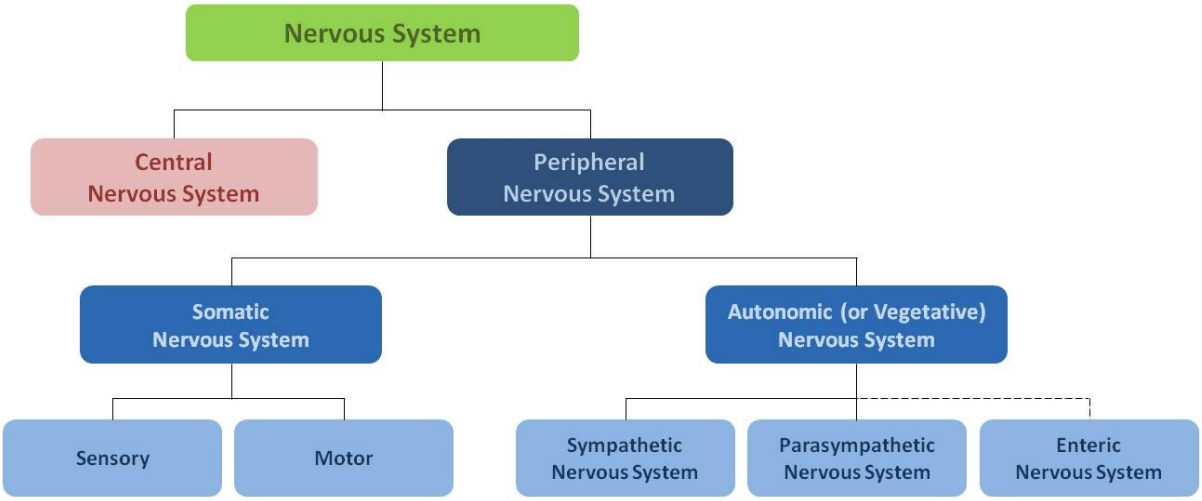

Figure 2 Schematic representation of Nervous System compartmentalization.

I.2. Development of the nervous system

The embryonic stages which lead to the complete formation of the nervous system, in humans, have been largely investigated. Nowadays, molecular mechanisms and pathways, as well as their regulating factors, are fully known. This is fundamental to better understand how human nervous system works, but also to be able to reproduce development processes, and induce neural differentiation in *in vitro* systems.

I.2.1. Formation of the neural tube

The nervous system is one of the earliest systems to form, since its development starts in the third week of embryogenesis. During the gastrulation, the blastula, a single-layered sphere of cells, modifies its structure to form the gastrula, which is composed of three different germ layers, called ectoderm, mesoderm and endoderm. In this phase, some mesenchymal cells move from primitive node (Hansens's node) to form the notochordal process. This is the first step of notogenesis, the

formation of notochord. Subsequently, notochordal process merges with the underneath endoderm layer, thickens, and originates the neural plate (Ramesh et al. 2017). When the neural plate invaginates, the neural groove takes shape in the middle, while borders create prominent neural folds on each side. With cellular growth, neural folds get close, fuse, and turn the neural plate into a neural tube (Simões-Costa and Bronner 2015).

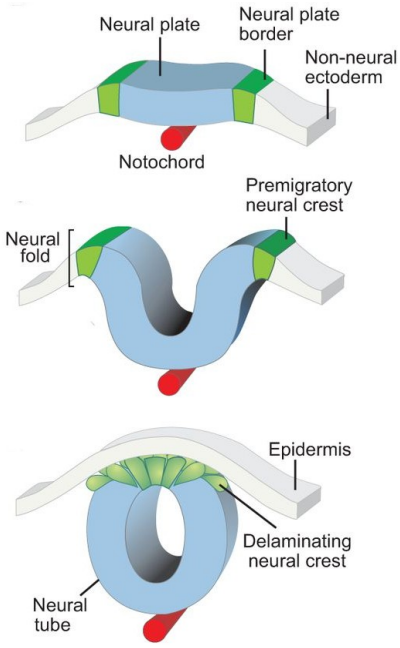

Figure 3 Development and evolution of the neural plate, and closure of the neural tube [Adapted from: (Simões-Costa and Bronner 2015)].

The closure of the neural tube plays a key role in the development of central and peripheral nervous systems. At this stage, the anterior part of the neural tube begins to expand and form the three primary brain vesicles: the prosencephalon, the mesencephalon and the rhombencephalon (Stiles and Jernigan 2010). By the end of the fifth week, these three structures give rice to the five secondary brain vesicles which will compose the adult central nervous system: the telencephalon, the diencephalon, the mesencephalon, the metencephalon and the myelencephalon (Stiles and Jernigan 2010).

Meanwhile, the development of the spinal cord begins with the formation of the neural tube. The neural tube is an empty channel whose internal wall is composed by the neuroepithelium, a floor of

rapidly dividing neural stem cells, which proliferate and differentiate into neuroblasts. The accumulation of neuroblasts originates the Mantle layer, the division which forms the grey matter of the spinal cord. The Mantle layer will be divided by the sulcuc limitans in an alar plate, predominantly made up of sensory neurons, and a basal plate, composed by motor neurons. On the other hand, the nerve fibers, coming from neuroblasts of the Mantle layer, organize in the Marginal layer. The Marginal layer surrounds the Mantle layer and forms the white matter of the spinal cord, when myelination of nerve fibers takes place.

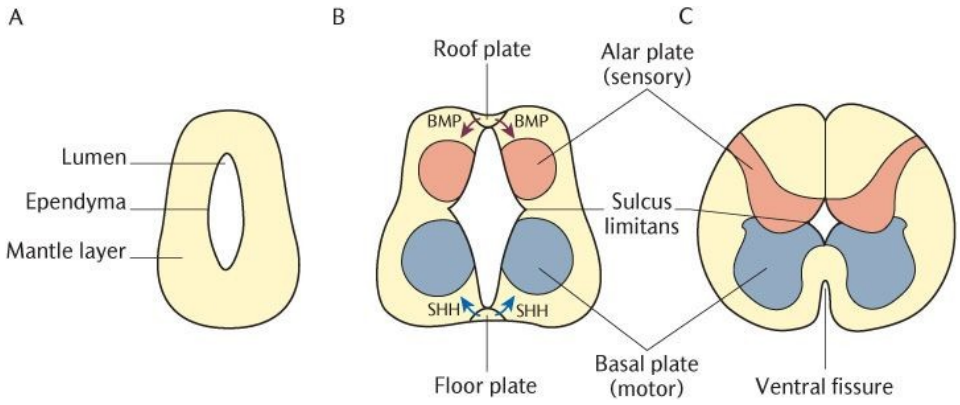

Figure 4 Formation of the spinal cord. Representation of the three layers of the neural tube: Lumen, Ependyma and Mantle layer (A). The Mantle layer will form the grey matter of the spinal cord, divided, by the sulcus limitans, in alar plate and basal plate; the Marginal layer, which surrounds the Mantle layer, will constitute the white matter (B and C). [From: (Martin, Radzyner, and Leonard 2012)].

At the same time, after the closure of the neural tube, neural crest cells, a population of cells located on the neural folds, turn from epithelial to mesenchymal state, and migrate to many localizations, differentiating into different cell types. Specifically, the trunk neural crest cells form the dorsal root ganglia, sympathetic neurons and Schwann cells, but also melanocytes and chromaffin cells. The parasympathetic ganglia originate from the vagal and sacral neural crest, while the cranial neural crest creates cranial neurons and glia, as well as cartilage, bones and connective tissue (Gilbert 2000) (Figure 5).

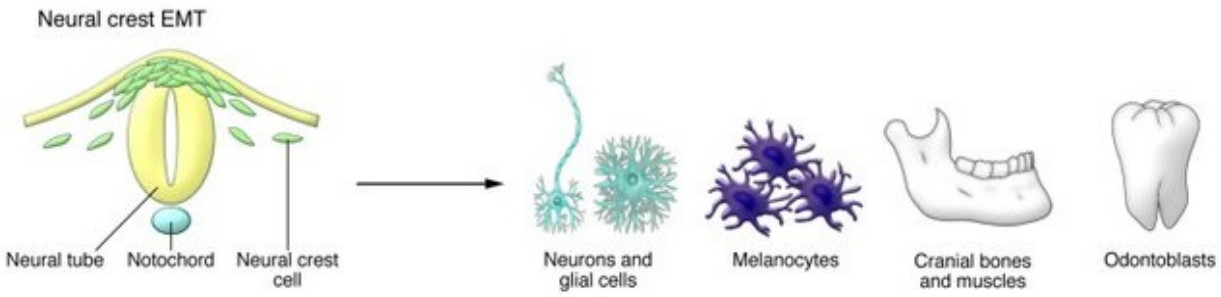

Figure 5 Neural crest cells migrate and differentiate into neural and non neural cell types [From: (Acloque et al. 2009)].

I.2.2. Molecular mechanisms of neural differentiation

The closure of neural tube is the most crucial event in the development of nervous system. The neural tube is a polarized structure, this means that it is organized along a dorsoventral (DV) axis, and an anteroposterior (AP) (or rostrocaudal (RC)), axis. The expression of specific transcription factors, involved in the differentiation process, depends on this organization. Consequentially, neural cells of the neural tube will have different fates of differentiation according to their position on DV and AP axes (Guillemot 2007).

Dorsoventral differentiation

Multiple factors act in DV differentiation events. They are often secreted by different sections of the neural tube, like the roof plate (the dorsal section) and the floor plate (the ventral section), or cells external to the neural tube. Bone morphogenetic protein (BMP) is a group of the transforming growth factor-β (TGF-β) superfamily, secreted by the roof plate and surrounding tissues. If, in early development stages, BMP inhibition is necessary to generate neuroectoderm from ectoderm, in this phase of the DV differentiation, BMP creates a gradient that regulates the expression patterning of several transcription factors (Bond, Bhalala, and Kessler 2012). BMP-regulated proteins are involved in generation of different populations of neural progenitors, in the dorsal and intermediate regions

of the neural tube (Timmer, Wang, and Niswander 2002). More than 20 BMP-ligands can act like antagonists and inhibit its expression, for example, noggin, chordin, follistatin. Proteins of the Wingless-type MMTV integration site (Wnt) family have a role similar to BMPs, since they participate in specification of dorsal interneurons (Muroyama et al. 2002).

The other factor with a key role in the DV differentiation is the Sonic Hedgehog (Shh) protein, expressed by cells of the ventral floor plate and the notochord (Yatsuzuka et al. 2019). Shh forms a ventral-to-dorsal gradient which controls the identity of progenitors in the ventral section of the neural tube (Le Dréau and Martí 2012).

Anteroposterior Differentiation

The earliest actor which acts in the anteroposterior patterning is *cyp26* (cytochrome P450 family 26) gene, expressed in the early anterior neural ectoderm and encoding the enzyme responsible for the degradation of Retinoic Acid (RA). RA is important in posteriorizing processes. So, in early stages, the activation of cyp26 inhibits RA, and most of developing events concern only the anterior portion of the neural tube, which organizes in primary vesicles. When Wnt and Fibroblast Growth Factor (FGF) pathways are activated, they suppress, independently, cyp26 activity, promoting RA expression. FGF, Wnt and RA can suppress further anterior markers, while FGF initiates the activation of posterior markers, in presence of RA pathway (Kudoh, Wilson, and Dawid 2002).

Main factors acting in DV and AP differentiation are reported in Figure 6.

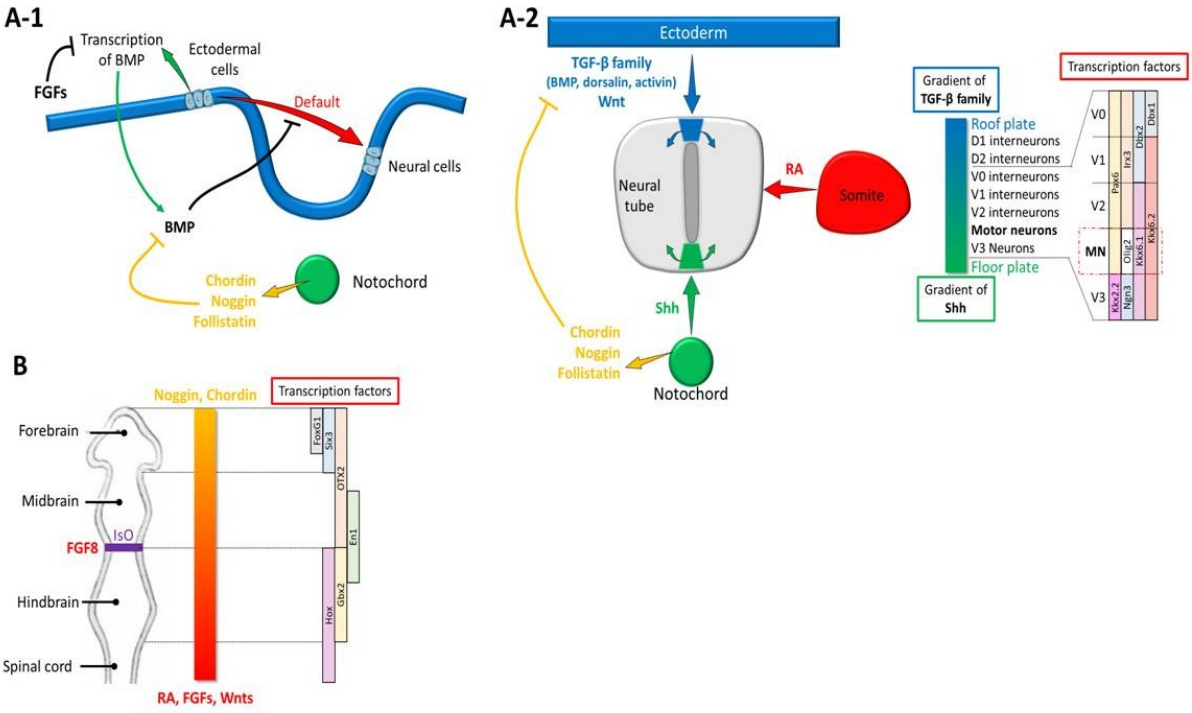

<u>Figure 6</u> Factors involved in dorsoventral polarity during the cord differentiation (A-1 and A-2), and factors involved in anteroposterior differentiation during neurulation (B) [From: (Faye et al. 2020)].

I.3. Peripheral nerve organization

I.3.1. Neurons

The neuron, or nerve cell, is the basic structural and functional unit of the nervous system. Neurons are excitable cells which communicate with each other or with other cell types by chemical synapses, in order to receive, elaborate, and transmit information. We can identify three major components in a neuron's structure: the cell body, the dedrites, and the axon (Figure 7).

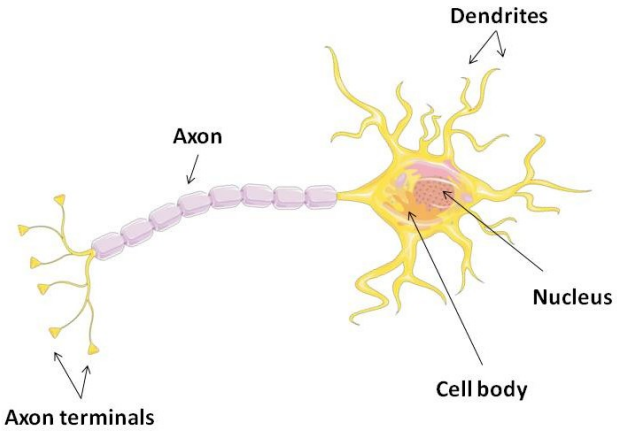

Figure 7 Schematic representation of a neuron.

I.3.1.1. The cell body

The cell body, or soma, is surrounded by a neural membrane which controls the cellular exchanges and establishes the electrical potential in the neuron. The cytosol is a potassium-rich solution which contains all the cellular organelles like the Golgi apparatus, the rough endoplasmic reticulum (RER), and mitochondria. Mitochondria, the "powerhouse" of the cell, play a key role in the soma since neurons require a large amount of energy. Moreover, in neuron body, we can find characteristic aggregates of RER granules, the Nissl bodies, important in the synthesis of proteins.

I.3.1.2. The dendrites

Dendrites are cytoplasmatic extensions of the cell, organized in a tree-like arborization ("dendritic tree") which allows to collect information coming from the external space and transmit it to the cell body. They are usually about 2 µm in length, while their number and their density can significantly vary, according to the neuron's function. Dentrites can present dendritic spines, small membranous protrusions that can rapidly change their form after signals' passage. These structures are

responsible for the so-called “dendritic plasticity”, the ability of neurons to adapt themselves to stimuli and change their connections in the neural network (Dharani 2015).

Concerning the dendrites’ composition, we observe the same organelles of the soma (Golgi apparatus, RER and mitochondria) and a large number of ribosomes, due to the high degree of protein synthesis.

I.3.1.3. The axon

The axon is a single long projection of the nerve cell that carries the neural information, so the electrical signal, away from the cell body. Its length can range from few millimeters to more than one meter. It arises in the axon hillock, a cellular region rich in ribosomes, and it is composed of three fragments: the initial segment, the shaft and the terminal arbor (or synaptic bouton), where neurotransmitters are stored in vesicles before being released. The axonal membrane is called the axolemma, while its cytoplasm is known as axoplasm. The main role of axolemma is to maintain the membrane potential of the axon thanks to the ion channels located along its surface. The axoplasm represents the main part of neuron’s cytoplasm. Its composition differs from soma and dendrites since it contains a reduced number of ribosomes associated to a large amount of elongated mitochondria and, above all, different cytoskeletal filaments: microtubules, microfilaments and neurofilaments (Morris and Lasek 1982).

Microfilaments (MFs) are made of globular actin monomers assembled to form a helical structure. They promote the expansion of axon growth cone during neurites formation process.

Neurofilaments (NFs) are composed of three subunit proteins: NF-L, NF-M, and NF-H. They act by stabilizing the cellular structure and by controlling the axon radial growth (Chevalier-Larsen and Holzbaur 2006).

Neural microtubules (MTs) are filaments of α and β tubulin heterodimers, forming a 25-nm-diameter hollow tube. Even if their structure is the same than MTs in the other body cells, neural MTs present

different isotypes of tubulin, with specific post-translational modifications, which can vary according to the localization. Moreover, it seems that, in contrast to dendrites, the polarity of axon MTs is uniform, considering that their "plus" end is always toward the axon terminal (Hammond 2015). The main role of MTs in the axon is related to the axonal transport activity. Since the axon lacks of ribosomes and ribonucleoprotein complexes, all the macromolecules need to be synthesized in the soma and transported along the axoplasm. Vesicles, mitochondria and other cellular organelles, require axonal transport, too. We can distinguish a retrograde axonal transport, from the periphery to the soma, and, vice versa, an anterograde axonal transport, from the soma to the periphery. Anterograde transport could be fast, up to 400 mm/day, or slow, 0.2 to 5 mm/day. If fast anterograde transport concerns mitochondria and vesicles containing neurotransmitters and enzymes, slow anterograde transport involves mostly cytoskeletal proteins, required to preserve cytoskeleton's structure integrity. Retrograde axonal transport is fast, 200 to 300 mm/day, and it carries old proteins and organelles to the soma to be degraded.

Two classes of motor proteins take part to axonal transport: the kinesin superfamily proteins, essential in the anterograde transport, and dyneins, essential in the retrograde transport (Chevalier-Larsen and Holzbaur 2006).

I.3.2. Classification of neurons

Neurons can be classified according to their structure or their function.

Basing on the neuron's structure we can distinguish (Figure 8):

- **Multipolar neurons** present a single axon and multiple dendrites, allowing interactions with multiple other neurons. They can be largely found in the CNS, specifically in cortex and spinal cord, but also in the PNS, in ganglia.

- **Bipolar neurons** possess two processes, one axon and one dendrite. They are generally involved in sensory pathway, that is why we can find them in eye's retina, in olfactory and vestibular nerves.
- **Unipolar neurons** have a single axon extending from the soma to the periphery. They are mostly present in invertebrates, like insects. In humans, unipolar neurons are generally "pseudounipolar". This means that these neurons present a single process, coming out from cell body, which splits, then, in two different branches. They are located in dorsal root ganglia, and conduct signals concerning touch, temperature, pain and vibration.

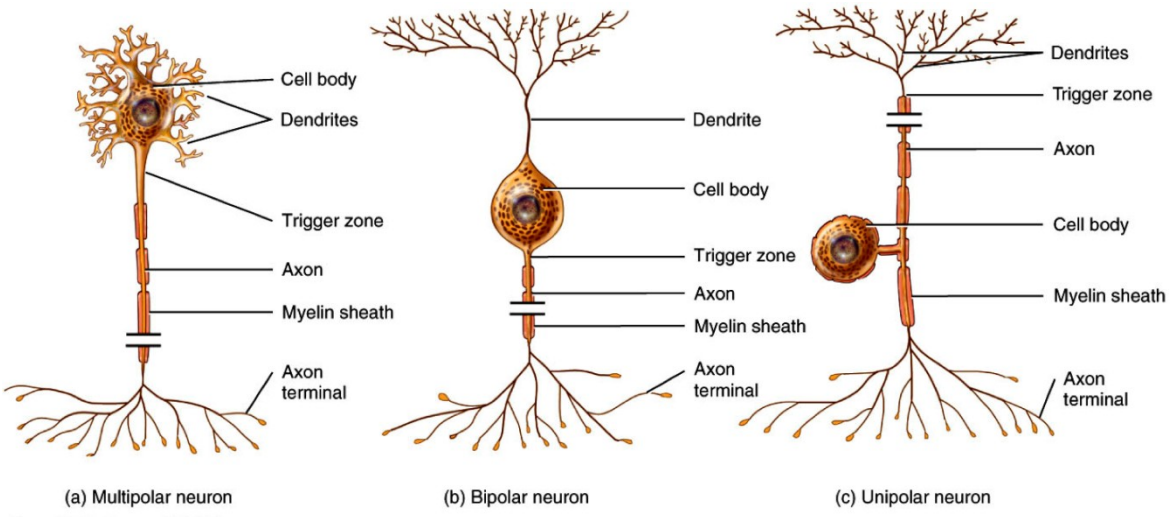

Figure 8 Structural classification of neurons [From:(Derrickson and Tortora 2017)].

According to their function, neurons can be classified in two main classes: sensory neurons and motor neurons.

- **Sensory neurons**, whose cell bodies are located in trigeminal ganglia and dorsal root ganglia, conduct stimuli from the periphery to the CNS, via afferent nerve fibers. Through their receptors, they receive three types of information: the proprioception, the sense of self-movement and body position; the nociception, which concerns the harmful stimuli; the mechanoreception and thermoception, activated by deformation and temperature information.

- **Motor neurons (MN)** form the efferent nerve fibers that carry information away from the CNS toward the peripheral effector organs. We can distinguish upper motor neurons, whose soma lie in the cortex, and lower motor neurons, whose soma reside in the brainstem or in the spinal cord. Upper motor neurons originate in the primary motor cortex, an area of the frontal lobe, and terminate within the brainstem and the spinal cord, where they synapse with lower motor neurons. They use glutamate as neurotransmitter. Lower motor neurons use acetylcholine as neurotransmitter and they transfer the information from upper motor neurons to target muscles. Lower motor neurons are classified according to their target: branchial, visceral and somatic MN.
    - Branchial motor neurons innervate branchial arch-derived muscles controlling face, jaw, larynx and pharynx. Their axons are assembled to form the trigeminal cranial nerve V, the facial cranial nerve VII, the glossopharyngeal cranial nerve IX, the vagal cranial nerve X, the spinal accessory cranial nerve XI (Chandrasekhar 2004).
    - Visceral motor neurons belongs to the ANS, and they are involved in the control of smooth muscles and glands. They are not directly connected to their effector organs but they allow the information moving from the CNS to the peripheral ganglionic neurons (Stifani 2014).
    - Somatic motor neurons are organized in three different group, on the basis of muscle fiber they innervate: alpha, beta, and gamma motor neurons. Alpha-motor neurons (αMN) innervate the extrafusal muscle fibers, the main fibers involved in muscle contraction. Beta-motor neurons (βMN) participate in contraction, and in responsiveness process too. They are less abundant than alpha and gamma motor neurons, and innervate intrafusal and extrafusal muscle fibers. Gamma-motor neurons (γMN) innervate intrafusal muscle fibers and they modulate the sensitivity of the muscle spindle to the phasic stretch and the tonic stretch, participating, in this way, to proprioception of the body.

I.3.3. Electrophysiological properties of neurons

Neurons are electrically excitable cells which can transfer information via electrical signals. They are characterized by two main properties: the excitability, the neural ability to respond to a stimulus, and the conductivity, the ability to conduct an electric message. These proprieties are due to voltage-gated ion channels, located on the plasmatic membrane of neurons, which allow the flow of different ions, specifically Na^+, K^+ and Ca^{2+}. When the neural cell is not excited, the resting potential is between -40 mV and -90 mV. This means that, according to the normal distribution of ions (mostly extracellular Na^+ and mostly intracellular K^+), there is an electric potential difference between the internal and the external sides of the membrane. Since the internal side is more negative than the external one, the membrane is defined "polarized". The cellular resting potential is maintained by the Na^+/K^+-pump which transports Na^+ and K^+ ions against their concentrations gradients, using adenosine triphosphate (ATP) hydrolysis as energy source. When the neuron is stimulated, it can elaborate different kinds of responses and the resting potential is perturbed in different ways:

- The *receptor potential* is a transient membrane potential activated by external stimuli like light, pressure, heat. It is typical of sensory neurons.
- The *synapse potential* is an alteration of membrane potential in a post-synaptic neuron, after the release of neurotransmitters in a synapse. It could be excitatory or inhibitory, and it is characterized by small amplitude and slow time course.

The receptor potential and the synapse potential are defined *graded potentials*, since they depend on the size of the stimulus and their amplitude is proportional to the strength of the stimulus. They differ from the action potential.

- The *action potential* is a rapid rise and subsequent fall of membrane resting potential. Specifically, it presents an initial rising phase or depolarization (opening of Na^+ channels),

followed by a falling phase or repolarization (closure of Na^+ channels and opening of K^+ channels), which brings the cell back to the resting potential, and it ends with an undershoot phase, or hyperpolarization, which makes the membrane potential more negative than the resting potential. After an action potential there is always a refractory period, during which it is not possible to evocate a new action potential. In contrast to graded potentials, actions potentials are "*all-or-none*". This means that they can occur only if the threshold is reached, or they do not occur at all. Their amplitudes, therefore, do not depend on stimuli intensity.

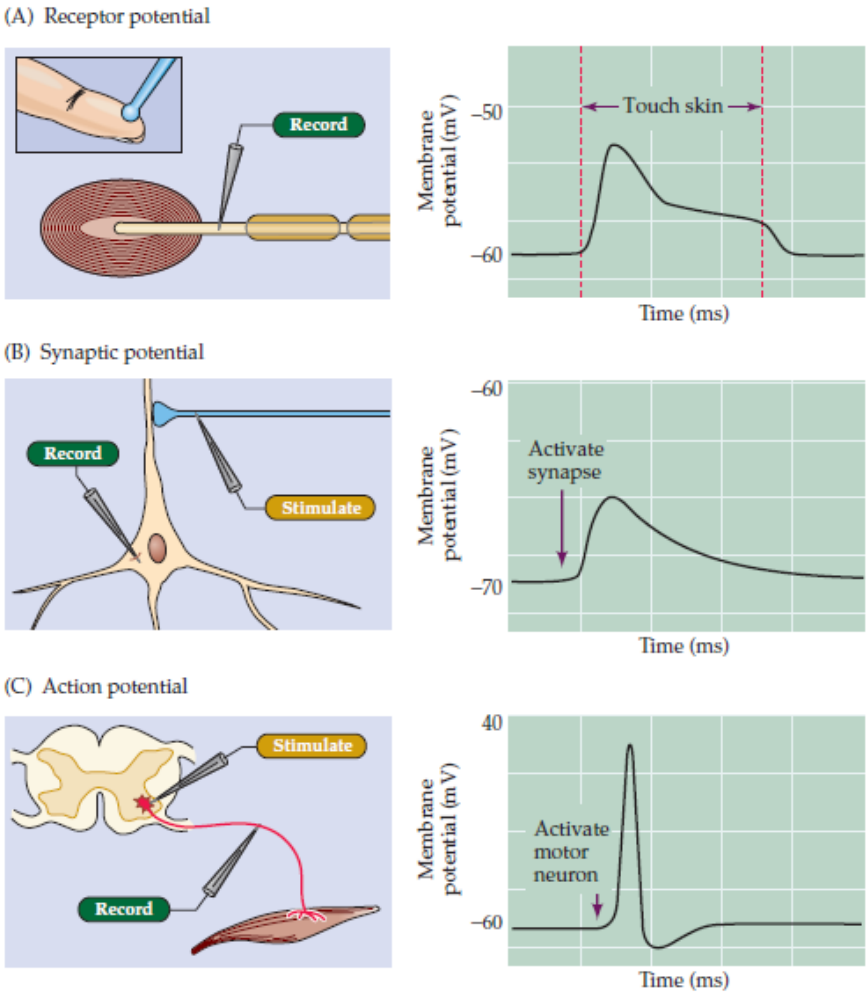

<u>Figure 9</u> Different electrical signals elaborated by neurons [From: (Purves 2004)].

I.3.4. Glial cells

Other than neurons, the nervous system consists of other cell types, gathered under the name of Glia, or Glial cells. Glial cells are more abundant than neurons but they do not produce and conduct electrical signals, even if they can participate indirectly to regulation of synaptic events. Their key role is to give physical support to nerve cells, control the uptake of nutrients and neurotransmitters, participate to myelin sheath creation, immune response and repair process. If, in the central nervous system, we can find oligodendrocytes, astrocytes, ependymal cells, and microglia, the peripheral nervous system presents only two main glial cells: satellite cells and Schwann cells (SC). Satellite cells are located in sensory and autonomic ganglia where they surround every neurons' soma (Gonçalves, Vægter, and Pallesen 2018). Schwann cells are the principal glial cells of the PNS.

I.3.4.1. Schwann Cells

Schwann cells originate from neural crest cells which migrate and differentiate themselves according to activation of specific transcription factors (Fröb and Wegner 2020). We can distinguish myelinating and non-myelinating SC. Both of them interact with neurons axons, but, if myelinating SC participate to myelin sheath creation around the axons, non-myelinating SC surround small-caliber axons just to isolate them from each other, without forming myelin sheath. Myelinating SC are analogous to oligodendrocytes in CNS, with the difference that, in PNS, the ratio axon/SC is 1:1, while oligodendrocytes can wrap multiple axons (Salzer 2008).

SC play also a key role in nerve repair and regeneration. For example, after a crush or cut injury of the nerve, SC can change their phenotype, produce survival signals for neurons, and, activating the immune response and macrophages recruitment, they can induce myelin clearance events (Jessen and Mirsky 2016). Moreover SC interact with proteins of extracellular matrix and basal lamina, and guide axonal growth during development (Chernousov and Carey 2000).

I.3.4.2. Myelin sheath

Myelin sheath is a lipid bilayers membrane that wraps multiple times nerve cells axons in the CNS and in the PNS, via the oligodendrocytes and the SC, respectively. It is organized in compact and non-compact components, with different structures and functions. Compact myelin is formed by tightly packed spiraling layers of membrane that lack cytoplasm. Non-compact myelin contains more cytoplasm and plays a role in signaling and transport of small metabolites (Ryu et al. 2008).

Myelin sheath is mainly composed by a high proportion of lipids (70-85%) and a smaller amount of proteins (15-30%), compared to other biological membranes. The most characteristic lipid of myelin is the galactosyl ceramide, but it presents also high levels of cholesterol and phospholipids (Quarles 2007). Concerning the protein composition, compact myelin contains four main proteins: Myelin Protein Zero (MPZ or P0), Proteolipid protein (PLP), Peripheral Myelin Protein 2 (PMP2 or P2) and Myelin Basic Protein (MBP). Another important myelin protein, known to be widely involved in neural physiopathology, is the Peripheral Myelin Protein 22 (PMP22). If PLP is specific of CNS, and MPZ, PMP2, and PMP22 are mostly expressed in PNS, MBP protein can be found in both of them. MPZ is the most abundant protein in peripheral myelin sheath (~50%) and it acts like structural element, stabilizing myelin through homophilic interactions (Quarles 2007). PMP2 seems to participate to myelin stabilization too, in addition to its role in lipid transport. MBP is important for the adhesion of the cytosolic surfaces of myelin (Boggs 2006), while PMP22 is involved in myelin formation, but also in SC proliferation and differentiation (Li, 2013). The main proteins of the non-compact myelin are Myelin Associated Glycoprotein (MAG), Connexin-32 (Cx32 or GJB1) and E-cadherin.

Myelin sheath acts like an insulator, helping the electric signals conduction, so enhancing the rapid propagation of action potentials along the axons. Each axon presents multiple myelinated segments, separated by short gaps, called nodes of Ranvier, where the axonal membrane is exposed to

extracellular space. Since voltage-gated sodium channels are located at nodes of Ranvier, when the axolemme is excited at this level, sodium ions enter in the neuron, leading to the depolarization of the membrane. This electrical signal, caused by ions diffusion, cannot flow through the high-resistance myelin sheath, and, consequentially, it reaches the next node of Ranvier, where a new segment of axolemme is depolarized. The membrane depolarization process, associated to the potassium channels-dependent repolarization, constitutes the action potential. As result of myelin sheath organization, the action potential jumps from a node of Ranvier to another along the axon, and for this reason its propagation is defined *saltatory* conduction.

In PNS, but not in CNS, the nodes of Ranvier are contacted by numerous microvilli, which are processes of Schwann cells, probably involved in ion buffering (Salzer 2008; Arancibia‐Carcamo and Attwell 2014). The myelinated segments between two nodes are called *internodes*, while the nodes-flanking regions are known as *paranodes* or *paranodal regions*. Paranodes are the site of tight junctions between the axon and the glial myelin, resulting from the action of multiple proteins like the contactin, the contactin-associated protein (Caspr) and the neurofascin 155 (Lyons and Talbot 2008; Uncini, Susuki, and Yuki 2013). Between internodes and paranodes, we find the *juxtaparanodal regions*, where most voltage-gated potassium channels are located (Arancibia‐Carcamo and Attwell 2014).

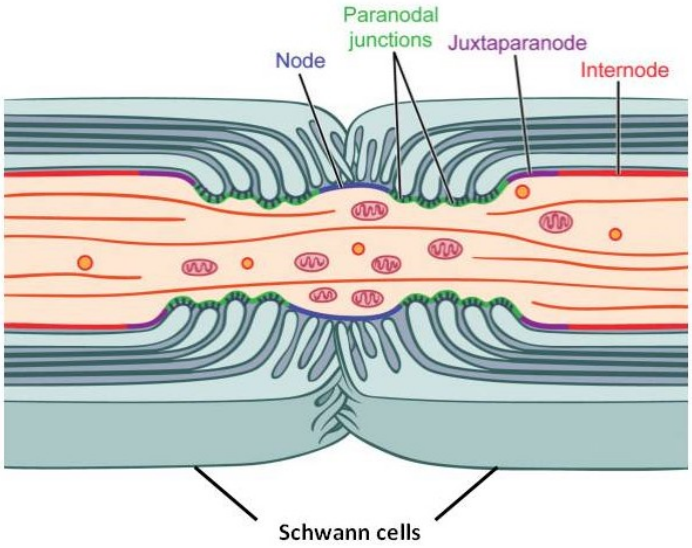

Figure 10 Organization of main domains in a node of Ranvier [Adapted from: (Salzer 2008)].

I.3.5. Nerve anatomy

The nerve is the main structure of the peripheral nervous system and it consists of a bundle of neurons' axons wrapped in the myelin sheath. In a nerve, every axon, with its myelin coating, is surrounded by the *endoneurium*, a layer of connective tissue composed of endoneurial cells. The endoneurium appears as an elastic channel since the collagen I and II represent its major components (Ju, Lin, and Chang 2017). It contains the endonerium fluid, with a protective role, comparable to the cerebrospinal fluid in CNS (Reinhold and Rittner 2017). Moreover, within a nerve, axons acting on the same anatomical area, are organized in fascicules (fasciculi), surrounded and held together by the *perineurium*. The perineurium is a dense sheath of connective tissue formed by multiple concentric layers of fibroblasts cells associated to type I and type II collagen fibers. In addition to its protective function, perineurium is important to regulate the inner pressure of the fascicule (Ju, Lin, and Chang 2017). Lastly, multiple nerve fascicles are kept together by the outer connective layer, the *epineurium*. The epineurium seems to be organized in two different layers: the external one consists in an areolar connective tissue with a vascular component, while the internal

one presents, above all, collagen fibers (Stolinski 1995). It acts like buffer barrier, protecting fascicles from the external space (Ju, Lin, and Chang 2017).

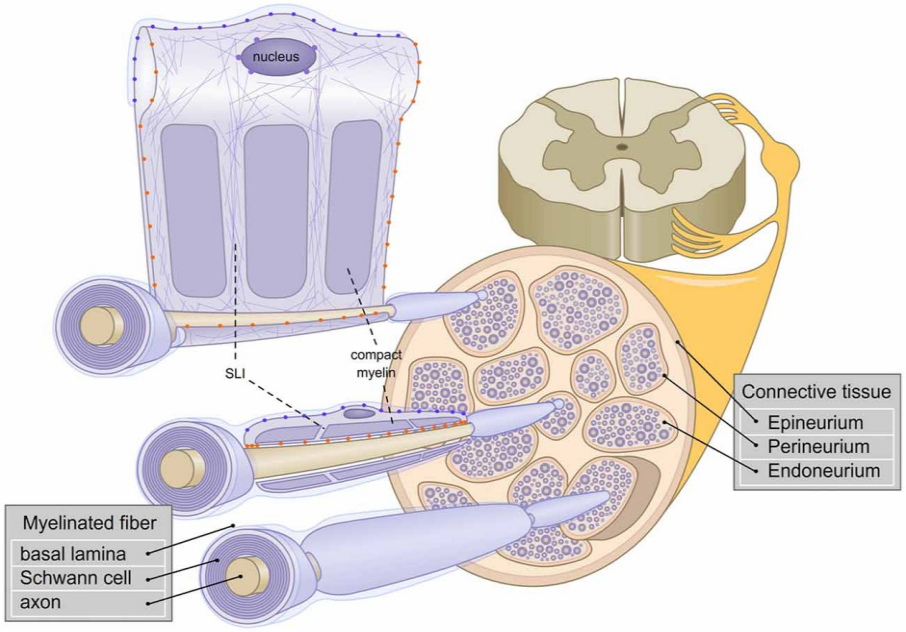

Figure 11 Nerve architecture. The Schwann cell, in blue, wraps around neuron's axon, in rose. They are surrounded by the endoneurium, within the nerve fascicule. Every fascicule is surrounded by the perineurium, and kept together with other fascicules, by the epineurium [From: (Belin, Zuloaga, and Poitelon 2017)].

I.4. PNS disorders: the peripheral neuropathies

I.4.1. Overview

A peripheral neuropathy is a pathological condition caused by the damage of a SNP structure (neuron cell body, axon, myelin sheath). Despite the lack of a large number of epidemiologic studies, it seems that peripheral neuropathies have a prevalence estimated between 2.4% and 7% (Callaghan, Price, and Feldman 2015). Their origin can vary considerably, as well as their symptomatology. According to the number of affected nerves, peripheral neuropathies can be classified in *mononeuropathies*, if they affect a single nerve, *mononeuritis multiplex* (or *multiple mononeuropathies*), if multiple non-contiguous nerve trunks are involved in an asymmetric way, and *polyneuropathies*, when the

disorder is diffuse and concerns the whole of the nerves. According to the kind of affected neurons, we can distinguish motor neuropathies and sensory neuropathies. On the other hand, basing on the type of affected nerves fibers, we can divide small fibers neuropathies, large fibers neuropathies, and autonomic neuropathies (Magy and Vallat 2009).

The peripheral disorders can involve different components of the PNS. This allows to further subdivide them in axonopathies, if they touch the axons, and myelinopathies, which concern the myelin sheath (Barohn and Amato 2013). In axonopathies, the axon degeneration leads to the aberration of terminal arbors of nerves, with the consequent disconnection of neurons from the neural network and loss of nerve fibers (Landowski et al. 2016; Burgess 2018). Distal axonopathies have generally a symmetric length-dependent evolution since symptoms appear in lower legs and feet. Myelinopathies are caused by myelin sheath damages and they are characterized by impaired conduction of electrical impulses. They could be length-dependent too.

The duration of symptoms in peripheral neuropathies makes it possible to distinguish acute forms (<4 weeks), subacute forms (4-12 weeks) and chronic forms (>12 weeks) (Misra, Kalita, and Nair 2008).

I.4.2. Etiology

The complexity of peripheral neuropathies diagnosis is associated to the large number of possible causes that can induce the onset of the disorder. Primarily, *acquired* neuropathies could be differentiated from *genetic* neuropathies.

I.4.2.1. Acquired neuropathies

We define “acquired”, a neuropathy not present at the beginning of patient’s life, so a condition resulting from environmental factors or other pathological events. Acquired neuropathies

represent the majority of peripheral neuropathies, and they can be further classified according to the specific associated cause (Lozeron, Trocello, and Kubis 2013).

- *Metabolic disorders*, alterations of normal metabolic processes in the body, can cause metabolic neuropathies. Among them, the most common pathologic condition is the *diabetic* neuropathy, which can affect up to 50% of adults with type 1 or type 2 diabetes mellitus. Frequent consequences are sensory loss, motor impairment, foot ulcers, sometimes lower limbs amputation, with a general worsening of life quality (Hicks and Selvin 2019).

- *Vascular disorders* can lead to decreased blood flow to upper and lower limbs and reduce oxygen supplied to nerves, inducing, in this way, nerve damage or death.

- *Kidney and liver disorders* may cause metabolic dysfunctions and increase the blood amount of toxic substances, damaging nerve tissue (Chaudhry et al. 1999; Arnold et al. 2016).

- *Imbalance of vitamins*, like Vitamin B12, B6, B1, or E, can result in axon and myelin dysfunction in PNS, as well as cognitive problems in CNS (Staff and Windebank 2014). Calcitriol, or 1,25-dihydroxyvitamin D3, seems to help axonogenesis and axon growth, myelination, and recovery of locomotor functions in trauma models. The calcitriol deficiency is associated to a higher risk of diabetes and related complications like neuropathies, but also reduction of nerve conduction velocity (Faye et al. 2019).

- *Autoimmune diseases* are due the abnormal response of immune system which mistakenly attacks a body part, such as a PNS structure. This is the case of Guillain-Barré syndrome, caused by bacterial or viral infections and characterized by a demyelination process mediated by T-cells and macrophages (Bourque, Chardon, and Massie 2015). Peripheral neuropathies can derive also from autoimmune diseases that not directly target the nervous system, like Lupus, rheumatoid arthritis, and Sjögren's syndrome.

- *Viral and bacterial infections* may have effects on the PNS. For example, up to 50% of patients with infection of human immunodeficiency virus (HIV) present distal polyneuropathy, while Herpes virus (herpes simplex type 1 and 2 and varicella-zoster virus) reside in ganglia and cause

manifestations on PNS when reactivate. *Flaviviridae*, like the West Nile virus or the Hepatitis C virus, may also affect sensory and motor systems (Brizzi and Lyons 2014). Among the bacteria, *Clostridium tetani*, *mycobacterium leprae*, and *Corynebacterium diphteriae*, are known to be associated to peripheral nerve damage (Carod-Artal 2018).

- *Cancers* seem to affect PNS through different pathophysiological mechanisms. Invasion processes, metastasis, metabolic imbalance and immune-mediated events can directly or indirectly induce nerve lesions (Zis and Varrassi 2017).

- *Drugs and toxins*. Chemotherapy drugs, like Platinum-Based Antineoplastics, Taxanes and Vinca Alkaloids, cause peripheral neuropathies in 19% to 85% of cases. Symptoms generally involve the sensory division and include numbness, altered touch and vibration senses, pain, paresthesias, dysesthesias, especially in hands and feet (Bessaguet et al. 2018; Zajączkowska et al. 2019). Toxins, above all heavy metals (plumb, arsenic, thallium, mercury) and industrial agents, are responsible for neurotoxicity in PNS (Staff and Windebank 2014).

- *Trauma* as falls, accidents, sport activities, often lead to nerve injuries, compression or crush, with consequent damage of myelin and/or axons (Menorca, Fussell, and Elfar 2013; Caillaud et al. 2018). According to several studies, brachial plexus, ulnar nerves, radial nerves and sciatic nerves are the most frequently involved (Kouyoumdjian 2006; Ciaramitaro et al. 2010).

I.4.2.2. Genetic neuropathies

Genetic or hereditary neuropathies are a heterogeneous group of disorders affecting the peripheral nervous system caused by genetic mutations, so by alterations of DNA sequence. The genetic mutations can involve a single nucleotide (point mutations), multiple nucleotides in small regions (small deletions and duplications), or they can concern large chromosomal regions (large deletions and duplications, chromosomal translocations and inversions). Pathological mutations can

be inherited, from parents, or *de novo*, if they appear in germline of parents or during a post-zygotic phase of the patient's embryogenesis. The mode of inheritance could be autosomal, dominant or recessive, or X-linked, dominant or recessive. Moreover, some cases of peripheral neuropathies, caused by mutations in mitochondrial DNA (mtDNA), have also been reported (Bouillot et al. 2002).

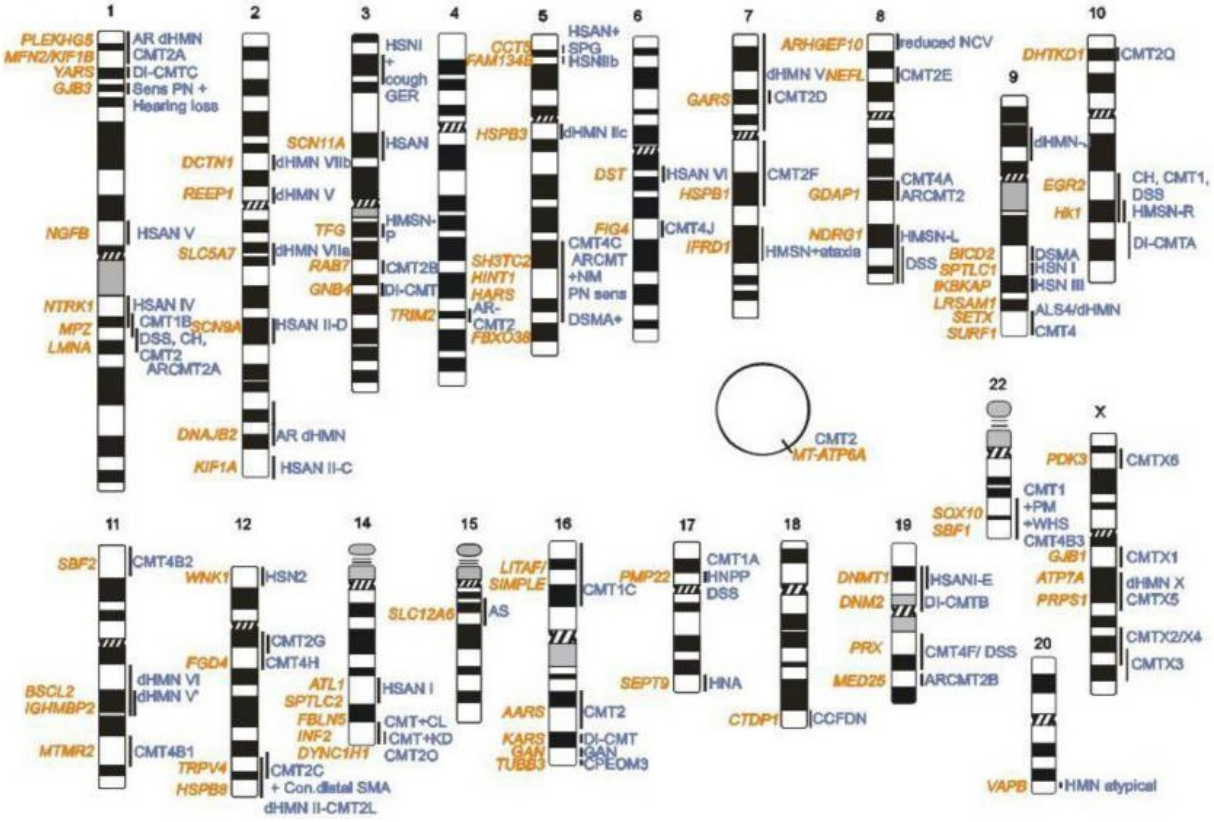

<u>Figure 12</u> Genomic localization of some nuclear and mitochondrial genes (in orange), and their associated inherited peripheral neuropathies (in blue) [From: (Timmerman, Strickland, and Züchner 2014)].

Among all the hereditary neuropathies, we distinguish genetic disorders mainly characterized by peripheral problems, and diseases in which the neuropathy is only an aspect of a more complex phenotype, like Friedreich ataxia (Rossor, Tomaselli, and Reilly 2016). The most common genetic peripheral neuropathies are:

Charcot-Marie-Tooth (CMT) disease, a sensory-motor neuropathy with impairment of both sensory and motor nerve fibers. It has a prevalence of 1/2,500 and it represents the most common hereditary neuropathy. More details about CMT disease are reported in Chapter 2.

Hereditary sensory and autonomic neuropathy (HSAN) or hereditary sensory neuropathy (HSN), which are characterized by a wide degree of sensory and autonomic fibers' impairment. The most frequent symptom is the loss of pain and temperature sensations, often followed by chronic ulcerations. Disturbances start distally in lower limbs, to spread later to upper limbs. Autonomic symptoms may also occur, like hyper-or-hypohidrosis, apnea, urinary incontinence (Rotthier et al. 2012).

Hereditary motor neuropathy (HMN), often known as distal hereditary motor neuropathy (dHMN). This is a group of slowly-progressive length-dependent disorders, defined by muscular atrophy and wasting, weakness, foot deformities (Bansagi et al. 2017). Reflexes are often abolished, amplitudes are reduced. Sensory disturbances are minor or absent (Rossor et al. 2012).

Small fibers neuropathy (SFN) which concerns small and myelinated Aδ fibers, and small and unmyelinated C fibers. Since sensory and autonomic fibers could be affected, main symptoms vary from case to case, but they often include alteration of thermal and pain sensation, like allodynia and hyperesthesia, but also paresthesia, numbness, bladder and gastric issues, cardiac alterations (Levine 2018).

Other hereditary pathologies, with a complex clinical manifestations, only partially characterized by peripheral neuropathy. For example, Hereditary Ataxia is a group of disorders defined by incoordination of muscles and gait disturbance, which result in altered speech and abnormal movement of hands and eyes (Bird 1993). It is normally associated to a cerebellar dysfunction and atrophy, but peripheral nervous system may be also implicated. Sometimes, peripheral, motor and sensory, signs are predominant in patient's phenotype, and Ataxia may be mistaken for "pure" peripheral neuropathy, like Charcot-Marie-Tooth disease (Salomão et al. 2017).

I.4.3. Clinical symptoms

Patients affected by peripheral neuropathies can show sensory and motor symptoms, both of them can be classified as *positive*, when there is a gain of function, or *negative*, with a loss of function.

- Typical positive sensory symptoms are: paresthesia, characterized by tingling and pricking; dysesthesia, the unpleasant sensation of touch; numbness; neuropathic pain, like coldness and burning sensations, electric shocks and «picks and needles» sensations.
- Typical negative sensory symptoms are: hypoesthesia and anesthesia, the reduction and the total loss of sensation, respectively; ataxia, the lack of coordination and balance functions.
- Typical positive motor symptoms are: cramps, sudden and involuntary contractions of muscles; muscle twitch (or fasciculations), the involuntary contraction of a group of muscle fibers.
- Typical negative motor symptoms are: muscular weakness, the decrease of muscle strength, with associated difficulties in daily activities; muscular atrophy, the decrease of muscle mass and size.

I.4.4. Medical history

Given the complexity of peripheral neuropathies, the patient medical history (or anamnesis) represents the first required step in the management of patients. It allows to collect all relevant information about medical events and problems of the person and the other family members, but also details about occurrence, evolution and distributions of symptoms. Anamnesis is essential to investigate the disorder and establish a good diagnosis.

I.4.5. Clinical examination

For peripheral neuropathies, the physical examination is the first process of patient's evaluation, and it is required for all individuals suspected to be affected by the pathology. It consists in the evaluation of muscular mass and strength, reflexes, sensory functions and possible physical deformities. After the physical exam, further tests are often necessary.

Electromyography and Nerve Conduction studies are commonly required, too. If electromyography (EMG), or needle EMG, measures the electrical activity in muscles, the nerve conduction study evaluates the velocity of nerve fibers in conducting electrical signals. Electrophysiological studies make it easier to identify the peripheral neuropathy form. More details about these analyses are reported in Chapter 2.

Sometimes, for deeper investigations, nerve, skin, or muscle biopsies are demanded. These tissues samples are used for the histopathological study, performed to explore eventually structure abnormalities induced by the peripheral pathology. For nerve biopsy, sural nerve and superficial peroneal nerve are often chosen when the disorder is predominant in lower limbs, superficial radial nerve and ulnar nerve are preferred when upper limbs are more involved (Said 2002). Nerve biopsy is an invasive procedure for patients, so its indication is restricted to specific cases. Skin biopsy, which is less invasive, is usually used in SFN examination, since it allows to quantify nerve fibers in epidermis. Muscle biopsy is performed to verify the functional consequence of nerve degeneration on the effector organ (muscles), but it seems to have also a key role in diagnosis of peripheral nerve vasculitis (Bennett et al. 2008).

Blood biochemical test can help in the identification of the disease's etiology, since it allows to detect vitamins imbalances, glucose level, kidney and liver disorders, thyroid issues, antibodies directed against pathogens or involved in autoimmune diseases.

In the event that the medical history, and the neurological and biochemical examinations, suggest a genetic cause for the peripheral neuropathy, the genetic analysis is generally conducted. It is

necessary to confirm the inherited origin of the disease, to identify the causing mutation and establish the inheritance mode of transmission, so to predict the pathological implications for the patient and the other family members. Moreover, this examination can help in the patient's follow-up and in the choice of a potential treatment. The genetic analysis is performed using molecular biology's tests. Most involved genes are often tested by Sanger Sequencing. Nevertheless, several gene panels for peripheral neuropathies have been designed to extend the analysis to a higher number of genes, using Next Generation Sequencing (NGS) strategies. Whole Exome Sequencing (WES) and Whole Genome Sequencing (WGS) are, currently, more and more employed, too. NGS data are then associated to a Bioinformatic analysis to be processed and interpreted.

Chapter II. Charcot-Marie-Tooth disease

II.1. Overview

Charcot-Marie-Tooth (CMT) disease, also called hereditary sensory-motor neuropathy, is the most common inherited peripheral disorder. Its prevalence has been estimated to be 1/2,500, even if epidemiological studies can considerably vary, from country to country, in quality and methodology, complicating the establishment of a correct global frequency (Barreto et al. 2016). Clinically, this heterogeneous group of peripheral neuropathies is mostly characterized by distal weakness and atrophy, sensory loss, reduced reflexes, balance troubles, and, sometimes, anatomical deformities, like *pes cavus*. First symptoms can appear early, in the first decade, or lately, in the adulthood.

CMT disease was described for the first time in 1886 in France, by Professor Jean-Martin Charcot and his student, Doctor Pierre Marie, who presented it like “a peroneal muscular atrophy”, characterized by muscular weakness and wasting. At the same time, in Cambridge, Howard Henry Tooth published his theses on the same subject. He was the first to realize that the “progressive muscular atrophy” could cover multiple disorders, characterized by atrophy, but due to different causes and with myelitic, neuropathic or myopathic origin (From the Archives: (Compston 2019)). Next studies allowed to discover further clinical cases of CMT disease, and associate additional symptoms and features to this pathology. First anatomical and histological analysis highlighted morphological abnormalities in nerve trunks and roots, as well as lesions in the spinal cord and schwannian hyperplasia (Sturtz, Chazot, and Vandenberghe 1992). In 1968 Dyck and Lambert, through electrophysiological analysis, showed, for the first time, that only some CMT families presented a reduced nerve conduction velocity, while it appeared preserved in other ones. Their study was fundamental for the first classification of CMT disease in demyelinating (CMT1) and axonal (CMT2) forms (Dyck and Lambert 1968).

CMT disease is part of genetic peripheral neuropathies, since it is caused by inherited or *de novo* mutations which can occur in a large panel of CMT-associated genes. It seems that the proportion of *de novo* mutations varies from gene to gene and it is related to severity of the pathological phenotype (Rudnik-Schöneborn et al. 2016). However, in most cases, CMT disease is inherited, in an autosomal, dominant or recessive, manner, or in a X-linked, dominant or recessive, manner. The most common CMT mutation is the duplication of *PMP22* gene, encoding the peripheral myelin protein 22.

II.2. Clinical presentation

As consequence of the wide range of possible causative mutations and associated genes, clinical manifestations of Charcot-Marie-Tooth disease are very heterogeneous, and they differ significantly from patient to patient. Age of onset, progression rate, or disease severity, are often difficult to predict and, sometimes, they can vary within the same family. Early troubles may appear in first years of childhood with difficulties in walking, stumbling and falls, clumsy movements. First distinctive symptoms are symmetric distal weakness, starting in feet and progressing in ankles and hands, and muscular atrophy, the wasting of muscles, in legs and arms (Szigeti and Lupski 2009). Consequentially, patients have often a feeling of fatigue and tiredness, even in easy efforts. These clinical signs are generally followed by depression or abolition of tendon reflexes, and, above all, sensory disorders. Concerning the sensory compound, patients usually experience loss or alteration of pain, touch and temperature perception, occasionally tingling and burning sensations (Gemignani et al. 2004). Neuropathic pain can be also present, as result of muscular weakness or skeletal deformities. The main anatomical deformities in CMT disease are the high-arched feet (or *pes cavus*), typically associated with curled toes (*hammertoes*), and the flat-arched feet (or *pes planus*). Lower legs can take the "inverted champagne bottle" appearance, due to the muscular wasting in lower

limbs. We can observe also deformities in hands, after protracted contraction of fingers, and scoliosis (Piazza et al. 2010).

With the progression of CMT disease, the persistent nerve damage can make more complicate, or impossible, daily easy tasks, deteriorating patients' quality of life. Difficulties in walking can evolve in severe mobility problems and need of walking aid like crutches and wheelchair.

In the analyses of CMT phenotype we can also include multiple, and sometimes rare, symptoms associated with specific CMT forms, such as pyramidal signs, mental retardation, cerebellar ataxia and visual or hearing problems.

II.3. Electrophysiological study

The electrophysiological study is often a required step in the diagnosis of CMT disease. It generally includes the needle electromyography (EMG) and the nerve conduction study (NCS).

The **needle EMG** is the analysis of muscular electrical activity, since it allows to record the electrical signals generated in muscle fibers. During this procedure, the recording needle electrode is inserted into the muscle and it records the electrical signal at rest and during voluntary contraction. The clinician skills, in interacting with the patient and handling the needle in the muscle, are important for the good efficiency of the procedure. The muscle chosen for the needle EMG depends on the patient's clinical condition (Rubin 2012).

The **nerve conduction study** (NCS) allows to measure the nerve conduction velocity (NCV), so the speed of an electrical signal which moves through a nerve segment. It is conducted on the largest and fastest myelinated fibers and it reflects the function of motor and sensory fibers. It is suitable, therefore, for detection and evaluation of peripheral nerve disorders (Moattari et al. 2018). NCS is generally performed on peroneal, tibial or sural nerves, in lower limbs, and median and ulnar nerves in upper limbs.

Specifically, NCS consists in a motor conduction study (MCS) and a sensory conduction study. To realize the MCS, the recording electrode is placed on the skin, over the nerve, while the stimulating electrode is placed at a known distance from it. The stimulating electrode provides a brief electrical shock, so an electrical impulse, which is conducted along the nerve to be detected by the recording electrode. The result of a MCS is the compound muscle action potential (CMAP) which represents the summation of all the action potentials of muscle fibers of the same region. A CMAP is characterized by the amplitude, the latency, the duration and the area (Figure 13).

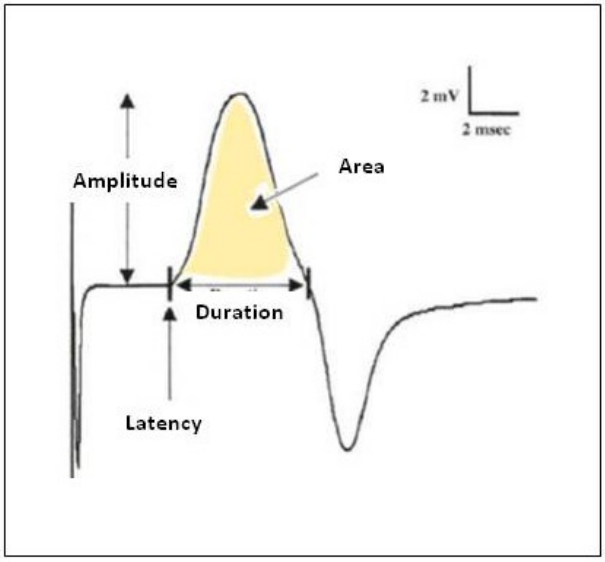

Figure 13 Latency, amplitude, duration, area, and latency of the compound muscle action potential (CMAP) [Adapted from (Moattari et al. 2018)]

The amplitude of the CMAP, measured from baseline to negative peak, depends on number of motor axons implicated. It is reduced in case of axonal loss, but also in demyelinating events (Mallik 2005; Tankisi et al. 2012).

CMAP duration is the time period between the onset of deflection and the return to the baseline. It increases in demyelinating disorders, since the myelin damage increases the temporal dispersion along the fibers (Isose et al. 2009). This means that in demyelinating neuropathies there is an inverse linear correlation between amplitude (decreased) and duration (increased), absent in axonal neuropathies.

CMAP area is defined by the baseline and the negative peak. It depends on amplitude and duration.

The latency, measured in milliseconds, is the time period between the stimulus and the beginning of the initial deflection (the response). If in axonal disorders it is usually normal, it increases in demyelinating disorders.

The latency is a required parameter to calculate the **motor nerve conduction velocity (MNCV)**.

$$\boldsymbol{MNCV} = \frac{Distance\ (between\ the\ proximal\ and\ the\ distal\ stimulation)}{Proximal\ latency - Distal\ latency}$$

The determination of the MNCV allows to distinguish two main classes of CMT disease: the demyelinating and the axonal forms.

II.4. CMT classification

II.4.1. CMT classification based on the electrophysiological study

Dyck and Lambert were the first, in 1968, to find out that nerve conduction velocity makes it possible to distinguish demyelinating peripheral neuropathies from axonal peripheral neuropathies (Dyck and Lambert 1968). These two clinical groups were better analyzed, in 1980, by Harding and Thomas, who set the NCV threshold at 38 m/s. Their study identified a more numerous group of patients, the HMSN type 1, presenting a NCV< 38m/s, and a second group, the HMSN type 2, with a NCV≥38 m/s (Harding and Thomas 1980).

Demyelinating forms derive from a damage or an alteration of the myelin sheath which surrounds neuronal axons in nerve fibers. Since myelin function is fundamental to ensure the rapid propagation of electrical signals, its injury leads inevitably to a reduction of NCV (<38 m/s). In axonal forms, neurons' axons are directly affected. Consequentially, CMT2 are characterized, at

electrophysiological level, by normal values of NCV, but reduced amplitudes of the CMAP. Today, the traditional classification of CMT disease in demyelinating forms (CMT1) and axonal forms (CMT2) is still conserved, in a general way.

In addition, several studies pointed out the presence of a third group, the so called “Intermediate CMT”. Intermediate CMT bring together clinical cases lying between axonal and demyelinating forms and sharing features with one and the other phenotype. The NCV of intermediate CMT are between 25 and 45 m/s (Liu and Zhang 2014; Berciano et al. 2017).

II.4.2. CMT classification based on the mode of inheritance

The mode of inheritance of CMT disease, so the manner of its genetic transmission from a generation to another, can largely vary among the different CMT forms. The autosomal mode of inheritance is related to genes located on autosomal chromosomes (any chromosome other than a sex chromosome), and it can be dominant or recessive. Other CMT forms have a X-linked mode of inheritance, since they are caused by genes located on the sex-determining X chromosome. As well as autosomal forms, they could be dominant or recessive.

II.4.3. A complete and complex CMT classification

The classification of all the CMT has been subjected to repeated revisions over the years and, still today, it remains a challenge. The detection of new CMT-associated genes, thanks to NGS technologies, and the understanding of related pathophysiological mechanisms, requires a continuous reworking and update of the existing nomenclature. Nowadays, multiple CMT classifications exist, but all of them usually consider the electrophysiological aspects of the disease (like the NCV), and the inheritance pattern (the mode of transmission). In addition, a

subcategorisation, based on the mutated gene responsible of the occurrence of the pathology, is often necessary. All these components allow to establish a more complete and complex organization of all the different CMT forms.

- **Demyelinating forms** are classified in **CMT1**, which present an autosomal dominant mode of inheritance, and **CMT4**, with an autosomal recessive mode of inheritance.
- **Axonal forms** are generally identified as **CMT2**. The typical transmission mode is autosomal dominant (**AD-CMT2**), but autosomal recessive forms are also described (**AR-CMT2**).
- Also the **intermediate forms** can follow an autosomal dominant or recessive mode of inheritance, so they are indicated, respectively, as **DI-CMT** and **RI-CMT**.
- The X-linked CMT (**CMTX**) are often considered a separate group, composed of dominant and recessive forms.

Moreover, basing on the observation of additional clinical features, three other CMT forms could occasionally be reported as **CMT3** (or Dejerine-Sottas disease), **CMT5** and **CMT6.**

In Table 1, a first detailed classification of CMT forms is reported. A letter, from A to Z, was attributed to each CMT form, following the order of discovery of the associated gene (e.g CMT1A for the duplication of *PMP22*) (Tazir et al. 2014).

Table 1 A first classification of Charcot-Marie-Tooth (CMT) diseases [AD = Autosomal Dominant; AR = Autosomal Recessive; XD = X-linked Dominant; XR = X-linked Recessive] [Adapted from: (Feely et al. 2011; Tazir et al. 2014; Wang and Yin 2016) and Online Mendelian Inheritance in Man (OMIM®) database].

Type	Subtype	Associated gene	Mode of inheritance
Demyelinating forms			
CMT1			
	CMT1A	PMP22	AD
	CMT1B	MPZ	AD
	CMT1C	LITAF	AD
	CMT1D	EGR2	AD
	CMT1E	PMP22	AD
	CMT1F	NEFL	AD
	CMT1G	PMP2	AD
CMT4			
	CMT4A	GDAP1	AR
	CMT4B1	MTMR2	AR
	CMT4B2	SBF2	AR
	CMT4B3	SBF1	AR
	CMT4C	SH3TC2	AR
	CMT4D	NDRG1	AR
	CMT4E	EGR2	AR
	CMT4F	PRX	AR
	CMT4G	HK1	AR
	CMT4H	FGD4	AR
	CMT4J	FIG4	AR
	CMT4K	SURF1	AR
Intermediate forms			
DI-CMT			
	DI-CMTA	10q24.1-q25.1	AD
	DI-CMTB	DNM2	AD
	DI-CMTC	YARS1	AD
	DI-CMTD	MPZ	AD
	DI-CMTE	INF2	AD
	DI-CMTF	GNB4	AD
RI-CMT			
	RI-CMTA	GDAP1	AR
	RI-CMTB	KARS1	AR
Additional forms			
CMT3		MPZ EGR2 PMP22 PRX	AD/AR AD/AR AD/AR AD/AR
CMT5		MFN2 (?)	
CMT6		MFN2	AD

Type	Subtype	Associated gene	Mode of inheritance
Axonal forms			
CMT2			
	CMT2A	MFN2	AD
	[CMT2A1	KIF1B]	AD
	CMT2B	RAB7	AD
	CMT2B1	LMNA	AR
	CMT2B2	MED25	AR
	CMT2B5	NEFL	AR
	CMT2C	TRPV4	AD
	CMT2CC	NEFH	AD
	CMT2D	GARS1	AD
	CMT2E	NEFL	AD
	CMT2F	HSPB1	AD
	CMT2G	12q12-q13.3	AD
	CMT2H	GDAP1	AR
	CMT2I	MPZ	AD
	CMT2J	MPZ	AD
	CMT2K	GDAP1	AD
	CMT2L	HSPB8	AD
	CMT2M	DNM2	AD
	CMT2N	AARS1	AD
	CMT2O	DYNC1H1	AD
	CMT2P	LRSAM1	AD/AR
	CMT2Q	DHTKD1	AD
	CMT2R	TRIM2	AR
	CMT2S	IGHMBP2	AR
	CMT2T	DNAJB2 MME	AR AR/AD
	CMT2U	MARS1	AD
	CMT2W	HARS1	AD
	CMT2X	SPG11	AR
	CMT2Z	MORC2	AD
X-linked forms			
CMTX			
	CMTX1	GJB1	XD
	CMTX2	Xp22.2	XR
	CMTX3	Xq26	XR
	CMTX4	AIFM1	XR
	CMTX5	PRPS1	XR
	CMTX6	PDK3	XD

Even if this current classification of CMT diseases is widespread, it could sometimes appear difficult to use. In fact, the same CMT-gene could have multiple modes of inheritance and induce both demyalinating and axonal forms, complicating the direct association of clinics and genetics. Moreover, the letter-based classification may be limited by the discovery of new associated genes, thanks to NGS strategies.

For all these reasons, a simpler and more "informative" classification has been proposed by *Mathis et al.*, in 2015. According to their method, the denomination of each CMT subtype should include the mode of inheritance (AD-, AR-, XL-), the electrophysiological information (de-, ax, in-), and the involved gene (Mathis et al. 2015). It is reported in Table 2.

Table 2 The alternative CMT classification proposed by Mathis et al .[From: (Mathis et al. 2015)].

	Proposed denomination	Gene	Chromosome	MIM	Present denomination
CMTde					
AD-CMTde	AD-CMTde-*PMP22dup*	*PMP22* (duplication)	17p12	118220	CMT1A
	AD-CMTde-*PMP22*	*PMP22*	17p12	118300	CMT1E
	AD-CMTde-*MPZ*	*MPZ/P0*	1q23.3	118200	CMT1B
	AD-CMTde-*LITAF*	*LITAF/SIMPLE*	16p13.13	601098	CMT1C
	AD-CMTde-*EGR2*	*EGR2/KROX20*	10q21.3	607678	CMT1D
	AD-CMTde-*NEFL*	*NEFL*	8p21.2	607734	CMT1F
	AD-CMTde-*FBLN5*	*FBLN5*	14q32.12	–	–
	AD-CMTde-*GJB3*	*GJB3/Connexin 31*	1p34.3	–	–
	AD-CMTde-*ARHGEF10*	*ARHGEF10*	8p23.3	608236	SNCV/CMT1
AR-CMTde	AR-CMTde-*GDAP1*	*GDAP1*	8q21.11	214400	CMT4A
	AR-CMTde-*MTMR2*	*MTMR2*	11q21	601382	CMT4B1
	AR-CMTde-*SBF1*	*SBF1/MTMR5*	22q13.33	615284	CMT4B3
	AR-CMTde-*SBF2*	*SBF2/MTMR13*	11p15.4	604563	CMT4B2
	AR-CMTde-*SH3TC2*	*SH3TC2/KIAA1985*	5q32	601591	CMT4C
	AR-CMTde-*NDRG1*	*NDRG1*	8q24.22	601455	CMT4D
	AR-CMTde-*EGR2*	*EGR2/KROX20*	10q21.3	605253	CMT4E
	AR-CMTde-*PRX*	*PRX*	19q13.2	614895	CMT4F
	AR-CMTde-*HK1*	*HK1*	10q22.1	605285	CMT4G
	AR-CMTde-*FGD4*	*FGD4*	12p11.21	609311	CMT4H
	AR-CMTde-*FIG4*	*FIG4/KIAA0274/SAC3*	6q21	609390	CMT4J
	AR-CMTde-*CTDP1*	*CTDP1*	18q23	604168	CCFDN
	AR-CMTde-*SURF1*	*SURF1*	9q34.2	–	–
CMTax					
AD-CMTax	AD-CMTax-*MFN2*	*MFN2*	1p36.22	609260	CMT2A2
	AD-CMTax-*RAB7*	*RAB7*	3q21.3	605588	CMT2B
	AD-CMTax-*TRPV4*	*TRPV4*	12q24.11	606071	CMT2C
	AD-CMTax-*GARS*	*GARS*	7p14.3	601472	CMT2D
	AD-CMTax-*AARS*	*AARS*	16q22.1	613287	CMT2N
	AD-CMTax-*MARS*	*MARS*	12q13.3	616280	CMT2U
	AD-CMTax-*HARS*	*HARS*	5q31.3	–	–
	AD-CMTax-*NEFL*	*NEFL*	8p21.2	607684	CMT2E
	AD-CMTax-*HSPB1*	*HSPB1/HSP27*	7q11.23	606595	CMT2F
	AD-CMTax-*HSPB8*	*HSPB8/HSP22*	12q24.23	608673	CMT2L
	AD-CMTax-*GDAP1*	*GDAP1*	8q21.11	607831	CMT2K
	AD-CMTax-*MPZ*	*MPZ/P0*	1q23.3	607677/607736	CMT2I/CMT2J
	AD-CMTax-*DNM2*	*DNM2*	19p13.2	606482	CMT2M
	AD-CMTax-*DYNC1H1*	*DYNC1H1*	14q32.31	60012	CMT2O
	AD-CMTax-*LRSAM1*	*LRSAM1*	9q33.3	614436	CMT2P
	AD-CMTax-*DHTKD1*	*DHTKD1*	10p14	615025	CMT2Q
	AD-CMTax-*TRIM2*	*TRIM2*	4q31.3	615490	CMT2R
	AD-CMTax-*VCP*	*VCP*	9p13.3	–	–
	AD-CMTax-*TFG*	*TFG*	3q12.2	604484	HMSNP
	AD-CMTax-*KIF5A*	*KIF5A*	12q13.3	604187	SPG10
	AD-CMTax-*mtATP6*	*mtATP6*	–	–	–
	AD-CMTax-*Unknown*	*Unknown*	12q12q13.2	608591	CMT2G
AR-CMTax	AR-CMTax-*LMNA*	*LMNA*	1q22	605588	CMT2B1
	AR-CMTax-*MED25*	*MED25*	19q13.33	605589	CMT2B2
	AR-CMTax-*GDAP1*	*GDAP1*	8q21.11	607731	CMT2H
	AR-CMTax-*IGHMBP2*	*IGHMBP2*	11q13.3	616155	CMT2S
	AR-CMTax-*C12ORF65*	*C12ORF65*	12q24.31	615035	SPG55
	AR-CMTax-*HSJ1*	*HSJ1*	2q35	604139	CMT2T
CMTin					
AD-CMTin	AD-CMTin-*DNM2*	*DNM2*	19p13.2	606482	CMTDIB
	AD-CMTin-*YARS*	*YARS*	1p35.1	608323	CMTDIC
	AD-CMTin-*MPZ*	*MPZ/P0*	1q23.3	607791	CMTDID
	AD-CMTin-*INF2*	*INF2*	14q32.33	614455	CMTDIE
	AD-CMTin-*GNB4*	*GNB4*	3q26.33	615195	CMTDIF
	AD-CMTin-*NEFL*	*NEFL*	8p21.2	–	–
	AD-CMTin-*Unknown*	*Unknown*	10q24.1–q25.1	606483	CMTDIA
AR-CMTin	AR-CMTin-*GDAP1*	*GDAP1*	8q21.11	608340	CMTRIA
	AR-CMTin-*KARS*	*KARS*	16q23.1	613641	CMTRIB
	AR-CMTin-*PLEKHG5*	*PLEKHG5*	1p36.31	615376	CMTRIC
	AR-CMTin-*COX6A1*	*COX6A1*	12q24	616039	CMTRID
XL-CMT	XL-CMTin-*GJB1*	*GJB1/Connexin 32*	Xq13.1	302800	CMTX1
	XL-CMTde-*GJB1*	*GJB1/Connexin 32*	Xq13.1	302800	CMTX1
	XL-CMTax-*GJB1*	*GJB1/Connexin 32*	Xq13.1	302800	CMTX1
	XL-CMT-*AIFM1*	*AIFM1*	Xq26.1	310490	CMTX4
	XL-CMT-*PRPS1*	*PRPS1*	Xq22.3	311070	CMTX5
	XL-CMT-*PDK3*	*PDK3*	Xp22.1	300905	CMTX6
	XL-CMT-*Unknown*	*Unknown*	Xp22.2	302801	CMTX2

AD, autosomal dominant; AR, autosomal recessive; MPZ, myelin protein zero (or P0); LMNA, lamin A/C; SPG, spastic paraplegia.

II.5. Genetics of CMT

The huge clinical and phenotypic variability of CMT disease reflects the high heterogeneity of its genetic context. In the last 40 years, more than 1,000 mutations in more than 80 genes have been identified to cause CMT disease (Bird 2020), and, probably, the discovery phase is not over yet. This discovery process is also complicated by the fact that the same gene can be involved in different CMT forms, with different modes of transmission, and, at the same time, mutations in different genes can result in the same phenotype. Moreover, we cannot exclude that multiple genomic mutations in different loci may co-occur and collaborate to a common complex clinical manifestation. This phenomenon is rarely investigated during CMT diagnosis ((Posey et al. 2017); Miressi, 2020 – *article in preparation*).

The first CMT locus was detected, in 1982, by Bird and colleagues, located at a distance of 10 cM from Duffy locus, lately identified as *MPZ* gene (Bird, Ott, and Giblett 1982; Hayasaka et al. 1993). On the other hand, *PMP22* was the first gene to be clearly associated with CMT disease. The duplication of 17p locus was linked to CMT1A form in 1989, and the candidate *PMP22* gene was confirmed to be contained in this genomic region in 1992 (Timmerman et al. 1992).

At the onset of the 21st century, these early genetic linkage studies were gradually replaced by the emergence of NGS technologies which have enabled a rapid and low-cost large-scale genomic sequencing, accelerating the discovery of new CMT-associated genes. Gene panels, WES and WGS represent today essential routine tools widely used in clinical and research laboratories.

II.5.1. CMT genes

The more than 80 CMT-genes encode for multiple proteins presenting different roles and different cellular localizations. This means that some proteins are expressed in mitochondria, endoplasmic

reticulum, Golgi apparatus, cytoskeleton, whereas other ones are part of myelin sheath, membrane channels, endosomal and proteaosomal systems.

We report here some of the most common genes associated with CMT disease:

PMP22

PMP22 (peripheral myelin protein 22) gene, located on chromosome 17, position 15,133,095-15,168,643, is the most frequent gene associated with CMT disease. The 1.5 Mb duplication in the genomic region 17p12-p11, containing *PMP22*, is responsible for ~70% of CMT1, and 15% of total CMT. Specifically, *PMP22* complete duplication is responsible for the CMT1A form, also called AD-CMTde-PMP22dup. Anyway, point mutations in *PMP22* have also been described to cause the demyelinating CMT1E (AD-CMTde-PMP22), always presenting an autosomal dominant mode of inheritance.

MPZ

MPZ (Myelin protein zero, or P0) gene is located on chromosome 1, position 161,274,525-161,279,762, in GrCh37 coordinates. It is the second most common gene involved in demyelinating CMT, with a global frequency of 3.1% (Murphy et al. 2012). Mutations in *MPZ* cause the demyelinating autosomal dominant CMT1B disease (AD-CMTde-MPZ), but also Dejerine-Sottas syndrome (CMT3), intermediate DI-CMTD (AD-CMTin-MPZ), and axonal CMT2I and CMT2J (AD-CMTax-MPZ).

MFN2

The CMT2A (AD-CMTax-MFN2), the most common axonal form, is caused by mutation in *MFN2* (Mitofusin 2) gene, located on chromosome 1, position 12,040,238-12,073,571. *MFN2* mutations are

transmitted with an autosomal dominant mode of inheritance, and present an estimated frequency of 2.8% (Murphy et al. 2012).

GDAP1

GDAP1 (ganglioside-induced differentiation-associated protein 1) gene is situated in chromosome 8: 75,233,365-75,401,107 position. Mutations in *GDAP1* are responsible for multiple Charcot-Marie-Tooth disease subtypes: CMT4A (AR-CMTde-GDAP1), the most common autosomal recessive demyelinating form, the axonal CMT2H (AR-CMTax-GDAP1) and CMT2K (AD-CMTax-GDAP1), and the intermediate RI-CMTA (AR-CMTin-GDAP1). *GDAP1* mutations' frequency seems to be approximately 0.5% (Murphy et al. 2012).

More details about *GDAP1* and its protein's functions are reported in Chapters 3 and 4.

CMT genes encode for different proteins, involved in different cellular processes and functions. For instance, many of them take part in myelination process (PMP22, MPZ), cellular transport (GJB1, NEFL), mitochondrial dynamics (MFN2, GDAP1), fundamental cellular events like protein translation (AARS1, GARS1) and signal transduction (SBF1, PRX).

II.6. Impaired mechanisms in CMT

Even if a large amount of genetic causative mutations has been detected for Charcot-Marie-Tooth disease, functional studies seem to show that the altered mechanisms, responsible for this disorder, may be common in different CMT forms. Since several CMT-genes share the same cellular localization and have related functions, the effects of their mutations may converge on the same pathway and lead to a similar impairment in cell viability.

Given their unique role in the body, neural cells are extremely susceptible to alterations of their fundamental functions, like axonal transport or energy requirement. Consequently, all the genomic mutations affecting these pathways, can have an adverse effect on the nerve activity and the proper functioning of peripheral nervous system. Some of pathophysiological mechanisms of peripheral neuropathies are reported in Figure 14. We analyze here the main ones.

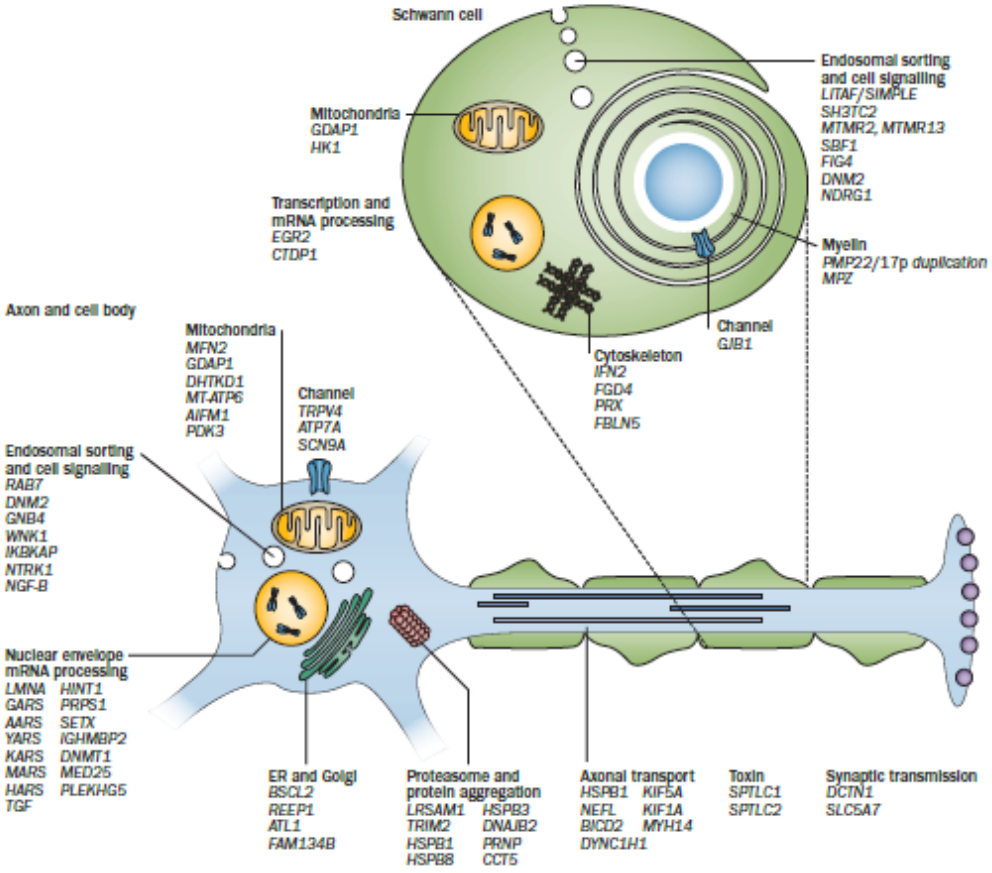

Figure 14 Localization and function of some CMT-associated genes [From: (Rossor et al. 2013)].

II.6.1. Axonal transport

As discussed in Chapter 1, the cytoskeleton in nerve cells is composed by microtubules, microfilaments and neurofilaments. It assures the characteristic structure of neurons, in the soma, the axon, and the dendrites, but it has also an active role in the axonal transport. The axonal transport is necessary to ensure the crosstalk between the cell body and the periphery of the cell, but also to preserve neural homeostasis and neural activities, like axonal outgrowth, cell repair, endocytosis and exocytosis events (Beijer et al. 2019). Multiple proteins participate to this complex organization, and some of them are encoded by genes whose mutations have been associated with CMT disease. Examples of these genes/proteins are: NEFL (neurofilament protein, light polypeptide) and LMNA (LAMIN A/C), which are part of cytoskeleton structure, KIF5A (kinesin family member 5a), involved in the anterograde axonal transport, and DYNC1H1 (dynein, cytoplasmic 1, heavy chain 1), participating in the retrograde axonal transport.

II.6.2. Endosomal trafficking

A portion of intracellular trafficking along microtubules concerns small vesicles, like endosomes and lysosomes, necessary to internalize, transport, and degrade, proteins and other macromolecules in nerve cells. RAB7 (ras-associated protein) and DNM2 (dynamin-2) proteins participate in endosomal trafficking, and they are known to be mutated in some forms of CMT disease.

II.6.3. Mitochondrial function and dynamics

Mitochondrial dysfunction is known to be implicated in multiple neurodegenerative and neuromuscular diseases, like Parkinson's disease and Alzheimer's disease, other than some forms of CMT disease. Peripheral nervous system, just like brain and muscles, is a complex organization with a high-en0ergy requirement: a constant ATP production is needed to assure the transport of organelles

and macromolecules in every cellular compartment, even at long distances. The maintaining of mitochondrial function is, therefore, fundamental for axonal and myelin formation and preservation. Classical mitochondrial mechanisms altered in neurodegenerative diseases concern the electron transport chain (ETC), ATP production, protection from reactive oxidative species (ROS), homeostasis of Ca^{2+}, and mitochondrial dynamics (Palau et al. 2009).

With mitochondrial dynamics we define the whole of mitochondrial fusion and fission processes. These events are necessary to determine mitochondrial shape, size and number, and they are regulated by various proteins, such as MFN1 and MFN2, OPA1, GDAP1, MFF, FIS1 (Pareyson et al. 2015). Here we focus on two of these proteins, whose role will be deepened in Chapter 3.

- Mfn2 protein, is located in the outer mitochondrial membrane (OMM) and, in small amounts, in endoplasmic reticulum (ER). In mitochondria Mfn2 protein plays a key role in fusion of OMM, in oxidative phosphorylation and in gradient coupling, while, in ER it seems to be important in defining ER morphology and mitochondria-ER interaction. It participates also in controlling the release of Ca^{2+} from ER and its uptake in mitochondria (de Brito and Scorrano 2008). In pathological conditions, mutated Mfn2 would impair mitochondrial fusion and mtDNA distribution, inducing the formation of mitochondria lacking electron transport activity (Chen, McCaffery, and Chan 2007). Other models suggest that mitochondrial morphological abnormalities, due to Mfn2 mutations, could alter mitochondria axonal transport. The consequence would be the accumulation of mitochondria in perinuclear area and their lack in distal regions, leading to axonal degeneration (Cartoni and Martinou 2009).
- GDAP1 protein is expressed on the MOM where it participates in mitochondrial fission and fusion events, together with regulation of glutathione metabolism and Ca^{2+} homeostasis (Niemann et al. 2005; Noack et al. 2012; Pla-Martín et al. 2013). Mutated forms of GDAP1 appeared to alter mitochondrial network's morphology and electron transport chain activity

(Complex I), and increase oxidative stress (Niemann et al. 2005; Noack et al. 2012; Cassereau et al. 2020).

II.6.4. Myelination and Schwann cells

Myelin sheath, formed by Schwann cells in peripheral nervous system, is the lipidic membrane that wraps neurons axons. Its presence is fundamental to allow the rapid propagation of electric signals along the axon, in a saltatory way. Demylination and dysmyelination, the loss and the abnormal formation of myelin, respectively, are most often the molecular cause of CMT manifestation. Since first linkage studies, genes coding for myelin proteins were identified to be associated with a large number of disease cases. Myelin dysfunction results in the increase of latencies and reduction of nerve conduction velocities.

- PMP22 protein is a component of myelin sheath, mainly expressed in PNS. Although its function is not completely understood, several studies suggest that, when wild-type *PMP22* is duplicated, PMP22 protein, overexpressed, accumulates in cytoplasmic aggresomes, perturbing the normal function of SC and leading them to apoptosis (Erdem, Mendell, and Sahenk 1998; Notterpek et al. 1999; Sancho, Young, and Suter 2001).
- MPZ (MYP0 or P0) protein is the major structural component of myelin, expressed only in the PNS. It is essential for myelination and compaction processes. The main effect of its mutation appears to be the accumulation of MPZ unfolded proteins in ER, that activates the unfolded protein response (UPR) and induces ER stress. These events may, therefore, result in Schwann cells death (Chang et al. 2019).

II.6.5. RNA Processing

Aminoacyl-tRNA-synthetases (ARS) are a class of enzymes necessary to catalyze the reaction between an amino acid and its tRNA. To date, six genes encoding ARS enzymes have been identified as CMT-causing genes: *GARS1* (glycyl-tRNA synthetase), *HARS1* (histidyl-tRNA synthetase), *AARS1* (alanine-tRNA synthetase), *YARS1* (tyrosyl-tRNA synthetase), *KARS1* (lysine-tRNA synthetase) and *MARS1* (methionyl-tRNA synthetase). ARS are ubiquitously expressed in human cells, so it is difficult to explain why the effect of their mutations can be observed only in PNS. There is the evidence of catalytic function impairment in CMT-ARS variants, which suggests a possible alteration of normal protein synthesis. Modification in dimerisation and cellular localization of these enzyme have been also evaluated as possible altered mechanisms (Boczonadi, Jennings, and Horvath 2018).

- GARS1 protein was the first ARS to be associated with axonal forms of CMT. *In vitro* and *in vivo* functional studies have highlighted multiple potential mechanisms linked to *GARS* mutations. Main hypotheses concern the alteration of dimer interactions and GARS conformation, but also the modification of enzyme ability to link glycine to its tRNA. Furthermore, Drosophila studies reveled a possible GARS role in neurite growth and arborization, even if supplementary analyses will be required (Motley, Talbot, and Fischbeck 2010).
- Multiple point mutations have been also described in *AARS1* gene (Latour et al. 2010; Bansagi et al. 2015). Even if the dimerization defect was excluded for mutated AARS1, the pathological mechanisms still rest unclear (Boczonadi, Jennings, and Horvath 2018).

The pathological mechanisms examined here describe only partially the complexity of CMT disorder. It is now clear that the different pathways are part of a unique intracellular organization and they are consequently correlated, even if resulting effects vary from mutations to mutations. The identification of new disease-causing genes and additional *in vivo* and *in vitro* analyses will help the understanding of unknown mechanisms, necessary to propose and develop new targeted therapies for demyalintaing and axonal Charcot-Marie-Tooth diseases.

Chapter III. Mitochondria

III.1. Overview

Identified for the first time during the 19th century, mitochondria are membranous cellular organelles located in the cytoplasm of most of eukaryotic organisms. Their origin has been studied for long time. According to the most corroborated hypothesis, mitochondria derive from the integration of an endosymbiotic α-proteobacterium into a precursor of the modern eukaryotic cell, around two billion years ago. These new organelles underwent a gradual evolution, modifying their genome and adapting their life cycle to that of the host cell (Roger, Muñoz-Gómez, and Kamikawa 2017).

Mitochondria have a really plastic structure and change constantly their shape, which varies from round to oval, while the diameter size ranges from 0.5 to 1 µm (Trushina 2016). The number of mitochondria in a cell depends on the organism and the tissue, in accordance with its energy requirement. In human body, for example, mitochondria are absent in red blood cells, but they could be hundreds or thousands in liver cells (Degli Esposti et al. 2012).

Within the cell, mitochondria are connected and form a complex dynamic network, which changes continuously its organization, thanks to mitochondrial fusion and fission events (Su et al. 2010). Moreover, they are strongly associated with cytoskeleton microtubules, that control their orientation and distribution, as well as their movement in the cell (Ishihara 2004).

The mitochondrion is traditionally considered the powerhouse of the cell, since it constitutes the site of oxidative phosphorylation and production of energy units, the ATP molecules. It is also involved in the control of oxidative stress, the production of precursors of macromolecules like lipids and proteins, the maintenance of ions homeostasis and Ca^{2+} storage, the control of cell cycle and apoptosis.

III.2. Mitochondrial structure

Each mitochondrion presents two lipid membranes, highly specific and different in their composition, which define two internal compartments in the organelle: an intermembrane space, between them, and an internal mitochondrial matrix. The internal mitochondrial organization is summarized in Figure 15.

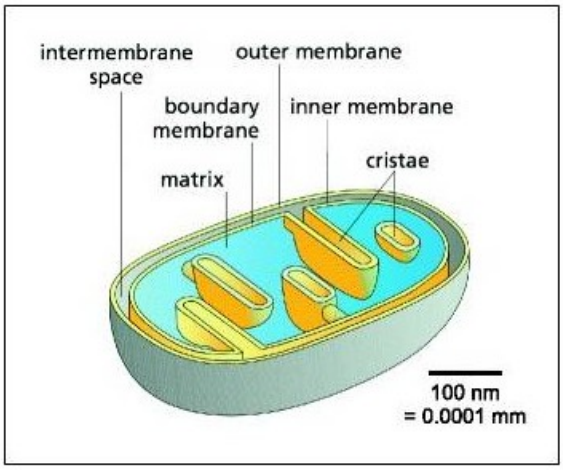

Figure 15 Mitochondrial membranes and compartments [From: (Kühlbrandt 2015)]

- **Outer membrane**

The outer mitochondrial membrane (OMM) separates the mitochondrion from the cellular cytoplasm and its composition is similar to the plasma membrane, in proportion of lipids and proteins. It is fairly porous and permeable to molecules up to 5,000 Da (Alberts 2002). Multiple transport proteins, called *porins*, are stuck in the OMM. Among the porins, the voltage-dependent anion channels (VDAC) are highly conserved channels, regulated by electrical potential, necessary to mediate the flow of metabolisms between the cytoplasm and the intermembrane space (Colombini 2012). The transport of larger molecules is assured by translocases (tranlocases of the outer membrane or TOM).

- **Intermembrane space**

The intermembrane space is a 20 nm gap between the outer and the inner mitochondrial membranes, corresponding to the *periplasm* of the ancestor bacteria. Given the high permeability of the OMM, the intermembrane space presents almost the same small molecules, like sugars, of the cytosol, while its protein composition differs because of the selective transport provided by porins. Although H^+ ions are pumped from the matrix to the intermembrane space, its pH is close to 7, as well as in the cytosol (Alberts 2002).

- **Inner membrane**

The inner mitochondrial membrane (IMM) is more selective than the OMM. It contains approximately 15%-20% of cardiolipin (CL), a phospholipid with four acyl chains, exclusively included in the IMM. Cardiolipin seems to reduce the membrane permeability to ions, but it has also an active role in mitochondrial functions, through its interaction with mitochondrial carriers and respiratory complexes (Paradies et al. 2019). The transport process across the IMM is regulated only by specific transport proteins and translocases of the inner membrane (TIM) (Kühlbrandt 2015).

The IMM is further subdivided in two structures: the inner boundary membrane and the cristae membrane. The boundary membrane is smooth and closer to the OMM. A large amount of carrier proteins is included in the inner boundary membrane. The cristae are invaginations of the IMM where almost all the complexes of the electron transport chain are located. They are therefore considered the site of oxidative phosphorylation (Colina-Tenorio et al. 2020). Cristae shape is quite variable, as well as their organization in accordance to the tissue. This means that cristae are closely stacked in high-energy required tissues, while they appear more spaced in low-energy demanding tissues (Kühlbrandt 2015). Crista junctions are membrane structures important to connect cristae with the inner boundary membrane.

- **Matrix**

The matrix, the aqueous compartment of mitochondria surrounded by the IMM, is the equivalent of cytoplasm in the ancestor bacteria. It contains ribosomes, selected ions, small molecules, and, above all, enzymes and cofactors involved in oxidative phosphorylation, citric acid cycle, oxidation of pyruvate and fatty acids. Furthermore, the matrix is the site where mitochondrial DNA (mtDNA) is located. As well as the nuclear DNA (nDNA), mtDNA is associated with proteins and organized in nucleoids (Mazunin et al. 2015). It is a circular double-stranded molecule, containing 37 genes, most of them coding for tRNA (transfer RNA), rRNA (ribosomal RNA), proteins of the electron transport chain (Chinnery and Hudson 2013). mtDNA is maternally inherited and its mutations may induce metabolism disorders, neurodegenerative diseases, or cancer (Schon, DiMauro, and Hirano 2012).

III.3. Mitochondrial functions

The main function of a mitochondrion is to be the cellular site of energy production. In a mitochondrion, sugars, fats and proteins are used as raw material to obtain usable energy in form of ATP molecules. Energy production is ensured especially through three processes: the Krebs cycle, the β-oxidation of fats, and the oxidative phosphorilation. On average, a cell of the body uses 10 billion ATP per day, this means that every adenosine diphosphate (ADP) molecule has to be transformed in an ATP molecule approximately 1,000 times in a day (Pizzorno 2014). This huge energy demand explains why mitochondrial machinery needs to work continuously and intensively in the cell, and why mitochondrial dysfunction often results in metabolic and degenerative diseases.

Aside the bionenergetic supply, four other relevant functions are associated with mitochondria: generation of reactive oxygen species (ROS), production of metabolic precursors for macromolecules, regulation of Ca^{2+} homeostasis and signaling, and control of cell cycle and cell apoptosis.

Here, we look in detail the energy production and the mitochondria role in oxidative stress.

III.3.1. Energy production

Glycolysis, β-oxidation and Krebs cycle

Glycolysis, the first step in degradation of glucose, and β-oxidation, the catabolic process of fatty acids, are two metabolic pathways converging on the production of acetyl-CoA, the "feeding molecule" of the Krebs cycle.

In glycolysis, which takes place in the cytoplasm, one molecule of glucose is converted in two molecules of pyruvate, with production of two molecules of ATP and two molecules of NADH (nicotinamide adenine dinucleotide).

$$Glucose + 2\ NAD^+ + 2\ ADP + 2Pi \rightarrow\ 2\ pyruvate + 2\ NADH + 2\ ATP + 2\ H_2O + 2\ H^+$$

Once pyruvate has been formed in cytosol, it needs to be transported in the mitochondrial matrix. Pyruvate transport across the OMM seems to involve VDAC or porins (McCommis and Finck 2015), while the pyruvate translocase mediates the pyruvate transport from the intermembrane space to the mitochondrial matrix. Here, the pyruvate is converted into acetyl-CoA, in an oxidative decarboxylation reaction catalyzed by pyruvate dehydrogenase (PDH).

$$pyruvate + NAD^+ + CoA - SH \rightarrow\ acetyl - CoA + CO_2 + NADH, H^+$$

At the same time, in the cell, fatty acids need to be activated to be degraded, through a two-step process promoted by the enzyme acyl-CoA synthetase. This reaction occurs in the cytoplasm and produces acyl-CoA.

$$fatty\ acid + ATP + CoA - SH \rightarrow acylCoA + AMP + 2Pi$$

Since the β-oxidation of fatty acids is carried out in the mitochondrial matrix, and given the impermeability of IMM, acyl-CoA exploits the specialized carnitine carrier system to be transported. The carnitine acyltransferase I (or carnitine palmitoyltransferase I, or CPT1), located on the OMM, transfers the acyl group of coenzyme A to carnitine to form acylcarnitine (or palmitoylcarnitine), which is passively transported in the intermembrane space, then shuttled across the IMM, by the carnitine acylcarnitine translocase (CACT). Once in mitochondrial matrix, the carnitine acyltransferase II (or carnitine palmitoyltransferase II, or CPT2), located on the IMM, dissociates the acylcarnitine in acyl-CoA and free carnitine, which passively returns to the cytoplasm to be reused (Longo, Frigeni, and Pasquali 2016)(Figure 16).

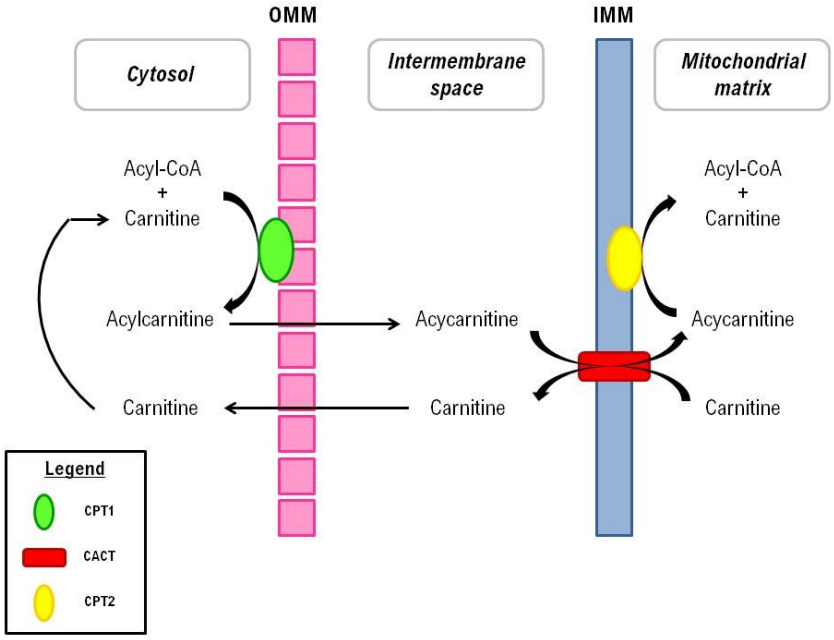

Figure 16 Transport of acyl-CoA into the mitochondrion through the carnitine carrier system.

In mitochondrial matrix, acyl-CoA molecules undergo the **β-oxidation**, a multistep-process, that sequentially removes two-carbons units at the C-terminal of the acyl-CoA, producing a molecule of acetyl-CoA, and reduced cofactors. This cycle is repeated until all the carbons are converted into acetyl-CoA (Figure 17).

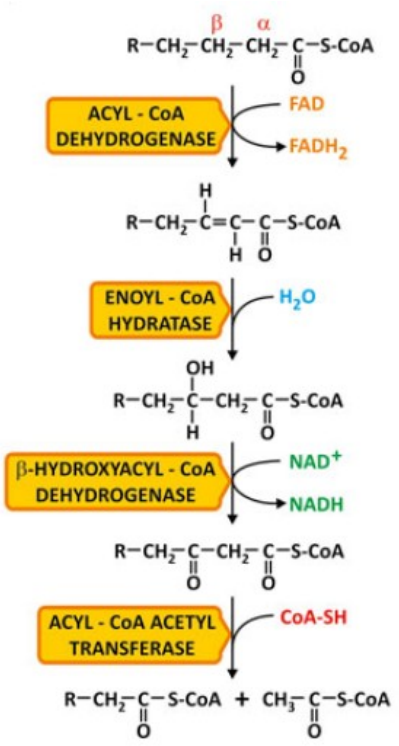

Figure 17 Reactions of β-oxidation [From: (Poian and Castanho 2015)].

Acetyl-CoA can derive, therefore, either from glycolysis and fatty acids β-oxidation, but also from amino acids produced by protein catabolism (not detailed). Figure 18 summarizes how carbohydrates', lipids', and proteins' catabolic pathways converge on acetyl-CoA.

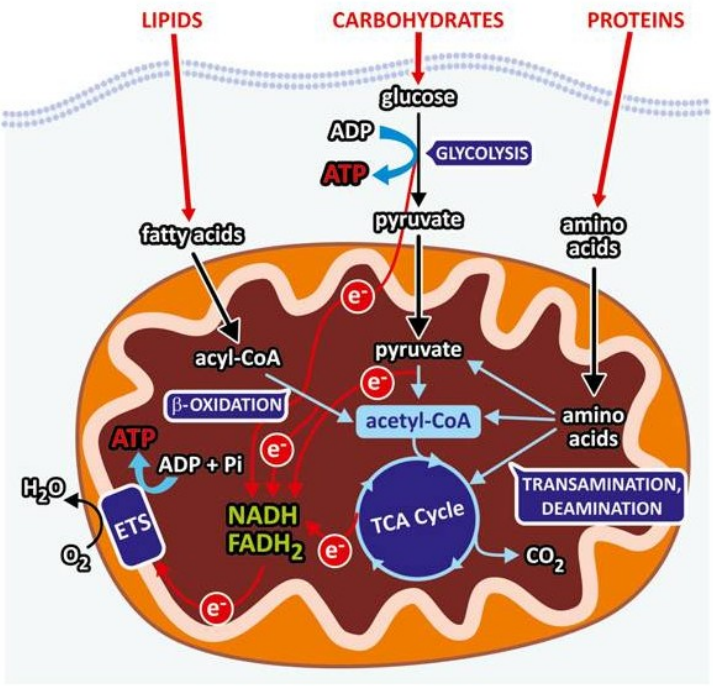

<u>Figure 18</u> Main pathways involved in energy production. Catabolism of carbohydrates, lipids, and proteins, produce acetyl-CoA which enters in the Krebs cycle (TCA Cyle). Krebs cycle allows the reduction of FAD and NAD^+ to $FADH_2$ and NADH, important to release electrons to the electron transport system (ETS). ETS is responsible for ATP synthesis [From: (Poian and Castanho 2015)].

In mitochondria matrix, acetyl-CoA enters in the Krebs cycle (or citric acid cycle, or tricarboxylic acid (TCA) cycle), where it first reacts with oxaloacetate, to form citrate. This reaction is followed by eight other reactions, which regenerate, at the end, a new molecule of oxaloacetate which can restart a new cycle. Moreover, every cycle originates two molecules of CO_2, one molecule of guanosine triphosphate (GTP, rapidly converted in ATP), three molecules of NADH, and one molecule of $FADH_2$ (flavin adenine dinucleotide).

$$acetyl - CoA + 3\,NAD^+ + \ FAD + GDP + Pi + 2\,H_2O \rightarrow$$
$$\rightarrow \ 2\,CO_2 + \ 3\,NADH, H^+ + FADH_2 \ + \ GTP + CoA - SH$$

NADH and $FADH_2$ are reduced cofactors that transfer high-energy electrons from a molecule to another. Once they are formed, in glycolysis or Krebs cycle for example, they reach the electron transport chain (ETC), where they are oxidized to provide electrons to chain complexes.

Oxidative phosphorylation

The oxidative phosphorylation (OXPHOS) is the final step of the cellular respiration process. It is a complex pathway that, in higher plants and animals, supplies most of the ATP required to maintain all cellular functions and metabolisms. Oxidative phosphorylation consists in two coupled events: the transfer of electrons in the ETC, driven by substrates oxidation, and the synthesis of ATP, by the ATP synthase. The electron transport chain is located on mitochondrial cristae, and it made up of four complexes, embedded in the IMM:

- Complex I or NADH-coenzyme Q oxidoreductase
- Complex II or Succinate-Q oxidoreductase or Succinate dehydrogenase
- Complex III or Q-cytochrome c oxidoreductase
- Complex IV or Cytochrome c oxidase

In addition to the four complexes, two mobile electron carriers are involved: the Coenzyme Q (CoQ) and the cytochrome C. Multiple ETC lie on the IMM of the same mitochondrion.

The electron transport is a series of redox reactions, in which electrons are transferred from an electron donor to an electron acceptor, more electronegative. These transfers are mediated by reducing equivalents NADH and $FADH_2$, generated by the Krebs cycle, β-oxidation, and other cellular processes. Specifically, electrons are transferred from NADH to Complex I, then to CoQ, while Complex II receives electrons from succinate and passes them to CoQ. From CoQ electrons are transferred to Complex III, so to Cytochrome C and, at the end, to Complex IV, where they are used to reduce oxygen to water (Figure 19). The energy liberated by the electron flow through the complexes of the ETC, promotes the transport of protons (H^+) across the IMM, from the matrix to the

intermembrane space. This proton movement, carried out by the proton pumps of Complex I, III and IV, creates an electrochemical gradient (or proton-motive force) across the membrane, constituted by two components: a H^+ ion concentration gradient (ΔpH), and an electrical potential, which constitutes the mitochondrial membrane potential (ΔΨm) and is due to the separation of charges across the membrane. The electrochemical proton gradient is the driving force of ATP synthesis by ATP synthase. The ATP synthase, or Complex V, presents two functional domains, F_0 (in IMM) and F_1 (in matrix). When protons, pumped across the IMM, need to come back to the matrix, they pass the F_0 subunit of ATP synthase, inducing the rotation of the central axle. This leads to a conformational change in the catalytic subunit of F_1 which favors the synthesis of ATP from ADP and Pi (Jonckheere, Smeitink, and Rodenburg 2012). It has been estimated that, from a molecule of glucose, about 30 molecules of ATP can be obtained, 26 of them from oxidative phosphorylation.

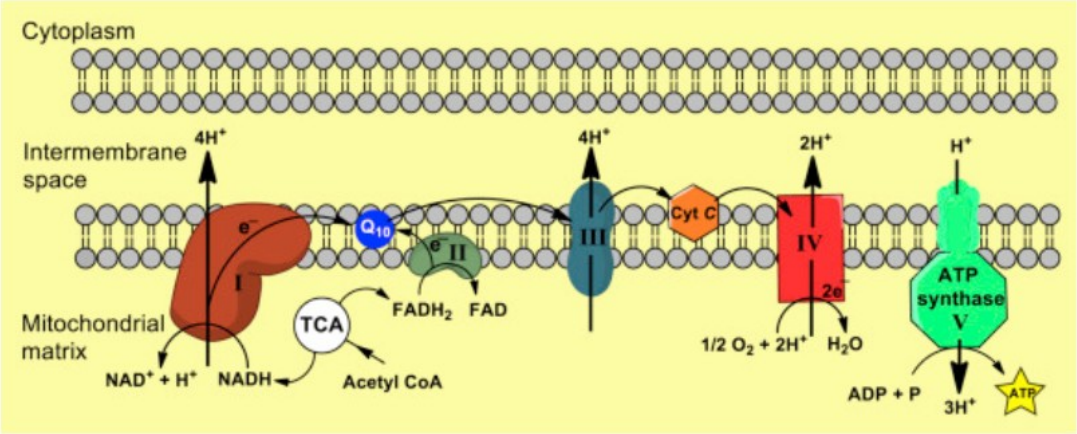

Figure 19 Representation of oxidative phosphorylation complexes and mechanism [From: (Mastroeni et al. 2017)]

III.3.1.1. Mitochondrial membrane potential (ΔΨm)

The mitochondrial membrane potential, indicated as ΔΨm, is a difference in electrical potential across the inner mitochondrial membrane. The result is a negatively charged inner side and a positively charged outer side of the IMM. The ΔΨm is generated by the activity of the electron transport chain, and it participates, together with the proton gradient (ΔpH), to define the *transmembrane potential of hydrogen ions* ($\Delta\mu H^+$). In particular, these two components, are linked by the relation:

$$\Delta\mu H+ = F\Delta\Psi m + 2.3RT\Delta pH$$

where F is the Faraday number, R is the gas constant, T is the absolute temperature (Zorova et al. 2018A)

It is difficult to establish a normal value of ΔΨm. We know that it is not always stable and short depolarization events can occur, induced by oscillations of the mitochondrial permeability transition (MPT). However, these brief episodes are not necessarily damaging for mitochondrial functions and, only when they last in time, they can lead to mitochondrion death.

The ΔΨm is strictly connected to ATP generation. It can be regarded as the energy storage which allows ATP synthase to form ATP molecules. Consequently, we can consider that ATP synthesis requires expense of ΔΨm, while ATP hydrolysis leads to generation of ΔΨm (Zorova et al. 2018B). Many other mitochondrial proteins participate in formation and maintaining of mitochondrial membrane potential, as for instance, the adenine nucleotide transporter (ANT).

In the mitochondrion, the ΔΨm plays a key role in several processes, necessary to conserve mitochondrial homeostasis. It is the driving force which guides the transport of cations and anions, but it seems also to be required for TIM-mediated protein transport across the IMM (Kulawiak et al. 2013). Moreover, it has been shown that a correlation exists between ΔΨm and the mitochondrial production of reactive oxygen species (ROS): at high values of ΔΨm, ROS production by ETC Complex I increases, while it is reduced when ΔΨm decreases (Suski et al. 2012). However, it is not clear if ΔΨm directly regulates ROS generation. It has been suggested that ΔΨm could be related to NADH redox state, which has itself a role in controlling ROS-producing site of Complex I (Starkov and Fiskum

2003). A chronic augmentation of ROS level (oxidative stress) may cause prolonged damaging effects on ROS targets and induce cell apoptosis. On the other side, a chronic reduction of ΔΨm and ROS, results in reductive stress, carrying, in the same way, to other deleterious consequences and cell death (Zorov, Juhaszova, and Sollott 2014).

III.3.2. Production of ROS and oxidative stress

III.3.2.1. ROS overview

ROS (Reactive Oxygen Species) are radical and non-radical species containing oxygen. Atomical oxygen has two unpaired electrons in separate orbitals in its outer shell, that's why it is more susceptible to radical formation. Reduction of oxygen leads to production of four main types of ROS:

- Superoxide or superoxide anion ($O_2^{\bullet-}$)
- Peroxide (O_2^{2-}) and hydrogen peroxide (H_2O_2)
- Hydroxyl radical (OH•)
- Singlet oxygen ($^1O_2$)

Superoxide derives from one-electron reduction of oxygen. Its dismutation, by superoxide dismutase enzymes, originates the hydrogen peroxide, a molecular specie less reactive than free radicals. Anyway, in presence of Fe^{2+} and Cu^+, H_2O_2 can be partially reduced to hydroxyl radical, via the Fenton reaction, or it can be fully reduced to water, by catalase (Turrens 2003). Hydroxyl radical is considered as the most reactive species of oxygen, since it can attack multiple organic molecules. Singlet oxygen, also high reactive, is produced, for example, during photosynthesis process in plants.
In addition to these ROS types, other reactive species have been identifies as Reactive Nitrogen Species or RNS, bearing both oxygen and nitrogen atoms. They include nitric oxide radical (NO or

NO•), nitrogen dioxide radical ($NO^{\bullet}_2$), nitrite (NO_2^-), and peroxynitrite ($ONOO^-$) (Krumova and Cosa 2016).

III.3.2.2. Sources of ROS

ROS are generated by internal cell processes and organelles, but they can be also the consequence of exogenous events.

Mitochondria are the main cellular producers of ROS. Specifically, seven separate sites have been identified in mitochondria to produce ROS, the most important of them are the complex I and complex III of the ETC. It has been observed that a leakage of electrons exists at these levels of the ETC and it induces the partial reduction of O_2 to $O_2^{\bullet-}$. Approximately 0.2% - 2.0% of O_2 used in the ETC is converted in superoxide, in physiological conditions. Once formed, $O_2^{\bullet-}$ is released by complex I in mitochondrial matrix, while complex III releases it in both mitochondrial matrix and mitochondrial intermembrane space (Li et al. 2013). The higher levels of superoxide are generated in sites IF (flavin mononucleotide (FMN)) and IQ of complex I, and the centre IIIQo of complex III (Brand 2010). Superoxide is rapidly converted in H_2O_2 by superoxide dismutases 1 and 2 (SOD1 and SOD2), respectively located in intermembrane space and mitochondrial matrix.

Other endogenous sources of ROS are the peroxisomes, the cytochrome P450, the transmembrane enzymes of NADPH oxidases (NOX) superfamily, the flavoenzyme ERO1 in the ER, the cyclo-oxygenase, the xanthine oxidase, the lipooxigenases (Krumova and Cosa 2016).

Multiple **exogenous**, or environmental, factors have been shown to have an effect on ROS production. Among them, it is important to mention ionizing and nonionizing radiations, heavy metals, pollution, but also cigarettes smoke, food, and some drugs (Bhattacharyya et al. 2014).

III.3.2.3. Role of ROS

Although reactive oxygen species are often associated with oxidative stress, biomolecules damage and occurrence of pathological conditions, it is now clear that their presence and activity are fundamental to preserve cellular homeostasis. In living organisms ROS have, therefore, a physiological role, so a positive involvement in cellular processes, which is counterbalanced by a negative effect, in case of ROS deregulation and accumulation (Figure 20).

Physiologically, several cellular mechanisms are regulated by ROS. In the immune system, for example, ROS would be implicated in both innate and acquired responses, since they favor and participate to the activation of phagocytes and T-lymphocytes, to combat the pathogen (Belikov, Schraven, and Simeoni 2015). Furthermore, ROS are involved in normal regulation of vessels diameter, but also in skeletal muscle contraction (Alfadda and Sallam 2012). Other positive ROS functions are linked to oxygen homeostasis, cell adhesion and migration, and response to stressors (Hurd, DeGennaro, and Lehmann 2012; You and Chan 2015).

On the other hand, ROS production can result in a harmful condition for the cell, called oxidative stress. **Oxidative stress** is defined as the imbalance between the reactive oxygen species and the antioxidant defenses, with consequent ROS excess, and alteration of redox state. First effects of oxidative stress can be seen on macromolecules and biological components. Proteins and lipids are considered the most concerned targets. They are often the substrate of oxidation and peroxidation reactions by ROS, especially on side-chain and backbone sites, for protein, and on polyunsaturated fatty acids (PUFA), for lipids (Su et al. 2019). In fact, oxidation of proteins can alter their chemical properties, their conformation and folding, as well as their interactions. Protein peroxides can, themselves, damage other targets. Also free amino acids can be attacked by free radicals (Davies 2016). Peroxidation of lipids can be deleterious for the integrity of membranes and the function of receptors and enzymes interacting with them. The third class of macromolecules mostly affected by oxidative stress are nucleic acids, in particular the DNA. Oxidation-caused lesions occur both in DNA sugars and bases, leading to strand breakage and genomic mutations. More than 100 types of DNA lesions, induced by ROS, have been identified (Cadet and Wagner 2013).

The increase of ROS levels in the cell may represent a starting signal to activate cell death pathways. It has been demonstrated that oxidative stress induces cell apoptosis, via the Fas activation pathway and the caspase cascade, but also necrosis, the uncontrolled cell death, and autophagy, the cellular self-degradation process (Ghosh et al. 2018). Consequentially, ROS have been shown to be implicated in the development of multiple pathological conditions, such as several types of cancer, neurological disorders (Alzheimer, Parkinson, Amyotrophic lateral sclerosis), cardiovascular diseases, chronic inflammation and autoimmune diseases (Brieger et al. 2012).

III.3.2.4. Antioxidant defenses

Within the cell, ROS level and activity are finely regulated by antioxidant (AO) systems, which control and reduce their potential damaging effect on macromolecules. These endogenous defenses have been classified in enzymatic and nonenzymatic systems.

Enzymatic antioxidants are capable to convert oxidative molecules and oxidized products into non-toxic substances, like water. Examples of these enzymes are the superoxide dismutases (SOD), the Catalase (CAT), and the glutathione peroxidase (GPx). SODs catalyze the dismutation reaction of superoxide radicals into hydrogen peroxide and molecular oxygen. In humans, three forms of SODs have been identified: SOD1, in cytosol and in mitochondrial intermembrane space, SOD2, in mitochondria, and SOD3, in the extracellular space. The CAT, mostly located in peroxisomes, but also in mitochondria and cytosol, converts H_2O_2 in water and molecular oxygen (Aguilar, Navarro, and Pérez 2016). The GPx, needed to reduce hydrogen and organic peroxides into water or alcohol, presents eight human isoforms, with different intracellular and extracellular localizations (Mbemba Fundu et al. 2020).

The most important **nonenzymatic** antioxidants are glutathione (GSH), Coenzyme Q (CoQ), and multiple metal-binding proteins (MBP), like Albumin, Transferrin, Ferritin (Mirończuk-Chodakowska, Witkowska, and Zujko 2018). CoQ, localized in the ETC and other internal membranes,

is important in preventing free radicals' damage on lipids, as well as on proteins and DNA (Saini 2011). MBPs, as Albumin, are considered to be the major antioxidants systems in plasma (Aguilar, Navarro, and Pérez 2016).

Glutathione is considered, together with enzymatic systems, the main antioxidant defense. Glutathione is a tripeptide, also called γ-l-glutamyl-l-cysteinyl-glycine, on the basis of its components. It is exclusively synthesized in cytosol, to be then distributed in other cellular organelles, like mitochondria and ER (Marí et al. 2009). Glutathione exists in two different forms: the reduced state (GSH) and the oxidized state (GSSG). In physiological conditions, the reduced state is more abundant than the oxidized one, with a ratio of 100:1 (Mirończuk-Chodakowska, Witkowska, and Zujko 2018). Glutathione molecules scavenge ROS through the oxidation of GSH into GSSG, in a reaction catalyzed by Gpx enzyme, in different subcellular organelles. Here, for example, we report the reduction reactions of H_2O_2 and peroxides, mediated by GSH:

$$HOOH + 2GSH \rightarrow 2H_2O + GSSG$$

$$ROOH + 2GSH \rightarrow ROH + H_2O + GSSG$$

Once formed, GSSG is then reduced back to GSH by glutathione reductase (GSR), in presence of NADPH:

$$GSSG + NADPH + H^+ \rightarrow 2GSH + NADP^+$$

GSR is present in both cytosol and mitochondria (Kelner and Montoya 2000).

Moreover, glutathione protects proteins against oxidative stress in a reversible or irreversible reaction, defined protein glutathionylation, with specific protein residues (Cooper, Pinto, and Callery 2011).

Since GSSG amount increases, and GHS decreases, in case of oxidative stress, it is clear that the GHS/GSSG ratio is an indicator of cellular health, and it can be measured to estimate oxidative stress severity in the cell. For example, it has been demonstrated that this ratio is significantly reduced during aging and in pathological conditions like neurodegenerative diseases (Parkinson's disease and

Alzheimer's disease), well known to be associate with an pro oxidant state (Owen and Butterfield 2010; Liu et al. 2017; Wojsiat et al. 2018).

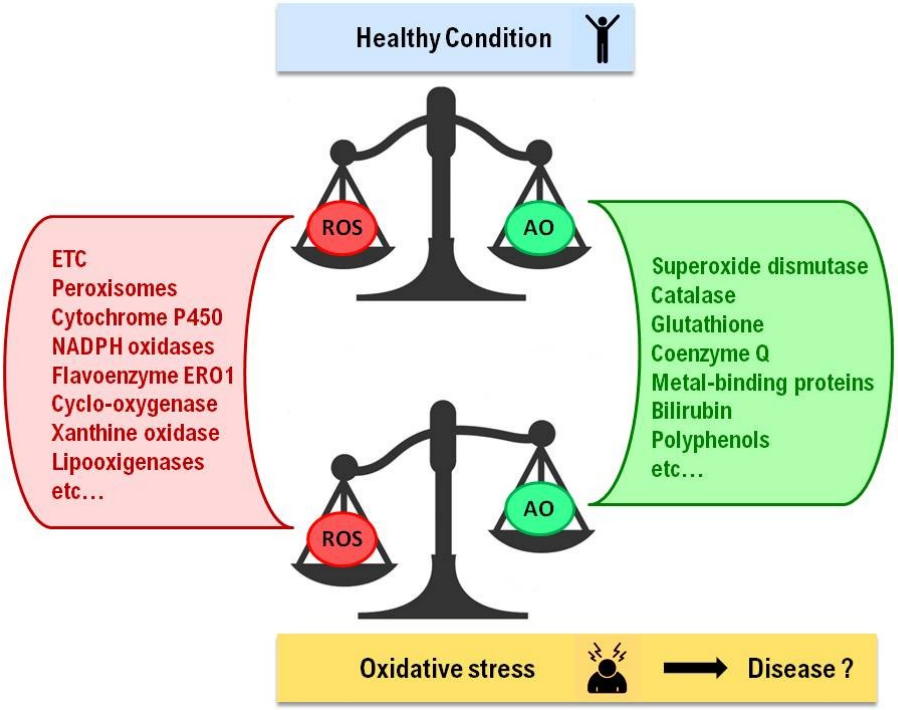

Figure 20 Redox balance and imbalance in physiological and pathological conditions.

III.4. Mitochondrial dynamics

Mitochondria are highly dynamic organelles that continuously change their organization and interactions, modifying their number, shape and localization in the cell. All these aspects are strictly connected to mitochondrial functions, like metabolism, signaling pathways, or ATP production. For example, the deregulation of mitochondrial morphology may alter mitochondria movement and distribution, impacting their physiological roles in the cell (Campello and Scorrano 2010). Impaired mechanisms of mitochondrial dynamics have emerged in pathological conditions, often neurodegenerative diseases, like the Alzheimer's disease, Parkinson's disease, Amyotrophic lateral sclerosis, Huntington's disease (Su et al. 2010).

We analyze here the main processes and protein actors of mitochondrial dynamics.

III.4.1. Mitochondria-Cytoskeleton interaction

Inside the cell, mitochondria are rarely organized as isolated discrete organelles, but they always interact to form a dynamic and ever changing network. Clusters of mitochondria move, change, divide, thanks to their interaction with the cytoskeleton, the supporting structure of the cell. All the cytoskeleton components seem to participate to mitochondrial dynamics and transport.

Microtubules (MT), made up of tubulin heterodimers, have been demonstrated to interact with mitochondria in many cell types (like fibroblasts, kidney cells, muscle cells, macrophages) (Heggeness, Simon, and Singer 1978). MT are necessary to transport mitochondria and distribute them where a high amount of energy is required (Puurand et al. 2019). Moreover, recent studies have focused on the role of unpolymerized tubulins and MT-associate tubulins. Unpolymerized tubulins, as βII- and βIII-tubulins, have been shown to regulate the VDAC permeability on the OMM (Puurand et al. 2019). γ-tubulin, which is involved in MTs polymerization, forms in the cell a complex structure called *γ-string meshwork*. It has been observed that this γ-string meshwork interacts with IMM and mtDNA, and it provides a fundamental structure element to organize and maintain mitochondrial network (Lindström et al. 2018).

In neurons, the proper distribution of mitochondria is extremely important, since the soma, and, above all, neurites and synapses, demand a continuous ATP supply. We know that the anterograde transport of mitochondria on MT tracks is mediated by kynesin proteins. The attachment of kynesin to mitochondria is made by the anchor proteins RhoT, a Mitochondrial Rho GTPase or Miro, and the motor adaptor TRAK/Milton (van Spronsen et al. 2013). The anchor proteins for dyneins in retrograde axonal transport are still unknown, but the involvement of Trak2 protein has been suggested (Mandal and Drerup 2019) (Figure 21).

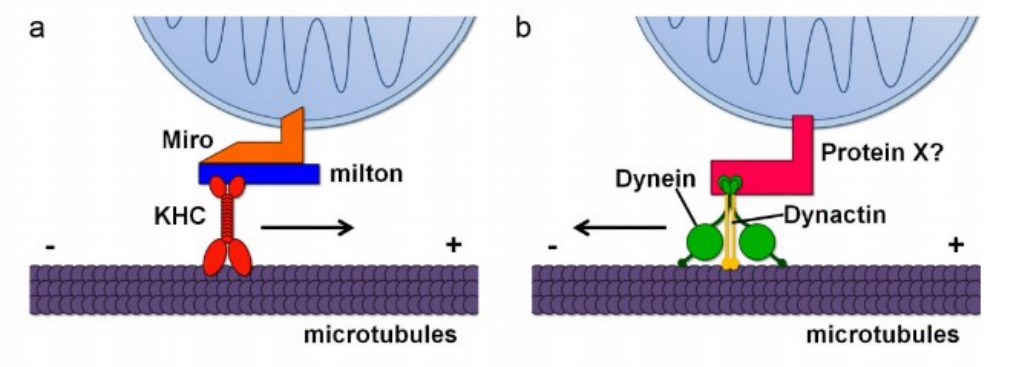

Figure 21 Schematic representation of mitochondria-microtubules interactions in anterograde (a) and retrograde (b) mitochondria transport [Adapted from: (Course and Wang 2016)].

Furthermore, it is important to underline that neural MT are not only responsible for mitochondrial movement, but they also control the stationary pool of mitochondria. In this stop function, MTs directly interact with the neuron-specific Syntaphilin (Snph), an anchor protein located on the OMM (Kang et al. 2008).

Actin microfilaments' (MF) role in mitochondrial dynamics has been less investigated over time. Most studies, conducted on simpler organisms like yeast, fungi and plants, confirmed the direct interaction of mitochondria with actin cytoskeleton and its involvement in mitochondrial transport, as for instance, during cell division (Fehrenbacher et al. 2004). In nerve cells, MF, organized in a meshwork structure, collaborate with MTs for mitochondrial movement along the axon. Several members of myosins family, like Myo19, work like motor proteins that bind mitochondria and guide them along actin tracks (Quintero et al. 2009). Furthermore, actin cytoskeleton appears involved in controlling the stationary state of mitochondria in the Nerve Growth Factor (NGF) signaling. This causes the immobilization and accumulation of the organelles in specific NGF stimulation regions of the neuron (Chada and Hollenbeck 2004).

Also **Intermediate filaments** (IF) have been shown to bind mitochondria, anchoring them to cytoskeleton, and regulate their general distribution in the cell. IF can influence not only mitochondrial motility, but also their morphology and function, revealing a strong connections

between them (Schwarz and Leube 2016). Neurofilaments (NF) replace intermediate filaments in neurons. The NFs-mitochondria interaction is mediated by the NF-H and NF-M sidearms, that probably recognize porins or other OMM proteins on mitochondria surface (Wagner et al. 2003).

III.4.2. Mitochondrial fusion

Mitochondrial fusion, a high conserved process in eukaryotes, is the merger of two mitochondria into one. It could occur as end-to-end or end-to-side fusion. It is a two-step process, since it requires the fusion of the outer and the inner mitochondrial membranes. Multiple proteins take part to these two events, even if the most involved are the GTP-hydrolyzing enzymes of the dynamin superfamily (Chan 2020).

The fusion of the **OMM** is managed by mitofusin 1 (**Mfn1**) and mitofusin 2 (**Mfn2**) proteins, members of the dynamin family and coded by *MFN1* and *MFN2* genes, respectively. These two proteins share ~80% of similarity in humans, consequently they present a similar structure and organization in functional domains. Both anchored in the OMM, Mfn1 and Mfn2 have two internal transmembrane (TM) domains, while the N-terminal and the small C-terminal segments are exposed in the cytoplasm. Moreover, they contain two hydrophobic heptad repeat domains (HR1 and HR2), beside the TM domains, and, closer to the N-terminus, a GTPase domain, responsible for mitofusins GTPase activity (Cartoni and Martinou 2009) (Figure 22). Mfn1 GTPase activity has been shown to be higher than that of Mfn2 (Ishihara 2004).

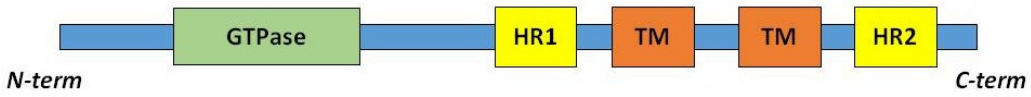

Figure 22 Schematic representation of Mfn1 and Mfn2 domains: one GTPase domain, two heptad repeat domains (HR1 and HR2), two transmembrane domains (TM).

Even if the fusion mechanism is still not completely understood, it seems that mitofusins on adjacent mitochondria form a *trans* interaction trough their HR2 domains, which dimerize in an antiparallel coiled-coil structure. Then, the GTPase activity modifies Mfn conformation and increases the contact surface between the two OMM, leading to their fusion (Tilokani et al. 2018) (Figure 24.1, 24.2, 24.3). Homozygous Mfn1-KO (Knock-out) and Mfn2-KO mice are unviable. Their cultured cells showed impaired mitochondrial fusion, and spherical or "fragmented" mitochondria (Chen et al. 2003). More than 100 mutations in *MFN2* gene have been reported to cause the axonal CMT2A. Most of them are missense mutations, located in all Mfn2 regions, but often within the GTPase domain or the coiled-coil motifs. Some of *MFN2* mutations have been associated with a "gain-of-function" effect, which causes mitochondria aggregation, while some others appear to compromise mitochondrial fusion, in a "loss-of-function" effect (Filadi, Pendin, and Pizzo 2018). In contrast to *MFN2*, disease-inducing mutations in *MFN1* have never been reported. Two main hypothesis have been suggested: *MFN1* mutations could be lethal for the embryo, and Mfn1 function cannot be compensated by Mfn2 protein; alternatively, Mfn1 function can be completely compensated by Mfn2, so its mutation does not induce any mitochondrial disorder (Li et al. 2019).

The fusion of the **IMM** is mediated by the Optic Atrophy 1 (**Opa1**) protein, a dynamin-related GTPase, included in the IMM. Opa1 protein derives from eight different RNA splice forms which are translated in eight Opa1 isoforms. All of them present a GTPase domain, a N-terminal mitochondrial targeting sequence (MTS), subsequently removed by the matrix processing protease (MPP), a transmembrane domain (TM), and a proteolysis site (S1), which can be cleaved by the OMA1 protease. Only four isoforms contain an additional S2 proteolysis site , which can be also cleaved by the Yme1L protease (Chan 2020). These different splice forms and different Opa1-processing result in the synthesis of short isoforms (S-Opa1) and long isoforms (L-Opa1) of Opa1 protein (Figure 23).

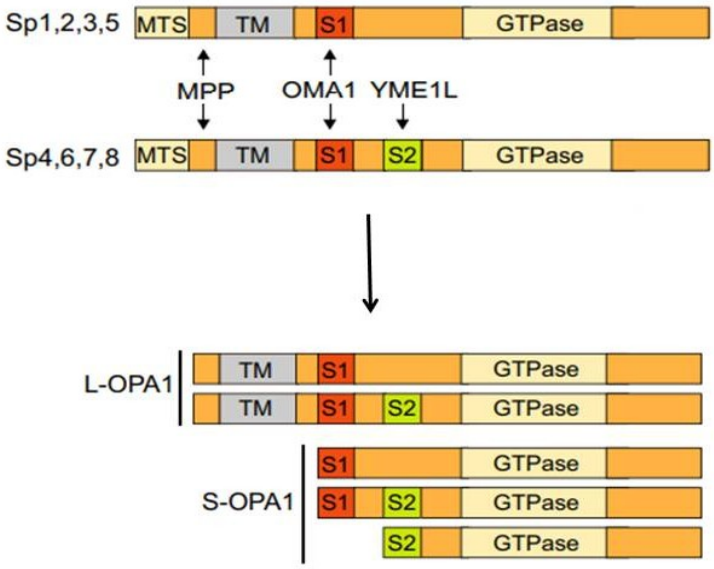

Figure 23 Opa1 isoforms and processing. The eight RNA splice forms of OPA1 are translated in eight isoforms (Sp 1-8), four of them (Sp 4, 6, 7, 8) containing an additional S2 proteolysis site. Constitutive processing, by OMA1 and YME1L enzymes, generate long (L-OPA1) and short (S-OPA1) isoforms [Adapted from: (MacVicar and Langer 2016)].

It seems that the relative abundance of these Opa1 isoforms may change in the cell types and have an effect in regulation of mitochondrial dynamics, although both short and long isoforms are always required. If molecular mechanism of IMM fusion are not entirely clear, recent studies highlighted that the membranes tethering may be mediated by the interaction between L-Opa1 and the IMM-specific cardiolipin. This first step would be followed by the GTP-hydrolysis-dependent fusion of inner membranes, regulated by S-Opa1 (Ban et al. 2017) (Figure 24.4 and 24.5).

Mutations in *OPA1* gene cause the autosomal dominant optic atrophy (ADOA), a progressive disorder due to the degeneration of the retinal ganglion cells. This pathology is clinically characterized by loss of visual acuity, scotomas and optic nerve atrophy. In some more complex cases, ADOA has been associated with peripheral neuropathy (Spinazzi et al. 2008). Most of disease-inducing mutations lie in the GTPase domain and in the dynamin central regions of Opa1 protein. OPA1-mutated cells show

alteration of mitochondrial morphology and fragmented mitochondrial network, but also swollen cristae structure and defects in respiratory chain (Nochez et al. 2009; J. Zhang et al. 2017). Opa1 is ubiquitously expressed, but the energetic impairment associated to *OPA1* mutations, seems to particularly affect the high vulnerable retinal ganglion cells (Amati-Bonneau et al. 2009).

A schematic model of mitochondrial fusion is reported in Figure 24.

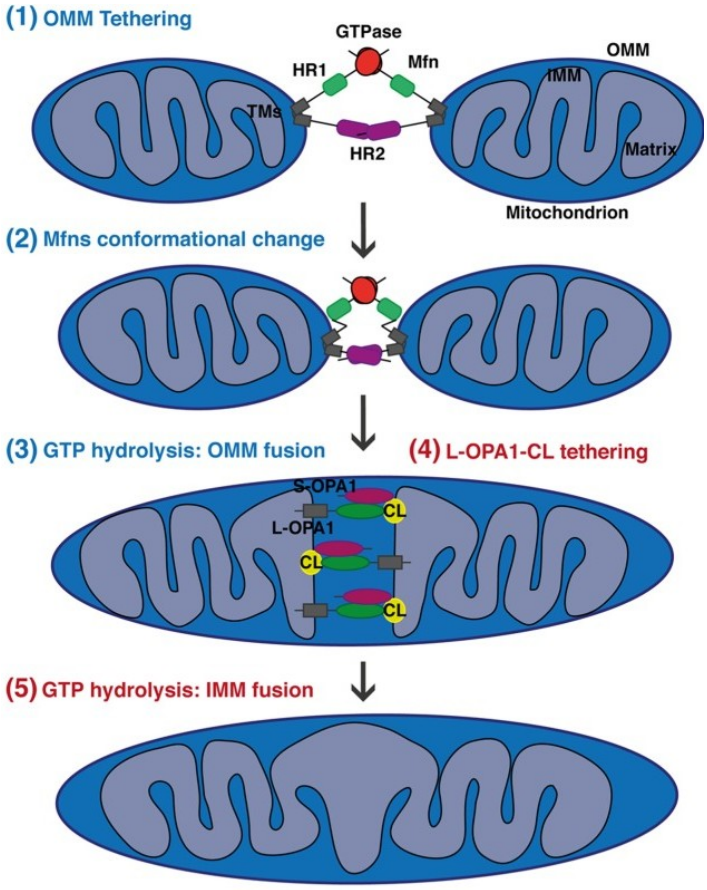

Figure 24 Representation of main known mechanisms of OMM and IMM fusions. (1) Trans interaction of Mitofusins HR2 domains on the OMM. (2) Mitofusins conformational change and increase of contact surface between membranes. (3) GTP hydrolysis and fusion of OMM. (4) IMM tethering trough the L-Opa1/cardiolipin interaction. (5) GTP hydrolysis and fusion of the IMM. [Adapted from: (Tilokani et al. 2018)].

As discussed here, the fusion of the OMM and the IMM present distinct players and regulatory mechanisms. However, it has been shown that these two events are strictly linked and closed in

time, suggesting that a synchronization process operates to coordinate them. In yeast, the most studied model for mitochondrial dynamics, Ugo1 protein has been identified as adaptor, or scaffold, to connect the outer and the inner mitochondrial membranes. In particular its N-terminus binds Fzo1 protein, the homolog of mammalian mitofusins, while its C-terminus is in contact with Mgm1 protein, the homolog of Opa1. In mammals this scaffold molecule has not been detected, but its existence is expected (Hoppins and Nunnari 2009).

III.4.3. Mitochondrial fission

In mitochondrial fission, one mitochondrion splits in two, often not equally sized, organelles. Mitochondrial fission, also known as mitochondrial division, was first studied in *Caenorhabditis elegans* and yeasts, before being explored in higher eukaryotes (Westermann 2010). It is a multi-step process, mostly mediated by **Drp1** (Dynamin-related protein 1), the mammalian homolog of Dnm1. Drp1, coded by *DNM1L* gene, is a GTPase with four domains: the GTPase domain in the N-terminus, the middle domain, the insert B, and the GTPase effector domain (GED) in the C-terminus (Pagliuso, Cossart, and Stavru 2018) (Figure 25).

Figure 25 Schematic representation of Drp1 domains: GTPase domain, middle domain, Insert B (Ins B) and GTPase effector domain (GED) [From: (Pagliuso, Cossart, and Stavru 2018)].

Drp1 protein has a predominant cytosolic localization, but it is recruited on the outer membranes of mitochondria and peroxisomes, to participate in mitochondrial and peroxisomal fissions. To promote mitochondrial fission process, small monomers of Drp1 self-assemble to form a multimeric spiral on the OMM. Then, GTP hydrolysis induces a conformational change in Drp1, which causes the compaction of the contractile ring and reduction of its diameter (Figure 26). Once this constriction

site is formed, the final physical scission of membrane is operated by Dnm2 (Dynamin 2) protein (Kraus and Ryan 2017). Other proteins take part to mitochondrial fission, helping Drp1 recruitment from cytosol to the OMM. Among them, it is important to mention the transmembrane receptors Fis1 (mitochondria, fission protein 1), Mff (mitochondrial fission factor), MiD49 and MiD51 (mitochondrial dynamics proteins of 49 and 51 kDa).

In homozygous KO mice, it has been shown that the complete deletion of Drp1 is embryonically lethal, and, in isolated MEF (mouse embryonic fibroblasts), it leads to impaired mitochondrial division and elongated peroxisomes, but not defects in energy production (Wakabayashi et al. 2009). Mutations in *DNM1L* gene have been reported, in few cases, to cause a complex phenotype, characterized by neonatal encephalopathy, microcephaly, developmental delay, optic atrophy (Fahrner et al. 2016).

Another protein that could contribute in regulating fission processes of mitochondrial network is **GDAP1**. GDAP1 overexpression, in transfected Cos7 cells, showed to cause mitochondrial fragmentation, while its knock-down, in N1E-115 cells, favors elongated mitochondria (Niemann et al. 2005). In any case, few functional studies on GDAP1 activity have been performed and its associated mechanisms rest to be understood. More details about GDAP1 are presented in Chapter 4.

Besides the active role of the aforementioned mitochondrial proteins in regulate mitochondrial fission, the involvement of other cellular organelles need to be considered. First of all, sites of interaction exist between the mitochondrion and the endoplasmic reticulum (ER). It seems that, where these physical ER-mitochondria contacts occur, the ER wraps around the mitochondrion, constricts it, and promote its division. It has been suggested that this ER-tag may then induce Drp1 or Mff recruitment (Friedman et al. 2011). Also the actin cytoskeleton could promote mitochondrial fission. Specifically, it has been shown that actin polymerization induces Drp1 recruitment, in a mechanism regulated by the inverted formin 2 (INF2), Spire1C protein, and the Cofilin1 (Rehklau et al. 2017).

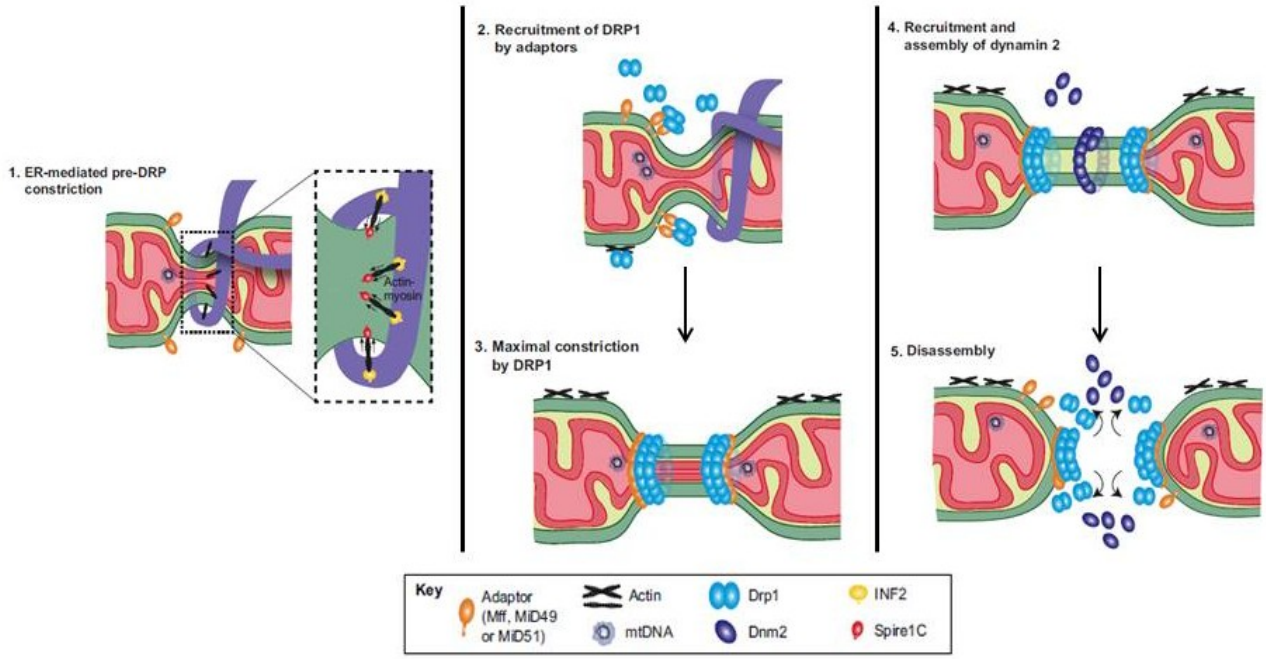

Figure 26 Representation of main known mechanisms of mitochondrial fission. (1) First ER-constriction of the mitochondrion. (2) Drp1 is recruited on the constriction site by fission adaptors. (3) Conformational change of Drp1 induced by GTP hydrolysis. (4) Recruitment of Dnm2 on fission site. (5) Completed mitochondrial scission [Adapted from: (Kraus and Ryan 2017)].

Mitochondrial fusion and fission occur simultaneously and continuously in the cell, finely regulated by multiple proteins and mechanisms. They allow the sharing of organelle contents, necessary in case of damage, and their balance is fundamental to organize mitochondrial structure and morphology. Moreover fusion and fission events are connected to mitophagy, the selective degradation of defective mithochondria, and apotosis, the programmed cell death (Scott and Youle 2010).

III.5. Mitophagy

The term “autophagy” derives from the Greek and it literally means “eating of self”. The autophagy is a programmed catabolic process, necessary to degrade cellular components, such as mitochondria, endoplasmic reticulum, peroxisomes, misfolded and aggregated proteins. It has been showed that two types of autophagy exist, the selective one and the non-selective one. Non-selective autophagy

occurs in case of privation of nutrients, since cells need to degrade macromolecules, like proteins, to refill nutrients stocks. On the other hand, the purpose of selective autophagy is to remove specific organelles in nutrient-rich conditions (Ding and Yin 2012). Mitophagy, the precise degradation of mitochondria, belongs to selective autophagy processes. It occurs when mitochondria are damaged, dysfunctional, or in excess. This mechanism has been largely investigated in yeast, and its factors have appeared to be conserved among the different species. In mammals, two main class of mitophagy have been identified, the ubiquitin-dependent and –independent pathways (Palikaras, Lionaki, and Tavernarakis 2018).

In the ubiquitin-independent, or receptor-mediated, pathway, NIX/BNIP3L and BNIP3, localized on the OMM, act like mitophagy receptors. Through their LIR motifs, they directly bind LC3/GABARAP, expressed on the autophagosome, a double-membrane vesicle. Once the autophagosome has incorporated the mitochondrion, it fuses with a lysosome, forming an autolysosome and causing the degradation of its own content (Glick, Barth, and Macleod 2010).

The ubiquitin-dependent pathway is also known as PINK1 (PTEN-induced putative kinase 1)/Parkin-mediated mitophagy. When the mitochondrion is damaged, the ΔΨm collapses and induces the accumulation and stabilization of PINK1 protein on the OMM. This is fundamental for the recruitment and the activation of the E3 ubiquitin ligase Parkin, which ubiquitinates several proteins of the OMM, enabling the targeting of the damaged mitochondrion by the autophagosome (Kubli and Gustafsson 2012).

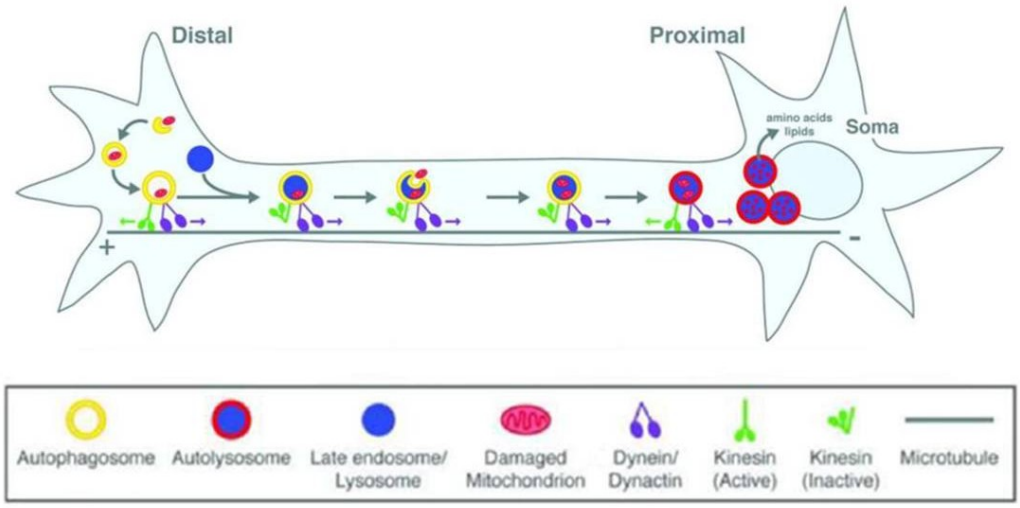

Figure 27 Autophagosomes biogenesis and maturation in neurons. Autophagosome (yellow ring), formed in neurites, incorporates damaged or dysfunctional mitochondria, and fuses with the lysosome (blue circle). With the autphagosome maturation, lysosomal acid proteases activate (red ring), degrading its contents [Adapted from: (Maday, Wallace, and Holzbaur 2012)]

It seems that mitochondrial mitophagy and dynamics are strictly connected events. In yeast and mammals, mitophagy is preceded by mitochondrial Drp1-mediated fission, probably in order to obtain smaller mitochondria, easier to be engulfed by autophagosomes (Youle and Narendra 2011). Moreover, Mitofusins 1 and 2, the main players of OMM fusion, have been demonstrated to be targets of Parkin ubiquitination. This interaction causes Mfn1 and Mfn2 degradation, which would be necessary to prevent the fusion of damaged mitochondria with the healthy ones (Kubli and Gustafsson 2012).

We know that mitochondria play a key role in neurons and nervous system, and their proper function is fundamental to ensure neural homeostasis. In neurons, most mitochondria localize in neurites, but, to be degraded, they need to be transported to cellular soma, which contains the higher amount of lysosomes. Nevertheless, we cannot exclude that mitophagy events may occur in peripheral axons too (Ashrafi et al. 2014). Even if mitophagy is a physiological process in neurons, activated to remove damaged mitochondria, when it is injured, it can be responsible for neurodegenerative diseases. For example, monogenic forms of Parkinson's disease have been associated with mutations in *PARK2* and

PARK6 genes, respectively coding Parkin and PINK1 proteins. The dysfunction of autophagy/mitophagy pathways has been suggested as pathological mechanism also in some cases of Alzheimer's disease, Amyotrophic lateral sclerosis, Huntington's disease (Martinez-Vicente 2017). Moreover, CMT2A iPS-derived motor neurons have shown that mutated *MFN2* induces enhanced levels of mitophagy, which seemed to be responsible of a striking reduction of mitochondria in affected neurons (Rizzo et al. 2016).

Chapter IV. The ganglioside-induced differentiation-associated protein 1 (GDAP1)

Since PNS is a high-energy requiring system, mutations in genes involved in mitochondria dynamics and activity, can lead to CMT disease. In particular, in this study, we have focused on the ganglioside-induced differentiation-associated protein 1 (*GDAP1*) gene, implicated in demyelinating and axonal CMT.

IV.1. *GDAP1* gene and transcripts

GDAP1 gene is located on chromosome 8, position 75,233,365-75,401,107, forward strand, in GRCh37 coordinates. It contains six exons and five introns, and it encodes for eight different transcripts, two of them protein coding. Specifically, GDAP1-001 is associated to the longer isoform, a 358-aa protein, while the transcript GDAP1-002 has been predicted to encode a 290-aa shorter isoform, with a smaller N-terminus (NCBI ID 54332, provided from RefSeq, Feb 2012). *GDAP1* expression was reported for the first time in 1999, by a Japanese team which isolated its cDNA from Neuro2a cells and showed it to be involved in Neuro2a differentiation into neuron-like cells (H. Liu et al. 2008).

Alignment studies have demonstrated that *GDAP1* orthologous genes exist in many other vertebrates, and sequence similarity has been observed also in few plants and bacteria. This data suggest that *GDAP1* may be occurred in genomes before the fish-tetrapod split, or, perhaps, even before the plant-animal split (Marco 2003). In humans, *GDAP1* has a paralog gene, the so-called *GDAP1L1* (Ganglioside-induced differentiation-associated protein 1-like 1). More details about GDAP1L are reported in paragraph 4.2.5.

IV.2. GDAP1 protein

GDAP1 is a 358-aa tail-anchored protein, integrated in the outer mitochondrial membrane, with its N-terminus situated in the cytosol, and the C-terminus in the mitochondrial intermembrane space (Pedrola et al. 2005; Niemann et al. 2005; Wagner et al. 2009).

IV.2.1. Protein expression

Expression studies have been performed on animal models, or cell cultures and tissues, through RT-PCR, Western blot, or Immunocytochemistry.

The first analysis, by Cuesta *et al.*, showed an ubiquitous GDAP1 expression in different human and murine tissues, particularly important in brain. Moreover, they verified that, in peripheral nerves, its expression occurs not only in neurons, but also in Schwann cells (Cuesta et al. 2002). These results were confirmed, in 2005, by Niemann *et al.*, who detected, on mice, a relevant GDAP1 expression in central neurons, motor and sensory peripheral neurons, and myelinating Schwann cells (Niemann et al. 2005).

Parallel studies, conducted by other authors on mice and rats, highlighted that GDAP1 is highly expressed in grey matter and in largest neurons, like neurons of the olfactory bulb, Purkinje neurons, pyramidal neurons of hippocampus and cortex. Instead, its levels are reduced in peripheral nerve and skeletal muscle, and absent in white matter and Schwann cells (Pedrola et al. 2005; 2008).

An *in vitro* study demonstrated that, in primary human skeletal muscle cells, GDAP1 expression is regulated by the AMP-activated protein kinase (AMPK). Specifically, when AMPK is activated, it would induce a reduced expression of GDAP1 (Lassiter et al. 2018).

IV.2.2. Protein structure

In GDAP1 structure, we can distinguish five main domains: the Glutathione-binding domain (G-Site or GST-N), the α-loop, the hydrophobic substrate-binding domain (H-Site or GST-C), the hydrophobic domain (HD1) and the transmembrane domain (TM). A schematic representation of GDAP1 protein is reported in Figure 28 (Cassereau et al. 2011A).

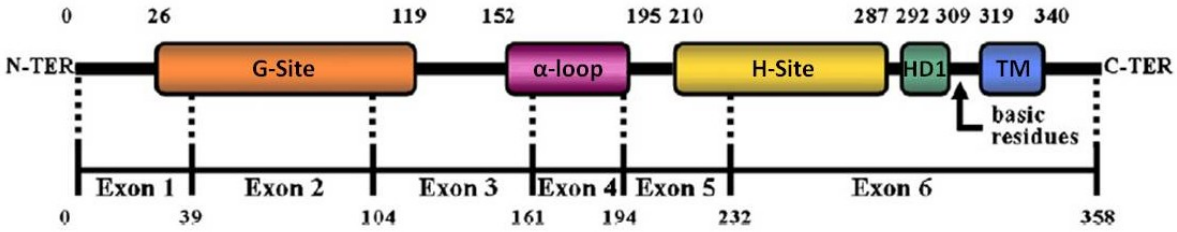

Figure 28 Predicted structure and domains of GDAP1 protein. G-site: Glutathione-binding domain; H site: hydrophobic substrate-binding domain; HD1: hydrophobic domain; TM: transmembrane domain. Numbers above and below the structure refer to amino acidic boundaries of protein domains and GDAP1 gene exons, respectively [Adapted from:(Cassereau et al. 2011A)].

Recently, thanks to x-ray crystallography, a 3D structural model for cytosolic portion of GDAP1 protein has been suggested. It has been developed on the murine GDAP1 protein, which share 94% identity with human GDAP1. This model was obtained, in particular, for the GDAP1 core (G- site and H-site), while the α-loop and the HD1 domains were added from structural bioinformatic predictions (I-TESSER server) (Googins et al. 2020) (Figure 29).

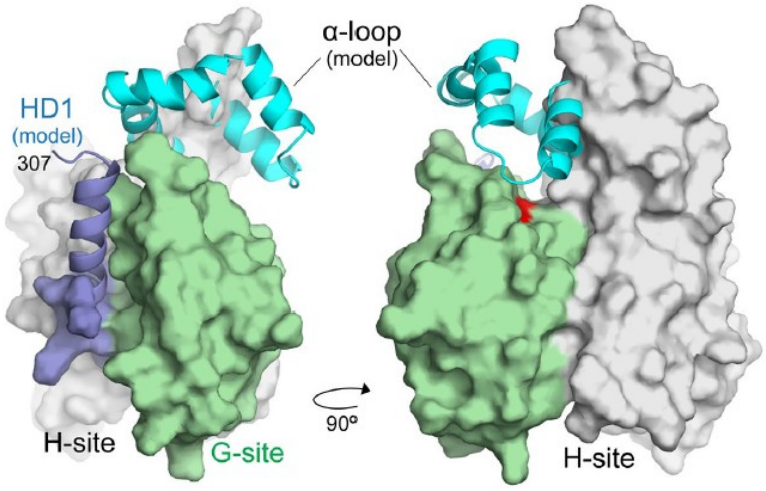

Figure 29 3D structural model for cytosolic GDAP1 murine protein: G-site (green), H-site (grey), α-loop (cyan), and HD1 domain (blue) [Adapted from: (Googins et al. 2020)].

GST domains and GST activity

GDAP1 protein presents two GST domains: the first is the glutathione-binding domain (G-site), located at the N-terminus, supposed to recognize glutathione molecules; the second, the hydrophobic substrate-binding domain (H-site), at the C-terminus, which would interact with a potential biological substrate.

The role of GDAP1 as glutathione transferase (or glutathione S-transferase, or GST) protein, as well as the activity of its GST domains, have always been matter of debate and the results of functional studies are controversial. In 2004, Marco *et al.* classified GDAP1 in a new class of GST-like proteins. Indeed, although its sequence similarity to other GST, some of its structural regions, as the α-loop and the TM domain, are absent in canonical GST, which are, usually, cytosolic enzymes (Marco 2003). The only study supporting the GDAP1 role as GST, was performed in 2016 by Huber *et al.*, who revealed, in soluble GDAP1 constructs, a theta-class-like GST activity, which would be regulated by the HD1 domain (Huber et al. 2016). This evidence was in contrast with all previous analysis. First functional investigations, in fact, tested GST activity of truncated GDAP1 on different substrates, and demonstrated that this protein had not GST activity (Pedrola et al. 2005; Shield, Murray, and Board

2006). A more in-depth study has recently examined GDAP1 domains through the expression of recombinant GDAP1 fragments, combined with crystallography strategy. The analysis confirmed that the GDAP1 G-site is not able to bind glutathione, since it lost some critical residues of the GST pocket, which are essential to glutathione-binding (Googins et al. 2020). On the other hand, Googins *et al*, demonstrated also that the H-site conserved its typical interactions and can create a robust binding with a GST substrate, like the ethacrynic acid (Googins et al. 2020).

Even if these results seem to support, in most cases, the absence of GST activity in GDAP1 protein, we cannot exclude an evolutional process of domains' structure, and the protein adaptation to alternative enzymatic and not enzymatic functions.

The α-loop

The α-loop is a large insertion between the G-site and the H-site, composed by one α4 and one α5 helix (Marco 2003). This is the most conserved region of GDAP1 protein, and it is not found in all GST. Analysis of the α-loop demonstrated its involvement in the substrate binding, since its deletion abolishes the interaction with the ethacrynic acid. Furthermore, it has been suggested a potential role of the α-loop in the interaction with the mitochondrial membrane (Googins et al. 2020).

The HD1 domain

In first studies, the GDAP1 hydrophobic domain 1 (HD1) has been shown to take part in mitochondrial fission events (Wagner et al. 2009; Huber et al. 2013). Later, its role in defining mitochondrial morphology has been confirmed using truncated GDAP1 variants (Googins et al. 2020). It seems also to interact with the α-loop and directly, or indirectly, participate in substrate-binding (Googins et al. 2020).

In the GDAP1 model, proposed by Huber in 2016, the HD1 domain would regulate the GST activity, promoting the active or the inactive conformations of GDAP1, in an autoinhibitory manner (Huber et al. 2016).

The TM domain

GDAP1 protein is integrated in the OMM and it presents, therefore, a transmembrane region (TM or TMD). The TMD is a single hydrophobic domain, located next to the cytosolic C-terminus, absent in the other GST (Wagner et al. 2009). It seems to be fundamental for the correct GDAP1 localization on the OMM. Consequently, truncated forms of the protein, lacking the TMD, were shown to diffuse in cytoplasm and nucleus (Pedrola et al. 2005).

IV.2.3. Protein dimerization

GST constitute a superfamily of enzymes, necessary for cellular detoxification from endogenous and exogenous compounds. They are dimeric proteins and their activity is deeply connected to this monomer-dimer equilibrium (Fabrini et al. 2009). It is for this reason that dimerization ability has been investigated in GDAP1 protein. In 2006, Shield *et al.* demonstrated, for the first time, that GDAP1 forms dimers of identical subunits (Shield, Murray, and Board 2006). The 2016 analysis by Huber *et al.* confirmed previous results, revealing that the formation of homodimers does not depend on TMD and HD1 domains (Huber et al. 2016). In the 3D model predicted for GDAP1, the dimerization interface would be located close to the α-loop, and it would concern the H-site of the first subunit and the G-site of the second one (Googins et al. 2020). However, recent analysis, conducted on truncated constructs, seem to suggest a monomeric stoichiometry of cytosolic portion of GDAP1 protein (Googins et al. 2020).

IV.2.4. Protein interactions

GDAP1 protein has been demonstrated to interact with three cellular proteins: the β-tubulin, RAB6B, and caytaxin (Estela et al. 2011; Pla-Martín et al. 2013). β-tubulin, coded by *TUBB* gene, is a

fundamental structural component of cytoskeleton microtubules. RAB6B is a member of RAB-GTPases family, specifically expressed in neuron cell types. It interacts with dynein/dynactin complex and takes part to retrograde transport in neuronal cells (Wanschers et al. 2007). Caytaxin protein (*ATCAY* gene) interacts with kinesin and may be involved in anterograde transport along microtubules structures (Aoyama et al. 2009). All these interactions with transport proteins, together with its localization on the OMM, suggest a potential role of GDAP1 in mitochondrial trafficking, not supported, so far, by additional evidence.

Furthermore, Pla-Martin *et al.* have observed that GDAP1 is located in MAMs (mitochondrial-associated membranes), and assumed that it could have a role in the interaction with the ER, via the RAB6B-binding (Pla-Martín et al. 2013). A proteomic analysis of MAMs composition confirmed the presence of GDAP1 at this level (Poston, Krishnan, and Bazemore-Walker 2013). Specifically, MAMs are sites of physical interaction and communication between the mitochondria and the ER, constituted by fragments of both membranes. These microdomains have been associated to multiple cellular functions, like the synthesis of lipids, the Ca^{2+} homeostasis, the cell survival and apoptosis (Perrone, 2020). Numerous proteins participate in MAMs organization and activity. Among them, Mfn1 and Mfn2, have been demonstrated to be necessary in mitochondria-RE tethering and Ca^{+2} uptake (de Brito and Scorrano 2008). GDAP1 role in MAMs has not be completely understood, but its deficiency reduces the connection between mitochondria and RE, and induces the formation of enlarged RE cisternae (Pla-Martín et al. 2013).

IV.2.5. GDAP1L1

GDAP1L1 gene, the paralog of *GDAP1*, is located on chromosome 20, coordinates 20: 42,875,887-42,909,013, on the forward strand. With six exons and five introns, it conserves the same genomic structure of *GDAP1*. Its 367-aa protein share 56% amino acidic identity with GDAP1 protein, and it maintains the same main functional domains (Shield, Murray, and Board 2006). GDAP1L1 is

expressed in the CNS, in cerebellum, cortex, hippocampus and Purkinje cells, but not in the PNS. It is normally located at cytosolic level. Nevertheless, *in vitro* functional studies demonstrated that it could translocate to mitochondria when oxidized glutathione concentrations increase. GDAP1L1 translocation may be mediated by its C-terminal targeting domain (Niemann et al. 2014). Moreover, it seems that GDAP1L1 could also be implicated in fission events, when GDAP1 expression is suppressed, compensating, in this way, its absence (Niemann et al. 2014).

IV.3. GDAP1 functions

Functional studies, performed on animal and cellular models, have allowed to identify multiple GDAP1 roles in the cell, most of them associated with mitochondrial dynamics and functions.

IV.3.1. Mitochondrial fission

Because of its localization on the outer mitochondrial membrane, the first aspect evaluated for GDAP1 concerned its possible effect on mitochondrial morphology and dynamics. GDAP1 has been shown to participate in mitochondrial fission events, since its overexpression, in transfected cells, resulted in an increased fragmentation of mitochondrial network. This means that mitochondria appeared less tubular and aggregated, modifying their whole architecture in the cell (Niemann et al. 2005). In contrast, GDAP1 knock-down led to increased tubular mitochondria (N1E-115 cells), not observed, nevertheless, in case of GDAP1 knock-out (SH-SY5Y cells and primary murine neurons) (Niemann et al. 2005; Pla-Martín et al. 2013; Barneo-Muñoz et al. 2015).

GDAP1-induced fragmentation seems to depend on Drp1 expression, the most crucial factor of mitochondrial fission, and be counterbalanced by Mfn1 and Mfn2 proteins, essential for mitochondrial fusion (Niemann et al. 2005). A structure-focusing analysis has shown that the integrity of the HD1 domain, as well as the conservation of its amino acidic sequence, are essential to

preserve GDAP1 mitochondrial fission activity (Wagner et al. 2009). In Huber model, HD1, together with GST domains, would regulate the switch between the active and the inactive states of GDAP1 fission activity (Huber et al. 2016).

IV.3.2. Mitochondrial fusion

Implication of GDAP1 in mitochondrial fusion has been investigated in just one study. It has been reported that, with some specific mutated forms of GDAP1 (p.Arg120Trp and p.Thr157Pro), mitochondrial fusion is impaired (Cos-7 cells). This would cause a partial alteration of the ΔΨm and a higher susceptibility to cellular apoptosis (Niemann et al. 2009).

IV.3.3. Peroxisomal fission

In addition to its mitochondrial localization and functions, GDAP1 has been shown to localize and operate also in peroxisomes. In particular, in Cos-7 cells, it has been observed that GDAP1 is targeted to peroxisomes through its binding with Pex19, a chaperon and import receptor (Huber et al. 2013). In peroxisomes, as well as in mitochondria, it appeared to participate in peroxisomal fission and fragmentation. This ability requires the integrity of its HD1 and TA (tail-anchored) domains. Lack of GDAP1 induces the apparition of tubular and elongated peroxisomes (Huber et al. 2013).

IV.3.4. Oxidative stress

An interesting GDAP1 role in cellular homeostasis is associated to oxidative stress and protection from ROS. First evidence of GDAP1 protective action has been reported, in 2011, by Noack *et al*., who observed that GDAP1 knock-down induced the increase of oxidative glutamate toxicity, in glutamate-

sensitive HT22 neuronal cells. On the other hand, they demonstrated that the overexpression of GDAP1 promoted the glutamate-resistance and increased levels of GSH, a fundamental cellular antioxidant (Noack et al. 2012). The direct relationship between GDAP1 expression and reduced glutathione content has been also confirmed in a *Drosophila melanogaster* model (López Del Amo et al. 2015). Moreover, GDAP1 seems to have a role in maintaining high levels of ΔΨm, which is reduced or disrupted in oxidative stress conditions (Noack et al. 2012). Consequently, when GDAP1 is mutated, it has been observed a significant augmentation of intracellular ROS, responsible for oxidative stress and damage of cellular components, which can favor cell death (Noack et al. 2012; Cassereau et al. 2020). All these observations corroborate the hypothesis that GDAP1 plays an important protective role against oxidative stress.

IV.3.5. Calcium homeostasis

GDAP1 has also been shown to participate in calcium homeostasis. The cell contains internal calcium stores, most notably the endoplasmic reticulum (ER). In response to specific agents, the ER empties, inducing the efflux of the Ca^{2+} from the cell. Since Ca^{2+} stores need to be refilled, Ca^{2+} is picked up from the external space through membrane channels. This Ca^{2+} entry across the plasma membrane is regulated by ER-Ca^{2+} levels, and it is known as "store-operated Ca^{2+} entry" or SOCE (Hogan and Rao 2015). It seems that mitochondria participate to SOCE activity and its modulation, even if mechanisms are still not clear (Malli and Graier 2017). Functional studies have shown that GDAP1 is implicated in calcium homeostasis and in SOCE regulation. First, it was observed that GDAP1 depletion impaired SOCE activity and reduced mitochondrial Ca^{2+} uptake, in cellular models (SH-SY5Y) (Pla-Martín et al. 2013; González-Sánchez et al. 2017). Moreover, further analyses reveled reduced cytosolic Ca^{2+} levels in GDAP1-lacking neurons of mice, maybe as consequence of impaired storage/release mechanisms (Barneo-Muñoz et al. 2015). It has been hypothesized that, when mitochondria lose GDAP1 function, their organization and dynamics in the cell are altered. This

would prevent the correct mitochondrial mobilization to plasma membrane and the SOCE-channels formation, in response to ER-Ca^{2+} emptying (Pla-Martín et al. 2013). This confirms that GDAP1 could mediate the interaction and tethering between the ER and the mitochondria, so the MAMs establishment, which is essential to preserve SOCE activity.

IV.3.6. Metabolic implication

GDAP1 involvement in mitochondrial energy production has been poorly investigated. It has been described that mutated forms of GDAP1 present, in fibroblasts, a deficiency of ETC Complex I activity, associated to reduced expression of SIRT1 deacetylase. Furthermore, the ATP production and the respiration rate appeared decreased, too. The activity of other OXPHOS complexes, as well as Krebs cycle, were preserved (Cassereau et al. 2009; 2020). Similar OXPHOS observations were reported in a study conducted on a GDAP1-deficient model of human skeletal muscle cells (Lassiter et al. 2018). In the same model, as regards the lipid metabolism, GDAP1 silencing has been shown to reduce β-oxidation levels (Lassiter et al. 2018). These results seem to disagree with the observation, on a GDAP1 *Drosophila* model, that both GDAP1 up- and down-regulations increase lipid β-oxidation in the cell (López del Amo et al. 2017).

Nevertheless, no mechanistic studies were performed to elucidate GDAP1 functions in bioenergetic regulation.

IV.3.7. Other GDAP1 implications

A recent and different topic of interest concerns the relationship between *GDAP1* gene and the alcohol/smoke additions. First, two studies highlighted that methylation of promoter region of *GDAP1* correlated with the severity of alcohol dependence in lymphocytes of diagnosed patients. In

particular, in patients with a higher severity of dependence, a *GDAP1* DNA hypomethylation was observed. It has been shown that this methylation status was reversible and it could return to normal values when patients started a treatment program (Philibert et al. 2014; Brückmann et al. 2016).

Secondly, in 2020, a third work has reported that exposure to cigarette smoke can alter the expression of *GDAP1* in some regions of murine hippocampus, maybe by methylation of its promoter (Mundorf et al. 2020).

A schematic representation of main GDAP1 functions is reported in Figure 30.

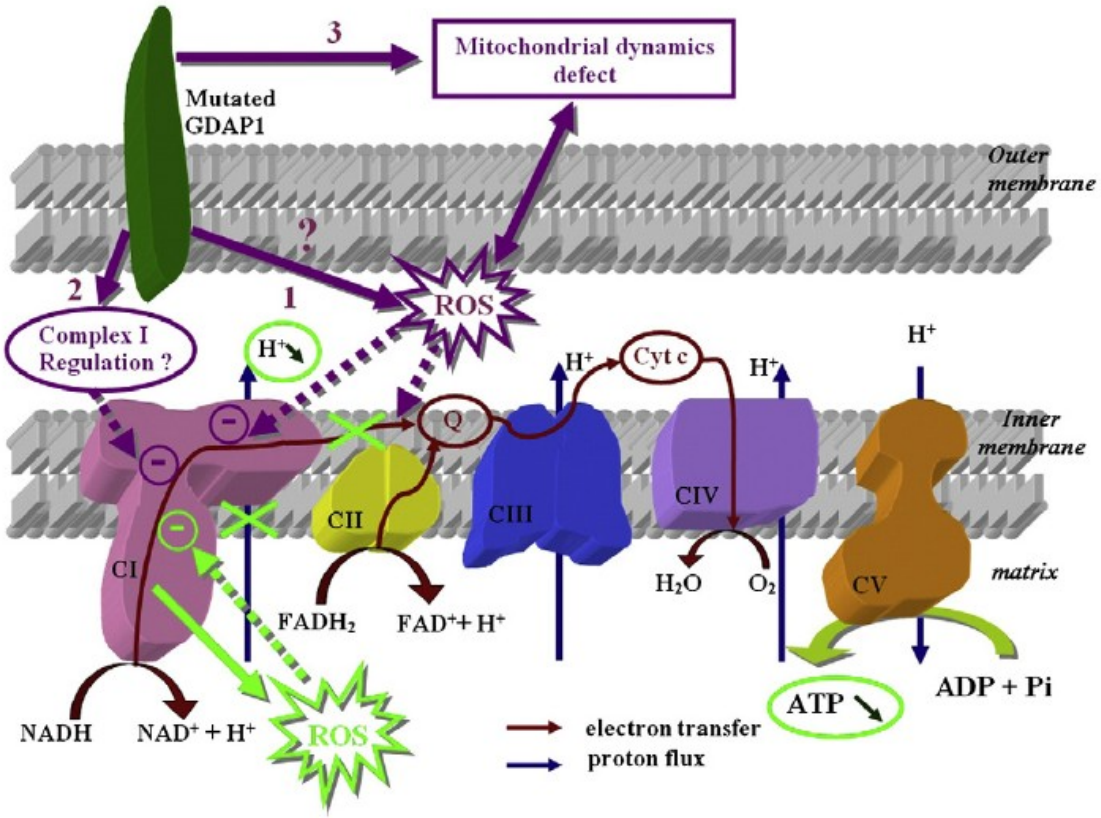

Figure 30 A suggested model of GDAP1 function and dysfunction: Effect of GDAP1 mutation on ROS production (arrow "1"), bioenergetic activity (arrow "2"), and mitochondrial dynamics (arrow "3") [From:(Cassereau et al. 2011A).]

IV.4. GDAP1 and Charcot-Marie-Tooth disease

IV.4.1. GDAP1 mutations

As discussed in Chapter 2, mutations in *GDAP1* gene are responsible for Charcot-Marie-Tooth disease. First mutations associated to CMT were simultaneously reported, in 2002, in two parallel studies (Baxter et al. 2002; Cuesta et al. 2002). To date, more than eighty mutations have been identified, the large majority of them consisting of single-base substitutions. However, rare cases reported small deletions or duplications, in *GDAP1*, to be responsible for CMT disease (García-Sobrino et al. 2017; Pakhrin et al. 2018).

Considering mutations' impact on protein structure, it appears that missense mutations constitute the higher proportion, followed by non-sense and frameshift mutations. Splicing mutations have been rarely described, both in exonic and intronic regions (Cassereau et al. 2011B; Rzepnikowska and Kochański 2018).

At protein level, GDAP1 mutations are mostly located in the α-loop and the GST-C domain, which reflects the presence of hot spots between the exon 3 and the exon 6 in its DNA sequence (Cassereau et al. 2011B).

In Figure 31, most of identified amino acidic substitutions are reported (Rzepnikowska and Kochański 2018).

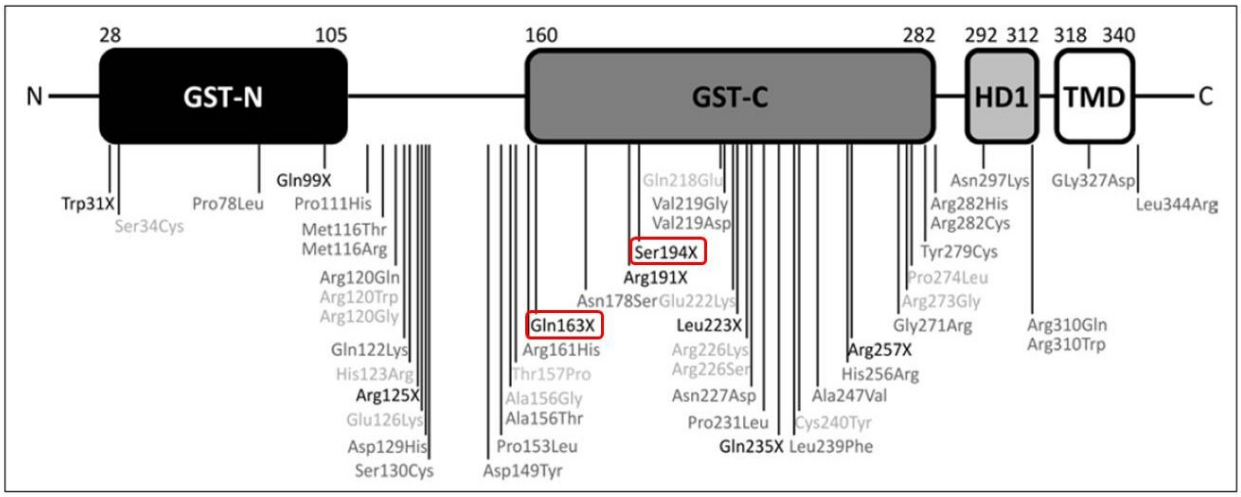

Figure 31 Structure and domains of GDAP1 protein (from Pfam database), and associated mutations: Recessively-inherited mutations are marked in black, if non-sense, and dark grey, if missense. Dominantly-inherited mutations are marked in light grey. We highlighted, in red, GADP1 mutations analyzed in our study [Adapted from: (Rzepnikowska and Kochański 2018)].

GDAP1 mutations are transmitted with in a recessive or dominant mode of inheritance. These CMT autosomal dominant and recessive forms present clearly distinctive features and clinical aspects.

IV.4.2. GDAP1 and autosomal recessive forms of CMT disease (AR-CMT)

IV.4.2.1. AR mutations

Most of CMT-associated mutations in *GDAP1* are recessively-inherited. In the case of AR mutations, both alleles need to be mutated to induce the emergence of the pathological manifestation. Their consequence is usually a loss-of-function effect, so to the dysfunction of the resulting protein. As regards AR-*GDAP1* mutations, this is observed for non-sense mutations, which lead to the formation of truncated proteins, and mutations falling in the C-terminal region, which is essential for the correct targeting on the OMM. Truncated and not-targeted proteins are often degraded, by endogenous cellular pathways. When AR-GDAP1 mutations are missense, mechanisms which induce

loss of protein function could be more complex to investigate (Rzepnikowska and Kochański 2018). According to functional studies performed on *GDAP1* models, the main impaired mechanisms induced by AR-mutations, may involve mitochondrial dynamics and interactions. It has been shown that AR-mutations in *GDAP1*, like p.Arg161His and p.Arg310Gln, impair mitochondrial fission, affecting the dynamic balance which controls mitochondrial morphology and, consequently, mitochondrial function (Niemann et al. 2005; 2009). Some missense mutations could also modify the interaction between GDAP1 and the transport proteins, affecting the mitochondrial axonal transport, a crucial mechanism for neuronal viability (Pla-Martín et al. 2013). Additionally, some AR-mutations, as p.Arg310Gln, seem to reduce the protective antioxidant role of GDAP1 protein (Noack et al. 2012).

IV.4.2.2. AR-CMT

Autosomal recessive GDAP1-CMT are generally severe, with an early age of onset, in the first decade of life, and a rapid progression. Clinically, mild inter- and intra-familial variability has been observed (Azzedine et al. 2003; Claramunt 2005). Common features are an important motor deficit and distal deformities, muscle weakness and atrophy, need of wheelchair before the third decade. Sensory symptoms are frequent, as well as vocal cord paresis and hoarseness of the voice, sometimes associated with respiratory problems (Sevilla et al. 2008; Sivera et al. 2017).

Considering the electrophysiological aspects, recessively-inherited *GDAP1*-mutations are responsible for the demyelinating CMT4A, most frequently, and the intermediate RI-CMTA. The rarer axonal AR-CMT, linked to *GDAP1*, is sometimes reported as AR-CMT2C (Kabzińska et al. 2011), elsewhere as AR-CMT2K (Fu et al. 2017) or CMT2H (N.607731 in OMIM database). In the case of CMT4A, recorded motor nerve conduction velocity (MNCV) are commonly lower than 25 m/s, even if they rest quite stable over the years. In contrast, CMAP amplitudes tend to progressively decrease, until reaching very low values, even smaller than 0.5 mV (Cassereau et al. 2011A). In the AR-intermediate form, demyelinating events, combined with axon degeneration, generate MNCV values between 25 and 38

m/s, on average, with reduced CMAP amplitudes (Senderek 2003; Crimella et al. 2010). As normal, in the *GDAP1* AR-axonal CMT, NCV are conserved, while amplitudes are strongly reduced (Kabzińska et al. 2011).

Histopathological analysis, generally conducted on patients' sural nerve biopsies, in light and electron microscopy, have been performed in some CMT4A cases. They show reduced number of large myelinated fibers and reduced thickness of myelin sheath. Moreover, clusters of regenerations and onion bulbs formations, surrounded by Schwann cells processes, are occasionally observed (Figure 32) (Nelis et al. 2002; Senderek 2003; Fu et al. 2017). These findings are consistent with an early myelin loss, which has been followed, with the progression of the disease, by the decay of large axons, indicating the occurrence of both demyelinating and axonal degeneration.

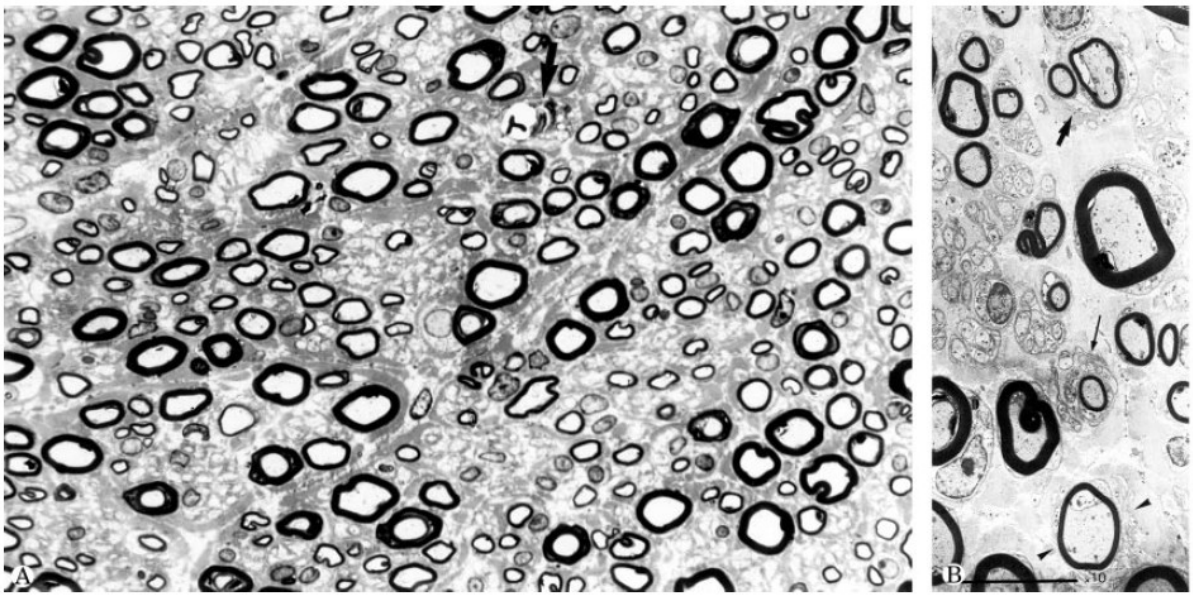

Figure 32 Transverse semithin section of sural nerve biopsy, from a CMT4A patient (GDAP1 homozygous p.Ser194 mutation). (A) Absence of large myelinating axons and reduced axonal thickness. (B) Electron micrograph. Clusters of axonal regeneration (thick arrow) and formation of onion bulbs (thin arrow). Scale bar = 10 µm [From: (Nelis et al. 2002)].*

In only one study, electron microscopy has reveled that mitochondria are more aggregated, and acquire a small and round morphology, in the sural nerve section of a CMT4A patient (Figure 33B)

(Tazir et al. 2014). Similar mitochondrial abnormalities in nerves have already been associated to a severe and early-onset axonal CMT, caused by different mutations in *MFN2* gene (Figure 33C) (Vallat et al. 2008).

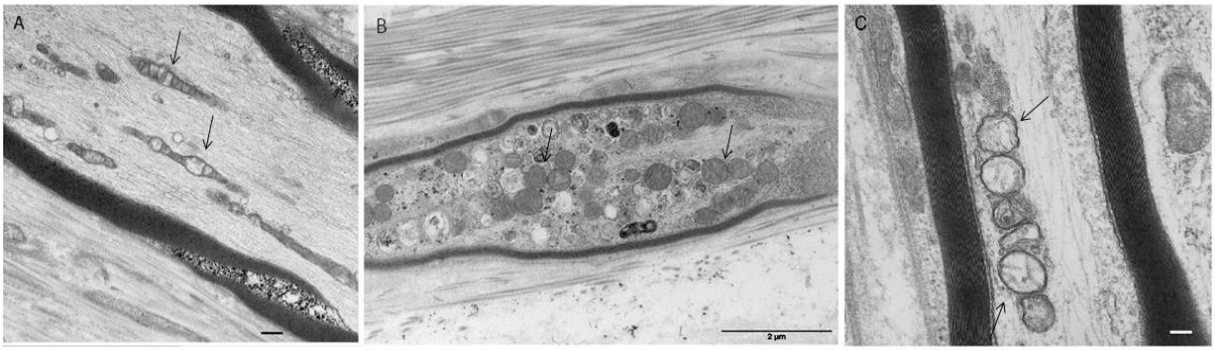

Figure 33 Electron microscopy on sural nerve sections. Mitochondria are indicated by black arrows. (A) Normal control with elongated mitochondria. Scale bar = 0.5 µm [From (Vallat et al. 2008)*]. (B) CMT4A patient (GDAP1 mutation not specified) with small, round, and aggregated mitochondria. Scale bar = 2 µm [from:* (Tazir et al. 2014)*]. (C) CMT2A patient (MFN2 compound heterozygous p.Asp214Asn and p.Cys390Arg mutations) with small, round, and aggregated mitochondria. Scale bar = 0.2 µm [From:*(Vallat et al. 2008) *].*

IV.4.3. GDAP1 and autosomal dominant forms of CMT disease (AD-CMT)

IV.4.3.1. AD-mutations

Autosomal dominant mutations in *GDAP1* are less frequently described, and they are, so far, always missense mutations. In this case, the alteration of a single allele is enough to induce the occurrence of the pathological phenotype. Dominant mechanisms are not always fully understood, but we can suppose that the mutated protein modifies some of its functional activities. Specifically, in human fibroblasts, carrying the AD p.Cys240Tyr mutation, a defect of ETC Complex I activity, as well as the increase of ROS, have been reported. This would reduce cellular ATP production and favor the

establishment of a chronic oxidative stress in the affected cells (Cassereau et al. 2009; 2020). Anyway, any of these alterations have been observed in fibroblasts carrying the AD p.Arg120Trp mutation, suggesting that mechanisms involved in the physiopathology may depend on mutation's localization (Cassereau et al. 2020). In transfected Cos-7 cells, the expression of GDAP1 p.Arg120Trp and Thr157Pro mutants, did not alter mitochondrial fission, as shown for AR-mutations, but it impaired mitochondrial fusion and destabilized the ΔΨm, making Cos-7 more susceptible to apoptosis (Niemann et al. 2009). Lastly, we cannot exclude a gain-of-function effect due to autosomal dominant *GDAP1* mutations. González-Sánchez *et al.* reported that p.His123Arg, p.Thr157Pro and p.Arg120Trp mutations are associated to an increased activity of SOCE, compared to wild-type GDAP1 expression (González-Sánchez et al. 2017).

IV.4.3.2. AD-CMT

Autosomal dominant CMT, associated with *GDAP1*, are normally reported as axonal forms, and they are known as CMT2K. They seem to be rarer and characterized by a milder phenotype, than recessively-inherited CMT, with symptoms onset generally during the second or third decade. However, a high variability has been described in CMT2K patients, as regards the age of onset and the symptoms' manifestation (Zimon et al. 2011). Generally, first signs appear as cramps, weakness and deformities in distal limbs, provoking walking difficulties. The progression of the disease is slower, and patients requiring wheelchair are often in old age. Respiratory complications and vocal cord paresis are described in sporadic cases (Sivera et al. 2017).

Although the relevant heterogeneity, the electrophysiological analysis, conducted on CMT2K patients, usually reveals normal NCV values, higher than 38 m/s. CMAP amplitudes are reduced (Zimon et al. 2011; Sivera et al. 2017).

Histological examinations have shown the predominant, but not pure, axonal nature of CMT2K. Light and electron microscopy on nerve biopsies have allowed to observe that the overall density of nerve

fibers was not significantly reduced in CMT2K patients. Anyway, they typically presented loss of large myelinated fibers, and presence of onion bulb structures, which revealed a demyelinating aspect of this autosomal dominant CMT form (Figure 34A and 34B). Another peculiar feature remarked is the accumulation of neurofilaments in giant unmyelinated axons (Figure 34C) (Fu et al. 2017).

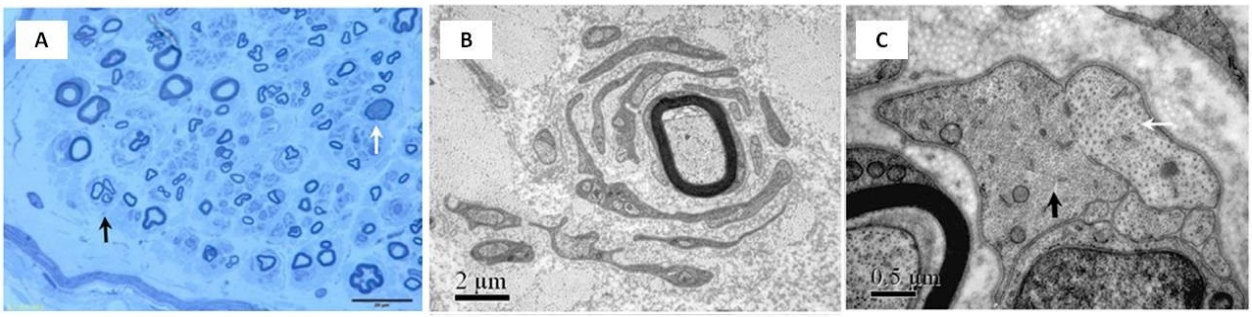

Figure 34 Histological findings in a semithin section of sural nerve biopsy, from a CMT2K patient with the heterozygous p.Arg120Trp mutation in GDAP1. (A) Loss of large myelinated fibers with regenerating clusters (black arrow) and abnormal structure of the axon (white arrow). Scale bar = 20 µm. (B) Onion bulb formation. Scale bar = 2 µm. (C) Neurofilaments' aggregation in giant axons (black arrow), compared with normal axons (white arrow). Scale bar = 0.5 µm. [From (Fu et al. 2017)].

IV.5. GDAP1 models

Expression studies have revealed that *GDAP1* is mainly expressed in neural cell types, like central and peripheral neurons, and Schwann cells (Niemann et al. 2005; Pedrola et al. 2005). Additionally, mutations in *GDAP1* have been only associated to Charcot-Marie-Tooth disease, a group of heterogeneous disorders affecting the peripheral nervous system. It is clear, therefore, that human neurons represent the most suitable model to investigate GDAP1-associated functions and implications in CMT physiopathology. They could be also important to evaluate and test potential therapeutic molecules and strategies. Anyway, peripheral human neurons cannot be easily obtained from CMT patients. That is why animal and cellular models have been developed to reproduce

GDAP1 expression and mutations, then to explore molecular mechanisms responsible for CMT manifestation.

IV.5.1. Animal models

Mice constitute the most employed animal model for GDAP1. Two research teams have generated, at the same time, *GDAP1* knock-out mice (*Gdap1-/-*), using the Cre-Lox recombination strategy, on two different sites (Niemann et al. 2014; Barneo-Muñoz et al. 2015).

Niemann *et al.* observed first signs of peripheral neuropathies when mice were 19-month-old and characterized by 25% reduced NCV. Histological studies confirmed a hypomyelination status in distal nerves. Furthermore, the study of axonal mitochondria revealed, in *Gdap1-/-* mice, increased mitochondrial size and altered mitochondrial transport, in anterograde and retrograde directions (Niemann et al. 2014).

The second *GDAP1* knock-out murin model was developed by a Spanish team. In this case, first motor problems appeared at the age of 3 months. In 5-month-old mice, CMAP amplitude was reduced, but no alteration in axons' number and organization, as well as in myelin thickness, was detected. However, motor neurons were demonstrated to be less healthy than control MN, and characterized by cellular lesions as vacuoles and chromatolysis. Ultrastructure analysis showed the presence of spheroid and larger mitochondria, with swollen cristae, but also vacuoles and phagolysosomes. A functional level, *Gdap1-/-* MN had a reduced cytosolic Ca^{2+} concentration and impaired Ca^{2+} homeostasis (Barneo-Muñoz et al. 2015).

Another *GDAP1* animal model was created using *Drosophila*, because it presents an orthologous gene of *GDAP1*, called *CG4623* (or *Gdap1*, in this study), which could be over-expressed, or silenced by RNA interference (RNAi). First, in both models, López del Amo *et al.* confirmed Gdap1 involvement in regulation of mitochondrial morphology and distribution. Smaller or aggregated mitochondria

were observed, respectively, when *Gdap1* was over-expressed or silenced, indicating, thereby, its role in mitochondrial fission (López Del Amo et al. 2015). Later, they demonstrated that alteration of *Gdap1* expression alters the energy metabolism, in particular at proteins', carbohydrates' and lipids' level. Specifically, it seems that *GDAP1* up- or down-regulation would induce the inactivation of the insulin pathway, and, consequentially, the accumulation of carbohydrates and the use of lipids as energy source (López del Amo et al. 2017).

A third GDAP1 model type has been proposed on the *Saccharomyces cerevisiae* yeast, by Estela *et al.*, in 2011, and Rzepnikowska *et al.*, in 2020 (Estela et al. 2011; Rzepnikowska et al. 2020).

In Estela's study, employed yeasts were defective for genes involved in mitochondrial fission and fusion. Even if *GDAP1* expression did not restore normal mitochondrial morphology in defective *S. cerevisiae*, the analysis allowed to highlight the interaction between GDAP1 protein and cytoskeleton's β-tubulins (Estela et al. 2011).

In a second yeast model, Rzepnikowska *et al.* expressed wild-type *GDAP1*, but also eight different *GDAP1* variants, carrying eight AR or AD pathological mutations, already associated with CMT disease. Some of studied mutations were shown to alter mitochondrial network structure, and/or increase the rate of mitochondrial DNA escape to the nucleus, which seems to be representative of mitochondrial abnormalities (Rzepnikowska et al. 2020).

Animal models have a fundamental role to explore a gene/protein expression, and to look for its WT or mutant effects, on the whole organisms. However, as we have seen here, some differences may emerge between two models generated in different species, but also between two models of the same animal species. Moreover, the animal physiology and pathophysiology could, sometimes, be far from real mechanisms in humans.

IV.5.2. Cellular models

Cellular models have allowed to detect and describe most of GDAP1 features and functions. They have been obtained from different cell types: primary cells, directly isolated from tissues or organs of living organisms; cells lines, immortalized cells which can proliferate for extended periods of time; human induced-pluripotent stem cells (hiPSC), generated by reprogramming of somatic cells.

IV.5.2.1. Primary cell cultures

Cells directly obtained from human or murine biopsies have been used, in some cases, as models for *GDAP1*. For humans, neural cells are not available, that's why the only studies were performed on dermal fibroblasts. Fibroblasts can be easily obtained from CMT patients, cultured, amplified, and employed for functional tests. The main limit of this strategy is that *GDAP1* is little, or no, expressed in fibroblasts, so this cell type could not show all the GDAP1-associated features. Cassereau *et al.* have worked on skin fibroblasts, obtained from CMT2K patients, carrying either the heterozygous p.Cys240Tyr or the heterozygous p.Arg120Trp mutations in *GDAP1* (Cassereau et al. 2009; 2020).
Other times, primary neural cell cultures were obtained from animals, in particular hippocampus and dorsal root ganglia neurons, from mice, and Schwann cells, from rats (Niemann et al. 2005; Pedrola et al. 2008; Huber et al. 2013).

IV.5.2.2. Cell lines cultures

Cell lines are immortal cells, largely used in research. They are generally easy to culture, amplify, and modify, providing an unlimited supply of cellular models. Cell lines can be originated from different tissues, and different organisms. In the studies on GDAP1, sometimes they have been used in their original state, sometimes they have been transfected to enable *GDAP1* expression.

SH-SY5Y are human neuroblastoma cells, that, given their neural origin, normally express *GDAP1*. They have been employed to detect GDAP1 protein localization in the cell, or to investigate the effects of *GDAP1* silencing, or knock-down, in a neural cell (Pedrola et al. 2005; Pla-Martín et al. 2013; González-Sánchez et al. 2017). In the same way, N1E-115 cells from mouse neuroblastoma, endogenously expressing *GDAP1*, have also been used (Niemann et al. 2005; 2009).

Cos-7 cells are fibroblast-like cells, derived from kidney tissue of monkeys. Normally, they do not express GDAP1. However, in many works, they have been transfected, with a *GDAP1*-expressing construct, in order to analyze which morphological and functional aspects are linked to GDAP1, and how they can be modified by mutant GDAP1 forms (Pedrola et al. 2005; Niemann et al. 2005; K. Wagner et al. 2009).

Other analysis have be conducted of different cell lines, like HeLa, HT22, HEK293T (Niemann et al. 2009; Noack et al. 2012; González-Sánchez et al. 2017).

IV.5.2.3. hiPSC cultures

hiPSC have the same features of human embryonic stem cells (hESC). The main advantage of hiPSC is that they can be easily obtained from adult cells, like fibroblasts, trough a "reprogramming" procedure, and, then, they can be potentially differentiated into any kind of human body's cell (Takahashi and Yamanaka 2006; Takahashi et al. 2007). This strategy has been exploited to obtain hiPSC from dermal fibroblasts of a CMT2K patient, carrying the heterozygous p.Gln163*/p.Thr288AsnfsX3 *GDAP1* mutations (Martí et al. 2017), and from a CMT4 patient with the heterozygous p.Leu193*/p.Arg341fs *GDAP1* mutations (Saporta et al. 2015). The same protocol has been also applied to generate murine iPSC from mouse embryonic fibroblasts (MEF) of *GDAP1*-null mice (Prieto et al. 2016). Anyway, it seems that, in all these cases, studies stopped at the stage of hiPSC, which were not differentiated in neurons, or other suitable cell types. No further works on iPS and *GDAP1* have been published since.

iPSC rest a relevant tool to recreate and cultivate human neurons, the most suitable cellular model for *GDAP1*. It is for this reason that, in the present study, we developed a cellular model of hiPSC-derived motor neurons, to investigate *GDAP1* functions and its involvement in CMT disease.

Objectives

This project entirely focused on Charcot-Marie-Tooth disease and associated peripheral neuropathies. In particular, it has been conceived with the purpose of better characterize this complex pathology affecting the peripheral nervous system with a frequency of 1/2500. In order to explore multiple aspects of CMT, we set two main objectives:

I – First, we wanted to improve the genetic diagnosis of CMT and hereditary peripheral neuropathies, which has currently a rate of resolution between 30 and 40%. We proposed a bioinformatic tool, CovCopCan, to promote the detection of Copy Number Variation (CNV) in CMT genes (Article 1). CNV have been rarely described to be responsible for CMT. Thus, we questioned about CNV occurrence in CMT, to understand if they could be more frequent than expected (Article 2). This study had also the objective to investigate the correlation between genotypic set-up and phenotypic manifestation in complex clinical cases of CMT (Article 3). This examination could be important to highlight never considered mechanisms behind the disease, which could help the diagnostic process. For all these analyses we exploited NGS technologies, "classical" molecular biology strategies, and bioinformatic tools. This part of the project was achieved thanks to the collaboration of the Biochemistry and Molecular Genetics Department of University Hospital of Limoges with our research team (EA6309), at University of Limoges.

II – The second part was definitely the central core of this project, since it has been developed for three years, in a continuous way. Its objective was to explore the molecular mechanisms associated with a specific axonal form of CMT disease, caused by a homozygous mutation in *GDAP1* gene. This part of the project was achieved thanks to the collaboration of the Neuropathies' Center of Reference of University Hospital of Limoges with our research team (EA6309), at University of Limoges. To reach our primary goal, we had to define two sub-objectives. First, we had to create a suitable cellular model to reproduce the human pathology. To do this, we cultivated dermal fibroblasts of the CMT patient and two control subjects, and reprogrammed them in human induced-

pluripotent stem cells (hiPSC). A differentiation protocol was then established to differentiate hiPSC into motor neurons, the most affected cells in this axonal CMT (Article 4). We also considered the role of additional factors, like the 1,25-Dihydroxyvitamin D3, or calcitriol, which can be included, in the future, in our differentiation protocol (Article 5). Secondly, after obtaining this model of MN, we wanted to discover the pathophysiological mechanisms, induced by *GDAP1* mutation, and responsible for the neural impairment and degeneration in the peripheral nervous system. Expression, morphological, and functional studies were so performed on MN of the three subjects (Article 6).

Overall, the present PhD project has been aimed at the exploration of CMT disease, from its genetic and clinical aspects, to the more complex functional characterization. Moreover, we developed a cellular model of MN, with the purpose to employ it in testing future innovative therapeutic strategies, still limited so far, for peripheral neuropathies.

Materials and Methods

I. Subjects

This study involved four groups of patients, and five control subjects.

Family 1

Family 1 presented two clinical cases: Patient 1-A and his brother, Patient 1-B (Figure 35). Patient 1-A was a 19-year old man, characterized by peripheral neuropathy and cerebellar ataxia. He showed abolished sensory reflexes, altered motor velocities, with a MNCV of 38 m/s on the median nerve. *Pes cavus* and abolished Achilles reflex were also observed. The 9-year old Patient 1-B presented peripheral neuropathy and motor disabilities, associated to balance troubles. Achilles reflex was diminished, too. Their not consanguineous parents, subjects 1-C (father) and 1-D (mother), were unaffected.

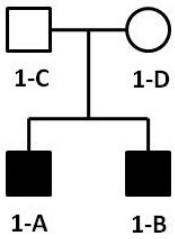

Figure 35 Pedigree of Family 1.

Family 2

In Family 2, Patient 2-A (mother) and Patient 2-B (daughter) were diagnosed with Charcot-Marie-Tooth type 2 disease (Figure 36). For Patient 2-A, a 58-year old woman, first difficulties in walking appeared at the age of two, to rapidly progress in loss of motor function, when she was 43. Clinical examination revealed, in lower limbs, abolished sensory responses and reduced motor responses, while the MNCV was 40 m/s. CMAP amplitudes were asymmetric. Her daughter, the Patient 2-B, was

born from not consanguineous parents. She was a 25-year old woman, exhibiting her first gait disturbances when she was 18-months. Moreover, she had learning difficulties and signs of mental retardation in the childhood. She presented the same asymmetric profile of her mother, with CMAP amplitudes abolished on the left side, and reduced on the right side. The MNCV, of the median nerve, was 50 m/s. Muscular atrophy and mild vermian atrophy were also observed.

No clinical signs were reported for the other members of Family 2, like subjects 2-C, 2-D, and 2-E, the maternal grand-mother and the maternal aunts of patient 2-B, respectively.

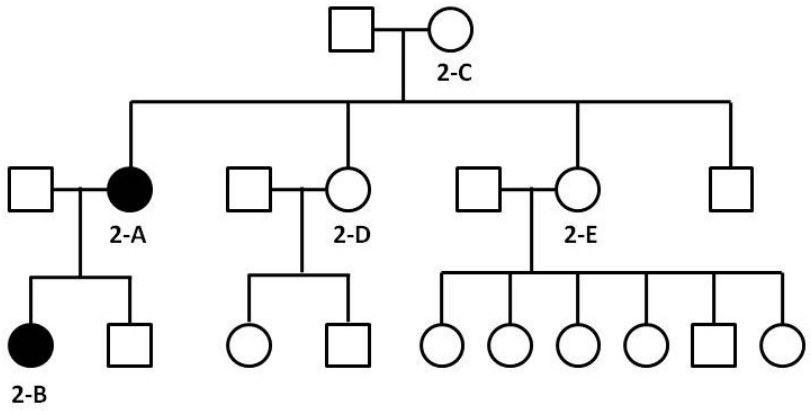

Figure 36 Pedigree of Family 2.

Family 3

In Family 3, two cases of Charcot-Marie-Tooth type 2 were reported (Figure 37). Patient 3-A was born in 2012 and showed severe axonal neuropathy associated with a polyvisceral disorder. His complex clinical condition led him to death when he was three. His brother, 4-year old, was characterized by motor deficit in lower limbs, distal atrophy, and abolition of deep tendon reflexes. Signs of mental retardation were also described. Patients 3-A had also an asymptomatic elder brother. His parents, unaffected, had first-degree of consanguinity.

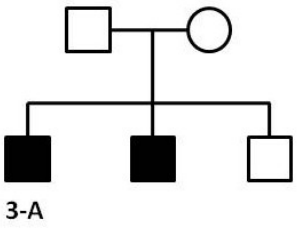

Figure 37 Pedigree of Family 3.

Family 4

Patient 4-A was a 23-year old man, experiencing, in the childhood, first motor difficulties, above all in lower limbs. They were followed by sensory troubles and weakness in the hands. After some years, progression of motor impairment led to the need of wheelchair. No response was obtained when muscles were stimulated in EMG analysis. Genealogic tree of Family 4 was not available.

Control subjects

We chose, as controls, five, seemingly healthy, subjects, two men and three women. Four of them were between 23- and 28-year old, the fifth was 56-year old.

II. Cell culture

II.1. Culture media

The detailed composition of main culture media is reported here:

Fibroblasts medium: RPMI 1640 medium (Thermo Fisher SCIENTIFIC), supplemented with 10% Fetal Bovine Serum (FBS) (Thermo Fisher SCIENTIFIC).

Mouse Embryonic Fibroblasts (MEF) medium: MEMα medium + GlutaMAX (Thermo Fisher SCIENTIFIC), supplemented with 10% FBS, 1% MEM non-essential amino acids (Thermo Fisher SCIENTIFIC), 0.1% Gentamycin (Thermo Fisher SCIENTIFIC).

Reprogramming medium: DMEM GlutaMAX medium (Thermo Fisher SCIENTIFIC), supplemented with 10% FBS, 1% MEM non-essential amino acids, 1% Sodium Pyruvate (Thermo Fisher SCIENTIFIC).

Human induced-Pluripotent Stem Cells (hiPSC) medium: KnockOut medium (Thermo Fisher SCIENTIFIC), supplemented with 20% KnockOut Serum Replacement (KSR) (Thermo Fisher SCIENTIFIC), 1% L-Glutamine (Thermo Fisher SCIENTIFIC), 1% MEM non-essential amino acid, 0.1% β-mercaptoethanol, 0.1% Gentamycin.

Differentiation medium: DMEM/F12 medium (Thermo Fisher SCIENTIFIC), 2% B27 supplement without Vitamin A (Thermo Fisher SCIENTIFIC), 5 µg/mL Heparin (Sigma-Aldrich, Merck), 0.1% β-mercaptoethanol (Thermo Fisher SCIENTIFIC).

Neural medium: 1:1 DMEM/F12 medium and Neurobasal A medium (Thermo Fisher SCIENTIFIC), supplemented with 2% B27 supplement without Vitamin A, 1% N2 supplement (Thermo Fisher SCIENTIFIC), and 0.1% β-mercaptoethanol.

II.2. Fibroblasts culture

Skin biopsies (1 mm^2) were obtained from five control subjects and two CMT patient (patient 3-A and patient 4-A), carrying respectively the homozygous mutation p.Ser194* and the homozygous mutation p.Gln163* in *GDAP1* gene. They were plated in 6-well plates, and cultured in CHANG Medium® D (Irvine Scientific) with 10% FBS, at 37°C in a water-saturated atmosphere with 5% CO_2. Medium was changed every two days. Two weeks later, after removing skin biopsies, surrounding fibroblasts were detached using 0.05% Trypsin EDTA solution (Thermo Fisher SCIENTIFIC), incubated 5 minutes at 37°C. Trypsin was inactivated with the complemented medium, and the cellular suspension collected and centrifuged 7 minutes at 200 x g. Supernatant was discarded and cells of the pellet were re-plated in a culture flask, to be amplified. Fibroblasts were first cultured in CHANG Medium® D 10% FBS, which was diluted, after three days, with RPMI 1640 medium (Thermo Fisher SCIENTIFIC), and finally replaced, after a week, by Fibroblasts medium. Fibroblasts were negative for mycoplasma (MycoAlert mycoplasma detection kit, Lonza).

II.3. Human induced-Pluripotent Stem cells (hiPSC) generation and culture

For hiPSC generation the iSTEM (INSERM / UEVE UMR 861, AFM-Téléthon, Genopole, Evry, France) protocol was followed. Fibroblasts were detached with Trypsin-EDTA solution and counted. Suspension of 600,000 fibroblasts was mixed with the Nucleofection mix solution and the plasmids mix. Plasmids mix was composed of three non-integrating plasmids, at 1 µg/mL concentration: Plasmid #27077 pCXLE-hOCT3/4-F shp53 Addgene, Plasmid #27078 pCXLE-hSK Addgene, Plasmid #27080 pCXLE- Hul Addgene. Nucleofection was performed with the Nucleofector II device (Amaxa, Lonza). Transfected cells were transferred in a 6-well plate, coated with Mouse Embryonic Fibroblasts (MEF) (tebu-bio), at a concentration of 25,000 MEF/cm^2. Cells were cultured in the

Reprogramming medium, adding, after the second day, 10 UI/mL gentamycin (Thermo Fisher SCIENTIFIC). They were incubated at 37°C, 5% CO_2, in a water-saturated atmosphere. At day 4, medium was replaced by the hiPSC medium, extemporaneously supplemented by 10 ng/mL FGF2 (Fibroblast Growth Factor 2) (Peprotech), 2 µM SB431542 (Tocris Bioscience), 0.5 µM PD0325901 (Miltenyi Biotech) et 500 µm Valproate (Sigma-Aldrich, Merck). It was changed every two days. At day 14 to 21 after nucleofection, 10-15 hiPSC colonies per patient were selected using a 25G needle and transferred to different MEF-coated culture dishes. Every day, hiPSC were "cleaned", removing differentiated cells with a 26G needle, and hiPSC medium was changed, extemporaneously complemented with 20 ng/mL FGF2. hiPSC colonies were passed once a week, cutting them with a 18G needle, to be amplified. At passage 15 all quality controls were performed: Alkaline Phosphatase staining, Pluripotence and Differentiation markers' staining, EB formation, Array-comparative genomic hybridization (aCGH) (detailed protocols in parts 3 and 4).

II.4 Motor neurons (MN) generation and culture

At day 0 of differentiation, two 60 mm culture dishes of hiPSC were cut in small squares using a 18G needle, and re-suspended using a pipette. Squares were transferred to a 15 mL tube in order to let them sediment at the bottom, and discard supernatant containing death cells and residual MEF. They were then collected with fresh hiPSC medium, without FGF2, and cultivated in 60 mm Ultra-Low Attachment dishes. At day 3/5, when Embryonic Bodies (EB) were well-formed, the hiPSC medium was replaced the Differentiation medium, adding, before use, 10 µM SB431542, 5 µM Dorsomorphin (Sigma-Aldrich, Merck), 100 ng/mL FGF2, and 10 ng/mL Noggin (PeproTech). Once EB have reached the right size and color, they need to be seeded. For this step a poly-L-ornithine/laminine coating was prepared. First, 20 µg/mL poly-L-ornithine (Sigma-Aldrich, Merck) solution was prepared in Boric Acid pH 8.4 buffer, and incubated in 3 mm or 6 mm dishes at 37°C, for, at least, 4 hours. Poly-L-ornithine solution was discarded, and dishes let dry, opened, under the hood. They were so washed three

times with Dulbecco's phosphate-buffered saline (DPBS), and let dry again. Laminine (Thermo Fisher SCIENTIFIC) was diluted, in a DMEM/F12 medium - Neurobasal A medium mix, to a final concentration of 20 µg/mL. It was added to dried dishes and incubated at 37°C, for, at least, 2 hours. On day 5/7, EB were plated in poly-L-ornithine/laminine-coated dishes, in Neural medium, extemporaneously complemented with 10 µM SB431542, 5 µM Dorsomorphin, 10 µM Retinoic Acid (RA) (Sigma-Aldrich, Merck), and, only when EB were seeded, 5 µM Y-27632 ROCK inhibitor (Calbiochem Millipore, Merck). It was changed every two days. At day 10/14, neural "rosettes", emerged in seeded EB, were picked up using a 25G needle, and collected in a tube. Once they sedimented, supernatant was discarded, and 1 mL 0.05% Trypsin-EDTA solution was added to allow rosettes' disaggregation. Cellular clusters were incubated at 37°C for 5 minutes to favor enzymatic activation, then softly dissociated with a mechanic action. In order to stop trypsin's activity, Neural medium, complemented with 10% FBS, was added to cellular suspension, which was then centrifuged at 200 x g for 5 minutes. Cellular pellet was resuspended with Neural medium, extemporaneously supplemented with 5 µM RA, 100 ng/mL Sonic Hedgehog (Shh) (PeproTech), 10 ng/mL Insulin-like Growth Factor 1 (IGF-1), 10 ng/mL Brain-Derived Neurotrophic Factor (BDNF), 10 ng/mL Glial cell-Derived Neurotrophic Factor (GDNF), and 5 µM Y-27632 ROCK inhibitor. Rosettes-derived neural progenitors (NP) were seeded at high density (>100,000 cells/cm^2), and passed every 3/4 days in poly-L-ornithine/laminine coated dishes. To induce the final differentiation of NP in motor neurons (MN), they were seeded at low density, between 20,000 and 30,000 cells/cm^2, in poly-L-ornithine/laminine coated dishes, and cultured in Neural medium, as previously described.

Table 3 Culture conditions of hiPSC differentiation into motor neurons.

Time (Days)	D -1	D 0	D 3/5	D 5/7	D 10/14	D 14/30	D 30/40
	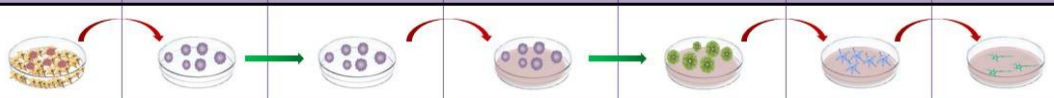						
Culture	Induced Pluripotent Stem cells (iPSc)	Embryonic Bodies (EB)	Embryonic Bodies (EB)	Embryonic Bodies (EB)	Rosettes	Neural Progenitors (NP)	Motor Neurons (MN)
Coating	Mouse Embryonic Fibroblasts (MEF)	/	/	20 µg/mL Poly-L-ornithine 20 µg/mL laminine	20 µg/mL Poly-L-ornithine 20 µg/mL laminine	20 µg/mL Poly-L-ornithine 3 µg/mL laminine	20 µg/mL Poly-L-ornithine 3 µg/mL laminine
Medium	hiPSC medium	hiPSC medium	Differentiation medium	Neural medium	Neural medium	Neural medium	Neural medium
Supplementary factors	20 ng/mL FGF2	/	10 µM SB431542, 5 µM Dorsomorphin 100 ng/mL FGF2 10 ng/mL Noggin	10 µM SB431542, 5 µM Dorsomorphin 10 µM RA	10 µM SB431542, 5 µM Dorsomorphin 10 µM RA	5 µM RA 100 ng/mL Shh 10 ng/mL IGF-1 10 ng/mL BDNF 10 ng/mL GDNF	5 µM RA 100 ng/mL Shh 10 ng/mL IGF-1 10 ng/mL BDNF 10 ng/mL GDNF

III. Molecular Biology

III.1. DNA

III.1.1. DNA Extraction

DNA was extracted either from blood either from *in vitro* cultured cells.

III.1.1.1. DNA Extraction from blood

Blood samples were collected in EDTA tubes, after providing informed consent (Families 1 and 2). Genomic DNA was extracted from white blood cells using the Illustra Nucleon Genomic DNA Extraction kit (GE Healthcare Life Sciences), following manufactory instructions. DNA extraction was carried out at Biochemistry and Molecular Genetics Department of University Hospital of Limoges.

III.1.1.2. DNA Extraction from cell culture

Genomic DNA was extracted from fibroblasts and hiPSC, using the Puregene Tissu kit (©QIAGEN) (Families 3 and 4, and controls). Cells of the dried pellet were lysed in the Lysis Buffer, incubated at 65°C for 15 minutes, then two minutes at 55°C. After adding the Proteinase K, the sample was again incubated at 55°C for 15 minutes. Then, RNA was degraded by the RNase A, and proteins were precipitated with the Protein Precipitation solution. After centrifugation, at 13,000 x g for 3 minutes, DNA-containing supernatant was transferred to a new tube, while protein pellet was discarded. Lastly, DNA was precipitated with Isopropanol 100%, isolated by centrifugation, washed once with ethanol 70%, and resuspended in 1X TE low EDTA buffer.

DNA concentration and purity were assessed using the NanoDrop 2000 spectrophotometer (Thermo Fisher SCIENTIFIC). Extracted DNA was conserved at -20°C.

III.1.2. Sanger Sequencing

Sanger Sequencing was performed in multiple steps. First, sequence of interest was amplified with a Polymerase Chain Reaction (PCR). Primers were designed using the Human GHCh37/hg19 genome as reference genome. Their sequences are reported in Table 4.

Table 4 MFN2, MORC2, and GDAP1, primers for Sanger Sequencing.

Gene	Transcript ID in Ensembl Genome Browser	Position in the gene	Sequence (5'->3')	Melting Temperature	Product size
MFN2	ENST00000235329.5	Ex 14	F: GTCAGCCTTCTGGGGTCAC	62°C	277 bp
			R: AAAGTCCTGATTTCTTTAGCTTG	62°C	
MORC2	ENST00000215862.4	Ex 11	F: GTGTCCAGTACTGTGGATCC	62°C	572 bp
			R: CAACCTGTCAATAATCAGTCC	60°C	
GDAP1	ENST00000220822.7	Ex 1	F: CCGGCGAAACTACATTTCC	58°C	328 bp
			R: TCAGAAGGAGCTGTCCCAGT	62°C	
		Ex 2	F: GTAACACAGGGAAGCCCAGA	62°C	413 bp
			R: CCAAACCACCATCATGACAC	60°C	
		Ex 3	F: GCTTTTGAGTGTAACAACTCATG	64°C	317 bp
			R: GACCATGAGACATGCTAGGTC	64°C	
		Ex 4	F: TGGTTCCATTTGAAAGGTGAG	60°C	417 bp
			R: AAAAGGAGAACATAAGCCAAAGG	64°C	
		Ex 5	F: TCTCGTTGTCTAAAATAGGCTGA	64°C	393 bp
			R: GGGTTTTTCTGGGTGCAATA	58°C	
		Ex 6	F: TCTGAGTGTGGCTGTCAAGAA	62°C	691 bp
			R: TGCTACCTGAACCCCTGTGT	62°C	

Samples were amplified with a positive and a negative control. Reactions were performed in the Mastercycler (Eppendorf®), setting standard parameters.

Amplifications products were displayed on a 1.5% agarose gel. Migration of samples and molecular weight maker (Gene Ruler 100 pb RTU, Fermentas, Thermo Fisher SCIENTIFIC) was run at 100 V for 20-30 minutes. Before performing the Sanger sequencing, PCR products were purified using the QIAquick gel extraction kit (© QIAGEN). Sequencing reactions were prepared with forward or reverse primers, and the BigDye® Terminator v3.1 Cycle Sequencing Kit (Thermo Fisher SCIENTIFIC). Lastly, after products' purification with the DyeEx 2.0 Spin Kit (© QIAGEN), sequencing was run on the Applied Biosystems 3130 xl Genetic Analyzer (Applied Biosystems), and sequences aligned and analyzed with the Sequencher 4.7 software.

III.1.3. Targeted NGS – CMT Panel

For the NGS analysis, a panel of 93 genes was used. 44 of them are known to be involved in Charcot-Marie-Tooth disease, 27 in Hereditary Sensory Neuropathies (HSN) and Hereditary Motor Neuropathies (HMN), and 22 in neuropathies of differential diagnosis. Their complete list is reported in Table 5.

Table 5 93-gene custom panel for CMT and hereditary neuropathies [R = recessively-inherited; D = dominantly-inherited].

GENE	CMT1D	CMT2D	CMT1R	CMT2R	HMN D	HMN R	HSN D	HSN R	Other
AARS		X							
ABHD12									R
AIFM1				X					
ARHGEF10									D
ATL1							X		
ATL3							X		
ATP7A						X			
BICD2					X				
BSCL2					X				
CCT5								X	
CTDP1								X	
C12ORF65									R
DCAF8									D
DCTN1					X				
DHTKD1		X							
DNAJB2				X					
DNM2	X	X							
DNMT1							X		
DST								X	
DYNC1H1		X							
EGR2	X		X						
FAM134B								X	
FBLN5									D/R
FBXO38					X				
FGD4			X						
FIG4			X		X				
GAN									R
GARS		X			X				
GDAP1		X	X	X					
GJB1	X	X							
GJB3									D/R
GNB4	X	X							
HARS		X							
HINT1									R
HK1			X						
HSPB1		X			X				
HSPB3					X				
HSPB8		X			X				
IFRD1									D
IGHMBP2				X		X			
IKBKAP								X	
INF2	X	X							
KARS			X	X					
KIF1A								X	
KIF1B		X							
KIF5A									D
LITAF	X								
LMNA				X					
LRSAM1		X							
MARS		X							
MED25				X					

GENE	CMT1D	CMT2D	CMT1R	CMT2R	HMN D	HMN R	HSN D	HSN R	Other
MFN2		X							
MPV17									R
MPZ	X	X	X						
MTMR2			X						
NDRG1			X						
NEFL	X	X							
NGF								X	
NTRK1								X	
PDK3		X							
PLEKHG5			X	X		X			
PMP22	X								
POLG									D/R
PRPS1				X					
PRX			X						
RAB7A		X							
REEP1					X				
SACS									R
SBF1			X						
SBF2			X						
SCN9A								X	
SCN10A							X		
SCN11A							X		
SEPT9									*D*
SETX					X				
SH3TC2			X						
SLC12A6									R
SLC5A7					X				
SMAD3									D
SOX10									D
SPTLC1							X		
SPTLC2							X		
SURF1			X						
TFG									D
TRIM2				X					
TRPV4		X			X				
TTR									D
TUBB3									D
UBQLN2					X				
VAPB									D
VCP									D
WNK1								X	
YARS	X	X							

Libraries were prepared using the Ion P1 HiQ Template OT2 200 kit (Ampliseq Custom, Life technologies), and sequenced on the Ion Proton sequencer (Life technologies), at Biochemistry and Molecular Genetics Department of University Hospital of Limoges.

III.1.4. Whole Exome Sequencing (WES)

For WES, genomic DNA was first fragmented using the Bioruptor® Pico Sonication System (Diagenode), to obtain fragments of 180-220 bp. Then, libraries' preparation, capture and

amplification, were performed with the NimbleGenSeqCapEZ-Library-SR-kits (Roche). Finally, libraries were sequenced on the NextSeq 500 System (Illumina®).

III.1.5. Real-Time Quantitative PCR (qPCR)

Relative qPCR on DNA was performed in order to confirm the occurrence of Copy Number Variations (CNV). Primers were designed in target genes, *AARS1* and *SACS*, and in a reference gene, *Albumin* (*ALB*), on Human reference genome GHCh37/hg19. Sequences of forward and reverse primers are reported in Table 6.

Table 6 ALB, AARS1, and SACS, primers for qPCR.

Gene	Transcript ID in Ensembl Genome Browser	Position in the gene	Sequence (5'->3')	Melting Temperature	Product size
ALB	ENST00000295897.4	Ex 1	F: ACACGCCTTTGGCACAATGA	60°C	90 bp
			R: TCTCGACGAAACACACCCCT	62°C	
AARS1	ENST00000261772.8	Ex 8	F: GTGTTGAGACGGATTCTCCG	62°C	93 bp
			R: GACAACATCCACTAACGTAGC	62°C	
SACS	ENST00000382298.3	Ex 8	F: GCAGGTGTACTTCTCAGAAC	60°C	117 bp
			R: AACAGCAGCATCCACATTCC	60°C	
		Ex 9	F: GATGATTGCTGTTCCTTTCC	58°C	88 bp
			R: AGGTGAGGTTTCAAGTTATCC	58°C	
		Ex 10	F: TGTGTGTACAACAACCAGCC	60°C	112 bp
			R: ATCCTATTCCATACTGTCCAG	60°C	

Reactions were prepared with the Rotor-Gene SYBR Green PCR Kit (400) (©QIAGEN), and performed on the Corbett Rotor-Gene 6000 Machine (© QIAGEN).

Resulting Ct values of target genes were first normalized using *Albumin* as endogenous control gene. Then, normalized Ct of patients (V1) were compared to normalized Ct of control subjects (V2), applying the following formulas:

$$V1 = \frac{2^{-(Ct\ target\ gene\ in\ patient)}}{2^{-}\ (Ct\ reference\ gene\ in\ patient)}$$

$$V1 = \frac{2^{-(Ct\ target\ gene\ in\ control)}}{2^{-}\ (Ct\ reference\ gene\ in\ control)}$$

$$X = \frac{V1}{V2}$$

All reactions were performed in triplicate.

III.1.6. Array Comparative Genomic Hybridization (aCGH)

For Array Comparative Genomic Hybridization, DNA samples were denatured and labeled, by random priming, with fluorescent dyes. Genome to be tested and reference genome were differently tagged with Cyanine 5 (Cy5, Red) or Cyanine 3 (Cy3, Green), then mixed together. After purification, samples were hybridized, for 24 hours, on G3 Human CGH microarrays 8x60K (Agilent Technologies) and analyzed with the Agilent CytoGenomics software (Agilent Technologies). aCGH was carried out at the Department of Cytogenetics of University Hospital of Limoges.

III.2. RNA

III.2.1. RNA extraction

Total RNA was extracted from fibroblasts, hiPSC, NP, and MN, using the miRNeasy Mini kit (©QIAGEN). After lysing cells with QIAzol, nucleic acids were isolated trough a phenol-chloroform extraction, then transferred to the RNeasy Mini columns to let them bind the silica gel membrane. DNA was digested by DNase I solution, while membrane-binding RNA, was washed twice, before

being eluted in RNase-free water. RNA was dosed with the NanoDrop 2000 spectrophotometer, and conserved at -80°C.

III.2.2. Evaluation of RNA integrity

The integrity of extracted RNA, given by the RNA Integrity Number (RIN), was tested by the Agilent 2100 Bioanalyzer, through the Agilent RNA 6000 Nano kit (© Agilent Technologies).

III.2.3. Reverse-Transcription PCR (RT-PCR)

For this two-step amplification, the QuantiTect® Reverse Transcription kit (©QIAGEN) was employed. Firstly, all residual DNA contaminations were eliminated during the 5-minute incubation with the gDNA Wipeout Buffer, at 42°C. Secondly, RNA was converted to complementary DNA (cDNA) in a Reverse-Transcription reaction, using a mix of both oligo-dT and random primers, allowing the cDNA synthesis from all the RNA regions.

III.2.4. Real-Time Quantitative PCR (qPCR)

For each primer pair of qPCR, at least one of forward and reverse primer was designed spanning the exon/exon boundaries. *TBP* was chosen as housekeeping gene, *GDAP1* was the gene to be tested. In Table 7, sequences of all primer pairs are reported.

Table 7 TBP and GDAP1 primers for qPCR.

Gene	Transcript ID in Ensembl Genome Browser	Position in the gene	Sequence (5'->3')	Melting Temperature	Product size
TBP	ENST00000392092.2	Ex 7-8	F: ACAGGTGCTAAAGTCAGAGC R: GAGGCAAGGGTACATGAGAG	60°C 62°C	107 bp
GDAP1	ENST00000220822.7	Ex 5-6	F: GCTGCTTGATCATGACAATGT R: CCTCTTCTGGGGTTTCTTCA	60°C 60°C	116 bp

As previously described in 2.1.4 Paragraph, samples were prepared with the Rotor-Gene SYBR Green PCR Kit (400), and reactions performed on the Corbett Rotor-Gene 6000 Machine. In this case, for each subject, *GDAP1* Ct values were normalized using *TBP* as reference gene.

$$V = \frac{2^{-(Ct\ target\ gene)}}{2^{-(Ct\ reference\ gene)}}$$

III.3. Bioinformatic Analysis

Variants detected by targeted NGS were annotated using Ion reporter. Variants' pathogenicity was tested by Alamut Mutation Interpretation Software (Interactive Biosoftware, Rouen, France). Databases as ExAC Genome browser (http://exac.broadinstitute.org), GnomAD browser (https://gnomad.broadinstitute.org/), dbSNP135 (National Center for Biotechnology Information [NCBI], Bethesda, Maryland, USA, http://www.ncbi.nlm.nih.gov/projects/SNP/), ClinVar (www.ncbi.nlm.nih.gov/clinvar) and HGMD professional (www.hgmd.cf.ac.uk), were also used to screen variants. The occurrence of Copy Number Variations (CNV) was evaluated with Cov'Cop software (Derouault et al. 2017) and with CovCopCan software (Derouault et al. 2020). These software allow to detect genomic duplications and deletions, using the read depth values of amplicons and comparing them among individuals of the same run.

IV. Biochemical analyses

IV.1. Imaging

IV.1.1. Immunocytochemistry (ICC)

For Immunocytochemistry, cells were fixed incubating them 10 minutes, at RT, with 4% paraformaldehyde (PFA) (Sigma-Aldrich, Merck). After washing three times with DPBS, cells were permeabilized using a 0.1% Triton-X 100 solution, prepared in 3% Bovine Serum Albumin (BSA) (Sigma-Aldrich, Merck) DPBS. Three 5-minute washes were done, before adding the primary antibody. Primary antibody solutions were prepared in 3% BSA-DPBS, and incubated with samples overnight, at 4°C. Antibodies' species and dilutions are reported in Table 8.

Table 8 Primary antibodies used for characterization of hiPSC and neural cells.

Antibody	Company	Cat. Number	Species	Dilution
		Pluripotency markers		
Sox2	Biolegend	630802	Rabbit	1:200
Oct3/4	Santa Cruz Biotech	sc-5779	Mouse	1:50
Nanog	DSHB	PCRP-NANOGP1-2D8-s	Mouse	1:5
		Germinal Layers markers		
α-SMA	DAKO	M0851	Mouse	1:500
Sox17	R&D	AF1924	Goat	1:100
MAP2	Merck	M-4403	Mouse	1:500
Pax6	Covance	PRB-278P	Rabbit	1:100
		Neural markers		
PGP9.5	Abcam	ab108986	Rabbit	1:100
Tuj1	R&D	MAB1195	Mouse	1:1000
HB9 = MNR2	DSHB	81.5C10	Chicken	1:100
Islet1	DSHB	40.2D6-c	Mouse	1:25
Islet1/2	DSHB	39.4D5-c	Mouse	1:25
Chat	Chemicon	AB144P	Goat	1:50
		Other		
GDAP1	Proteintech	13152-1-AP	Rabbit	1:100
P4HB	OriGene	AF0910-1	Mouse	1:100
Ki-67	Leica	NCL-L-Ki67-MM1	Mouse	1:100

The next day, cells were washed three times, then labeled with the secondary antibody, conjugated with the Alexa Fluor™ 488 or the Alexa Fluor™ 594 (Molecular Probes, Thermo-Fisher SCIENTIFIC). Secondary antibodies were incubated 1 hour at RT. Nuclei were stained with 4',6-diamidino-2-phenylindole (DAPI) (Sigma-Aldrich, Merck), incubated 10 minutes at RT. ICC images were acquired using the Leica DM IRB microscope, and the confocal laser Zeiss LSM 510 Meta microscope. They were analyzed and treated with the NIS Element BR software, the Zen lite software, and the Image J software.

IV.1.2. 3,3'-Diaminobenzidine (DAB) staining

The DAB staining was performed with the VECTASTAIN® Elite ABC kit (Vector Laboratories). As well as in ICC, cells were fixed, permeabilized, and incubated with the primary antibody overnight, at 4°C.

After washing them, they were incubated with the biotinylated secondary antibody for 30 minutes, at RT. Cells were washed once again, for 5 minutes, and incubated for 30 minutes with the VECTASTAIN Elite ABC Reagent, composed of the Avidin DH and the biotinylated Horseradish Peroxidase H. After a 5-minute wash, the DAB+ chromogen, i.e. the peroxidase substrate solution, was added, and incubated until the staining appeared. Images were acquired using a Nikon microscope and a digital camera Nikon D90®.

IV.1.3. Electron microscopy

Cells were fixed in 2.5% glutaraldehyde for 30 minutes at RT, then in 2% osmium tetroxide (OsO_4) (Euromedex) for 30 minutes at RT. Fixation was followed by a water-wash, and the dehydration phase in a series of ethanol dilutions (30%, 50%, 70%, 95%, 100%). After a 30-minute incubation in a 100% ethanol/epon mix, cells were embedded in epoxy resin overnight, at 4°C. Next day, they were polymerized 48 h at 60 °C, and ultrathin sections (80/100 nm) were prepared to be stained with uranyl acetate and lead citrate. Images were acquired with the TEM JEM-1011 (JEOL), at Anatomy Pathology Department of University Hospital of Limoges.

IV.2. Functional tests

IV.2.1. Alkaline phosphatase test

HiPSC were tested for alkaline phosphatase, highly expressed and active in pluripotent stem cells. Test was performed using the SIGMAFAST™ BCIP®/NBT, or BCIP®/NBT Alkaline Phosphatase Substrate (Sigma-Aldrich, Merck), which is converted, by the AP, in a blue-purple product. hiPSC were first fixed with 95% ethanol, incubated 10 minutes, at RT. They were then washed three times with DPBS 1X, and incubated 8 minutes, at 37°C, with the SIGMAFAST™ BCIP®/NBT Alkaline Substrate,

extemporaneously dissolved in Ultra Pure Water. When blue/purple staining appeared, solution was discarded, and cells were washed three times with DPBS.

IV.2.2. Adenosine Triphosphate (ATP) quantification

Cells (fibroblasts, MN) were plated in 96-wells plates, preparing 6 wells for each subject. After 3 to 7 days, ATP was dosed using CellTiter-Glo® Luminescent Cell Viability Assay kit (Promega), following manufacturer's instructions. The employed kit was based on the conversation of Luciferin, in presence of ATP molecules, in Oxyluciferin and light (Figure 38). Luminescent signal was then recorded by the Fluoroskan Ascent®FL (Thermo Fisher), and normalized to number of cells, measured with DAPI staining. The experiment was reproduced three times, for each cell type.

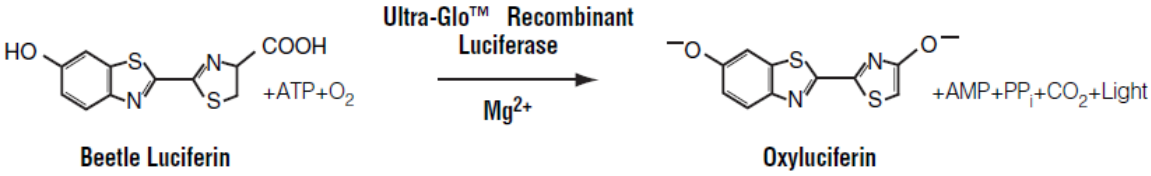

Figure 38 Luciferase reaction's method in the CellTiter-Glo® Luminescent Cell Viability Assay kit. Luciferin, in presence of ATP, molecular oxygen, and Mg2+, is converted, by Luciferase, in Oxyluciferin and light. Recorded light is proportional to ATP content [From: CellTiter-Glo® Luminescent Cell Viability Assay kit User's Guide, Promega].

IV.2.3. Succinate dehydrogenase (Complex II) activity

Cells (Fibroblasts, MN) were plated in 96-wells plates, preparing three wells for each condition. Succinate dehydrogenase activity was measured using the Cell Proliferation Kit I (Roche), based on the conversion of the yellow 3-[4,5-dimethylthiazol-2-yl]-2,5-diphenyl tetrazolium bromide (MTT) salt into purple formazan crystals, by the succinate dehydrogenase enzyme (Figure 39). Cells were first incubated with the MTT to favor formations of formazan crystals. After 2 to 4 hours, according to the cell type, the solubilization solution was added, to dissolve crystals, and let act overnight, at 37°C.

Next day, absorbance values, at 595 nm, were recorded with the Multiskan™ FC Microplate Photometer (Thermo Fisher), and normalized to number of cells, measured with DAPI staining. The experiment has been reproduced three times, for each cell type.

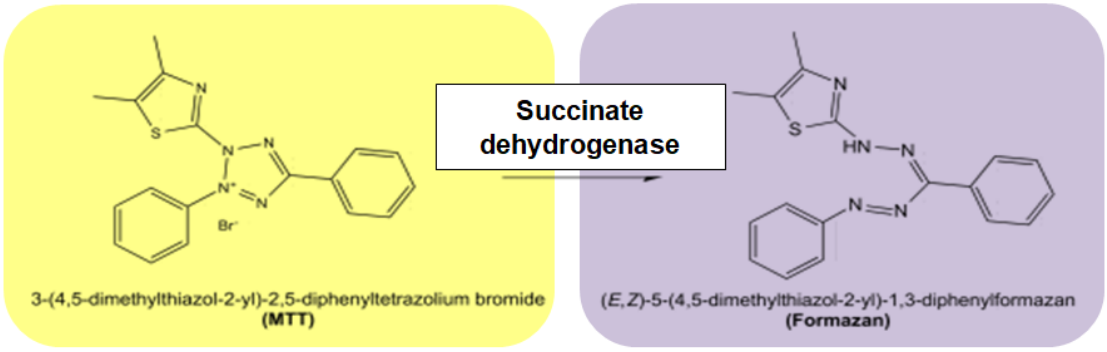

Figure 39 The succinate dehydrogenase enzyme catalyzes the conversion of yellow MTT in purple formazan crystals.

IV.2.4. Superoxide anion analysis

Cells (Fibroblasts, MN) were plated in 48-well plates, 6 wells for each subject. Half of the wells were treated, 2 hours at 37°C, with 1mM H_2O_2, prepared in culture medium. Then, medium was removed from all the wells, and 5 µM MitoSOX™ Red mitochondrial superoxide indicator (Molecular Probes, Thermo-Fisher SCIENTIFIC), prepared in DPBS, was added and incubated 10 minutes at 37°C, protected from the light. After removing MitoSOX solution, cells were washed once, fixed with 4% PFA, and nuclei were stained with DAPI. Images were acquired using the Leica DM IRB microscope, and analyzed with ImageJ software. Fluorescent signal was normalized by the number of cells. The experiment was reproduced three times, for each cell type.

IV.2.5. Total (GSH) and oxidized (GSSG) glutathione quantification

Cells (Fibroblasts, NP, MN) were plated in 35-mm dishes or in 12-well plates, three times for each cell type. The Glutathione Assay Kit (Cayman Chemical) was used for the quantification of total and oxidized glutathione, according to manufacturer's instructions. Briefly, cells were collected in 1X 2-

(N-morpholino)ethanesulphonic acid (MES) with a cell scraper, then sonicated using the VibraCell 75186 sonicator (Sonics and Materials, Inc.). Lysates were deproteinated in an equal volume of metaphosphoric acid (MPA) (Sigma-Aldrich, Merck), centrifuged, and the supernatant mixed with the triethanolamine (TEAM) Reagent. For GSSG measurement, GSH was derivatized adding 2-vinylpyridine solution, in deproteinated samples and in the standards, which were then incubated 1 hour at RT. All samples and standards were added to the 96-well plate, followed by the Assay Cocktail, containing enzymes, cofactors, and 5,5-dithio-bis-(2-nitrobenzoic acid) (DNTB), in the suitable buffer, to induce the reaction reported in Figure 40. Absorbance values, at 405 nm, were recorded by Multiskan® EX (Thermo Fisher) and concentrations, of GSH and GSSG, were calculated from the standard curve.

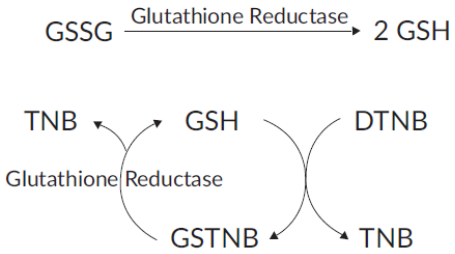

Figure 40 GSH recycling method for quantification of GSH. GSH reacts with DTNB to form the yellow colored 5-thio-2-nitrobenzoic acid (TNB), and the GSTNB, which is reconverted to GHS and TNB. Absorbance at 405 nm of TNB is proportional to TNB amount and GSH concentration in the sample [From: Glutathione Assay Kit User's Guide (Cayman Chemical)].

IV.2.6. Mitochondrial membrane potential measurement

The mitochondrial membrane potential (ΔΨm) was assessed with the 5,5',6,6'-Tetrachloro-1,1',3,3'-tetraethylbenzimidazolocarbocyanine iodide (JC-1) dye (Sigma-Aldrich, Merck). JC-1 monomers, with a fluorescence emission at ~530 nm, enter in the cell, then in mitochondria, where they are converted, by the ΔΨm, in JC-1 aggregates, with an emission of ~590 nm. In apoptotic cells, the ΔΨm is perturbed and JC-1 monomers accumulate in cytoplasm.

For the JC-1 analysis, cells (Fibroblasts, MN) were cultured in 60 mm dishes. They were detached trough trypsinazation, centrifuged and resuspended in DPBS/5% FBS solution. containing 1 µg/mL JC-1 dye. After 30-minute incubation at 37°C, the excess of JC-1 was discarded by centrifugation and cells collected in FACS tubes with DPBS. 1 µM TO-PRO-3 (Thermo-Fisher SCIENTIFIC) was added for nuclear counterstaining. Analysis of 590 and 530 nm emissions for JC-1, and 661 nm emission for TO-PRO-3, was performed with the FACSCalibur (BD biosciences), and the CellQuest software (BD biosciences).

V. Statistical analyses

All statistical analyses were performed using the Graphpad Prism 5 software (GraphPad Software, Inc.). Data were expressed as mean ± SEM (Standard Error of the Mean). They were compared using the nonparametric Mann–Whitney U test.

Results

Results - Part I
Genetic analysis of hereditary peripheral neuropathies

<u>Article 1</u> - CovCopCan: An efficient tool to detect Copy Number Variation from amplicon sequencing data in inherited diseases and cancer

Published in PLOS Computational Biology (12 February 2020)

The molecular investigation is a fundamental step in the analysis of inherited and somatic diseases. The identification of genetic mutations responsible for the pathological condition may help, not only the diagnostic process, but also the choice of the more appropriate therapeutic strategy. NGS technology, and, in particular, amplicon sequencing, is widely employed for the detection and discovery of single-nucleotide mutations or short indels, while Copy Number Variations (CNV) are less often explored, since analysis software are limited. In this work we presented CovCopCan, the more advanced version of the bioinformatic tool Cov'Cop. CovCopCan allows to detect CNV, as large deletions or duplications, using data of amplicon sequencing. Specifically, it analyses and compares read-depth values of amplicons of one patient, to read-depth of amplicons of the other patients examined in the same run. The main advantage of CovCopCan is that is can be used in inherited pathologies, like hereditary peripheral neuropathies, but also in somatic diseases, like cancers. In this case, it is capable of detect CNV, even if the ratio of mutated cells to healthy cells is low. Moreover, in this paper, we presented all CovCopCan implementations, as regards the statistical approach and the software visualization and interface, proposing a more efficient and user-friendly tool.

For this work, all the software conception and implementation took place at University Hospital of Limoges, while its validation was supported by the EA6309 research team, at University of Limoges. Specifically, I collaborated to the confirmation, by Real-time qPCR, of multiple CNV detected by CovCopCan, a necessary step to test CovCopCan sensitivity and further optimize its performance.

PLOS COMPUTATIONAL BIOLOGY

RESEARCH ARTICLE

CovCopCan: An efficient tool to detect Copy Number Variation from amplicon sequencing data in inherited diseases and cancer

Paco Derouault[1], Jasmine Chauzeix[2,3], David Rizzo[2,3], Federica Miressi[4], Corinne Magdelaine[4,5], Sylvie Bourthoumieu[4,6], Karine Durand[7,8], Hélène Dzugan[4,5], Jean Feuillard[2,3], Franck Sturtz[4,5], Stéphane Mérillou[9], Anne-Sophie Lia[1,4,5]*

1 CHU Limoges, UF de Bioinformatique, Limoges France, **2** CHU Limoges, Service Hématologie Biologique, Limoges, France, **3** Univ. Limoges, UMR CNRS 7276 CRIBL, Limoges, France, **4** Univ. Limoges, MMNP, EA 6309, Limoges, France, **5** CHU Limoges, Service Biochimie et Génétique Moléculaire, Limoges France, **6** CHU Limoges, Service de Cytogénétique, Limoges, France, **7** CHU Limoges, Service Anatomie Pathologie, Limoges, France, **8** Univ. Limoges, EA CAPTur, Limoges, France, **9** Univ. Limoges, UMR-7252X-LIM, Limoges, France

* anne-sophie.lia@unilim.fr

Citation: Derouault P, Chauzeix J, Rizzo D, Miressi F, Magdelaine C, Bourthoumieu S, et al. (2020) CovCopCan: An efficient tool to detect Copy Number Variation from amplicon sequencing data in inherited diseases and cancer. PLoS Comput Biol 16(2): e1007503. https://doi.org/10.1371/journal.pcbi.1007503

Editor: Aaron E. Darling, University of Technology Sydney, AUSTRALIA

Received: May 13, 2019

Accepted: October 23, 2019

Published: February 12, 2020

Data Availability Statement: All relevant data are within the manuscript and its Supporting Information files.

Funding: The authors received no specific funding for this work.

Competing interests: The authors have declared that no competing interests exist.

Abstract

Molecular diagnosis is an essential step of patient care. An increasing number of Copy Number Variations (CNVs) have been identified that are involved in inherited and somatic diseases. However, there are few existing tools to identify them among amplicon sequencing data generated by Next Generation Sequencing (NGS). We present here a new tool, CovCopCan, that allows the rapid and easy detection of CNVs in inherited diseases, as well as somatic data of patients with cancer, even with a low ratio of cancer cells to healthy cells. This tool could be very useful for molecular geneticists to rapidly identify CNVs in an interactive and user-friendly way.

This is a *PLOS Computational Biology* Software paper.

Introduction

Identifying mutations responsible for inherited or somatic diseases can be essential to define the appropriate therapy for the efficient treatment of patients. For example, this is true for patients presenting an amyloid neuropathy due to Transthyretin (*TTR)* point mutations, who can benefit from new treatments, such as Tafamidis [1]. This is also true for cancer, for which it is important to rapidly detect certain Copy Number Variations (CNVs), such as the 17p deletion, a recurrent abnormality in Chronic Lymphocytic Leukemia (CLL), with major therapeutic implications. Because this acquired chromosomal abnormality directly impairs the *TP53* gene [2, 3], it is now recommended to test this CNV before each treatment for CLL [4]. Indeed, TP53 alterations in CLL are responsible for primary resistance to fludarabine and survival of such patients is clearly improved by new-targeted therapies, such as ibrutinib [5, 6].

High-throughput sequencing techniques allow partial or total sequencing of a patient's genome. Amplicon sequencing is one of the techniques that enables the sequencing of several thousand exons at a very low cost. Although this method is robust for the discovery of small genetic mutations, such as single-nucleotide polymorphisms or short indels, only a few tools are available for the detection of larger variations, such as deletions or duplications in amplicon sequencing data. Some of these tools require control samples to establish a reference set of data (ONCOCNV [7]). For others (ExomeDepth [8], IonCopy [9], DeviCNV [10], Cov'Cop [11]), control samples are not necessary. Indeed, if the CNV is rare, the other patient samples tested in the same run can serve as controls. In this strategy, multiple patients are tested at the same time, potentially shortening the time to diagnosis.

Most available tools based on the read depth method to detect CNVs include robust statistical methods. ExomeCopy [12] proposes a hidden Markov model to detect CNVs from raw read count data. CONVector [13] was built on a machine-learning algorithm to associate PCR-efficiency correlations for subsets of amplicons. Here, we propose a new tool, CovCopCan, based on the initial read-depth method developed in Cov'Cop, with additional statistical methods and features that allow the rapid and easily detection of CNVs in inherited diseases, as well as somatic data of patients with cancer, even with a low ratio of cancer cells to healthy cells (data sets described in S1 File). CovCopCan includes heuristic methods to compare the value of each amplicon of a patient to those of other patients sequenced in the same run. CovCopCan focuses on data manipulation and results exploration for the interpretation of CNVs. Users have access to an overview of the results for each patient through an interactive visualization, allowing, for example, the exclusion of low-quality amplification from the analysis and quickly restarting CNV detection. In addition, several statistics methods (Loess regression, Cumulative summary) can help in the interpretation of the results.

Design and implementation

CNV-detection algorithm

Z-score-based CNV detection: "Z-detection". From the raw read count of each amplicon, CovCopCan applies the same corrections and normalization as the Cov'Cop tool [11], resulting in a normalized read count value (NRC) for each amplicon (see S1 File). Starting from this point, we developed a new CNV-detection algorithm, based on the z-score. The z-score is calculated for each amplicon in each patient, according to the following formula:

$$z - score_{p\_i} = \frac{NRC_{p\_i} - \mu_p}{\sigma_p}$$

NRC_{p_i} is the normalized read count of the amplicon i in the patient p, μ_p the NRC average of the patient p, and σ corresponds to the standard deviation of the patient p. The z-score follows a standard normal distribution $N(0;1)$. We fixed a threshold corresponding to a significance level of 0.01 for both deletion and duplication events by a one-tailed test. Thus, a negative z-score with a p-value < 0.01 indicates a deleted amplicon, whereas a positive z-score with a p-value < 0.01 indicates a duplicated amplicon. This algorithm automatically determines the best deletion and duplication thresholds based on the variability of a patient's data. The users are free to determine the minimum number of concurrent amplicons required to call a CNV. No minimum distance between amplicons is required, but they have to be on the same chromosome. By default, a minimum of three successive amplicons on the same chromosome was used for all data in this paper.

Two-stage ratio to optimize CNV detection. The last normalization step of CovCopCan results in a ratio of standardized patient values that gives a theoretical value of 1 for a gene

present in two copies, 0.5 for a deletion event, and 1.5 for a duplication. In this last step, each amplicon value is divided by the median of the same amplicon from the other samples. Once this first ratio is calculated and the first round of CNV detection is performed, a second ratio is calculated excluding all amplicons located inside the initially detected CNVs from each sample, and final CNV detection is achieved. This approach is used to improve standardization in regions in which the same CNV event is present in many patients.

Merging CNVs. We provide a "merge" option to reduce the impact of false-negative amplicons on CNV detection. If two CNV areas located on the same chromosome are disjointed by only one amplicon with a z-score duplicated or deleted at a significance level of 0.05, CovCopCan will then merge the two CNV areas to easily highlight this global CNV. In addition, the user can also define the maximum distance value between two CNVs to be merged.

Reference amplicon selection or exclusion. For the normalization step, CovCopCan selects a set of amplicons, consisting of those that are the most stable among the patients of a run. These amplicons are then used to normalize the values of the other amplicons. The user can indicate specific amplicons to use for this normalization step (see S1 File). Inversely, our tool also provides the possibility to manually exclude some amplicon data for the last ratio step of normalizations (see S1 File).

Control samples. Although CovCopCan works without control samples, it is possible to exploit the presence of controls if they are available. In such a case, the median of the last standardization step is no longer calculated using all the samples but only the controls. Then for each patient, the amplicon values are divided by the median calculated for the controls, according to the following formula:

$$Ratio_{i\_patj} = \frac{NRC_{i_{patj}}}{Md(NRC_{i_{controls}})}$$

$NRC_{i_{patj}}$ is the normalized read count of the amplicon i in the patient j.

$Md(NRC_{i_{controls}})$ is the median of the normalized read count of the control samples.

CovCopCan can be run with only one control sample but more control samples will improve the result.

2D interactive visualization

An interactive 2D visualization is available for each patient (Fig 1). The amplicons are represented by dots over their chromosomal positions on the x-axis and their normalized values on the y-axis. Users can interactively zoom in on specific regions and navigate between data in an intuitive and interactive way, allowing simple navigation. Several types of information described below have also been added to the graphical representation.

Local regression curve. We introduced the possibility to display regression curves on the presented chart to optimize visual CNV detection. We chose to implement the Loess local regression algorithm [14] to easily visualize a sudden change. The Loess regression is calculated for each chromosome. By default, the bandwidth parameter is fixed to 0.25, but it is possible to interactively fine tune it to more or less smoothen the curve. The Loess regression is represented by a green curve on the chart (see S1 File).

CUSUM charts. For data generated from cancer or mosaic samples, a sample may simultaneously contain "normal" and deleted/duplicated cells. The deletion/duplication detection accuracy depends on the proportion of deleted/duplicated cells relative to that of the normal cells and the normalized values can be close to 1. CNVs will then be very difficult to detect. Consequently, we added a visual method called CUmulative SUMmary control chart (CUSUM; [15])

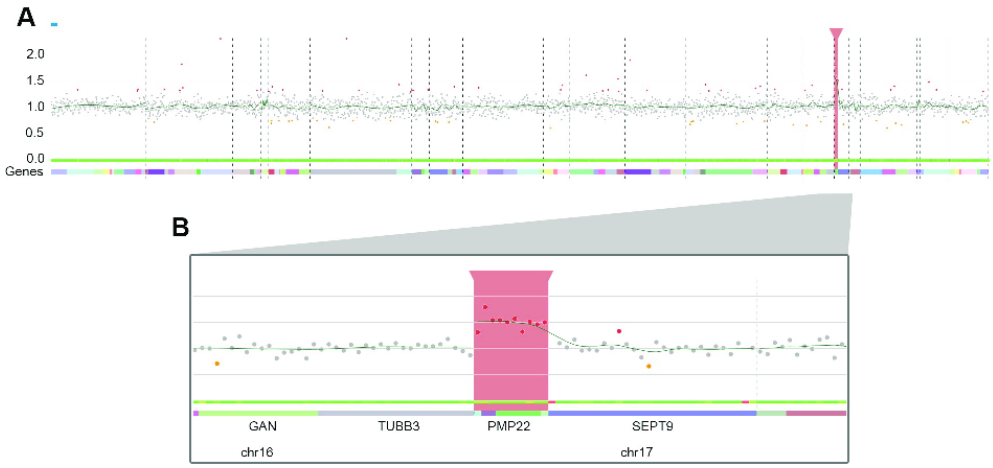

Fig 1. Visualization of CovCopCan. A. General view. Each dot corresponds to an amplicon. The amplicons are distributed on the x-axis according to their genomic position. The y-axis corresponds to the normalized values. Grey dots indicate a "normal" value, whereas red or orange dots indicate duplicated and deleted amplicons, respectively. The names of the gene and chromosome number are located at the bottom of the figure. The green curve shows the Loess regression. The thick green ribbon is a noise heatmap in which green indicates a stable amplicon in all samples (see S1 File). The red rectangle highlights a CNV region. B. Zoom on the duplicated region covered by 10 amplicons (*PMP22*).

https://doi.org/10.1371/journal.pcbi.1007503.g001

to be able to observe a slight increase or decrease in values. For each chromosome, this algorithm calculates the cumulative sum of the positive deviations (values > patient's average) for deletions and negative deviations (values < patient's average) for duplications. It can be useful for detecting a slight deviation of the values due to cancer data or mosaicism, as well as small CNVs in inherited diseases.

$$S_n^+ = \max(0,\ S_{n-1}^+ + x_n - (\bar{x} + \sigma))$$

$$S_n^- = min(0,\ S_{n-1}^- + x_n - (\bar{x} - \sigma))$$

Here, x_n corresponds to the value of one amplicon, $\bar{x}$ is the mean value of all the patient's amplicons, and σ is the standard deviation. In the visualization of CovCopCan, a blue shape indicates a possible deletion, whereas a pink shape indicates a potential duplication. Although this method makes it possible to highlight potential CNVs, it does not allow precise definition of their breakpoints (see S1 File).

Results

Two-stage ratio

We visualized the result of the two-stage ratio using sequencing data from panel 2 (see S1 File for details). This gene panel, designed by Ion AmpliSeq designer software, includes 1,206 amplicons on 70 genes. The run presented here was performed on an Ion Proton device and included seven patients. A deletion on chromosome 13 was shared by three of the seven patients (verified by karyotyping). Examples of the visualization obtained for two of the patients (patient 1 normal and patient 2 "deleted") are presented in Fig 2. Without the two-stage ratio, the region in non-deleted patients was disturbed and a false positive duplication event was detected by CovCopCan

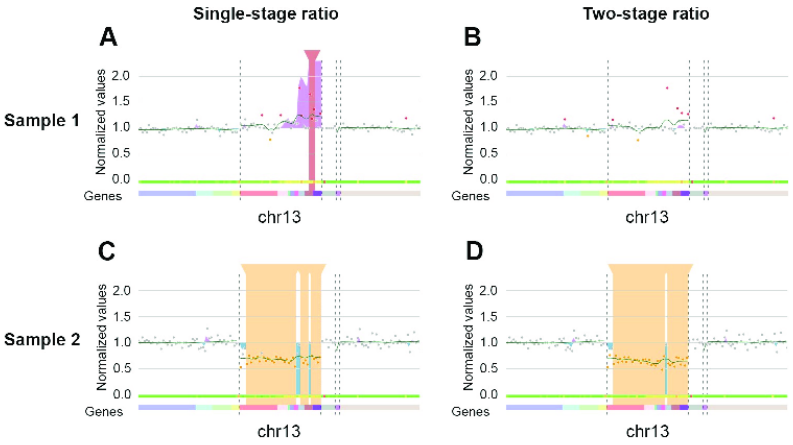

Fig 2. Comparison of single-stage and two-stage ratio results. A. Without the two-stage ratio, a disturbed region showed a false-positive duplication on chromosome 13 covered by three amplicons. B. The two-stage ratio improved the stability of the region and the false duplication was no longer detected. C. Without the two-stage ratio, six amplicons (grey dots in Chr13 area) were not detected as deleted throughout chromosome 13 (39 amplicons) and three separated CNVs were detected. D. With the two-stage ratio, only three false-negative amplicons (grey dots in chr13 area) were present among the 39 amplicons of chromosome 13 and only one amplicon split the total deletion of the chromosome (partial screenshots from CovCopCan).

https://doi.org/10.1371/journal.pcbi.1007503.g002

in both (highlighted by a vertical red rectangle, as for patient 1, Fig 2A). The two-stage ratio improved the stability of the values so that no false duplication event was detected by CovCopCan, thus increasing the specificity (Fig 2, compare A and B). This method also improved the detection of deletions (highlighted by a vertical orange rectangle) in the true deleted patients, decreasing the number of false-negative amplicons (Fig 2C and 2D).

Merging CNVs

To reduce the effect of individual false negative amplicons, CovCopCan relaxes the significance threshold when a single non-significant amplicon is flanked on both sides by significant amplicons. For this specific amplicon, the threshold will be automatically switched to 0.05. If this amplicon becomes significantly duplicated, it will be merged with the initial duplicated detected areas. The grey dot in the graph will stay grey, indicating that it is a merged area. Deletions are treated the same way. Here, we show the results of this merging option on a complete chromosome X duplication. A single duplication covering the entire gene is detected by CovCopCan, whereas six successive duplications would have been found without this merging option (Fig 3).

Control samples

We tested this method with the Panel 2 data (Fig 4). Seven samples were simultaneously sequenced on an Ion Proton sequencer (three controls and four patients). The four patients share the same region q deletion on chromosome 13. Without defining controls, CovCopCan detected a correct deletion (highlighted by the vertical orange rectangle) for one of the four patients and only a partial deletion for another. In addition, two false-positive duplications (highlighted by the vertical red rectangle) were detected in two controls. When the control samples were defined (here three controls without the chromosome 13q deletion), CovCopCan

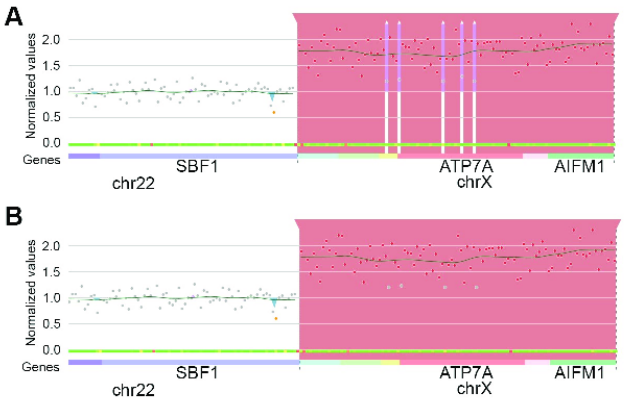

C

```
##fileformat=VCFv4.1
##fileDate=20190826
##INFO=<ID=SVLEN,Number=.,Type=Integer,Description="Difference in length between REF and ALT
alleles">
##INFO=<ID=SVTYPE,Number=1,Type=String,Description="Type of structural variant">
##INFO=<ID=END,Number=1,Type=Integer,Description="End position of the variant described in this
record">
##ALT=<ID=DEL,Description="Deletion">
##ALT=<ID=DUP,Description="Duplication">
##FORMAT=<ID=GT,Number=1,Type=String,Description="Genotype">
#CHROM POS  ID REF  ALT  QUAL FILTER INFO FORMAT IonXpress_013
chrX 24483480 . C  <DUP>  . PASS SVTYPE=DUP;END=129299679;SVLEN=104816199 GT 0/1
```

Fig 3. Example of CNV merging on a chromosome X duplication. A. Entire duplication of chromosome X. CovCopCan detects six CNV areas without the merging CNV algorithm. B. By using the merging CNV algorithm, the duplication detected includes all of chromosome X, although some amplicons appear as neutral (grey dots). C. The exported CNV in the VCF format contains only one line corresponding to the duplication of chromosome X (partial screenshots from CovCopCan).

https://doi.org/10.1371/journal.pcbi.1007503.g003

efficiently detected two total q deletions on chromosome 13 and two partial deletions for the two other positive patients. In addition, no false-positive duplications were detected in the three controls.

Performance on germline data

Amplicon sensitivity and specificity. We first tested our algorithm on germline data. We used several coverage files obtained after Proton sequencing of our "CMT-89" Ampliseq library (see S1 File, panel 1).

We calculated the sensitivity of CovCopCan, by amplicon, using 22 positive controls confirmed by karyotype, real-time PCR, or Multiplex Ligation-dependent Probe Amplification (MLPA). The detected CNVs were present in 22 patients, sequenced in 11 runs (Table 1). Of the 22 CNVs, 15 are covered by more than 10 amplicons. We used a range of CNV sizes from 4 (TFG) to 98 amplicons (chromosome X duplication). CovCopCan was used with the default settings, with all options active. Raw read values of less than 20 were deleted.

The 22 CNVs are covered by a total of 461 amplicons. CovCopCan correctly detected 403 of 461 deleted/duplicated amplicons, giving an amplicon sensitivity of 0.87. If considering CNV detection, CovCopCan was able to detect 22 of the 22 CNVs tested, leading to a sensitivity of 1.

In addition, we analyzed the *PMP22* gene to calculate the specificity of CovCopCan by amplicon. Indeed, the *PMP22* duplication is the most frequent known mutation responsible

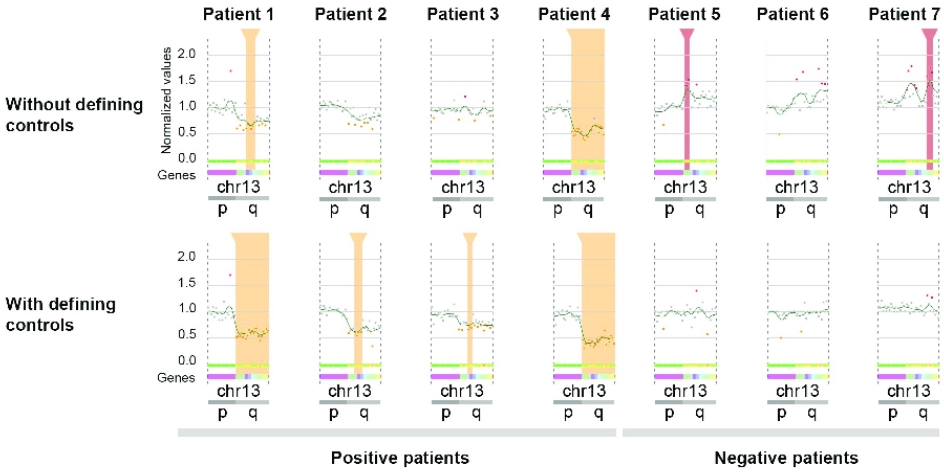

Fig 4. Visualization of chromosome 13 in seven samples. Each dot corresponds to an amplicon. Orange and red rectangles correspond to deletions and duplications, respectively. The green curve shows the Loess regression. Patients 1 to 4 share a q arm deletion. Samples 5 to 7 do not present this deletion. Without defining samples 5 to 7 as controls, only one deletion was correctly detected in patient 4. A partial deletion was detected in patient 1. False-positive deletions were detected in two of the three controls. By defining samples 5 to 7 as controls, two deletions were correctly detected in patients 1 and 4. Two partial deletions were found in both patients 3 and 4. No duplication was found in the controls (partial screenshots from CovCopCan).

https://doi.org/10.1371/journal.pcbi.1007503.g004

Table 1. Details of the 22 positive-control CNVs used for germline analysis, with chromosomal locations of the CNVs. **a**: Number of amplicons covering the CNVs. **b:** Number of amplicons correctly detected as duplicated or deleted by CovCovCan.

Sample	Gene	Chrom.	Start	End	Length (pb)	Amps[a]	Positives Amps[b]	Type
R1_S3	PMP22	chr17	14593353	15167670	574318	10	8	Gain
R1_S8	KIF1A	chr2	241656712	241709233	52522	58	43	Gain
R1_S9	-	chrX	24483480	129299679	104816200	98	94	Gain
R2_S2	AARS	chr16	70286552	70316749	30198	25	22	Gain
R2_S15	DHTKD1	chr10	12110948	12162941	51994	25	25	Loss
R3_S3	KIF1A	chr2	241656712	241709233	52522	58	45	Gain
R4_S4	TFG	chr3	100432328	100439067	6740	4	4	Gain
R4_S12	KIF1A	chr2	241656712	241709233	52522	58	45	Gain
R5_S3	AARS	chr16	70286552	70316749	30198	25	23	Gain
R5_S15	PMP22	chr17	14593353	15167670	574318	10	10	Gain
R5_S16	PMP22	chr17	14593353	15167670	574318	10	10	Loss
R6_S2	PMP22	chr17	14593353	15167670	574318	10	10	Gain
R6_S9	TFG	chr3	100432328	100439067	6740	4	4	Gain
R7_S2	TFG	chr3	100432328	100439067	6740	4	4	Gain
R7_S6	PMP22	chr17	14593353	15167670	574318	10	8	Gain
R8_S8	PMP22	chr17	14593353	15167670	574318	10	10	Loss
R9_S6	PMP22	chr17	14593353	15167670	574318	10	10	Loss
R10_S10	REEP1	chr2	86444070	86509447	65378	7	7	Gain
R10_S16	TFG	chr3	100432328	100439067	6740	4	4	Gain
R11_S8	PMP22	chr17	14593353	15167670	574318	10	10	Gain
R11_S14	TFG	chr3	100432328	100439067	6740	4	3	Gain
R11_S15	REEP1	chr2	86444070	86509447	65378	7	6	Gain

https://doi.org/10.1371/journal.pcbi.1007503.t001

for CMT disease and all patients were initially screened by MLPA to detect this gene duplication. The *PMP22* region was covered by 10 amplicons and the entire design contains 2,394 amplicons. We used 456 patients who had no CNV on *PMP22* to estimate the specificity of the CovCopCan algorithm. Of the 4,560 *PMP22* amplicons tested, 4,375 were indeed tagged as "normal" and only 185 were false positives, leading to a specificity of 0.96.

Comparison with other tools. We compared CovCopCan with three other tools: IonCopy, DeviCNV, and ExomeDepth. IonCopy and DeviCNV are designed to analyze amplicon sequencing data without a control set. ExomeDepth uses a robust model for the read count data and to build an optimized reference set.

We used the shiny version of the software IonCopy (v. 2.1.1), with the gene-wise analysis mode and default parameters. DeviCNV (v. 1.5.1) was launched with the recommended parameters, detailed in the manual. ExomeDepth (v.0.1) was also launched with the default parameters. We tested these tools on the same dataset, already described, containing the 22 CNVs. We only considered CNVs supported by at least three amplicons for all the tools. The results are presented in Table 2 as the number of CNVs detected.

CovCopCan, IonCopy, DeviCNV, and ExomeDepth each detected 22, 20, 18, and 19 CNVs, respectively (Table 2). Only CovCopCan detected all CNVs for a sensitivity of 1. IonCopy, DeviCNV, and ExomeDepth showed sensitivity of 0.91, 0.82, and 0.86, respectively. It was impossible to verify all the other CNVs found by the various tools. Thus, we could not calculate specificity based on these data. However, a small number of CNVs would be expected, since the data correspond to germline samples. Thus, with only seven CNVs detected in addition to the 22 controls, CovCopCan must have had the best specificity for this dataset.

Performance on cancer data

Low cell fraction. CovCopCan can also process cancer data. The main difference between germline and somatic data is that a cancer tissue sample may simultaneously contain both healthy cells and cancer cells. A low proportion of cancer cells may interfere with the detection of CNVs. We estimated the minimum proportion of cancer cells required for CNV detection by simulating the complete deletion of a gene covered by 80 amplicons using panel 1 (2,394 amplicons). We used a coverage matrix containing the data of 16 patients sequenced by an Ion Proton Sequencer. The deletion of the entire gene was simulated following this method:

$$SRC_i = RRC_i \times (1 - CancerCellProportion) + {}^{RRC_i}/_{2} \times CancerCellProportion$$

SRC_i is the simulated value of the amplicon i, RRC_i the Raw Read Count of the amplicon i, and *CancerCellProportion* the proportion of cancer cells ($0 <$ values < 1). We simulated a proportion of cancer cells ranging from 0 to 1, in steps of 0.05. The first CNV was detected by the cumulative summary chart for 15% of cancer cells and clearly identifiable for 20%. Using only "Z-detection", the CNV was detected when 40% of the cells contained the deletion, whereas

Table 2. Comparison of the performance of CovCopCan and other CNV callers for 22 positive-control CNVs from 22 samples.

	True positives (total = 22)	Other CNVs	Total
CovCopCan	22	7	29
IonCopy	20	3914	3934
DeviCNV	18	117	135
ExomeDepth	19	218	237

https://doi.org/10.1371/journal.pcbi.1007503.t002

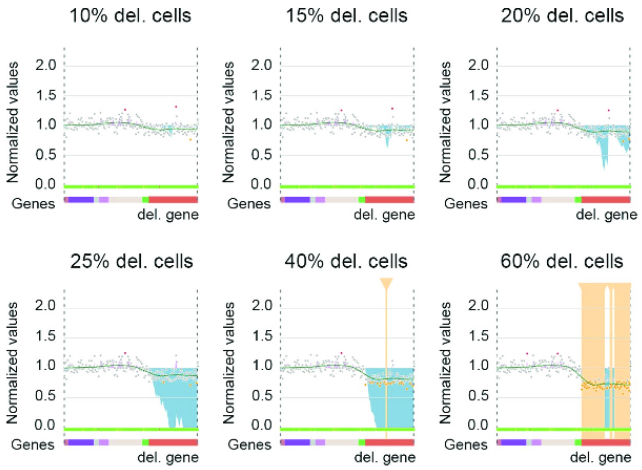

Fig 5. Gene deletion simulation (gene visualized in red), with various proportions of cells containing this deletion. The cumulative summary chart (blue shading) first detected the deletion with 15 to 20% of the cells containing the deletion (partial screenshots from CovCopCan).

https://doi.org/10.1371/journal.pcbi.1007503.g005

almost the entire gene (67/80 amplicons) was detected by "Z-detection" as deleted for 60% of cancer cells (Fig 5).

We confirmed the results obtained from these simulated data using real data. We sequenced five patient samples harboring various amounts of positive cancer cells carrying the same *ATM* gene deletion and previously explored with conventional cytogenetics (karyotype and FISH). The data were obtained using panel 2 without control samples. The cumulative algorithm first detected the deletion from 19.5% cancer cells (Fig 6). These results show that CovCopCan can detect CNVs within a heterogeneous sample if the cancer cells make up at least 15 to 20%.

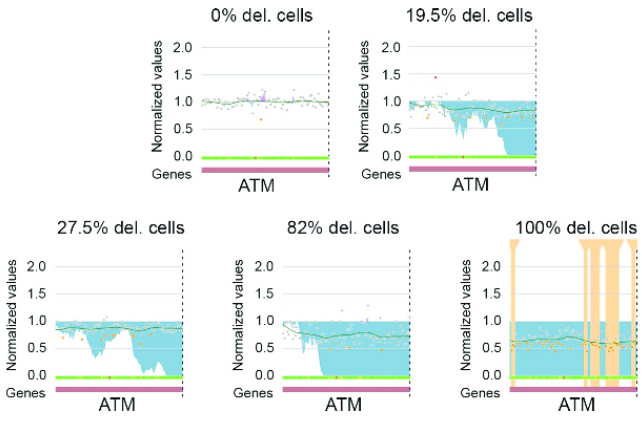

Fig 6. Detection of the entire *ATM* gene deletion in patients DNA, in which the percentage of cancer cells was estimated based on 200 FISH metaphases per patient. The Cumulative summary detected the deletion starting from 19.5% estimated cancer cells (partial screenshots from CovCopCan).

https://doi.org/10.1371/journal.pcbi.1007503.g006

Table 3. Detection of a CNV according to the proportion of cancer cells. "No" indicates no detection of the CNV, whereas "Yes" indicates correct detection of the CNV.

Cancer cell fraction	CovCopCan	IonCopy	DeviCNV	ONCOCNV
0%	No	No	No	No
19.5%	Yes	Yes	No	Yes
27.5%	Yes	Yes	No	Yes
82%	Yes	Yes	Yes	Yes
100%	Yes	Yes	No	Yes

https://doi.org/10.1371/journal.pcbi.1007503.t003

Comparison with other tools. We compared the performance of CovCopCan against IonCopy, DeviCNV, and ONCOCNV. First, we used these three tools on the deletion of the *ATM* gene described above. Like CovCopCan, both IonCopy, and ONCOCNV correctly detected the CNV with 19.5% of cancer cells, but not DeviCNV (Table 3).

In addition, we used another dataset obtained using panel 2. We sequenced the DNA of 54 patients in eight runs. Eighteen patients had a partial deletion of a chromosome arm, whereas two had a complete deletion of this same chromosome arm. The partial deletion was covered by 21 amplicons, whereas the entire deletion involved 39. In this study, we did not consider the percentage of cells presenting the CNVs. CovCopCan was used with the default settings, with all options active. Raw read values of less than 20 were deleted. IonCopy was used in the gene-wise mode with the default parameters. DeviCNV was used with the recommended settings. ONCOCNV (v 6.9) was used with the default settings. As with the germline data, we set the minimum number of amplicons to detect CNVs to three for each tool. DeviCNV failed to analyze a run due to a low number of samples (5) and detected four CNVs from the other

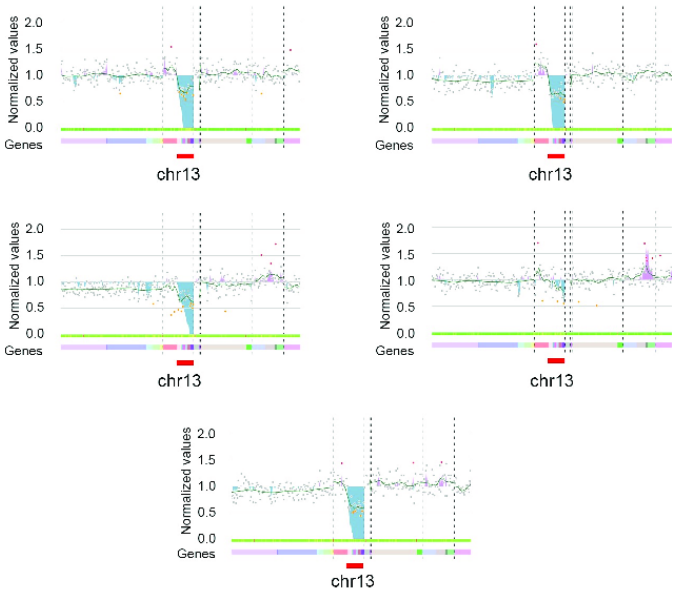

Fig 7. Deletion of the arm of chromosome 13 detected by CovCopCan using the Cumulative Summary Chart. The deletion is highlighted in the blue area.

https://doi.org/10.1371/journal.pcbi.1007503.g007

patients. IonCopy detected nine CNVs. ONCOCNV correctly detected the 20 CNVs but required at least three controls in a run to call them. CovCopCan was able to detect CNVs, with or without controls. Without defining control samples, CovCopCan automatically detected 13 of 20 CNVs. When defining controls, the number of correct CNVs increased to 15 and using the interactive visualization option, such as the CUSUM chart, CovCopCan clearly indicated the presence of a deletion in at least four of the five additional samples (Fig 7).

Availability and future directions

CovCopCan sources are available on GitHub: https://git.unilim.fr/merilp02/CovCopCan/tree/master. Pre-complied binaries can be downloaded from this page of the GitHub repository: https://git.unilim.fr/merilp02/CovCopCan/tree/master.

CovCopCan offers a wide range of features to interpret data from amplicon sequencing to detect CNVs. This tool works on data generated from Ion Designer (Life Technologies, CA, USA) as well as that from Illumina DesignStudio (Illumina Inc., San Diego, CA, USA). The user-friendly interface associated with our 2D visualization facilitates data exploration and manipulation allowing complex analyses such as those from cancer data. CovCopCan also offers the possibility to export the results in VCF format [16] or graphical output for publications. It can also be used in command-line mode to be integrated into various pipelines (see S1 File).

Future development of CovCopCan will involve the possibility to exploit the variant allele fraction (VAF) to improve the statistical detection of CNVs.

We will also improve memory consumption and parallelism to ensure that CovCopCan can work on a minimal configuration.

Supporting information

S1 File. Supplementary information of this article. The supplementary document provides information on the panels used in this article, a guideline to create an optimized panel to call CNVs, the workflow of CovCopCan algorithm, information on the possibility to define manually reference amplicons, details on graphical visualization elements and command line interface data.
(DOCX)

Acknowledgments

We thank Dr. Emilie Guerin, Dr. Valentin Tilloy and Pr. Sophie Alain from the Sequencing platform of the Limoges CHU for their help on this project.

Author Contributions

Conceptualization: Paco Derouault, Jasmine Chauzeix, David Rizzo, Jean Feuillard, Franck Sturtz, Stéphane Mérillou, Anne-Sophie Lia.

Data curation: David Rizzo, Corinne Magdelaine, Sylvie Bourthoumieu.

Formal analysis: Paco Derouault, Stéphane Mérillou, Anne-Sophie Lia.

Investigation: Jasmine Chauzeix, Federica Miressi, Sylvie Bourthoumieu, Karine Durand, Hélène Dzugan.

Methodology: Paco Derouault, David Rizzo, Stéphane Mérillou, Anne-Sophie Lia.

Project administration: Stéphane Mérillou, Anne-Sophie Lia.

Software: Paco Derouault, Stéphane Mérillou.

Supervision: Stéphane Mérillou, Anne-Sophie Lia.

Validation: Paco Derouault, Jasmine Chauzeix, David Rizzo, Federica Miressi, Sylvie Bourthoumieu, Karine Durand, Hélène Dzugan, Stéphane Mérillou, Anne-Sophie Lia.

Visualization: Paco Derouault, Jasmine Chauzeix, David Rizzo, Stéphane Mérillou, Anne-Sophie Lia.

Writing – original draft: Paco Derouault.

Writing – review & editing: Jasmine Chauzeix, David Rizzo, Federica Miressi, Jean Feuillard, Franck Sturtz, Stéphane Mérillou, Anne-Sophie Lia.

References

1. Zhao Y, Xin Y, Song Z, He Z, Hu W. Tafamidis, a Noninvasive Therapy for Delaying Transthyretin Familial Amyloid Polyneuropathy: Systematic Review and Meta-Analysis. J Clin Neurol. 2019; 15 (1):108–15. https://doi.org/10.3988/jcn.2019.15.1.108 PMID: 30618225; PubMed Central PMCID: PMCPMC6325356.
2. Dohner H, Fischer K, Bentz M, Hansen K, Benner A, Cabot G, et al. p53 gene deletion predicts for poor survival and non-response to therapy with purine analogs in chronic B-cell leukemias. Blood. 1995; 85 (6):1580–9. PMID: 7888675.
3. Dohner H, Stilgenbauer S, Benner A, Leupolt E, Krober A, Bullinger L, et al. Genomic aberrations and survival in chronic lymphocytic leukemia. N Engl J Med. 2000; 343(26):1910–6. https://doi.org/10.1056/NEJM200012283432602 PMID: 11136261.
4. Malcikova J, Tausch E, Rossi D, Sutton LA, Soussi T, Zenz T, et al. ERIC recommendations for TP53 mutation analysis in chronic lymphocytic leukemia-update on methodological approaches and results interpretation. Leukemia. 2018; 32(5):1070–80. https://doi.org/10.1038/s41375-017-0007-7 PMID: 29467486; PubMed Central PMCID: PMCPMC5940638.
5. Hallek M, Cheson BD, Catovsky D, Caligaris-Cappio F, Dighiero G, Dohner H, et al. iwCLL guidelines for diagnosis, indications for treatment, response assessment, and supportive management of CLL. Blood. 2018; 131(25):2745–60. https://doi.org/10.1182/blood-2017-09-806398 PMID: 29540348.
6. Hallek M, Shanafelt TD, Eichhorst B. Chronic lymphocytic leukaemia. Lancet. 2018; 391(10129):1524–37. https://doi.org/10.1016/S0140-6736(18)30422-7 PMID: 29477250.
7. Boeva V, Popova T, Lienard M, Toffoli S, Kamal M, Le Tourneau C, et al. Multi-factor data normalization enables the detection of copy number aberrations in amplicon sequencing data. Bioinformatics. 2014; 30(24):3443–50. https://doi.org/10.1093/bioinformatics/btu436 PMID: 25016581 PubMed Central PMCID: PMCPMC4253825.
8. Plagnol V, Curtis J, Epstein M, Mok KY, Stebbings E, Grigoriadou S, et al. A robust model for read count data in exome sequencing experiments and implications for copy number variant calling. Bioinformatics. 2012; 28(21):2747–54. https://doi.org/10.1093/bioinformatics/bts526 PMID: 22942019; PubMed Central PMCID: PMCPMC3476336.
9. Budczies J, Pfarr N, Stenzinger A, Treue D, Endris V, Ismaeel F, et al. Ioncopy: a novel method for calling copy number alterations in amplicon sequencing data including significance assessment. Oncotarget. 2016; 7(11):13236–47. https://doi.org/10.18632/oncotarget.7451 PMID: 26910888; PubMed Central PMCID: PMCPMC4914355.
10. Kang Y, Nam SH, Park KS, Kim Y, Kim JW, Lee E, et al. DeviCNV: detection and visualization of exon-level copy number variants in targeted next-generation sequencing data. BMC Bioinformatics. 2018; 19 (1):381. https://doi.org/10.1186/s12859-018-2409-6 PMID: 30326846; PubMed Central PMCID: PMCPMC6192323.
11. Derouault P, Parfait B, Moulinas R, Barrot CC, Sturtz F, Merillou S, et al. 'COV'COP' allows to detect CNVs responsible for inherited diseases among amplicons sequencing data. Bioinformatics. 2017; 33 (10):1586–8. https://doi.org/10.1093/bioinformatics/btx017 PMID: 28137711.
12. Love MI, Mysickova A, Sun R, Kalscheuer V, Vingron M, Haas SA. Modeling read counts for CNV detection in exome sequencing data. Stat Appl Genet Mol Biol. 2011; 10(1). https://doi.org/10.2202/1544-6115.1732 PMID: 23089826; PubMed Central PMCID: PMCPMC3517018.
13. Demidov G, Simakova T, Vnuchkova J, Bragin A. A statistical approach to detection of copy number variations in PCR-enriched targeted sequencing data. BMC Bioinformatics. 2016; 17(1):429. https://doi.org/10.1186/s12859-016-1272-6 PMID: 27770783; PubMed Central PMCID: PMCPMC5075217.

14. Cleveland WS. Lowess—a Program for Smoothing Scatterplots by Robust Locally Weighted Regression. Am Stat. 1981; 35(1):54–. https://doi.org/10.2307/2683591 WOS:A1981LF14200011.

15. Page E. Continuous inspection schemes. Biometrika. 1954; 41:100–15. https://doi.org/10.2307/2333009

16. Danecek P, Auton A, Abecasis G, Albers CA, Banks E, DePristo MA, et al. The variant call format and VCFtools. Bioinformatics. 2011; 27(15):2156–8. https://doi.org/10.1093/bioinformatics/btr330 PMID: 21653522; PubMed Central PMCID: PMCPMC3137218.

Conclusion

CovCopCan software has been designed and created with the purpose of increasing information achievable from NGS, since it allows to detect CNV, often underestimated. It cannot detect, however, different Structural Variants (SV), as translocations and inversions, where the number of genomic copies is not modified. In a general way, we think that CovCopCan could be an important tool to increase the rate of positive diagnosis, which rests pretty low for some hereditary pathologies, like, for instance, peripheral neuropathies. Furthermore, it can be necessary not only in the identification of already described CNV, but, above all, in discovery of new duplications and deletions, elucidating unknown mechanisms associated with the diseases. It is for this reason, that CovCopCan arose from the interaction between the diagnostic field, at Biochemistry and Molecular Genetics Department of University Hospital of Limoges, and the research field, at University of Limoges.

<u>Article 2</u> - A mutation can hide another one: Think Structural Variants!

Published in Computational and Structural Biotechnology Journal (online 2 August 2020)

As previously discussed, molecular analyses of hereditary diseases, by NGS, generally focuses on single-nucleotide polymorphisms. Consequentially, SV, like CNV, are often neglected, also for the lack of valid analysis tools. In Charcot-Marie-Tooth disease, 15% of cases are associated with the duplication of *PMP22* gene (CMT1A). Anyway, evaluation of SV in other 80 and more CMT-genes is rarer. The paper reported here is the genetic investigation of the patient 1-A (described in Materials and Methods, Chapter I), presenting peripheral neuropathy and cerebellar ataxia. The targeted NGS analysis, conducted with a 93-genes custom panel for CMT and associated neuropathies, had revealed the homozygous c.5744_5745delAT in exon 10 of *SACS* gene, inducing a frameshift and the production of a truncated protein. Since mutations in *SACS* were consistent with the observed phenotype, we could suppose to have identified the correct genetic cause. Nevertheless, Sanger sequencing detected the same mutation, in homozygous state, in the affected brother (patient 1-B), in heterozygous state, in his father (patient 1-C), but not in his mother (patient 1-D). Only looking for CNV in NGS data, by CovCopCan analysis, we detected, in patient 1-A, a heterogygous deletion in exon 10 of *SACS*, never described before. It was then confirmed, in heterozygous state, also in the affected brother and the unaffected mother. Patient 1-A, as well as his brother, was, therefore, a compound heterozygous for *SACS*, since he carried two different *SACS* mutations (c.5744_5745delAT and deletion) on its two alleles.

This study highlighted the importance of exploring both point mutations, small indels, and large SV, during the diagnostic procedure. The validation of results with multiple technical approaches, and an in-depth analysis of the genotype-phenotype correlation, could help, as in the present case, the detection of the genetic cause inducing the pathological condition.

Also this work, started at the Biochemistry and Molecular Genetics Department of University Hospital of Limoges, was developed thanks to the collaboration with the EA6309 research team, for the investigation of CNV.

Computational and Structural Biotechnology Journal 18 (2020) 2095–2099

COMPUTATIONAL AND STRUCTURAL BIOTECHNOLOGY JOURNAL

journal homepage: www.elsevier.com/locate/csbj

Communications

A mutation can hide another one: Think Structural Variants!

Federica Miressi [a], Pierre-Antoine Faye [a,b], Ioanna Pyromali [a], Sylvie Bourthoumieux [a,c], Paco Derouault [d], Marie Husson [e], Frédéric Favreau [a,b], Franck Sturtz [a,b], Corinne Magdelaine [a,b], Anne-Sophie Lia [a,b,d,*]

[a] Univ. Limoges, MMNP, EA 6309, F-87000 Limoges, France
[b] CHU Limoges, Service de Biochimie et Génétique Moléculaire, F-87000 Limoges, France
[c] CHU Limoges, Service de Cytogénétique, F-87000 Limoges, France
[d] CHU Limoges, Service de Bioinformatique, F-87000 Limoges, France
[e] CHU Bordeaux, Service de Neurologie, F-33076 Bordeaux, France

ARTICLE INFO

Article history:
Received 29 February 2020
Received in revised form 29 June 2020
Accepted 25 July 2020
Available online 2 August 2020

Keywords:
Structural Variants
Diagnosis
Charcot-Marie-Tooth
NGS
CovCopCan

ABSTRACT

Next Generation Sequencing (NGS) using capture or amplicons strategies allows the detection of a large number of mutations increasing the rate of positive diagnosis for the patients. However, most of the detected mutations are Single Nucleotide Variants (SNVs) or small indels. Structural Variants (SVs) are often underdiagnosed in inherited genetic diseases, probably because few user-friendly tools are available for biologists or geneticists to identify them easily. We present here the diagnosis of two brothers presenting a demyelinating motor-sensitive neuropathy: a presumed homozygous c.5744_5745delAT in exon 10 of *SACS* gene was initially detected, while actually these patients were heterozygous for this mutation and harbored a large deletion of *SACS* exon 10 in the other allele. This hidden mutation has been detected thanks to the user-friendly CovCopCan software. We recommend to systematically use such a software to screen NGS data in order to detect SVs, such as Copy Number Variations, to improve diagnosis of the patients.

1. Introduction

Inherited genetic diseases are due to germline mutations. Thanks to Next Generation Sequencing (NGS), an increasing number of these mutations are detected every day improving patients' diagnosis. Therefore, molecular diagnosis may influence patients' care through the choice of adapted treatments, for instance in neurological diseases and particularly in genetic epilepsies [1]. However, to date, the majority of the reported mutations are Single Nucleotide Variants (SNVs) and Structural Variants (SVs) have rarely been described, probably due to the analytic methods used to analyze NGS data, comparing patients' sequences to a reference one.

In Charcot-Marie-Tooth disease (CMT), the most common hereditary neuropathy characterized by damages of both motor and sensory peripheral nerves, the most frequent mutation involved in this disease is the *PMP22* duplication, explaining around 15% of CMT patients. It has been identified by Southern-Blot in 1992 [2]. Since this date, more than other 90 genes have been identified to be involved in this disease and in associated peripheral neuropathies [3]. Most of the detected mutations are SNVs or small indels [4,5], and Structural Variants (SVs) have rarely been described [6].

NGS techniques allow partial or total sequencing of a patient's genome. Sequenced libraries can be prepared by capture or by amplicons. Both methods are efficient for the detection of single-nucleotide variants or short indels, however only a few tools are available for the detection of large deletions or duplications, especially with amplicon sequencing data, such as Cov'Cop and CovCopCan [7,8]. Molecular diagnosis being an essential step of patient care, we believe it is crucial to improve the detection of SVs to increase the rate of positive diagnosis by using several bioinformatics approaches to analyze NGS data.

By presenting the diagnosis of a specific patient harboring a peripheral neuropathy, we show here how it is important to look for all kind of variants to provide an accurate diagnosis to the patients. Indeed one mutation could hide another one, such as Structural Variant.

2. Material and methods

2.1. Patients

Our current study focused on a family with two cases of peripheral neuropathy: Patients A (propositus) and B (affected brother),

* Corresponding author at: 2 rue du Docteur Raymond Marcland, 87000 Limoges, France.
E-mail address: anne-sophie.lia@unilim.fr (A.-S. Lia).

https://doi.org/10.1016/j.csbj.2020.07.021
2001-0370/

both with learning disabilities. Patient A is a 19 year-old man, presenting peripheral neuropathy (EMG: abolished sensitive potential and altered motor velocities, with elongated distal latencies and altered F-waves – Median nerve conduction velocity: 38 m/s). He also has pes cavus, progressive cerebellar ataxia and abolished Achilles reflex. His brother, Patient B, is a 9 year-old boy, presenting peripheral neuropathy, exhibiting progressive walking difficulties, fine motor skill disabilities, balance disorder with intermittent falls and Achilles reflex decrease. We accessed to the DNA of the four members of this family: Patients A (propositus) and B (affected brother), and patients C and D, the unaffected father and mother respectively.

2.2. DNA extraction

Blood samples were collected in EDTA tubes after providing informed consent. The protocol was in accordance with the French ethics legislation and the Declaration of Helsinki. Genomic DNA was extracted by standard methods (Illustra DNA Extraction kit BACC3, GEHC).

2.3. Sequencing

NGS strategy was performed on patient A using a 93-genes-custom panel designed for CMT and associated neuropathies diagnosis (Supplementary Table 1). The amplified library was prepared with Ion P1 HiQ Template OT2 200 kit (Ampliseq Custom, Life technologies), sequenced on Proton sequencer (Life technologies), and mapped to the human reference sequence hg19/GHCh37. Mutations of interest were verified by Sanger sequencing using forward and reverse primer pairs.

2.4. Bioinformatics analyses

Variants detected by targeted NGS were annotated using Ion reporter software. They were evaluated with Alamut Mutation Interpretation Software (Interactive Biosoftware, Rouen, France). Databases such as ExAC Genome browser (http://exac.broadinstitute.org), dbSNP135 (National Center for Biotechnology Information [NCBI], Bethesda, Maryland, USA, http://www.ncbi.nlm.nih.gov/projects/SNP/), ClinVar (www.ncbi.nlm.nih.gov/clinvar) and HGMD professional (www.hgmd.cf.ac.uk) were also screened. Cov'Cop and CovCopCan, interactive powerful software, were used to detect Copy Number Variations (CNV) [7,8]. Briefly, using the read depth value of each amplicon, these software simultaneously analyze all the patients of the run. The algorithm is based on the concept that in common cases, both alleles have to be similarly amplified within each amplicon. Several normalization steps, guided by carefully chosen references amplicons, permit to compute a score for each amplicon. Theoretical score of 1 is the normal case while low (<0.5) or high (>1.5) values respectively reveal deletions or duplications. Cov'Cop and CovCopCan were used with the default settings, with all options active and we defined a minimum threshold of three successive amplicons on the same chromosome to highlight a CNV. For the tested patient, mean read depth value of the 93 tested genes was 1624 X and the mean value for the 78 amplicons covering *SACS* was 660 X (minimum: 64 X and maximum: 2603 X). The coverage of *SACS* was 100%.

2.5. Quantitative real-time Q-PCR

Primers were designed in exon 9 and 10 of *SACS* gene and in exon 1 of Albumin gene, chosen as reference gene. Rotor-Gene SYBR Green PCR Kit (400) (©QIAGEN) was used following the standard protocol. Reactions were performed on the Corbett Rotor-

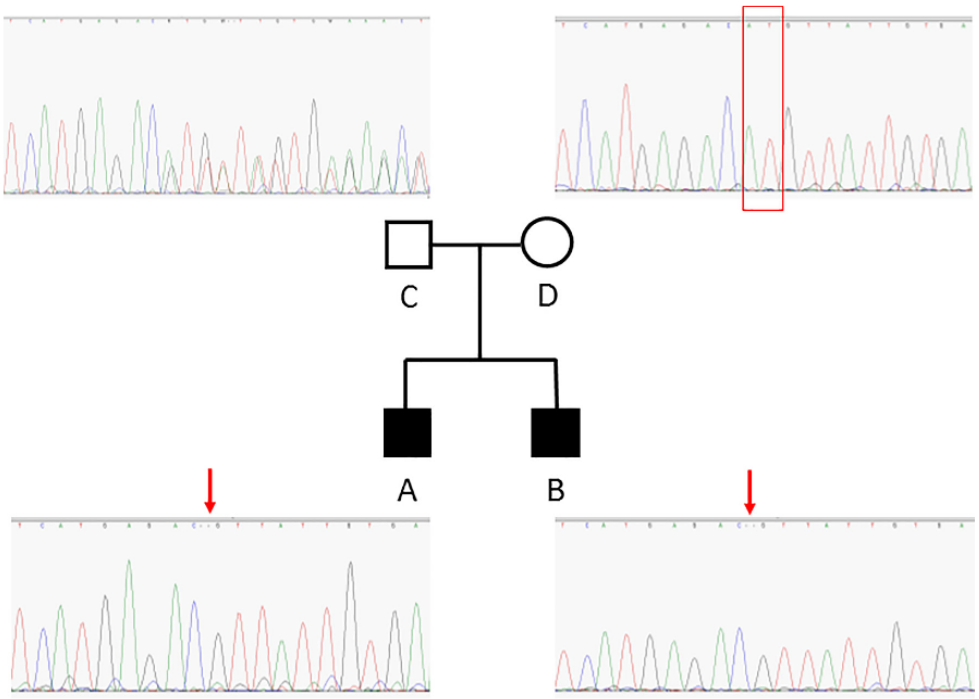

Fig. 1. Family tree associated with Sanger sequencing of SACS exon 10.

Fig. 2. Visualization of CovCopCan results. Each dot corresponds to an amplicon. The amplicons are distributed on the x-axis according to their genomic position. The y-axis corresponds to the normalized values. Grey dots indicate a "normal" value, whereas red or orange dots indicate duplicated and deleted amplicons, respectively. A) Patient A analysis in which one can see a partial deletion of SACS gene, highlighted in orange; B) A control sample analysis in which no deletion or duplication can be detected. (For interpretation of the references to colour in this figure legend, the reader is referred to the web version of this article.)

Gene 6000 Machine (© QIAGEN). The Ct values of each Real-Time reaction were normalized, using Albumin as endogenous control gene, and then compared to the normalized Ct values of three control samples.

3. Results

3.1. Detection of presumed homozygous mutation in SACS gene

Targeted NGS of Patient A DNA, revealed the presence of mutation c.5744_5745delAT in exon 10 of *SACS* gene. This mutation results in a frameshift, leading to truncated protein p. His1915Argfs*19. This mutation is very rare (1/125568 in ExAc) and is predicted as pathogenic in ClinVar. The normal allele has not been sequenced suggesting the presence of mutation c.5744_5745delAT at homozygous state, confirmed by Sanger sequencing (Fig. 1-A). No other rare Single Nucleotide Variant or short InDels has been detected in this patient. Mutations in *SACS* have already been reported to be responsible of spastic ataxia of Charlevoix-Saguenay, an early-onset neurodegenerative disease. The transmission follows an autosomal recessive manner and two mutations are expected in a patient.

3.2. Problematic familial segregation

Sanger Sequencing surrounding the mutation was then performed on the affected brother B and on father C and mother D, both asymptomatic. As expected, only the c.5744_5745delAT mutation was detected in patient B (Fig. 1-B), heterozygous mutation was detected in the father (Fig. 1-C), but no mutation was detected in the mother (Fig. 1-D), showing that only the normal allele could be sequenced in this case and suggesting the potential presence of a deletion of this area, that had to be defined more precisely.

3.3. Detection of Structural Variant using CovCopCan

We then used the new CovCopCan software, a user-friendly tool, based on the read-depth analysis of NGS data, that allows the rapid and easily detection of Structural Variants (SVs) in inherited diseases but also in Cancer [8]. Using CovCopCan, we identified easily the presence of a heterozygous deletion in *SACS* gene (Fig. 2A) in comparison to a control (Fig. 2B). We could also define, thanks to CovCopCan, the boundaries of the deletion. Indeed, we could see that amplicons on exon 9 were not deleted (value around 1 in CovCopCan) and that amplicons on exon 10 were deleted (value around 0.5) (Fig. 3A and 3B). This new SV has never been described (SV-GnomAD) and it could lead to the production of a truncated protein.

3.4. Confirmation of Structural Variant and correct segregation

We confirmed the presence of exon 10 deletion in Patient A by Real-Time qPCR. We investigated the other individuals of the family: as expected, the affected brother and the mother presented the exon 10 deletion, but not the father. Normal value has been obtained for exon 9 in all the family members confirming that the deletion does not overlap the first exons of *SACS* gene.

4. Discussion

We showed here the importance of complete bioinformatics analysis of NGS data to perform an accurate diagnosis. In this family, the presumed homozygous mutation c.5744_5745delAT has been detected in *SACS* gene by classical variants detection software

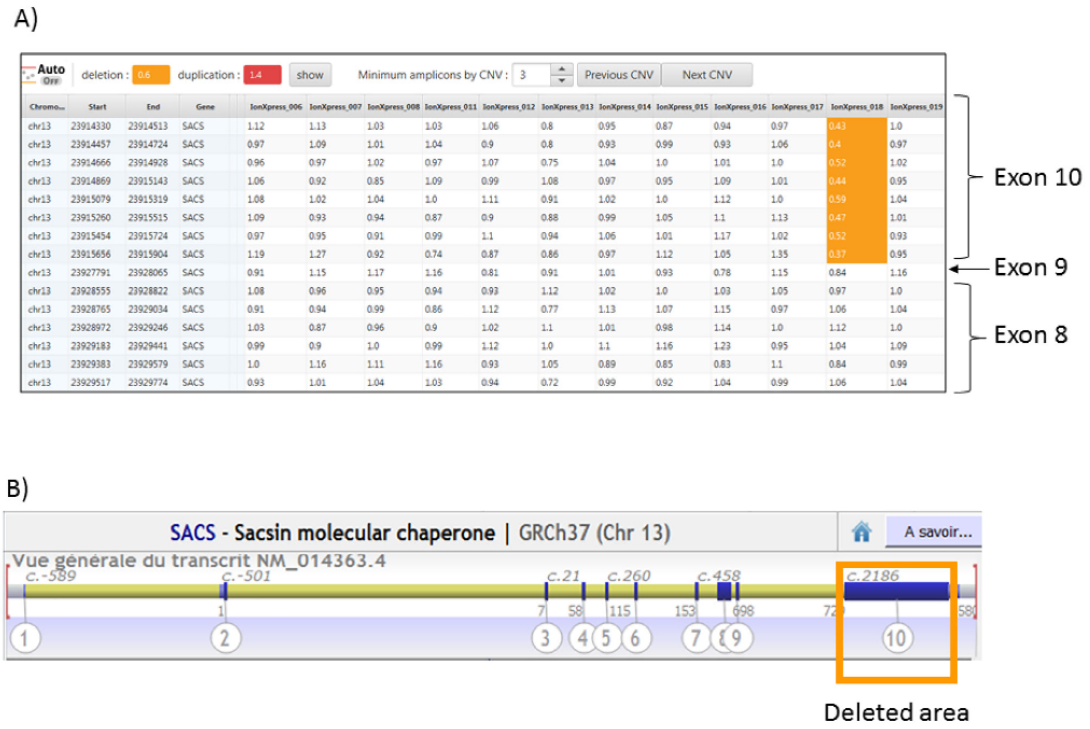

Fig. 3. Detection of SACS Exon 10 deletion – A) Overview of CovCopCan table results, values around 0.5 (highlighted in yellow) show a deletion of this area in patient A (Xpress 18), but not in the other patients tested in the same NGS Run; B) Alamut Overview of SACS gene and of the deleted area. (For interpretation of the references to colour in this figure legend, the reader is referred to the web version of this article.)

such as Ion Reporter in Patient A. This conclusion was actually not accurate. Indeed, Patient A presents in fact one allele with c.5744_5745delAT mutation and one allele with a Structural Variation: a large deletion of *SACS* exon 10. This SV has been detected thanks to CovCopCan Software, a new user-friendly tool allowing the detection of Copy Number Variations (CNVs) in NGS data generated from amplicons sequencing.

Few user-friendly tools are easily usable for biologists and geneticists to detect SVs, such as CNVs, in amplicons sequencing data. In addition to CovCopCan, ExomeDepth [9], IonCopy [10], DeviCNV [11], Cov'Cop [7], are also available and have to be tested by the users to define their preferred tools to detect these SVs. We believe tools detecting SVs, such as CNVs, have to be used systematically on NGS data analysis in addition to the classical variants detection tools highlighting only Single Nucleotide Variants and small indels.

However, it is important to notice that these tools using the read-depth to detect CNVs, will not be able to detect easily SVs such as inversion or translocation. To date, we do not know the percent of CNVs responsible for inherited diseases in comparison to others SVs, such as inversion or translocation, because all of them were poorly detected until now. In addition, we do not know the percent of pathogenic CNVs in comparison to SNVs or some indels.

Nevertheless, we estimated in our cohort of 695 CMT patients analysed by NGS using an amplicon targeted sequencing panel of 93 genes of Charcot-Marie-Tooth disease and associated neuropathies, that CNVs were present in 107 patients (15.4% of the patients), showing a large amount of CNVs in our cohort. Twenty-eight were small deletions (3–6 amplicons), 10 were large deletions, 49 were small duplications and 20 were large duplications. We now investigate the pathogenicity of these new SVs and we presented one of them in this article: a large deletion of *SACS* exon 10, which appeared to be pathogenic.

Currently, in the diagnosis of peripheral neuropathy, we reach between around 40% of positive diagnosis using only classical variants detection software highlighting SNVs or some indels. By using, in addition, tools such as CovCopCan, allowing the detection of SVs, such as CNVs, we hope to increase the rate of positive diagnosis for our patients. Indeed, to date, a patient with a homozygous SV was not diagnosed positively using the classical tools, this was also the case for male patients harboring, for example, a deletion on X chromosome gene, while these kind of SVs could be pathogenic mutations. Thanks to CovCopCan, or equivalent tools, all these patients will be diagnosed positively. Of course, CovCopCan can detect CNVs on all the inherited diseases. This tool works on data generated from Ion Designer (Life Technologies, CA, USA) as well as that from Illumina DesignStudio (Illumina Inc., San Diego, CA, USA). The user-friendly interface associated with our 2D visualization facilitates data exploration.

5. Conclusion

Structural Variants are probably underdiagnosed and should be more looked for to improve inherited diseases diagnosis. It is crucial for physicians to be aware that a potential homozygous variation can hide a Structural Variant. In addition, if no pathogenic SNV was found by NGS sequencing, SVs should be systematically inves-

tigated. Detection of such variants would then help to better understand the physiopathology involved in inherited diseases, in order to develop, in fine, therapeutic approaches.

6. Author statement

All authors have reviewed and edited the manuscript.

FM: participated to the bioinformatics study, performed experiments and proofread the manuscript

PAF: participated to the bioinformatics study, participated to the writing and proofread the manuscript

IP: participated to the bioinformatics study and performed experiments

SB: performed experiments

PD: participated to the bioinformatics study and proofread the manuscript

MH: reported clinical study

FF: performed a critical revision of the manuscript

FS: contributed to the interpretation of the results and proofread the manuscript

CM: planned the experiments, contributed to the interpretation of the results and proofread the manuscript.

ASL: initiated the work, designed and planned the experiments, analyzed the results and wrote most of the manuscript.

Declaration of Competing Interest

The authors declare that they have no known competing financial interests or personal relationships that could have appeared to influence the work reported in this paper.

Acknowledgment

We would like to thank the Sequencing GenoLim team of the Limoges CHU, especially Emilie Guerin, Valentin Tilloy and Sophie Alain.

Appendix A. Supplementary data

Supplementary data to this article can be found online at https://doi.org/10.1016/j.csbj.2020.07.021.

References

[1] Striano P, Vari M, Mazzocchetti C, Verrotti A, Zara F. Management of genetic epilepsies: from empirical treatment to precision medicine. Pharmacol Res 2016;107:426–9.
[2] Timmerman V, Nelis E, Van Hul W, Nieuwenhuijsen BW, Chen KL, Wang S, et al. The peripheral myelin protein gene PMP-22 is contained within the Charcot-Marie-Tooth disease type 1A duplication. Nat Genet 1992;1(3):171–5. Erratum in: Nat Genet 1992 Sep;2(1):84.
[3] Timmerman V, Strickland AV, Züchner S. Genetics of Charcot-Marie-Tooth (CMT) disease within the frame of the human genome project success. Genes (Basel) 2014;5(1):13–32.
[4] Lerat J, Cintas P, Beauvais-Dzugan H, Magdelaine C, Sturtz F, Lia AS. A complex homozygous mutation in ABHD12 responsible for PHARC syndrome discovered with NGS and review of the literature. J Peripher Nerv Syst 2017;22(2):77–84.
[5] Lerat J, Magdelaine C, Roux AF, Darnaud L, Beauvais-Dzugan H, Naud S, et al. Hearing loss in inherited peripheral neuropathies: molecular diagnosis by NGS in a French series. Mol Genet Genomic Med 2019;7(9).
[6] Mortreux J, Bacquet J, Boyer A, Alazard E, Bellance R, Giguet-Valard AG, et al. Identification of novel pathogenic copy number variations in Charcot-Marie-Tooth disease. J Hum Genet 2020;65(3):313–23.
[7] Derouault P, Parfait B, Moulinas R, Barrot CC, Sturtz F, Merillou S, Lia AS. 'COV'COP' allows to detect CNVs responsible for inherited diseases among amplicons sequencing data. Bioinformatics 2017;33(10):1586–8.
[8] Derouault P, Chauzeix J, Rizzo D, Miressi F, Magdelaine C, Bourthoumieu S, et al. CovCopCan: an efficient tool to detect Copy Number Variation from amplicon sequencing data in inherited diseases and cancer. PLoS Comput Biol 2020;16(2).
[9] Plagnol V, Curtis J, Epstein M, Mok KY, Stebbings E, Grigoriadou S, et al. A robust model for read count data in exome sequencing experiments and implications for copy number variant calling. Bioinformatics 2012;28 (21):2747–54.
[10] Budczies J, Pfarr N, Stenzinger A, Treue D, Endris V, Ismaeel F, et al. Ioncopy: a novel method for calling copy number alterations in amplicon sequencing data including significance assessment. Oncotarget 2016;7(11):13236–47.
[11] Kang Y, Nam SH, Park KS, Kim Y, Kim JW, Lee E, et al. DeviCNV: detection and visualization of exon-level copy number variants in targeted next-generation sequencing data. BMC Bioinf 2018;19(1):381.

Conclusion

We reported here a family case of peripheral neuropathy, whose diagnosis was complicated by the unexpected genetic set-up. If we had limited our analysis to single-nucleotide mutations and small indels, obtained from NGS data, we would definitely identify the c.5744_5745delAT mutation, in *SACS*, as the only cause of the pathology. With this example, we wanted to show how, sometimes, a restricted molecular analysis, can lead to a partial, or incorrect, diagnosis. We think that this is a widespread phenomenon, partially responsible for several undiagnosed clinical cases of peripheral neuropathies (Mortreux et al. 2020). The routine employment of bioinformatics tools, as Cov'Cop and CovCopCan, could significantly help to overcome the diagnostic challenge.

Article 3 - One Multilocus Genomic Variation is responsible for a severe Charcot-Marie-Tooth axonal form: a singular case report

Article under review in Brain Sciences

The occurrence of multiple mutations, in different genomic loci, is rarely described in peripheral neuropathies. In CMT, two disease-inducing mutations, at most, have been occasionally reported for the same patient. In this work, we presented one case of peripheral neuropathy associated with three mutations in three different CMT-genes. In this family (described as Family 2, in Materials and Methods, Chapter I), the daughter (patient 2-B) had a more severe CMT2 form, with signs of mental retardation and learning problems. Her mother (patient 2-A) presented classical motor and sensory deficit. Three different strategies were combined to assess the correct molecular diagnosis. First, targeted NGS revealed, only in the daughter, the heterozygous p.Arg468His mutation in *MFN2*, not explaining, however, the mother's phenotype. Cov'Cop analysis detected the complete heterozygous duplication of *AARS1* gene, in the two affected subjects, but also in the unaffected sisters of patient 2-A (subjects 2-D and 2-E). Lastly, WES analysis allowed the identification, exclusively in patients 2-A and 2-B, of the heterozygous missense mutation c.754C>T (p.Arg252Trp) in *MORC2*.

Three different mutations (*MORC2*, *MFN2*, *AARS1*) were, therefore, present in patient 2-B, the more affected subject, two mutations (*MORC2*, *AARS1*) in patient 2-A, only one mutation (*AARS1*) in two unaffected family members. We can consider that the *MORC2* mutation is, presumably, the main cause of CMT in the Family 2, while the *MFN2* mutation may participate in aggravate the 2-B pathological state, as already described in previous works. The role of *AARS1* duplication rests unclear.

In this clinical case, the inconsistency between the genetic findings and the clinical manifestation led us to test different approaches during the molecular diagnosis. Unfortunately, the molecular exploration does not often take into account the "multilocus" possibility, overlooking further genomic alterations which could participate in establishing the whole patient's phenotype.

brain sciences

MDPI

Case Report

One Multilocus Genomic Variation is responsible for a severe Charcot-Marie-Tooth axonal form.

Federica Miressi [1,*], Corinne Magdelaine [1,2], Pascal Cintas [3], Sylvie Bourthoumieux [1,4], Angélique Nizou [1], Paco Derouault [5], Frédéric Favreau [1,2], Franck Sturtz [1,2], Pierre-Antoine Faye [1,2] and Anne-Sophie Lia [1,2,5]

[1] Univ. Limoges, MMNP, EA 6309, F-87000 Limoges, France
[2] CHU Limoges, Service de Biochimie et Génétique Moléculaire, F-87000 Limoges, France
[3] CHU Toulouse, Service de Neurologie, F-31000 Toulouse, France
[4] CHU Limoges, Service de Cytogénétique, F-87000 Limoges, France
[5] CHU Limoges, Service de Bioinformatique, F-87000 Limoges, France
* Correspondence: federica.miressi@unilim.fr

Received: date; Accepted: date; Published: date

Abstract: Charcot-Marie-Tooth (CMT) disease is a heterogeneous group of inherited disorders affecting the peripheral nervous system, with a prevalence of 1/2500. So far, mutations in more than 80 genes have been identified causing either demyelinating forms (CMT1) or axonal forms (CMT2). Consequentially, the genotype-phenotype correlation is not always easy to assess. Diagnosis could require multiple analysis before the correct causative mutation is detected. Moreover, it seems that approximately 5% of overall diagnosis for genetic diseases involves multiple genomic loci, although they are often underestimated or underreported. In particular, the combination of multiple variants is rarely described in CMT pathology and often neglected during the diagnostic process. Here, we present the complex genetic analysis of a family including two CMT cases with various severities. Interestingly, Next Generation Sequencing (NGS) associated with Cov'Cop analysis, allowing Structural Variants (SV) detection, highlighted variations in *MORC2* (microrchidia family CW-type zinc-finger 2) and *AARS1* (alanyl-tRNA-synthetase) genes for one patient and an additional mutation in *MFN2* (Mitofusin 2) in the more affected patient.

Keywords: Multilocus disease; Charcot-Marie-Tooth; Diagnosis; CNV; NGS

1. Introduction

Charcot-Marie-Tooth (CMT) disease, the most common peripheral neuropathy, is a hereditary disorder associated to numerous genomic mutations, which can occur in different genes and in different loci of the same gene. Even if Next Generation Sequencing (NGS) strategies, like Whole Exome Sequencing (WES) and Whole Genome Sequencing (WGS), are now largely used to investigate human variations, CMT molecular diagnosis still remains difficult. Furthermore, Posey *et al.*, showed, on a wild range of genetic pathologies, that phenotypical manifestations are the result of the combination of multiple genomic mutations in 4.9% of cases [1].

We describe here the genetic analysis of a family with two CMT2 cases: Patient A (mother), characterized by axonal impairment, and patient B (daughter), with a more severe clinical condition. NGS analyses associated with Cov'Cop analysis, allowing to detect Structural Variants (SV) [2], showed that both of them present a known pathological mutation in *MORC2* (microrchidia family CW-type zinc-finger 2) and a never described *AARS1* (alanyl-tRNA-synthetase) duplication. In addition, the more affected daughter had a third variation in *MFN2* (Mitofusin 2).

With this clinical case report, we want to highlight how CMT disease may belong to multilocus genetic pathologies. It could be relevant to take into account the possibility of a combined effect of multiple genomic mutations in order to explain the high heterogeneity of this complex clinical condition. Until now, this aspect has been poorly explored in CMT, often inducing uncompleted diagnosis and complicating the understanding of correlation between the genomic modifications and the phenotypic manifestations.

2. Case presentation

This study focused on a large family with two cases of CMT2 (Figure 1). Ethics approval was obtained from the ethic committee of Limoges University Hospital: N 386-2020-42, as well as the informed consent of all participants. This study was performed in accordance with the Declaration of Helsinki. We accessed to the DNA of five members of this family who were clinically examined by a neurologist. Patients A (mother) and B (daughter) exhibited neuropathic disease phenotypes, but not individuals C, D, and E, the maternal grand-mother and the maternal aunts of patient B, respectively. Patient A is a 58-year-old woman of French origin an atypical asymmetric proximal and distal neuropathy. Her symptoms started at the age of two with gait disturbances, which progressed to a complete loss of ambulation at 43 years old. Clinically, the deficit affected the proximal and distal regions and the upper and lower limbs equally but very asymmetrically. The nerve conduction study revealed an axonal asymmetric sensory and motor neuropathy (Table 1). Median motor nerve conduction velocity (MNCV) was 40 m/s. The clinical history of patient B is slightly different from those of her mother. Patient B, a 25-year-old woman, experienced her first difficulties in walking at the age of 18 months, followed by learning problems and signs of mental deficiency in the childhood. Medical examination revealed an asymmetric distal predominant sensory and motor deficit of upper and of lower limbs, prevalent on the left side. Mild muscular atrophy was observed in both hands in association with a dystonic disorder in the finger. The examination confirmed the presence of cerebellar ataxia, with a nystagmus. There were no pyramidal signs, no diaphragmatic paralysis, no thoracic deformity or vocal cords involvement. The asymmetry of the axonal sensory and motor neuropathy observed for patient A was confirmed in the daughter (Table 1). Encephalic MRI showed mild vermian atrophy, without cerebellar defects. Nystagmus was also present. No clinical signs have been observed in the other family members (C, D, and E).

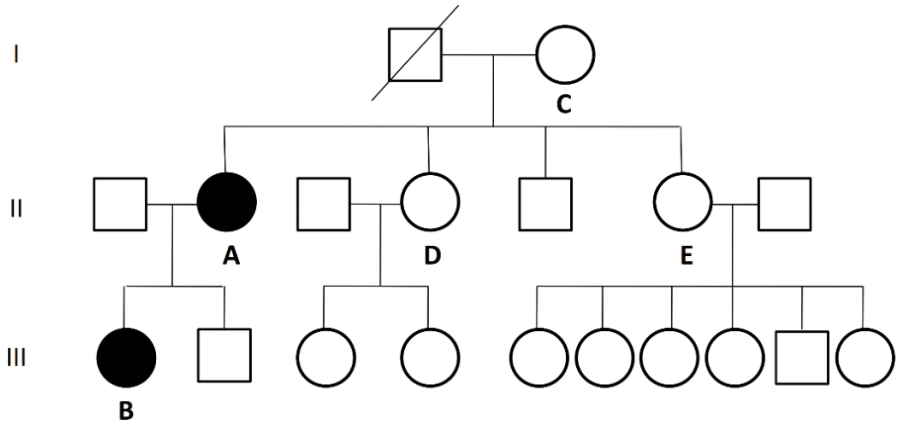

Figure 1. Family pedigree: the affected members are marked with black symbols.

Table 1. Neurophysiological recordings of patient A and patient B (Amp: amplitude; CMAP: compound motor action potential; CV: conduction velocity; NR: no response; SNAP: sensory nerve action potential).

Subjects	Peroneal		Sural		Median						Ulnar			
	Right	Left	Right	Left	Right			Left			Right		Left	
	CMAP Amp (mV)	CMAP Amp (mV)	SNAP Amp (µV)	SNAP Amp (µV)	CMAP Amp (mV)	CV (m/s)	SNAP Amp (µV)	CMAP Amp (mV)	CV (m/s)	SNAP Amp (µV)	CMAP Amp (mV)	SNAP Amp (µV)	CMAP Amp (mV)	SNAP Amp (µV)
Patient A	0.5	0.5	NR	NR	0.9	50	1.5	2.1	45	2.5	2.3	2.3	1.3	NR
Patinet B	2.7	NR	NR	NR	4.7	50	3.2	3.2	45	2.8	4.1	1.2	5.7	1.0

3. Materials and Methods

3.1. DNA extraction

Blood samples were collected in EDTA tubes. Genomic DNA was extracted by standard methods (Illustra DNA Extraction kit BACC3, GEHC).

3.2. Sequencing

First, NGS strategy was performed on patients A and B using a 92-genes-custom panel designed for CMT and associated neuropathies diagnosis (Supplementary data). The amplified library was prepared with Ion P1 HiQ Template OT2 200 kit (Ampliseq Custom, Life technologies), sequenced on Proton sequencer (Life technologies), and mapped to the human reference sequence hg19/GHCh37. Secondly, for WES, performed for patients A, B and E, libraries were prepared with NimbleGenSeqCapEZ-Library-SR-kits (Roche) and sequenced on a NextSeq-500-System (Illumina®). Mutations of interest were verified by Sanger sequencing using forward and reverse primer pairs.

3.3. Bioinformatics analysis

Variants detected by targeted NGS and by WES were annotated using Ion reporter and Annovar software respectively. They were evaluated with Alamut Mutation Interpretation Software (Interactive Biosoftware, Rouen, France). Databases such as ExAC Genome browser (http://exac.broadinstitute.org), dbSNP135 (National Center for Biotechnology Information [NCBI], Bethesda, Maryland, USA, http://www.ncbi.nlm.nih.gov/projects/SNP/), ClinVar (www.ncbi.nlm.nih.gov/clinvar) and HGMD professional (www.hgmd.cf.ac.uk) were also screened. Cov'Cop and CovCopCan, two interactive powerful software, were used to detect Copy Number Variations (CNV) [2] [3].

3.4. Array-comparative genomic hybridization (aCGH)

Array Comparative Genomic Hybridization (aCGH) was performed using G3 Human CGH microarrays 8x60K (Agilent Technologies) following the manufacturer's instructions. Agilent CytoGenomics software (Agilent Technologies) was used to visualize, detect and analyze copy number changes.

3.5. Quantitative real-time PCR (Q-PCR)

q-PCR reactions were carried out on genomic DNA extracted from blood samples. Primers were designed in exon 8 of *AARS1* gene and in exon 1 of *Albumin* gene, chosen as reference gene. Rotor-Gene SYBR-Green PCR Kit (400) (©QIAGEN) was used following the standard protocol. Reactions were performed on the Corbett Rotor-Gene 6000 Machine (© QIAGEN). The Ct values of each Real-Time reaction were normalized, using *Albumin* as endogenous control gene, and then compared to the normalized Ct values of three control samples.

The experiment was performed in triplicate. The normalized raw data of samples was analyzed by Student's t-test, comparing them with the normalized raw data of the controls. All results were statistically significant.

4. Results

Targeted NGS strategy revealed, only on patient B, a heterozygous c.1403G>A mutation in *MFN2* gene (NM_014874.3), resulting in the amino acidic substitution p.Arg468His. No other potentially pathological mutation has been detected for patient B by targeted NGS. Sanger sequencing confirmed the presence of *MFN2* c.1403G>A mutation in patient B, and excluded it in the other family members (Figure 2A). Given the unclear role of MNF2 p.Arg468His in CMT pathophysiology and its absence in the affected subject A, we expanded our study looking for CNV with the bioinformatics tools Cov'Cop and CovCopCan [2][3]. We detected, among the 92 sequenced genes investigated, a complete duplication of *AARS1* gene (NM_001605.2) in both patients [ClinVar accession number: SCV001167105]. *AARS1* duplication was confirmed by aCGH which allowed to identify a 231 kb duplication, whose start and stop coordinates were identified in positions chr16:70185757 and chr16:70416579, respectively. Other genes were included in the detected duplication and they are listed in Supplementary Table 2. Although no neuropathic clinical cases caused by *AARS1* duplication have already been reported, we investigated the unaffected individuals of the same family by Real-Time qPCR. There was no *AARS1* duplication in subject C, but it was present in unaffected subjects D and E, suggesting that *AARS1* duplication by itself is not the major cause of CMT disease of patients A and B (Figure 2B).

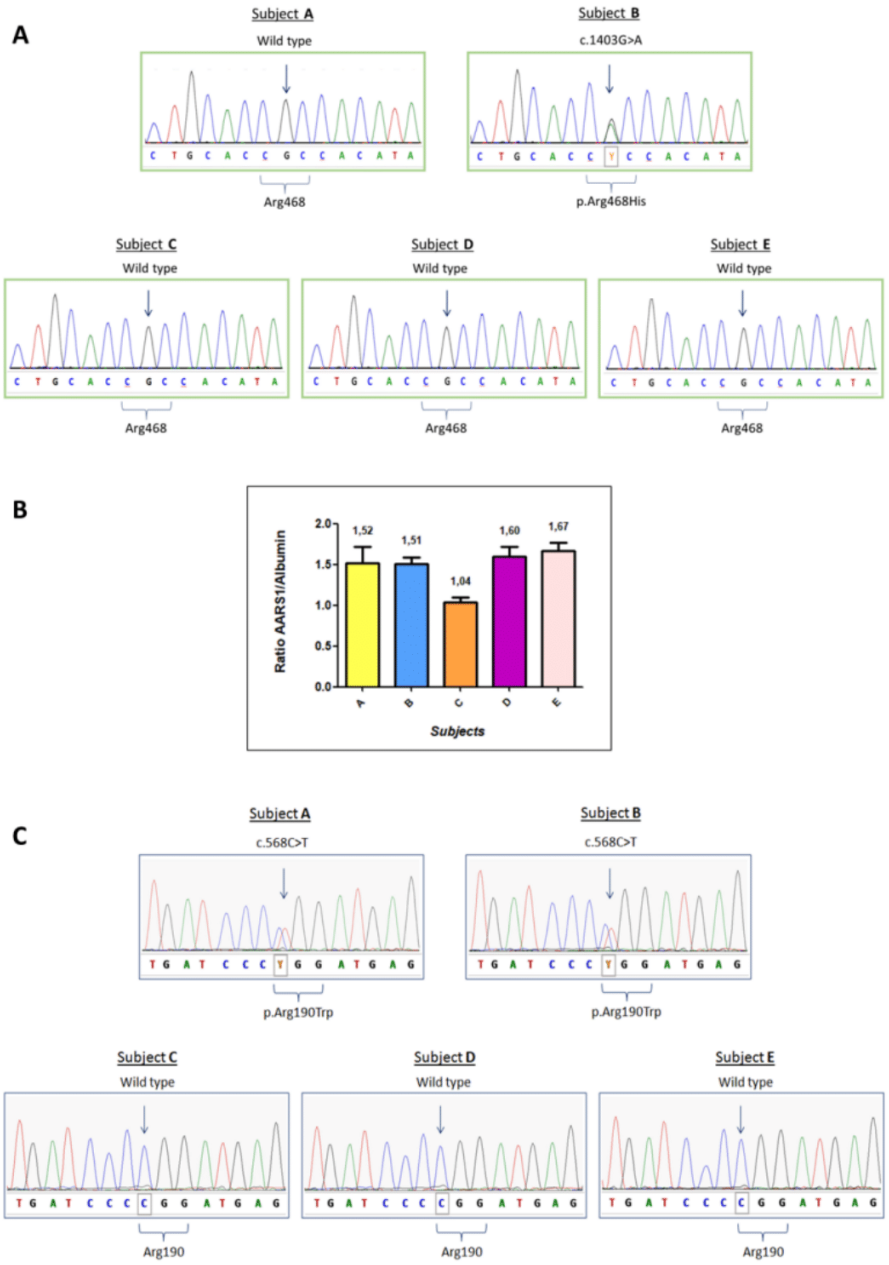

Figure 2 – Molecular analysis of patients A to E. A) Sanger Sequencing of *MFN2* gene regarding the variation c.1403G>A, p.Arg468His. B) Real-Time qPCR results for *AARS1* duplication. The expected ratio is approximately 1.5 in case of duplication (three copies versus two copies) or 1 if there are no copy number variations. Plot report ratios' means and standard deviations for each subject. C) Sanger sequencing analysis of *MORC2* gene regarding the variation c.568C>T, p.Arg190Trp.

To elucidate the genetic cause of the disease, we performed WES of three different members of the family: subjects A, B, and E, who is the mother of six unaffected children, reinforcing the hypothesis that she does not carry a pathological mutation responsible for CMT disease in this family. Interestingly, WES data showed a heterozygous missense mutation c.568C>T (p.Arg190Trp)

in *MORC2* gene (NM_014941), which was detected in the affected individuals (A and B) but not in the healthy one (E). c.568C>T is a known *MORC2* mutation, already described in literature [4]. Sanger sequencing confirmed the presence of the *MORC2* mutation in subjects A and B, and its absence in subjects C, D and E. Sanger sequencing results are reported in Figure 2C. The results of the three genetic variants are summarized in Figure 3.

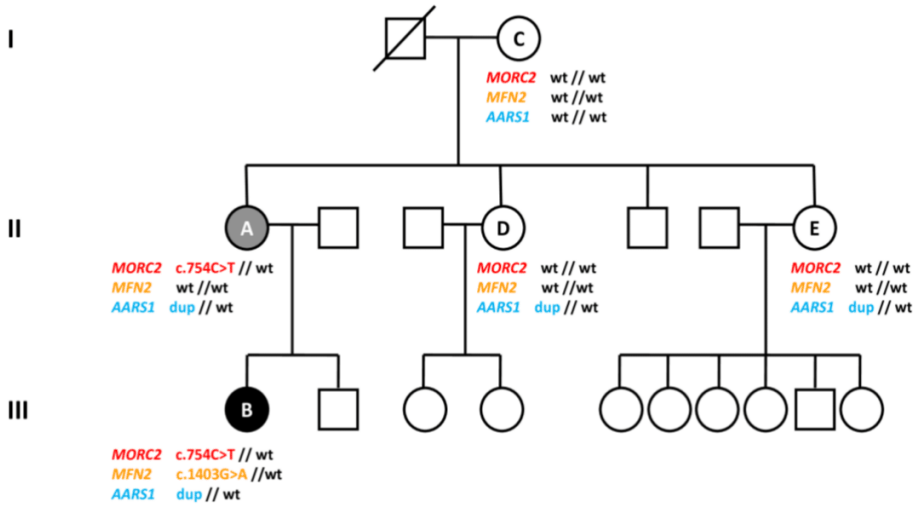

Figure 3: Family pedigree and summary of genetic results. The affected members are marked with black (more severe condition) or grey (less severe condition) symbols. Patients tested are indicated by letters A to E and their genotypes specified below (wt: wildtype; dup: duplication).

5. Discussion

The role of the three genetic variations (*AARS1* duplication, *MORC2* and *MFN2* mutations) in the clinical manifestation of CMT disease in our patients appears to be complex, but does not seem so rare according to Posey *et al.* who found that 4.9% of their diagnosed patients with genetic pathologies presented two or more disease loci [1].

MORC2 belongs to a family of transcriptional regulators conserved in eukaryotes and, interacting with the Human Silencing Hub (HUSH) complex, it participates in heterochromatin regulation [5,6]. Li *et al.* described that, when radiation-induced double-strand breaks occur, MORC2 protein interacts with DNA repair processes to induce chromatin relaxation [7]. Concerning its pathogenic involvements, it seems that altered MORC2 expression or function could promote tumor growth, invasion, and metastasis in several cancers [8,9]. However, *MORC2* mutations are usually associated with axonal Charcot-Marie-Tooth disease type 2Z. [4,10]. Classically, this *MORC2*-dependent form of CMT has an early age of onset and it is characterized by distal weakness of the lower limbs, muscular hypotonia and atrophy, foot deformities, such as pes cavus, sensory impairment, and areflexia. These clinical signs result in difficulty in walking and the need of canes or wheelchair. The *MORC2* heterozygous mutation c.568C>T (p.Arg190Trp), is, sometimes, also reported as c.754C>T (p.Arg252Trp), based on the isoform encoded by the NM_001303256 *MORC2* transcript. It has been described for the first time in 2016 [4], and it appears as a hot spot, located within the GHL-ATPase domain of the MORC2 protein [4,10]. It seems to hyperactivate HUSH-mediated silencing, whereas its effect on ATPase activity remains unclear [5,11]. Moreover, in patients-derived fibroblasts, p.Arg190Trp alters the transcriptional regulation of more than 800

target genes, like ZNFs, homeobox genes, helicases and metallothionein genes [11]. According to our findings and previous results, the heterozygous *MORC2* mutation c.568 C>T is likely the main cause of the axonal neuropathy of patient A.

However, patient B was characterized by a more severe phenotype than patient A. This phenotypic difference may be related to the *MFN2* missense mutation c.1403G>A (p.Arg468His), which was found only in the more affected daughter (B). *MFN2* gene encodes a mitochondrial membrane protein which plays a crucial role in mitochondrial fission and mitochondrial pathway's organization. The amino acidic substitution p.Arg468His is located between the transmembrane domain and the C-terminal coiled coil region of the MFN2 protein [12]. It has already been described as the causative mutation of the axonal CMT2A, but its pathogenicity rests unclear and in ClinVar database its interpretation is mentioned as conflicting. Engelfried *et al.* reported it in two patients, the first with muscular atrophy and sensory loss, the second with Parkinson and distal neuropathy, but also in an asymptomatic individual [12]. This *MFN2* variation was also found in two members of a Spanish family with mild CMT phenotype and discrete symptoms of neuropathy [13]. Given the highly variability of the associated phenotype and its uncertain pathogenicity, functional studies were conducted on human fibroblasts carrying the p.Arg468His substitution, demonstrating a mitochondrial coupling defect and a reduced ATP production [13]. In 2011, p.Arg468His was reported to be a disease-causing mutation in association with *GDAP1* nonsense mutation p.Gln163* [14]. The clinical condition of the patient was more complex than that of her brother, who bore only the *MFN2* mutation. As well as *MFN2* and *GDAP1*, the simultaneous occurrence of two disease-causing mutations in CMT pathology (digenic inheritance) has been described for other combinations of genes, sometimes associated with intrafamilial variability [15–17]. This corroborates the idea that, even if the *MFN2* p.Arg468His mutation is not the primary genetic cause, it may impact the symptomatology's severity of patient B, in our clinical case. The role of *MFN2* p.Arg468His mutation as modifier allele, in CMT, has already been suggested in a previous publication [18].

Moreover, in our family, we detected a third variation, the complete duplication of *AARS1* gene, a SV never described before and not recorded in GnomAD database. *AARS1* encodes the alanyl-tRNA-synthetase, the enzyme that catalyzes proper attachment of Alanine to its tRNA. In 2010, Latour *et al.* showed for the first time that an *AARS1* missense mutation was responsible for axonal Charcot-Marie-Tooth disease in a French family [19]. Further *AARS1* pathological mutations were then reported to be associated to CMT disease [20,21]. As well as AARS1, several other tRNA-synthases were shown to be involved in peripheral neuropathies. In these cases, dominant mutations resulted in pathological mutant proteins, and toxic gain-of-function effects, or in protein's loss of function [22]. However, overexpression of wildtype tRNAs has never been described to cause CMT disease and overexpression of wildtype GARS1 in mice showed no pathological effect [23]. In our case, the presence of *AARS1* duplication also in two unaffected family members, suggests that the overproduction of AARS1 enzyme would not alter the translation process and is not enough by itself to induce CMT. However, we cannot exclude that *AARS1* duplication, just like *MFN2* mutation, may modulate the phenotypic manifestation of this CMT axonal form, acting as "modifier allele". In recent years, the role of modifier alleles has been reported and analyzed in some cases of CMT disease [24,25].

6. Conclusions

In summary, in our study, the *MORC2* mutation (p.Arg190Trp) alone is likely responsible for axonal CMT disease (patient A). When the *MFN2* mutation (p.Arg468His) is associated with it, their effects are probably combined in a synergistic way, resulting in a more severe phenotype with additional symptoms (patient B). Lastly, an additional pathogenic role of the newly described *AARS1* duplication cannot be excluded. This genomic analysis shows how it could be complex to investigate a family clinical case if diagnosis is not complete and genetic variations are only partially detected. We believe that, for heterogeneous diseases like Charcot-Marie-Tooth, a more accurate investigation supported by Next Generation Sequencing technologies, would promote the discovery

of new genes-associations, so the understanding of further molecular interactions and impaired mechanisms in this pathology.

Supplementary Materials: The following are available online at [www.mdpi.com/xxx/s1]. Supplementary Table 1: 92-gene panel used for NGS. It includes the 44 known CMT genes, 27 genes involved in HSN (Hereditary Sensitive Neuropathy) and HMN (Hereditary Motor Neuropathy) and 21 other genes of interest involved in neuropathies of differential diagnosis [R = recessively-inherited; D = dominantly-inherited].

Author Contributions: Conceptualization, A.-S.L; software, P.D.; validation, F.M., and C.M.; formal analysis, F.M., P.D., and A.-S.L.; investigation, F.M., C.M., P.C., S.B., and A.N.; resources, C.M., and P.C.; data curation, C.M., and S.B.; writing—original draft preparation, F.M., and A.-S.L.; writing—review and editing, C.M., P.C., P.D., S.B., A.N., F.F., F.S., and P.-A.F.; visualization, F.M., F.F., F.S., P.-A.F., and A.-S.L.; supervision, P.-A.F., and A.-S.L.; project administration, A.N., P,-A,F., and A.-S.L.; funding acquisition, F.S., and A.-S.L.. All authors have read and agreed to the published version of the manuscript.

Funding: This research received no external funding.

Acknowledgments: We would like to acknowledge the GENOLIM-tool and Emilie GUERIN, as well as the PEIRENE laboratory, Lionel FORESTIER, and Nathalie DUPRAT.

Conflicts of Interest: The authors declare no conflict of interest.

References

1. Posey, J.E.; Harel, T.; Liu, P.; Rosenfeld, J.A.; James, R.A.; Coban Akdemir, Z.H.; Walkiewicz, M.; Bi, W.; Xiao, R.; Ding, Y.; et al. Resolution of Disease Phenotypes Resulting from Multilocus Genomic Variation. *N Engl J Med* **2017**, *376*, 21–31, doi:10.1056/NEJMoa1516767.
2. Derouault, P.; Parfait, B.; Moulinas, R.; Barrot, C.-C.; Sturtz, F.; Merillou, S.; Lia, A.-S. " COV'COP" allows to detect CNVs responsible for inherited diseases among amplicons sequencing data. *Bioinformatics* **2017**, *33*, 1586–1588, doi:10.1093/bioinformatics/btx017.
3. Derouault, P.; Chauzeix, J.; Rizzo, D.; Miressi, F.; Magdelaine, C.; Bourthoumieu, S.; Durand, K.; Dzugan, H.; Feuillard, J.; Sturtz, F.; et al. CovCopCan: An efficient tool to detect Copy Number Variation from amplicon sequencing data in inherited diseases and cancer. *PLoS Comput Biol* **2020**, *16*, e1007503, doi:10.1371/journal.pcbi.1007503.
4. Sevilla, T.; Lupo, V.; Martínez-Rubio, D.; Sancho, P.; Sivera, R.; Chumillas, M.J.; García-Romero, M.; Pascual-Pascual, S.I.; Muelas, N.; Dopazo, J.; et al. Mutations in the MORC2 gene cause axonal Charcot–Marie–Tooth disease. *Brain* **2016**, *139*, 62–72, doi:10.1093/brain/awv311.
5. Tchasovnikarova, I.A.; Timms, R.T.; Douse, C.H.; Roberts, R.C.; Dougan, G.; Kingston, R.E.; Modis, Y.; Lehner, P.J. Hyperactivation of HUSH complex function by Charcot–Marie–Tooth disease mutation in MORC2. *Nat Genet* **2017**, *49*, 1035–1044, doi:10.1038/ng.3878.
6. Douse, C.H.; Bloor, S.; Liu, Y.; Shamin, M.; Tchasovnikarova, I.A.; Timms, R.T.; Lehner, P.J.; Modis, Y. Neuropathic MORC2 mutations perturb GHKL ATPase dimerization dynamics and epigenetic silencing by multiple structural mechanisms. *Nat Commun* **2018**, *9*, 651, doi:10.1038/s41467-018-03045-x.
7. Li, D.-Q.; Nair, S.S.; Ohshiro, K.; Kumar, A.; Nair, V.S.; Pakala, S.B.; Reddy, S.D.N.; Gajula, R.P.; Eswaran, J.; Aravind, L.; et al. MORC2 Signaling Integrates Phosphorylation-Dependent, ATPase-Coupled Chromatin Remodeling during the DNA Damage Response. *Cell Reports* **2012**, *2*, 1657–1669, doi:10.1016/j.celrep.2012.11.018.
8. Liao, X.-H.; Zhang, Y.; Dong, W.-J.; Shao, Z.-M.; Li, D.-Q. Chromatin remodeling protein MORC2 promotes breast cancer invasion and metastasis through a PRD domain-mediated interaction with CTNND1. *Oncotarget* **2017**, *8*, 97941–97954, doi:10.18632/oncotarget.18556.
9. Zhang, F.-L.; Cao, J.-L.; Xie, H.-Y.; Sun, R.; Yang, L.-F.; Shao, Z.-M.; Li, D.-Q. Cancer-Associated MORC2-Mutant M276I Regulates an hnRNPM-Mediated CD44 Splicing Switch to Promote Invasion and

Metastasis in Triple-Negative Breast Cancer. *Cancer Res* **2018**, *78*, 5780–5792, doi:10.1158/0008-5472.CAN-17-1394.

10. Laššuthová, P.; Šafka Brožková, D.; Krůtová, M.; Mazanec, R.; Züchner, S.; Gonzalez, M.A.; Seeman, P. Severe axonal Charcot-Marie-Tooth disease with proximal weakness caused by de novo mutation in the MORC2 gene. *Brain* **2016**, *139*, e26–e26, doi:10.1093/brain/awv411.
11. Sancho, P.; Bartesaghi, L.; Miossec, O.; García-García, F.; Ramírez-Jiménez, L.; Siddell, A.; Åkesson, E.; Hedlund, E.; Laššuthová, P.; Pascual-Pascual, S.I.; et al. Characterization of molecular mechanisms underlying the axonal Charcot–Marie–Tooth neuropathy caused by MORC2 mutations. *Human Molecular Genetics* **2019**, *28*, 1629–1644, doi:10.1093/hmg/ddz006.
12. Engelfried, K.; Vorgerd, M.; Hagedorn, M.; Haas, G.; Gilles, J.; Epplen, J.T.; Meins, M. Charcot-Marie-Tooth neuropathy type 2A: novel mutations in the mitofusin 2 gene (MFN2). *BMC Med Genet* **2006**, *7*, 53, doi:10.1186/1471-2350-7-53.
13. Casasnovas, C.; Banchs, I.; Cassereau, J.; Gueguen, N.; Chevrollier, A.; Martinez-Matos, J.A.; Bonneau, D.; Volpini, V. Phenotypic spectrum of MFN2 mutations in the Spanish population. *Journal of Medical Genetics* **2010**, *47*, 249–256, doi:10.1136/jmg.2009.072488.
14. Cassereau, J.; Casasnovas, C.; Gueguen, N.; Malinge, M.-C.; Guillet, V.; Reynier, P.; Bonneau, D.; Amati-Bonneau, P.; Banchs, I.; Volpini, V.; et al. Simultaneous MFN2 and GDAP1 mutations cause major mitochondrial defects in a patient with CMT. *Neurology* **2011**, *76*, 1524–1526, doi:10.1212/WNL.0b013e318217e77d.
15. Chung, K.W.; Sunwoo, I.N.; Kim, S.M.; Park, K.D.; Kim, W.-K.; Kim, T.S.; Koo, H.; Cho, M.; Lee, J.; Choi, B.O. Two missense mutations of EGR2 R359W and GJB1 V136A in a Charcot–Marie–Tooth disease family. *Neurogenetics* **2005**, *6*, 159–163, doi:10.1007/s10048-005-0217-4.
16. Vital, A.; Latour, P.; Sole, G.; Ferrer, X.; Rouanet, M.; Tison, F.; Vital, C.; Goizet, C. A French family with Charcot–Marie–Tooth disease related to simultaneous heterozygous MFN2 and GDAP1 mutations. *Neuromuscular Disorders* **2012**, *22*, 735–741, doi:10.1016/j.nmd.2012.04.001.
17. Yoshimura, A.; Yuan, J.-H.; Hashiguchi, A.; Ando, M.; Higuchi, Y.; Nakamura, T.; Okamoto, Y.; Nakagawa, M.; Takashima, H. Genetic profile and onset features of 1005 patients with Charcot-Marie-Tooth disease in Japan. *J Neurol Neurosurg Psychiatry* **2019**, *90*, 195–202, doi:10.1136/jnnp-2018-318839.
18. McCorquodale, D.S.; Montenegro, G.; Peguero, A.; Carlson, N.; Speziani, F.; Price, J.; Taylor, S.W.; Melanson, M.; Vance, J.M.; Züchner, S. Mutation screening of mitofusin 2 in Charcot-Marie-Tooth disease type 2. *J Neurol* **2011**, *258*, 1234–1239, doi:10.1007/s00415-011-5910-7.
19. Latour, P.; Thauvin-Robinet, C.; Baudelet-Méry, C.; Soichot, P.; Cusin, V.; Faivre, L.; Locatelli, M.-C.; Mayençon, M.; Sarcey, A.; Broussolle, E.; et al. A Major Determinant for Binding and Aminoacylation of tRNAAla in Cytoplasmic Alanyl-tRNA Synthetase Is Mutated in Dominant Axonal Charcot-Marie-Tooth Disease. *The American Journal of Human Genetics* **2010**, *86*, 77–82, doi:10.1016/j.ajhg.2009.12.005.
20. McLaughlin, H.M.; Sakaguchi, R.; Giblin, W.; NIH Intramural Sequencing Center; Wilson, T.E.; Biesecker, L.; Lupski, J.R.; Talbot, K.; Vance, J.M.; Züchner, S.; et al. A Recurrent loss-of-function alanyl-tRNA synthetase (AARS) mutation in patients with charcot-marie-tooth disease type 2N (CMT2N). *Hum. Mutat.* **2012**, *33*, 244–253, doi:10.1002/humu.21635.
21. Bansagi, B.; Antoniadi, T.; Burton-Jones, S.; Murphy, S.M.; McHugh, J.; Alexander, M.; Wells, R.; Davies, J.; Hilton-Jones, D.; Lochmüller, H.; et al. Genotype/phenotype correlations in AARS-related neuropathy

in a cohort of patients from the United Kingdom and Ireland. *J Neurol* **2015**, *262*, 1899–1908, doi:10.1007/s00415-015-7778-4.

22. Boczonadi, V.; Jennings, M.J.; Horvath, R. The role of tRNA synthetases in neurological and neuromuscular disorders. *FEBS Lett* **2018**, *592*, 703–717, doi:10.1002/1873-3468.12962.
23. Motley, W.W.; Seburn, K.L.; Nawaz, M.H.; Miers, K.E.; Cheng, J.; Antonellis, A.; Green, E.D.; Talbot, K.; Yang, X.-L.; Fischbeck, K.H.; et al. Charcot-Marie-Tooth–Linked Mutant GARS Is Toxic to Peripheral Neurons Independent of Wild-Type GARS Levels. *PLoS Genet* **2011**, *7*, e1002399, doi:10.1371/journal.pgen.1002399.
24. Kousi, M.; Katsanis, N. Genetic Modifiers and Oligogenic Inheritance. *Cold Spring Harbor Perspectives in Medicine* **2015**, *5*, a017145–a017145, doi:10.1101/cshperspect.a017145.
25. Bis-Brewer, D.M.; Fazal, S.; Züchner, S. Genetic modifiers and non-Mendelian aspects of CMT. *Brain Research* **2020**, *1726*, 146459, doi:10.1016/j.brainres.2019.146459.

348 **Supplementary Materials**

349

350 Supplementary Table 1: 92-gene panel used for NGS. It includes the 44 known CMT genes, 27 genes
351 involved in HSN (Hereditary Sensitive Neuropathy) and HMN (Hereditary Motor Neuropathy) and
352 21 other genes of interest involved in neuropathies of differential diagnosis [R =
353 recessively-inherited; D = dominantly-inherited].

GENE	CMT1D	CMT2D	CMT1R	CMT2R	HMN D	HMNR	HSN D	HSN R	Other
AARS		X							
ABHD12									R
AIFM1				X					
ARHGEF10									D
ATL1							X		
ATL3							X		
ATP7A						X			
BICD2					X				
BSCL2					X				
CCT5								X	
CTDP1								X	
C12ORF65									R
DCAF8									D
DCTN1					X				
DHTKD1		X							
DNAJB2				X					
DNM2	X	X							
DNMT1							X		
DST								X	
DYNC1H1		X							
EGR2	X		X						
FAM134B								X	
FBLN5									D/R
FBXO38					X				
FGD4			X						
FIG4			X		X				
GAN									R
GARS		X			X				
GDAP1		X	X	X					
GJB1	X	X							
GJB3									D/R
GNB4	X	X							
HARS		X							
HINT1									R
HK1			X						
HSPB1		X			X				
HSPB3					X				
HSPB8		X			X				
IFRD1									D
IGHMBP2				X		X			
IKBKAP								X	
INF2	X	X							
KARS			X	X					
KIF1A								X	
KIF1B		X							
KIF5A									D
LITAF	X								
LMNA				X					
LRSAM1		X							
MARS		X							
MED25				X					
MFN2		X							
MPV17									R
MPZ	X	X	X						
MTMR2			X						
NDRG1			X						
NEFL	X	X							

354

NGF								X	
NTRK1								X	
PDK3		X							
PLEKHG5			X	X		X			
PMP22	X								
POLG									D/R
PRPS1				X					
PRX			X						
RAB7A		X							
REEP1					X				
SBF1			X						
SBF2			X						
SCN9A								X	
SCN10A							X		
SCN11A							X		
SEPT9									D
SETX					X				
SH3TC2			X						
SLC12A6									R
SLC5A7					X				
SMAD3									D
SOX10									D
SPTLC1							X		
SPTLC2							X		
SURF1			X						
TFG									D
TRIM2				X					
TRPV4		X			X				
TTR									D
TUBB3									D
UBQLN2					X				
VAPB									D
VCP									D
WNK1								X	
YARS	X	X							

Supplementary Table 2: All genes included in the detected chromosome 16 duplication (from chr16:70185757 to chr16:70416579) (bp: base pair).

Gene stable ID	Gene stable ID version	Gene name	Gene start (bp)	Gene end (bp)	Gene description
ENSG00000090857	ENSG00000090857.9	**PDPR**	70147529	70195203	pyruvate dehydrogenase phosphatase regulatory subunit
ENSG00000157335	ENSG00000157335.15	**CLEC18C**	70207225	70221264	C-type lectin domain family 18, member C
ENSG00000223496	ENSG00000223496.1	**EXOSC6**	70284134	70285833	exosome component 6
ENSG00000090861	ENSG00000090861.11	**AARS1**	70286198	70323446	alanyl-tRNA synthetase
ENSG00000157349	ENSG00000157349.11	**DDX19B**	70323566	70369186	DEAD (Asp-Glu-Ala-Asp) box polypeptide 19B
ENSG00000168872	ENSG00000168872.11	**DDX19A**	70380732	70407286	DEAD (Asp-Glu-Ala-Asp) box polypeptide 19A
ENSG00000157350	ENSG00000157350.8	**ST3GAL2**	70413338	70473140	ST3 beta-galactoside alpha-2,3-sialyltransferase 2
ENSG00000157353	ENSG00000157353.12	**FUK**	70488324	70514177	fucokinase
ENSG00000103051	ENSG00000103051.14	**COG4**	70514471	70557468	component of oligomeric golgi complex 4
ENSG00000189091	ENSG00000189091.8	**SF3B3**	70557691	70608820	splicing factor 3b, subunit 3, 130kDa
ENSG00000157368	ENSG00000157368.6	**IL34**	70613798	70694585	interleukin 34
ENSG00000132613	ENSG00000132613.10	**MTSS1L**	70695107	70719969	metastasis suppressor 1-like

Conclusion

In this study, we demonstrated that multiple genomic mutations may be simultaneously involved in inducing CMT disease. The phenotypic heterogeneity observed in Family 2 is probably related to a different gene-association in different family members, even if molecular mechanism are still unknown. As shown for other genetic diseases (Posey et al. 2017; Karaca et al. 2018), we think that multilocus genomic mutations may be more common than expected, also in CMT pathology, and their occurrence must be more frequently considered during the molecular diagnosis. Given the huge number of data we can obtained from NGS analysis, and the increasing number of bioinformatic tools, this phenomenon will be more and more explored in next future.

Results - Part II
A cellular model for hereditary peripheral neuropathies

<u>Article 4</u> - Optimized Protocol to Generate Spinal Motor Neuron Cells from Induced Pluripotent Stem Cells from

Published in Brain Sciences (27 June 2020)

Once examined the genetic aspects of peripheral neuropathies, molecular mechanisms associated with genomic mutations need to be explored, using cellular models. In particular, we created a cellular model of motor neurons (MN) for an axonal form of CMT disease (CMT2H), caused by homozygous codon-stop mutations in *GDAP1* gene. In the study reported here, we present the protocol we have developed to generate MN from human induced-pluripotent stem cells (hiPSC), for five unaffected control subjects, and two CMT-patients, one (patient 3-A) carrying the nonsense c.581C>G (p.Ser194*) mutation in *GDAP1*, the other (patient 4-A) carrying the nonsense c.487C>T (p.Gln163*) mutation, always in *GDAP1* gene. First, we obtained dermal fibroblasts from skin biopsies of the seven subjects, and we cultivated and reprogrammed them into hiPSC, employing the strategy elaborated by Pr Yamanaka, in 2006 (Takahashi and Yamanaka 2006). hiPSC were then selected, amplified, and checked for all quality controls, before being differentiated in MN. The differentiation protocol is presented in detail in this article. It has been established looking at molecular pathways involved in embryonic development, with the aim to choose the main MN-inducing factors, to mimic, *in vitro*, the same differentiation events. This protocol has allowed to obtain, from hiPSC, 100% cells expressing neuronal markers and 80% spinal MN markers. It requires 20 to 30 days, and it is easy to reproduce.

brain sciences

MDPI

Article

Optimized Protocol to Generate Spinal Motor Neuron Cells from Induced Pluripotent Stem Cells from Charcot Marie Tooth Patients

Pierre-Antoine Faye [1,2,*], Nicolas Vedrenne [3], Federica Miressi [2], Marion Rassat [2], Sergii Romanenko [4], Laurence Richard [2,5], Sylvie Bourthoumieu [2,6], Benoît Funalot [7,8], Franck Sturtz [1,2], Frederic Favreau [1,2] and Anne-Sophie Lia [1,2,9]

1 CHU de Limoges, Service de Biochimie et Génétique Moléculaire, F-87000 Limoges, France; franck.sturtz@unilim.fr (F.S.); frederic.favreau@unilim.fr (F.F.); anne-sophie.lia@unilim.fr (A.-S.L.)
2 Université de Limoges, Maintenance Myélinique et Neuropathies Périphériques, EA6309, F-87000 Limoges, France; federica.miressi@unilim.fr (F.M.); marion.rassat@gmail.com (M.R.); laurence.richard@unilim.fr (L.R.); sylvie.bourthoumieu@unilim.fr (S.B.)
3 Université de Nantes, RMeS Regenerative Medicine and Skeleton, ONIRIS, INSERM UMR 1229, F-44042 Nantes, France; Nicolas.Vedrenne@univ-nantes.fr
4 Bogomoletz Institute of Physiology, Department of Sensory Signaling, 01601 Kyiv, Ukraine; S.Romanenko@nas.gov.ua
5 CHU de Limoges, Service de Neurologie, F-87000 Limoges, France
6 CHU de Limoges, Service de Cytogénétique, F-87000 Limoges, France
7 CHU Henri-Mondor, Département de Génétique, F-94000 Créteil, France; benoit.funalot@aphp.fr
8 Université Paris-Est-Créteil, Inserm U955-E10, F-94000 Créteil, France
9 CHU de Limoges, UF de Bioinformatique, F-87000 Limoges, France
* Correspondence: pierre-antoine.faye@unilim.fr; Tel.: +33-555-056-341

Received: 29 May 2020; Accepted: 24 June 2020; Published: 27 June 2020

Abstract: Modelling rare neurogenetic diseases to develop new therapeutic strategies is highly challenging. The use of human-induced pluripotent stem cells (hiPSCs) is a powerful approach to obtain specialized cells from patients. For hereditary peripheral neuropathies, such as Charcot–Marie–Tooth disease (CMT) Type II, spinal motor neurons (MNs) are impaired but are very difficult to study. Although several protocols are available to differentiate hiPSCs into neurons, their efficiency is still poor for CMT patients. Thus, our goal was to develop a robust, easy, and reproducible protocol to obtain MNs from CMT patient hiPSCs. The presented protocol generates MNs within 20 days, with a success rate of 80%, using specifically chosen molecules, such as Sonic Hedgehog or retinoic acid. The timing and concentrations of the factors used to induce differentiation are crucial and are given hereby. We then assessed the MNs by optic microscopy, immunocytochemistry (Islet1/2, HB9, Tuj1, and PGP9.5), and electrophysiological recordings. This method of generating MNs from CMT patients in vitro shows promise for the further development of assays to understand the pathological mechanisms of CMT and for drug screening.

Keywords: induced pluripotent stem cells; hiPSC; spinal motor neurons; cellular models; peripheral nervous system; Charcot-Marie-Tooth; CMT; peripheral neuropathy

1. Introduction

Peripheral nerves are critical for the functioning of the nervous system, as they forward information to the spinal cord and encephalon and provide the periphery (muscles, organs, skin, blood vessels) with adapted signals. As such, peripheral nerve illnesses constitute an important source of medical problems and a large group of neurological diseases of various origins. Among them, hereditary

peripheral neuropathies, such as Charcot–Marie–Tooth disease (CMT) disease, have a prevalence of 1:2500 and often affect patients during their entire lives. The use of next-generation sequencing has tremendously improved the molecular diagnosis of these diseases in recent years by efficiently determining the mutations involved. However, even when a gene mutation is identified, the molecular and cellular pathways involved in the pathophysiology remain difficult to decipher. Because of the numerous mutations and various genes involved, animal models are of limited utility and are highly difficult to study, aside from the potential ethical problems. As an alternative, in vitro cellular models appear to be a promising path for the expeditious development of therapeutic strategies.

In this context, human-induced pluripotent stem cells (hiPSCs) generated from patients, associated with their ability to differentiate toward the cell type of interest, appear to be a potentially powerful tool, as it is very difficult, if not impossible, to study live peripheral nerve cells. The work of Yamanaka et al. on iPSCs opened the way to creating dedifferentiated cells and, later, to observing the behavior of previously unattainable cells [1,2]. They showed that the reprogrammation of dermal fibroblasts using non-integrative plasmids that included the Oct4, Sox2, Klf4, and l-Myc genes induces hiPSCs that can be subsequently differentiated into many cells types [3]. The differentiation of hiPSCs into neuronal cells is an essential step.

Several protocols have been developed to differentiate human embryonic stem cells (hESCs) [4,5] or hiPSCs [6–10] into spinal motor neurons (MNs). In the peripheral neuropathy field and, in particular, in CMT diseases, several groups have attempted to obtained spinal MNs [11] and more recently differentiate hiPSCs into Schwann cells [12,13]. However, cells from patients are not always easily reprogrammed and differentiated. Based on an extensive review of the literature and results obtained in our laboratory, we developed a robust and reproducible protocol to improve MNs differentiation of hiPSCs obtained from CMT patients.

2. Materials and Methods

2.1. Cell Culture Media

iPSC medium: KO-DMEM (Life Technologies, Carlsbad, CA, USA), supplemented with 20% KnockOut Serum Replacement (Life Technologies), 1X MEM non-essential amino acids (Life Technologies), 2 mM Glutamine (Life Technologies), 50 µM β-mercaptoethanol (Life Technologies), and 10 UI/mL gentamycin (Life Technologies).

Differentiated medium: DMEM/F12 (Life Technologies), 2% B27 without vitamin A (Life Technologies), 5 µg/mL heparin (Sigma-Aldrich, Saint-Quentin Fallavier, France), and 100 µM β-mercaptoethanol (Life Technologies).

Neural induction medium: 1:1 DMEM/F12 (Life Technologies) and Neurobasal A (Life Technologies), 1% N2 supplement (Life Technologies), 2% B27 without vitamin A (Life Technologies), and 100 µM β-mercaptoethanol (Life Technologies).

2.2. Experimental Design

2.2.1. Generation of hiPSCs

HiPSCs were obtained as previously described [14]. Briefly, human dermal fibroblasts, negative for HVB, HVC, and HIV virus (Hospital virology department, Limoges, France) and mycoplasma (MycoAlert mycoplasma detection kit, Lonza) were used to generate hiPSCs. Three plasmids (Plasmid #6: pCXLE-hOCT3/4 shp53-F Addgene (Watertown, Massachusetts, USA), Plasmid #7: pCXLE-hSK Addgene, and Plasmid #8: pCXLE-hUL Addgene) at 1 µg/mL were used to reprogram fibroblasts into hiPSCs using a Nucleofector II device (Amaxa, Lonza AAD-10015, (Bâle, Switzerland). Directly after nucleofection, 100,000 cells were seeded on mitomycin mouse embryonic fibroblasts with culture medium consisiting of DMEM GlutaMAX (Life Technologies) supplemented with 10% fetal bovine serum (FBS) (Life Technologies) and 1X MEM non-essential amino acids (Life Technologies) and

incubated at 37 °C in a water-saturated atmosphere with 5% CO_2. At day 1, the medium was replaced by the same culture medium supplemented with 10 UI/mL gentamycin (Life Technologies). At day 4, the culture medium was replaced with hiPSC medium and this medium changed every day up to day 10. Then, hiPSC colonies were picked 2–4 weeks post-nucleofection. Fifteen days after nucleofection, the morphology of the fibroblasts changed to form colonies with a typical morphology (Figure S1). Approximately 40 colonies per patient or control were isolated for further expansion. HiPSC colonies were cultivated on mitomycin mouse embryonic fibroblasts (CF 1 MEF 4M Mito C, TebuBio) seeded on 0.1% gelatin (G1393-100ML, Sigma-Aldrich, Merck). Every day, hiPSC colonies were cleaned to remove the differentiated cells using a needle (26G, Dutscher, Brumath, France) and the culture medium was changed with complete fresh hiPSC medium supplemented with 20 ng/mL FGF2 (fibroblast growth factors). The hiPSCs were characterized at passage 15 (Figure S2, Appendix A).

The CMT2 patients included in this study were two men of three and 23 years of age. The younger patient carried a homozygous nonsense mutation in *GDAP1* (p.Ser194*, c. 581C>G). He developed a severe form of CMT2 with multiorgan failure, leading to an early death at three years of age. The older patient has a different homozygous nonsense mutation in *GDAP1* (p.Gln163*, c. 487C>T) and is currently using a wheelchair. The first signs of the disease appeared during his childhood, with motor problems observed more in the lower than upper limbs, followed by sensitive troubles. No response was obtained when muscles were stimulated during an electromyogram. The healthy controls consisted of three women and two men (ranging from 24 to 56 years of age) without peripheral neuropathy nor any mutation in *GDAP1*, investigated by sequencing (data not shown).

2.2.2. Generation of Motor Neurons

The protocol is summarized in the scheme in Figure 1. At day 0, hiPSC colonies were cut into homogenous squares using a StemPro® EZPassage™ (Life Technologies; Figure 2A). Colonies were collected and suspended in 60-mm ultralow-attachment dishes (Corning Incorporated, New York, NY, USA) in 5 mL hiPSC medium without FGF2. At day 1, the medium was changed by sedimentation: dead cells were discarded with the supernatant, whereas sedimented cells were transferred to a new 60-mm ultralow-attachment dish using 5 mL fresh iPSC medium. At day 3, when embryoid bodies (EBs) are fully formed, differentiation medium was applied, extemporaneously supplemented with 10 µM SB431542 (Tocris Bioscience, Minneapolis, MN, USA), 5 µM Dorsomorphin (Sigma-Aldrich, Merck), 100 ng/mL FGF2 (PeproTech Inc., Rocky Hill, NJ, USA), and 10 ng/mL Noggin (PeproTech Inc.). The culture medium was renewed daily up to day 5 and detached cells in the supernatant were isolated by sedimentation and plated in a new dish as already described (Figure 2B). From day 5, the cells required a specific coated-plate. Thus, the plate was incubated with 20 µg/mL poly-L-ornithine (Sigma-Aldrich, Merck) for 4 h at 37 °C. Excess poly-L-ornithine in the dish was discarded and the plate dried for 30 min at room temperature. After washing three times with sterile water or saline buffer, the dish was dried at room temperature (opened under the hood). For the upper coating, laminin (Invitrogen, Thermo Fisher Scientific) was diluted with fresh neural induction medium (without supplement) to a final concentration of 20 µg/mL. The solution was added to cover the entire dish surface and incubated overnight at 37 °C. On days 5–7, EBs were sequentially seeded on the 60-mm coated dishes in 5 mL neural induction medium supplemented with 10 µM SB431542 (Tocris Bioscience), 5 µM Dorsomorphin (Sigma-Aldrich), and 10 µM retinoic acid (RA) (Sigma-Aldrich). Prior to treatment, EBs needed to be of the same size, circular, smooth, and brownish, without black spots, to maximize the efficiency of the protocol. Every two days, fresh supplemented neural induction medium was added to the dish until "rosette" formation. Mature "rosettes" were observed on day 10 (Figure 2C).

"Rosettes" were isolated from the other cells using a simple needle to make the smallest squares possible and collected in a tube containing a small volume of Dulbecco's phosphate-buffered saline (DPBS) to wash them. Trypsin solution (Gibco, Thermo Fisher) was added to facilitate cell dissociation. After 5 min of incubation at 37 °C in a water-saturated atmosphere and 5% CO_2, "rosettes" were gently mechanically dissociated under the microscope until a homogeneous cell suspension was obtained.

Then, fresh neural induction medium containing 10% FBS was added to the suspension to stop enzyme activity. After centrifugation at 200× *g* for 5 min, the supernatant was discarded and the cells plated at 100,000 cells per cm^2 in a 96- or 48-well plate coated with 20 µg/mL poly-L-ornithine and 3 µg/mL laminin (Figure 2D). The neural induction medium was supplemented with 100 ng/mL Sonic Hedgehog (Shh) (PeproTech Inc.), 5 µM RA, 10 µM Y-27632 ROCK inhibitor (Calbiochem, Billerica, MA, USA), 10 ng/mL BDNF (brain-derived neurotrophic factor), 10 ng/mL GDNF (glial cell line-derived neurotrophic factor), and 10 ng/mL IGF-1 (insulin-like growth factor-1) (PeproTech Inc.) to generate neuronal precursors. This supplemented culture medium was renewed every two days, except for the Y-27632 ROCK inhibitor, which was added only after passing the cells. The neural progenitors needed to be passed every 3–4 days using the trypsin method, as already described. Neuronal precursors were plated at a density of 20,000 to 40,000 cells/cm^2 in the same supplemented medium to generate completely differentiated MNs. First, neurites were observed 24 h after plating (Figure 2E,F). Neural precursors may also be stored by freezing at this stage. Briefly, they were collected as described, centrifuged for 5 min at 200× *g* and cryopreserved in CryoStor CS10 (Stemcell Technologies, Grenoble, France) added to the cell pellet. The frozen vials were then stored long-term in standard liquid nitrogen storage containers.

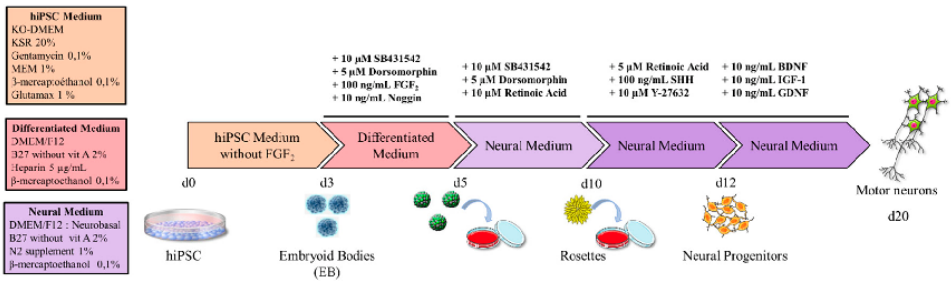

Figure 1. Schematic representation of motor neuron induction with all media and factors.

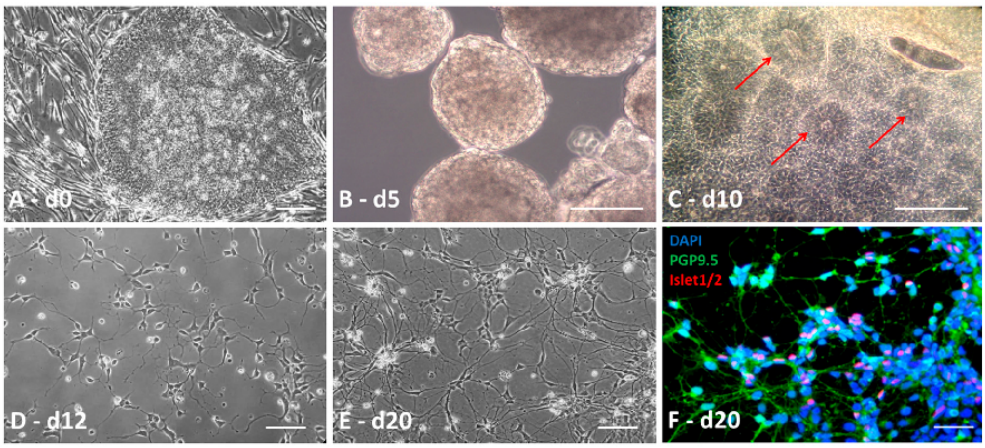

Figure 2. Induction of spinal motor neurons. HiPSc colonies (**A**) were cut into large squares to generate EBs (embryoid bodies) (**B**) and grown in classical medium for three days. EBs evolved in differentiated medium for two days and were seeded on a poly-L-ornithin/laminin plate in neural induction medium up to the apparition of rosettes (**C**, red arrows). Rosettes were gently manually removed and dissociated. Single cells were seeded on poly-L-ornithin/laminin dishes at 100,000 cells/cm^2 to generate neuronal precursors (**D**). Neuronal precursors were then dissociated and seeded at 20,000 to 40,000 cells/cm^2 (**E**) to generate motor neurons. The proportion of motor neurons increased from 10% to 80% following maturation from day 15 to day 20 ((**F**) 4′,6′-diamidino-2-phénylindole dihydrochloride (DAPI) in blue, PGP9.5 in green, and Islet cocktail in red). Scale bar = 50 µm.

2.3. Immunostaining

Staining was performed to characterize hiPSCs and effective neuronal differentiation. Cells were fixed in 4% paraformaldehyde (Sigma-Aldrich, Saint-Quentin Fallavier, France) for 10 min at room temperature and rinsed three times with 1X DPBS for 5 min. The cells were permeabilized with 0.2% Triton X-100 (Sigma-Aldrich, Saint-Quentin Fallavier, France) and 3% bovine serum albumin (BSA) in 1X DPBS for 1 h at room temperature. Cells were washed and incubated with primary antibodies in 3% BSA overnight at 4 °C (Table 1). Cells were subsequently labeled with the appropriate fluorescently-tagged secondary antibodies, Alexa fluor 488 (green fluorescence) and Alexa fluor 594 (red fluorescence) (Molecular Probes, Eugene, OR, USA). Cells were then counterstained with 1 mg/mL 4',6'-diamidino-2-phénylindole dihydrochloride (DAPI, Sigma-Aldrich) to stain the nuclei. Cells were observed with a fluorescence microscope (Leica DM IRB, Nanterre, France) and a confocal microscope LSM 880 (Zeiss, Germany). Images were obtained using NIS Element BR and Zen software and treated with image J software (NIH, Bethesda, MD, USA).

Table 1. Primary antibodies used for human-induced pluripotent stem cell (hiPSC), neuron, and motor neuron characterization.

Antibody	Company	Cat Num	Species/Type	Dilution
		Pluripotency		
Nanog	Abcam	130095632	Rabbit poly IgG	1:100
Oct3/4	Santa Cruz Biotech	sc-5279	Mouse Mono IgG2B	1:100
Sox2	Chemicon	AB5603	Rabbit poly IgG	1:100
		Spontaneous Differentiation in Three Germinal Layers		
Pax6	Covance	PRB-278P	Rabbit poly IgG	1:100
αSMA	DAKO	M0851	Mouse IgG2A	1:500
Sox17	R&D	AF1924	Goat IgG	1:100
		Neuronal and Motor Neuronal		
Tuj1	R&D	MAB1195	Mouse Mono IgG	1:500
PGP9.5	Ultraclone	Ra95101	Rabbit poly IgG	1:500
HB = MNR2	DSHB	81.5C10	Chicken	1:100
Islet1	DSHB	40.2D6-c	Mouse Mono IgG	1:25
Islet1/2	DSHB	39.4D5-c	Mouse Mono IgG	1:25
ChAT	Chemicon	AB144P	Goat IgG	1:20
		Other		
Ki-67	Leica	NCL-L-Ki67-MM1	Mouse Mono IgG	1:200

2.4. Electrophysiology

Cells were covered with an approximately 1.5-mm-thick fluid layer (Saline solution, Live Cell Imaging Solution, Life Technologies) and placed under an inverted microscope (IX70, Olympus, Shinjuku, Tokyo, Japan). Cells were illuminated with an upright microscope condenser and a 4x objective was used to distinguish the neuronal shapes. For electrophysiological recordings, patch electrodes were generated by pulling borosilicate capillary glass (1.5/0.75 mm OD/ID, 1B150F-4, WPI, Sarasota, FL, USA) associated with a microelectrode filled with an intracellular solution with a resistance between 3 MOhm and 4 MOhm. The solution composition was: 140 mM K-gluconate, 10 mM HEPES, 2 mM Mg-ATP, and 1.1 EGTA, with the pH adjusted to 7.3 with KOH; the sodium channel recording solution composition was: 135 mM Cs-gluconate, 5 mM CsF, 10 mM HEPES, 2 mM Mg-ATP, and 1.1 EGTA, with pH adjusted to 7.3 with CsOH. All electrophysiological recordings were performed using a microelectrode amplifier (PC-ONE Patch/Whole Cell Clamp, CORNERSTONE Series, Dagan, USA) in the voltage-clamp mode, with a holding potential of −70 mV in the whole-cell configuration. Acquired transmembrane current alterations were digitized online at 20 kHz after

passing through a low-pass Bessel filter with the setting at 10 kHz using data acquisition hardware (DigiData 1440A; Molecular Devices) and software (Whole Cell Electrophysiology Analysis Program V4.8.2, (c) John Dempster, University of Strathclyde 1996–2014). Leak current and stray capacitance were instrumentally pre-compensated and residual capacitance and related artifacts were subtracted using the P/N method. Electrophysiological recordings were performed using the Stimulus Protocol mode and processed offline using data analysis software (Whole Cell Electrophysiology Analysis Program V4.8.2, (c) John Dempster, University of Strathclyde 1996–2014, and OriginPro 8). Whole-cell currents were measured in response to the voltage ramp command protocol from −80 mV to 50 mV (with a rate of voltage augmentation of 0.65 mV/msec) (n = 4).

3. Results

3.1. Obtaining iPSCs from Patients

We launched this study to define a robust protocol to obtain and differentiate cells obtained from CMT patients into MNs. The hiPSCs from five healthy controls and two CMT2 patients were generated and characterized according to a procedure developed by iStem (INSERM/UEVE UMR 861, AFM, Genopole, Evry, France) (Figures S1 and S2 and Appendix A). At this step, there were no observable morphological differences between hiPSCs from the healthy controls and patients (data not shown). However, it was more difficult to obtain the hiPSCs from the CMT2 patients than the controls, perhaps due to the mutation (one patient carrying a *GDAP1* homozygous nonsense mutation p.Gln163*, c. 487C > T and the other a *GDAP1* homozygous nonsense mutation p.Ser194*, c. 581C > G). Nevertheless, it was possible to obtain hiPSCs from both.

3.2. Definition of the Factors and the Timeframes for MN Differentiation

We first tested various published protocols to generate MNs from our iPSCs but with limited success. This led us to test several conditions and factors. We first investigated the factors involved in embryonic development towards the neuronal lineage. According to the literature [7,11,15,16], Shh and RA are key factors. However, the MN differentiation rate was still too low (20%) when we tested these factors. To increase the MN differentiation rate, we tried other factors, in addition to RA and Shh, such as Noggin, dorsomorphine, BDNF, IGF-1, GDNF, SB431542, and Y-27632, with the aim to activate different pathways involved in differentiation, as described in Figure 3. After numerous attempts (up to six months), we defined an optimized protocol that enables the generation of MNs in 20 days with a MN differentiation rate of approximately 80%. The factors, concentrations, and timepoints are given in the Materials and Methods section and summarized in Figure 1.

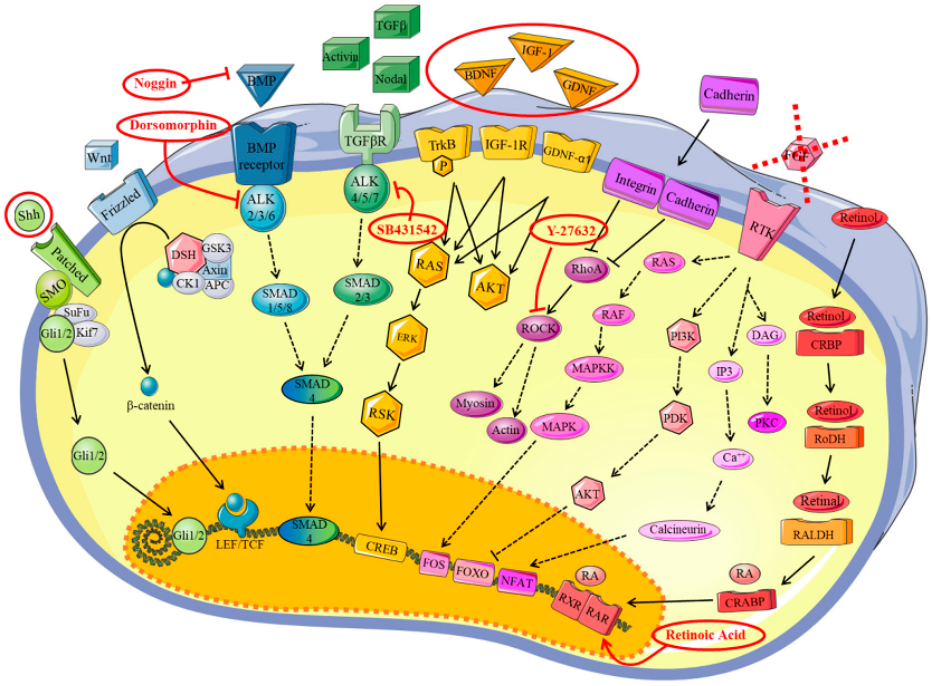

Figure 3. A schematic representation of the trophic factor pathways used for motor neuron differentiation in this study. Sonic Hedgehog (Shh) pathway in green [17]; Wnt pathway in clear blue [18]; BMP (morphogens bone morphogenetic proteins) pathway in dark blue [19]; transforming growth factor-β (TGF-β) pathway [20]; BDNF (brain-derived neurotrophic factor), IGF-1 (insulin-like growth factor-1), and GDNF (glial cell line-derived neurotrophic factor) pathways in yellow [21–23]; Rock inhibitor pathway in purple [24]; FGF2 (fibroblast growth factors) pathway in pink [25]; retinoic acid pathway in red [26]. Red circles indicate the trophic factors used in this study.

3.3. Differentiation into Motor Neurons

MNs were generated by dissociating and seeding neuronal precursors at 20,000 cells/cm^2 to 40,000 cells/cm^2 in supplemented differentiation medium (Figure 2E). After five days, spinal cells were characterized by immunochemistry (Figure 4A–D,I–L). All cells expressed PGP9.5 and 10% were Islet positive, which are specific markers of neuronal cells and MNs, respectively. Five days later, the proportion of MNs increased to up to 80% due to a maturation process (Figure 4E–H,M–Q)) and 80% of the cells were HB9 positive, which is a specific nuclear label of MNs, thus confirming their ventral spinal cord phenotype (Figure 5A–F). The expression of Islet at d20 was not significantly different between the control and patient groups (Student t test). Moreover, ChAT immunostaining was performed at d15 on neuronal progenitors from a healthy control. The neuronal progenitors already expressed ChAT (approximately 31%), suggesting that our MNs may be cholinergic (Figure S3). Based on the immunocytochemistry results (Figure 4D,H,L,P) and visual observation by optic microscopy (Figure 2E,F), the morphology appeared to be typical of MNs, with long processes, a small soma, and a process network. Thus, Ki-67 immunostaining was performed on the neuronal progenitors from a healthy control. Only 32% of the cells were Ki-67 positive versus 87% at the iPSC stage, in support of a weak ratio of progenitors undergoing cell proliferation (Figure S4).

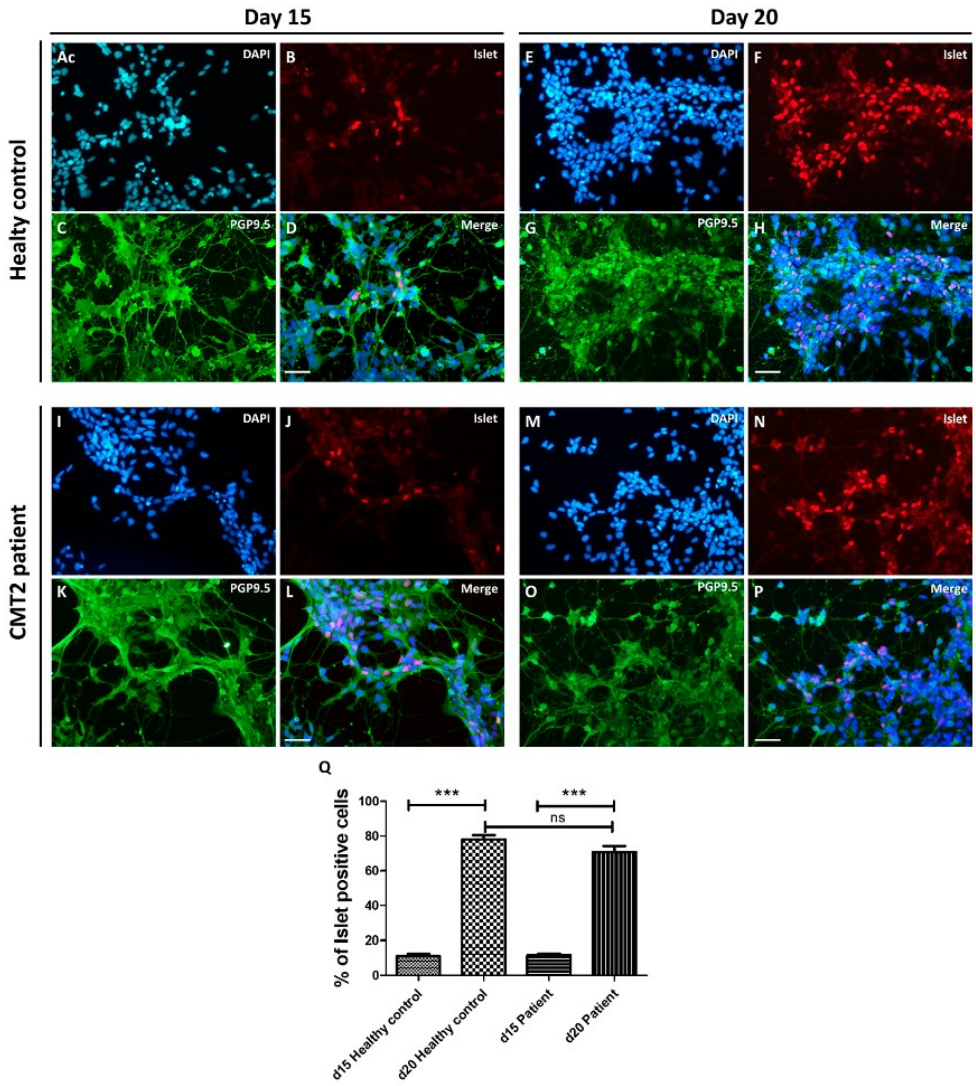

Figure 4. hiPSC differentiation into motor neurons at d15 and d20 from healthy control (**A**–**H**) and CMT2 patient (**I**–**P**). Immunocytochemistry was performed at d15 and d20. Nuclei were stained with DAPI (blue **A**,**E**,**I**,**M**), neurons with PGP9.5 (green **C**,**G**,**K**,**O**), and motor neurons with an Islet cocktail (red **B**,**F**,**J**,**N**). At day 15, all cells were differentiated into neurons (100% PGP9.5) and 10% were Islet positive (**A**–**D**,**I**–**L**). Five days later (day 20), the proportion of motor neurons increased to up to 80% due to a maturation process (**E**–**H**,**M**–**P**). Scale bar = 50 µm. Histograms showed the progressive maturation of cells to the motor neuron (MN) phenotype between d15 and d20 for healthy control and patient (**Q**) (Student T Test, $n = 4$ to 7, *** $p < 0.001$).

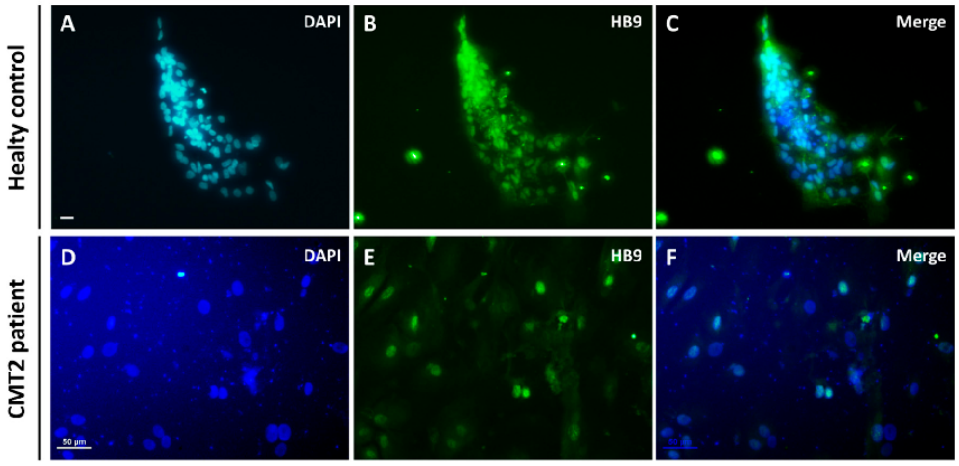

Figure 5. hiPSC differentiation into motor neurons at d20. Nuclei were stained with DAPI (blue **A**,**D**) and motor neurons with HB9 (green **B**,**E**). **A–C** show immunocytochemistry for healthy control cells and **D–F** for CMT2 patient cells. Scale bar = 50 µm.

We performed electrophysiological recordings to estimate alterations in transmembrane currents in both control and patient MNs (Figure 6). The typical electrophysiological characteristics of MNs were compared between groups and are supported by previous studies [11,27]. In particular, CMT2-patient derived MNs showed stronger inward currents, in the range of 40–30 mV, and weaker outward currents than the control group. Both differences are consistent with previously reported intrinsic hyperexcitability for CMT MNs [11].

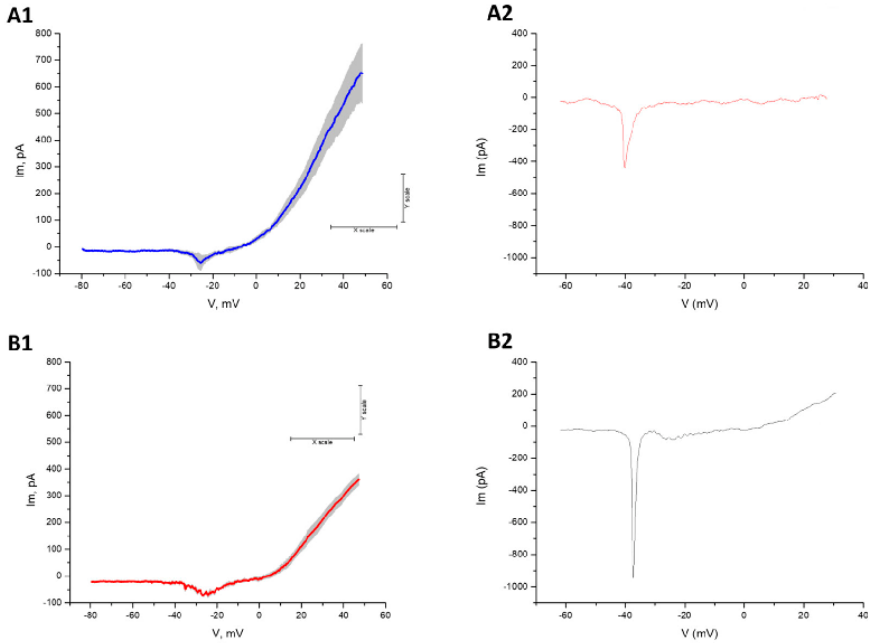

Figure 6. Healthy control (**A1** and **A2**) and CMT2 patient (**B1–B2**) motor neuron electrophysiology (n = 4). (**A1**,**B1**) Averaged traces with SE shadow, showing a persistent inward current and strong outward current. (**A2–B2**) Individual traces obtained with high a Cs^+ inside solution, showing a fast transient inward current.

4. Discussion

We aimed to create a robust protocol to obtain hiPSCs differentiated into MNs from CMT patients. We also aimed to use only a limited number of factors that mimic embryonic development to stimulate the various pathways (summarized in Figure 3) within a defined timeframe. This protocol allowed us to obtain 100% cells expressing neuronal markers and 80% spinal MNs in only 20 days. MNs could be used up to d30 without any sign of degeneration.

We returned to embryology to handpick efficient differentiating factors. Indeed, the balance between activation and inhibitory pathways during embryonic development must be understood to choose MN-inducing factors (Figure 3) [28–30]. Neural tube development follows two axes (Figure S5A1). Dorso-ventral differentiation is controlled by opposite gradients of the morphogens bone morphogenetic proteins (BMP) and Shh. Approximately 30 types of BMPs (family members of transforming growth factor-β (TGF-β)) are expressed during embryonic development [31,32] and their activities are inhibited by three molecules from the chord: noggin, chordin, and follistatin, promoting neural-tube formation [31,33]. Shh is synthesized by the notochord and neural-tube floor, promoting interneurons and MN differentiation (Figure S5A1,A2). Specific transcription factors, such as Pax6, Olig2, Nkx6.2, and Nkx6.1 are stimulated by these gradients [34,35]. Antero-posterior differentiation is based on morphogen signals through RA, FGF, or Wnt production by the axial and paraxial mesoderma and endoderma [36]. The gradient is distributed from the caudal to cranial section and is involved in modification of the hindbrain or, in the anterior section, the spinal cord [35,37] (Figure S5B). We applied this knowledge to define the best factors.

Few protocols have been proposed for MNs differentiation, all showing various rates. Wichterle et al. reported the differentiation of mouse ESCs into MNs using RA and Shh agonists [15], with a rate of differentiation of 20% to 40%. Their protocol was modified by Miles et al. and the proportion increased to 60% to 80% using N2 supplement in the culture medium [16]. During differentiation, human rosettes appear later than those of mice and a specific cocktail containing BDNF [21,38], IGF-1 [22,39–41], and GDNF [23,42] was found to be essential for the survival and growth of neural progenitors. However, the proportion of MNs obtained by Singh Roy et al. was approximatly only 10% after 28 days and 50% after 35 days [5]. Dimos et al. generated MNs using Shh and RA for amyotrophic lateral sclerosis [7]. They reported that 20% of the cells expressed HB9, a cholinergic neuronal marker, of which more than 90% expressed Islet1/2 [7]. Based on a study of Watanabe et al., we chose to add a ROCK inhibitor (Y-27632) to protect cells from apoptosis and promote neuronal differentiation [24]. Hu et al. obtained MNs in 35 days and functionally mature MNs were generated in 56–70 days, with a final proportion of approximately 50%. Interestingly, at the MN generation step, the cells required limited concentrations of Shh and RA to prevent inhibition of MN differentiation [9]. After 14 days, Chambers et al. obtained 30% Islet-positive cells and 60% were HB9 positive [6]. Kim et al. reported that SB431542 and dorsomorphin (used in our protocol), inhibitors of both the activin/nodal and BMP pathways, improved the neural differentiation of hESCs and hiPSCs by more than 90% [10]. This led us to supplement the medium with the following factors: RA, Shh, Noggin, dorsomorphine, BDNF, IGF-1, GDNF, SB431542, and Y-27632.

Only a limited number of groups have worked on MNs derived from hiPSCs in CMT disease, despite the fact that more than 90 genes are involved [43,44]. In the realm of axonal CMT, Saporta et al. and Juneja et al. studied the *NEFL*, *MFN2*, *HSPB8*, and *HSPB1* mutations [11,45]; Ohara et al. studied those of *MFN2* [46]; and Kim et al. studied those of *HSPB1* [47], whereas nobody has studied mutations of *GDAP1*, according to our knowledge. In their protocol, Saporta et al. used SMAD signaling inhibition, Shh, and RA [11], obtaining mature spinal MNs in 35 days, as in the protocol of Ohara et al. [46]. Kim et al. [47] obtained mature spinal MNs in 21 to 28 days. We obtained mature spinal MNs in 20 days using our protocol. The ratio of spinal MNs was not mentioned in these publications and this has presented problems in deciphering the mechanisms involved in this disease and in performing drug screening, as not all the cells were MNs.

In the future, it may be worth testing the use of a Wnt pathway activator, as demonstrated, to further increase the rate of MN differentiation [18]. It may aso be worth would testing calcitriol, as it has a synergic effect with Wnt, Shh, or Klotho, and binds to the vitamin D receptor, which is associated with the nuclear receptor of RA [48]. In addition, calcitriol is involved in various processes, such as neural stem cell differentiation, axon genesis, and the growth of MNs [48]. Furthermore, the high purity of the cells obtained with this protocol could be further improved by sedimentation field flow fractionation (SdFFF), which makes it possible to obtain neural and endothelial precursors after spontaneous differentiation in basic medium, with no added factors [49].

Finally, we defined the cells we obtained as spinal MNs by morphological observation, immunostaining for seveal markers, and electrophysiological recordings. This characterization is already convincing. However, it would be informative to co-culture these MNs with myotubes or Schwann cells to verify that they function properly.

We applied this efficient protocol to three controls (two women and one man, ranging from 24 to 56 years of age) and two patients (two males, three and 23 years of age) to generate mature MNs, supporting this robust method. We believe that this protocol could also be applied to various types of patient cells (various ages and different sex) and used to obtain hiPSCs from CMT patients with different gene variations (*MFN2*, *PMP22*, etc.).

The optimized method that we have developed to generate MNs provides a true opportunity to discover new therapeutics. With this in vitro model, the screening of potential therapeutic molecules is possible, directing efficient molecules towards animal models and clinical trials. This model is also relevant for generating MNs or neural progenitors harboring various mutations from the fibroblasts of patients for an injection of their corrected cells by the promising CRISPR Cas9 technique. This method could be applied not only to CMT patients but also those with other genetic peripheral neuropathy diseases.

5. Conclusions

This protocol should aid researchers to easily and rapidly differentiate hiPSCs into MNs (only 20 days for the first MNs) using a limited number of growth factors, with a high success rate (approximately 80% vs 10% to 60% for other protocols). This technique to derive MNs from hiPSCs is a critical step to mimic neurological diseases of genetic origin, such as CMT, in vitro. These models will allow investigation of the molecular pathways involved in the disease and, hopefully, help in the development of new therapeutic strategies, particularly as a tool for drug screening.

Supplementary Materials: The following are available online at http://www.mdpi.com/2076-3425/10/7/407/s1, Figure S1. Schematic representation of hiPSC induction. Dermal fibroblasts were reprogrammed with Yamanaka's cocktail (Oct4, Sox2, Klf4, c-Myc) into induced pluripotent stem cells. HiPSC clones were generated in 18 days and then amplified to passage 15; Figure S2. hiPSC generated from a healthy control (A1–P1) and a CMT2 patient (A2-P2). HiPSC colonies have a typical morphology (A1, A2), with a nucleus/cytoplasma ratio of 1:1. Embryoïd bodies (B1, B2) could be differentiated into cell types from the three embryonic germ layers following spontaneous differentiation (C1, C2) and labelling with α-SMA ((E1, E2) mesoderma), PAX6 ((F1, F2) ectoderma), and Sox17 ((G1,G2) endoderma). HiPSCs expressed pluripotency markers, including Nanog, Oct3/4, and Sox2 (I1-P1, I2, P2), were positive for alkaline phosphatase (D1, D2), and had normal karyotypes (H1, H2); Figure S3. ChAT immunostaining performed at d15 on neuronal progenitors from a healthy control; Figure S4. Ki-67 immunostaining performed at d0 (iPSC stage A-B, E) and d15 (neuronal progenitor C-D, E) from a healthy control. (E) Histograms showed the KI-67 positives cells betwenn hiPSCs (d0) and neuronal progenitor (d15) from a healthy control (Student T Test, $n = 4$ to 7, *** $p < 0.001$); Figure S5. Factors involved in dorsal-ventral polarity during cord differentiation (A), factors involved in antero-posterior differentiation during neurulation (B), and MN markers during differentiation (C) adapted from Casarosa et al., 2013 and Davis-Dusenbery et al., 2014 [35,37].

Author Contributions: Conceptualization: F.S., B.F., and A.-S.L.; methodology and experiments: P.-A.F., N.V., F.M., M.R., and S.R.; formal analysis, P.A.F, N.V., F.M., and S.R.; data curation: L.R. and S.B.; writing—original draft preparation: P.A.F and N.V.; writing—review and editing: P.-A.F., N.V., F.M., M.R., L.R., S.R., S.B., B.F., F.S., F.F., and A.-S.L.; supervision: B.F., F.S., and A.-S.L. All authors have read and agreed on the published version of the manuscript.

Funding: This research was funded by the French Ministery of higher education and research.

Acknowledgments: The authors thank the "Région Limousin", "Club 41", "Lions Club" and "Mairie de St Yrieix La Perche", and the Limoges Hospital for their support. We also thank the I-Stem institute (INSERM/UEVE UMR 861, AFM, Genopole, Evry, France) and the AFM-Téléthon institute for the training they offered to help us to generate our hiPSC.

Conflicts of Interest: The authors declare no conflict of interest.

Ethics Statements: All subjects gave their informed consent for inclusion before participating in the study. The study was conducted in accordance with the Declaration of Helsinki.

Appendix A. HiPSC Characterization

a. Morphology

The HiPSC colonies, EBs, and spontaneous differentiation were observed by light microscopy. The images were captured with a Nikon D90® digital camera.

b. The alkaline phosphatase

Alkaline phosphatase was determined according to the manufacturer's guidelines (Sigma, Fast BCIP/NBT SIGMA B5655).

c. Karyotyping

Metaphase cells were obtained after cell-cycle arrest in mitosis by the addition of demecolcine solution (10mg/mL, Sigma) to the cultures for 2 h after the end of exposure. Mitotic arrest was followed by treatment with a hypotonic solution (diluted fetal calf serum) to increase the cell volume and disrupt cell membranes. The cells were then fixed in 3:1 methanol:acetic acid before being spread onto microscope slides. Chromosomes were stained by the R-banding method, which produces a pattern of bands on chromosomes. R-banding was obtained by heating slides at 88 °C in Earle's buffer followed by Giemsa staining. Metaphase cells were observed under the microscope (Zeiss Axioplan 2 imaging) and karyotyped using the CytoVysion image analysis system (Applied Imaging).

References

1. Takahashi, K.; Yamanaka, S. Induction of pluripotent stem cells from mouse embryonic and adult fibroblast cultures by defined factors. *Cell* **2006**, *126*, 663–676. [CrossRef] [PubMed]
2. Takahashi, K.; Tanabe, K.; Ohnuki, M.; Narita, M.; Ichisaka, T.; Tomoda, K.; Yamanaka, S. Induction of pluripotent stem cells from adult human fibroblasts by defined factors. *Cell* **2007**, *131*, 861–872. [CrossRef] [PubMed]
3. Lancaster, M.A.; Knoblich, J.A. Organogenesis in a dish: Modeling development and disease using organoid technologies. *Science* **2014**, *345*, 1247125. [CrossRef] [PubMed]
4. Li, X.-J.; Du, Z.-W.; Zarnowska, E.D.; Pankratz, M.; Hansen, L.O.; Pearce, R.A.; Zhang, S.-C. Specification of motoneurons from human embryonic stem cells. *Nat. Biotechnol.* **2005**, *23*, 215–221. [CrossRef] [PubMed]
5. Singh Roy, N.; Nakano, T.; Xuing, L.; Kang, J.; Nedergaard, M.; Goldman, S.A. Enhancer-specified GFP-based FACS purification of human spinal motor neurons from embryonic stem cells. *Exp. Neurol.* **2005**, *196*, 224–234. [CrossRef] [PubMed]
6. Chambers, S.M.; Fasano, C.A.; Papapetrou, E.P.; Tomishima, M.; Sadelain, M.; Studer, L. Highly efficient neural conversion of human ES and iPS cells by dual inhibition of SMAD signaling. *Nat. Biotechnol.* **2009**, *27*, 275–280. [CrossRef]
7. Dimos, J.T.; Rodolfa, K.T.; Niakan, K.K.; Weisenthal, L.M.; Mitsumoto, H.; Chung, W.; Croft, G.F.; Saphier, G.; Leibel, R.; Goland, R.; et al. Induced pluripotent stem cells generated from patients with ALS can be differentiated into motor neurons. *Science* **2008**, *321*, 1218–1221. [CrossRef]
8. Ebert, A.D.; Yu, J.; Rose, F.F.; Mattis, V.B.; Lorson, C.L.; Thomson, J.A.; Svendsen, C.N. Induced pluripotent stem cells from a spinal muscular atrophy patient. *Nature* **2009**, *457*, 277–280. [CrossRef]
9. Hu, B.-Y.; Zhang, S.-C. Differentiation of spinal motor neurons from pluripotent human stem cells. *Nat. Protoc.* **2009**, *4*, 1295–1304. [CrossRef]
10. Kim, D.-S.; Lee, J.S.; Leem, J.W.; Huh, Y.J.; Kim, J.Y.; Kim, H.-S.; Park, I.-H.; Daley, G.Q.; Hwang, D.-Y.; Kim, D.-W. Robust Enhancement of Neural Differentiation from Human ES and iPS Cells Regardless of their Innate Difference in Differentiation Propensity. *Stem Cell Rev. Rep.* **2010**, *6*, 270–281. [CrossRef]

11. Saporta, M.A.; Dang, V.; Volfson, D.; Zou, B.; Xie, X.S.; Adebola, A.; Liem, R.K.; Shy, M.; Dimos, J.T. Axonal Charcot-Marie-Tooth disease patient-derived motor neurons demonstrate disease-specific phenotypes including abnormal electrophysiological properties. *Exp. Neurol.* **2015**, *263*, 190–199. [CrossRef] [PubMed]
12. Maciel, R.; Correa, R.; Bosso Taniguchi, J.; Prufer Araujo, I.; Saporta, M.A. Human Tridimensional Neuronal Cultures for Phenotypic Drug Screening in Inherited Peripheral Neuropathies. *Clin. Pharmacol. Ther.* **2019**. [CrossRef] [PubMed]
13. Besser, R.R.; Bowles, A.C.; Alassaf, A.; Carbonero, D.; Claure, I.; Jones, E.; Reda, J.; Wubker, L.; Batchelor, W.; Ziebarth, N.; et al. Enzymatically crosslinked gelatin-laminin hydrogels for applications in neuromuscular tissue engineering. *Biomater. Sci.* **2020**, *8*, 591–606. [CrossRef] [PubMed]
14. Okita, K.; Matsumura, Y.; Sato, Y.; Okada, A.; Morizane, A.; Okamoto, S.; Hong, H.; Nakagawa, M.; Tanabe, K.; Tezuka, K.; et al. A more efficient method to generate integration-free human iPS cells. *Nat. Methods* **2011**, *8*, 409–412. [CrossRef] [PubMed]
15. Wichterle, H.; Lieberam, I.; Porter, J.A.; Jessell, T.M. Directed Differentiation of Embryonic Stem Cells into Motor Neurons. *Cell* **2002**, *110*, 385–397. [CrossRef]
16. Miles, G.B.; Yohn, D.C.; Wichterle, H.; Jessell, T.M.; Rafuse, V.F.; Brownstone, R.M. Functional properties of motoneurons derived from mouse embryonic stem cells. *J. Neurosci.* **2004**, *24*, 7848–7858. [CrossRef]
17. De Luca, A.; Cerrato, V.; Fucà, E.; Parmigiani, E.; Buffo, A.; Leto, K. Sonic hedgehog patterning during cerebellar development. *Cell. Mol. Life Sci.* **2016**, *73*, 291–303. [CrossRef]
18. Komiya, Y.; Habas, R. Wnt signal transduction pathways. *Organogenesis* **2008**, *4*, 68–75. [CrossRef]
19. Wang, R.N.; Green, J.; Wang, Z.; Deng, Y.; Qiao, M.; Peabody, M.; Zhang, Q.; Ye, J.; Yan, Z.; Denduluri, S.; et al. Bone Morphogenetic Protein (BMP) signaling in development and human diseases. *Genes Dis.* **2014**, *1*, 87–105. [CrossRef]
20. Akhurst, R.J.; Hata, A. Targeting the TGFβ signalling pathway in disease. *Nat. Rev. Drug Discov.* **2012**, *11*, 790–811. [CrossRef]
21. Kowiański, P.; Lietzau, G.; Czuba, E.; Waśkow, M.; Steliga, A.; Moryś, J. BDNF: A Key Factor with Multipotent Impact on Brain Signaling and Synaptic Plasticity. *Cell. Mol. Neurobiol.* **2018**, *38*, 579–593. [CrossRef] [PubMed]
22. Iams, W.T.; Lovly, C.M. Molecular pathways: Clinical applications and future direction of insulin-like growth factor-1 receptor pathway blockade. *Clin. Cancer Res.* **2015**, *21*, 4270–4277. [CrossRef] [PubMed]
23. De Tassigny, X.d.; Pascual, A.; Lopez-Barneo, J. GDNF-based therapies, GDNF-producing interneurons, and trophic support of the dopaminergic nigrostriatal pathway. Implications for parkinson's disease. *Front. Neuroanat.* **2015**, *9*, 1–15. [CrossRef]
24. Watanabe, K.; Ueno, M.; Kamiya, D.; Nishiyama, A.; Matsumura, M.; Wataya, T.; Takahashi, J.B.; Nishikawa, S.; Nishikawa, S.; Muguruma, K.; et al. A ROCK inhibitor permits survival of dissociated human embryonic stem cells. *Nat. Biotechnol.* **2007**, *25*, 681–686. [CrossRef]
25. Goetz, R.; Mohammadi, M. Exploring mechanisms of FGF signalling through the lens of structural biology. *Nat. Rev. Mol. Cell Biol.* **2013**, *14*, 166–180. [CrossRef] [PubMed]
26. Maden, M. Retinoid signalling in the development of the central nervous system. *Nat. Rev. Neurosci.* **2002**, *3*, 843–853. [CrossRef]
27. Powers, R.K.; Binder, M.D. Persistent sodium and calcium currents in rat hypoglossal motoneurons. *J. Neurophysiol.* **2003**, *89*, 615–624. [CrossRef]
28. Harfe, B.D.; Scherz, P.J.; Nissim, S.; Tian, H.; McMahon, A.P.; Tabin, C.J. Evidence for an expansion-based temporal Shh gradient in specifying vertebrate digit identities. *Cell* **2004**, *118*, 517–528. [CrossRef]
29. Bergmann, S.; Sandler, O.; Sberro, H.; Shnider, S.; Schejter, E.; Shilo, B.-Z.; Barkai, N. Pre-steady-state decoding of the Bicoid morphogen gradient. *PLoS Biol.* **2007**, *5*, e46. [CrossRef]
30. Gregor, T.; Tank, D.W.; Wieschaus, E.F.; Bialek, W. Probing the limits to positional information. *Cell* **2007**, *130*, 153–164. [CrossRef]
31. Andrews, M.G.; Kong, J.; Novitch, B.G.; Butler, S.J. *New Perspectives on the Mechanisms Establishing the Dorsal-Ventral Axis of the Spinal Cord*, 1st ed.; Elsevier Inc.: New York, NY, USA, 2019; Volume 132, ISBN 9780128104897.
32. Ducy, P.; Karsenty, G. The family of bone morphogenetic proteins. *Kidney Int.* **2000**, *57*, 2207–2214. [CrossRef] [PubMed]

33. Bier, E.; De Robertis, E.M. BMP gradients: A paradigm for morphogen-mediated developmental patterning. *Science* **2015**, *348*. [CrossRef] [PubMed]
34. Gilbert, S.F. *Developmental Biology*, 6th ed.; Sinauer Associates Inc.: Sunderland, MA, USA, 2000; p. 695.
35. Casarosa, S.; Zasso, J.; Conti, L. Systems for Ex-Vivo Isolation and Culturing of Neural Stem Cells. *Neural Stem Cells New Perspect.* **2013**. [CrossRef]
36. Kudoh, T.; Wilson, S.W.; Dawid, I.B. Distinct roles for Fgf, Wnt and retinoic acid in posteriorizing the neural ectoderm. *Development* **2002**, *129*, 4335–4346. [PubMed]
37. Davis-Dusenbery, B.N.; Williams, L.A.; Klim, J.R.; Eggan, K. How to make spinal motor neurons. *Development* **2014**, *141*, 491–501. [CrossRef]
38. Cardenas-Aguayo, M.D.C.; Kazim, S.F.; Grundke-Iqbal, I.; Iqbal, K. Neurogenic and Neurotrophic Effects of BDNF Peptides in Mouse Hippocampal Primary Neuronal Cell Cultures. *PLoS ONE* **2013**, *8*, e53596. [CrossRef]
39. Jung, H.J.; Suh, Y. Regulation of IGF −1 signaling by microRNAs. *Front. Genet.* **2015**, *5*, 472. [CrossRef]
40. Dyer, A.H.; Vahdatpour, C.; Sanfeliu, A.; Tropea, D. The role of Insulin-Like Growth Factor 1 (IGF-1) in brain development, maturation and neuroplasticity. *Neuroscience* **2016**, *325*, 89–99. [CrossRef]
41. Wrigley, S.; Arafa, D.; Tropea, D. Insulin-like growth factor 1: At the crossroads of brain development and aging. *Front. Cell. Neurosci.* **2017**, *11*, 14. [CrossRef]
42. Takahashi, M. The GDNF/RET signaling pathway and human diseases. *Cytokine Growth Factor Rev.* **2001**, *12*, 361–373. [CrossRef]
43. Timmerman, V.; Strickland, A.V.; Züchner, S. Genetics of Charcot-Marie-Tooth (CMT) Disease within the Frame of the Human Genome Project Success. *Genes Basel* **2014**, *5*, 13–32. [CrossRef] [PubMed]
44. Juneja, M.; Burns, J.; Saporta, M.A.; Timmerman, V. Challenges in modelling the Charcot-Marie-Tooth neuropathies for therapy development. *J. Neurol. Neurosurg. Psychiatry* **2019**, *90*, 58–67. [CrossRef] [PubMed]
45. Juneja, M.; Azmi, A.; Baets, J.; Roos, A.; Jennings, M.J.; Saveri, P.; Pisciotta, C.; Bernard-Marissal, N.; Schneider, B.L.; Verfaillie, C.; et al. PFN2 and GAMT as common molecular determinants of axonal Charcot-Marie-Tooth disease. *J. Neurol. Neurosurg. Psychiatry* **2018**, *89*, 870–878. [CrossRef] [PubMed]
46. Ohara, R.; Imamura, K.; Morii, F.; Egawa, N.; Tsukita, K.; Enami, T.; Shibukawa, R.; Mizuno, T.; Nakagawa, M.; Inoue, H. Modeling Drug-Induced Neuropathy Using Human iPSCs for Predictive Toxicology. *Clin. Pharmacol. Ther.* **2017**, *101*, 754–762. [CrossRef]
47. Kim, J.Y.; Woo, S.Y.; Hong, Y.B.; Choi, H.; Kim, J.; Choi, H.; Mook-Jung, I.; Ha, N.; Kyung, J.; Koo, S.K.; et al. HDAC6 Inhibitors Rescued the Defective Axonal Mitochondrial Movement in Motor Neurons Derived from the Induced Pluripotent Stem Cells of Peripheral Neuropathy Patients with HSPB1 Mutation. *Stem Cells Int.* **2016**, *2016*, 9475981. [CrossRef]
48. Faye, P.A.; Poumeaud, F.; Miressi, F.; Lia, A.S.; Demiot, C.; Magy, L.; Favreau, F.; Sturtz, F.G. Focus on 1,25-dihydroxyvitamin D3 in the peripheral nervous system. *Front. Neurosci.* **2019**, *13*, 348. [CrossRef]
49. Faye, P.-A.; Vedrenne, N.; De la Cruz-Morcillo, M.A.; Barrot, C.-C.; Richard, L.; Bourthoumieu, S.; Sturtz, F.; Funalot, B.; Lia, A.-S.; Battu, S. New Method for Sorting Endothelial and Neural Progenitors from Human Induced Pluripotent Stem Cells by Sedimentation Field Flow Fractionation. *Anal. Chem.* **2016**, *88*, 6696–6702. [CrossRef]

Conclusion

In our study, we presented an efficient protocol to generate MN from hiPSC, in 20-30 days. It is based on specific and accurately balanced differentiation factors, and it does not require any particular cellular manipulation, like virus transduction (Wang et al. 2017). Moreover, as shown by neural markers staining, it allows to obtain a quite pure culture of MN, with a higher efficiency rate than that reported in previous protocols (Chambers et al. 2009; Hu and Zhang 2009).

hiPSC are widely employed to recreate suitable cellular models. Our protocol could provide a new strategy in modeling of peripheral neuropathies, like CMT disease, which is fundamental in the exploration of their impaired molecular mechanisms.

<u>Article 5</u> - Focus on 1,25-Dihydroxyvitamin D3 in the Peripheral Nervous System

Published in Frontiers in Neuroscience (12 April 2019)

The 1,25-dihydroxyvitamin D3, or calcitriol, is the active form of the vitamin D or calciferol. It has long been associated with the phosphocalcium metabolism, but more recent studies highlighted its involvement also in tissue proliferation, cell differentiation, and apoptosis. In this review, we focused on calcitriol role in nervous system, and, in particular, in PNS. In CNS, vitamin D participates in several processes, like calcium trafficking, and regulation of neural proteins', neurotrophic factors', and neurotransmitters' synthesis. Its deficiency, therefore, seems to promote neurodegenerative diseases, like Parkinson's disease, Alzheimer's disease, multiple sclerosis. In the PNS, vitamin D has been shown to favor axonal formation and regeneration, but also myelin production and remyelination events. On the contrary, its levels appeared reduced in some cases of peripheral neuropathies, such as chemotherapy-induced peripheral neuropathy and diabetic neuropathy. At molecular level, it has demonstrated that vitamin D could participate in different pathways, as Wnt, Sonic hedgehog, and Klotho pathways, which are essential in nervous system development. Lastly, on the basis of all previous findings, we suggested that it could be interesting to investigate, with *in vitro* and *in vivo* studies, whether and how supplementation of calcitriol can contribute to peripheral nervous system maintenance and function.

frontiers in Neuroscience

REVIEW
published: 12 April 2019
doi: 10.3389/fnins.2019.00348

Focus on 1,25-Dihydroxyvitamin D3 in the Peripheral Nervous System

Pierre Antoine Faye[1,2†], François Poumeaud[1†], Federica Miressi[1], Anne Sophie Lia[1,2], Claire Demiot[1], Laurent Magy[3], Frédéric Favreau[1,2] and Franck G. Sturtz[1,2*]*

[1] EA 6309, Myelin Maintenance and Peripheral Neuropathies, Faculties of Medicine and Pharmacy, University of Limoges, Limoges, France, [2] Department of Biochemistry and Molecular Genetics, University Hospital of Limoges, Limoges, France, [3] CHU de Limoges, Reference Center for Rare Peripheral Neuropathies, Department of Neurology, Limoges, France

In this review, we draw attention to the roles of calcitriol (1,25-dihydroxyvitamin D3) in the trophicity of the peripheral nervous system. Calcitriol has long been known to be crucial in phosphocalcium homeostasis. However, recent discoveries concerning its involvement in the immune system, anti-cancer defenses, and central nervous system development suggest a more pleiotropic role than previously thought. Several studies have highlighted the impact of calcitriol deficiency as a promoting factor of various central neurological diseases, such as multiple sclerosis, amyotrophic lateral sclerosis, Parkinson's disease, and Alzheimer's disease. Based on these findings and recent publications, a greater role for calcitriol may be envisioned in the peripheral nervous system. Indeed, calcitriol is involved in myelination, axonal homogeneity of peripheral nerves, and neuronal-cell differentiation. This may have useful clinical consequences, as calcitriol supplementation may be a simple means to avoid the onset and/or development of peripheral nervous-system disorders.

Keywords: calcitriol, peripheral nervous system, neuronal-cell differentiation, synergistic effects, myelin process

OPEN ACCESS

Edited by:
Stanko S. Stojilkovic, National Institutes of Health (NIH), United States

Reviewed by:
Elena Gonzalez-Rey, Instituto de Parasitología y Biomedicina López Neyra (IPBLN), Spain
A. J. van Ballegooijen, VU University Medical Center, Netherlands

***Correspondence:**
Frédéric Favreau
frederic.favreau@unilim.fr
Franck G. Sturtz
franck.sturtz@unilim.fr

†These authors have contributed equally to this work

Specialty section:
This article was submitted to Neuroendocrine Science, a section of the journal Frontiers in Neuroscience

Received: *11 January 2019*
Accepted: *26 March 2019*
Published: *12 April 2019*

Citation:
Faye PA, Poumeaud F, Miressi F, Lia AS, Demiot C, Magy L, Favreau F and Sturtz FG (2019) Focus on 1,25-Dihydroxyvitamin D3 in the Peripheral Nervous System. Front. Neurosci. 13:348. doi: 10.3389/fnins.2019.00348

EPIDEMIOLOGICAL DATA AND THE GENERAL FUNCTION OF VITAMIN D3

For decades, the role of calcitriol was thought to be limited to phosphocalcium metabolism. Recent results have highlighted the role of this hormone in other functions (Garabédian, 2000; Christakos et al., 2016), which include the regulation of tissue proliferation, cell differentiation, and apoptosis, as well as regulation of the cardiovascular and immune systems. Indeed, the active form of vitamin D3 has been shown to regulate inflammation by regulating the synthesis of several cytokines and lymphocyte migration, with anti-cancer activities (Baeke et al., 2010). Based on cellular and animal models, Kalueff and Tuohimaa (2007) suggest that calcitriol has a major role in the genesis, development, and maintenance of central nervous system in adulthood. As shown in animal experiments, calcitriol may regulate rat brain development. Rats born to a mother that was vitamin D3-depleted during pregnancy were shown to have brain malformations, such as cortical atrophy associated with ventricular dilation (Eyles et al., 2005). Another study has reported the synthesis of calcitriol within the central nervous system, thus regulating its functioning and exerting neuroprotective effects (Eyles et al., 2003). Marini et al. (2010) observed that *in vitro* calcitriol delays cell proliferation and induces cell differentiation in HN9.10 embryonic hippocampal cells, with the formation of axons and dendrites. Overall, these findings suggest that vitamin D3 has activities

similar to other neuroactive steroids in the central nervous system (Emmanuel et al., 2002; Melcangi and Panzica, 2009). However, the exact role of calcitriol in the peripheral nervous system is still unclear. The aim of this review was to gather available data concerning the role of calcitriol in the peripheral nervous system during its development and maintenance.

Although all the calcitriol functions may not yet be known, the chemical characteristics have been extensively investigated. The precursor of calcitriol is vitamin D or calciferol, which is synthesized in the skin or ingested with food. This precursor is biologically inactive and subjected to double hydroxylation, first in the liver and then in the kidney, to produce the biologically active compound, 1,25-$(OH)_2$-vitamin D3 or calcitriol (**Figure 1**). It is well known to regulate the expression of numerous target genes through the nuclear vitamin D receptor (VDR), which belongs to a common family of steroid receptors that also includes steroid, glucocorticoid, and retinoic acid receptors (Kalueff and Tuohimaa, 2007). Vitamin D deficiency is widely found worldwide (Holick, 2006). For example, the prevalence of vitamin D insufficiency was 77% in the United States population in 2004 (Ginde et al., 2009). However, reference values vary widely between countries. According to Rosen (2011) only 25-OH-vitamin D3 prohormone blood levels can accurately estimate vitamin D3 input from cutaneous synthesis and dietary intake, in contrast to 1,25-$(OH)_2$-vitamin D3. The measurement of 1,25-$(OH)_2$-vitamin D3 is mainly reserved for patients with kidney insufficiency. Several countries consider that serum levels of 25-OH-vitamin D3 below 10 ng/ml indicate vitamin D deficiency. Vitamin D "insufficiency" is characterized by serum levels between 10 and 30 ng/ml, an "appropriate" level between 30 and 100 ng/ml, and a "toxic" level by values above 100 ng/ml (Rosen, 2011). However, in the United States, the Endocrine Society has established different threshold levels. Vitamin D deficiency is diagnosed in patients with serum levels of 25-OH-vitamin D3 below 20 ng/ml, "sufficiency" between 30 and 40 ng/ml, and toxicity above 50 ng/ml (Ross et al., 2011). In addition, these different thresholds are those used to measure phosphocalcium homeostasis. These thresholds could be different for other functions of the nervous system and, if so, they are yet to be determined.

MECHANISTIC AND MOLECULAR INTERACTIONS OF VITAMIN D3

Systemic action of Vitamin D3 requires a metabolization and an activation. Vitamin D3 metabolism is a multiple-step multiple-organ process which will be recalled thereafter. Once activated vitamin D3 will act upon several genes at a transcriptional level, in cooperation with other factors such as fat-soluble vitamin derivatives.

Vitamin D3 Metabolism

Calcitriol levels are precisely regulated by the mitochondrial hydroxylases, cytochrome P450C1α (CYP27B1) and P450C24 (CYP24), which catalyze the bioactivation and degradation of vitamin D3 metabolites in most target cells (Hii and Ferrante, 2016). The blood level of calcitriol is auto-regulated through the stimulation of the CYP24 enzyme (VanAmerongen et al., 2004). In addition, calcitriol also inhibits CYP1 (renal 1 α hydroxylase involved in the second hydroxylation of vitamin D3) activity, thus forming a negative feedback loop to maintain normal levels (Issa et al., 1998). Finally, most calcitriol is excreted as calcitroic acid. The serum half-life of 1,25-$(OH)_2$-vitamin D3 is approximately 4–6 h, whereas the serum half-life of 25-OH-vitamin D3 is approximately 10–21 days (Kumar, 1986). These different serum half-lives explain why 25-OH-vitamin D3 is the classical form used in serum-level measurements in humans to evaluate the body level of vitamin D3. In addition, standard protocols in the clinical lab appear to be poorly adapted to measure calcitriol levels. Indeed, liquid chromatography coupled to tandem mass spectrometry (LC-MS/MS) appears to be the most appropriate, but it is expensive and not used by most laboratories (Spanaus and von Eckardstein, 2017). This sensitive technique is used for calcitriol measurement because absolute levels of 25-OH-vitamin D3 and 1,25-$(OH)_2$-vitamin D3 differ by a factor of 1000. The renal 1-alpha hydroxylation of 25-OH-vitamin D3 to 1,25-$(OH)_2$-vitamin D3 is highly regulated by the serum concentration of parathyroid hormone, calcium, and phosphate. It is well known that a wide variety of extra-renal cells can produce calcitriol from 25-OH-vitamin D3 by the enzyme 1 α hydroxylase *in vitro*, including activated macrophages, keratinocytes, and cells of the central nervous system, such as neurons and microglial cells. However, the regulation of hydroxylation in these cells has not been fully explored and such production of calcitriol appears to not be finely regulated by renal production (VanAmerongen et al., 2004). Most circulating vitamin D metabolites in blood under normal physiological conditions are bound to vitamin D-binding protein or albumin and transported to a large number of target organs (VanAmerongen et al., 2004).

Vitamin D3 and the Vitamin D Receptor (VDR)

Vitamin D is converted into its hydroxylated derivative, 1,25-$(OH)_2$-vitamin D3, by two successive hydroxylations, one in the liver and one in the kidneys. Its liposolubility allows calcitriol to pass through cell membranes without a transporter. Within the cell, the vitamin D receptor (VDR), a member of the nuclear-receptor superfamily, mediates the biological activity of 1,25-$(OH)_2$-vitamin D3 by regulating gene expression, similarly to other steroid hormone receptors (**Figure 2**). Following a conformational change, the VDR regulates gene transcription by binding to hexameric core-binding motifs in the promoter regions of target genes (Issa et al., 1998). The vitamin D-VDR endocrine system has been identified in nearly all nucleated cells. Microscopic autoradiography of the VDR has identified the target organs for vitamin D, especially the brain and spinal cord, for which there is a high binding rate (Stumpf, 2012). Although not fully understood, VDR could be involved in the development of a variety of neurological illnesses.

When entering a target cell, calcitriol dissociates from vitamin D-binding protein (the transporter of vitamin D in blood),

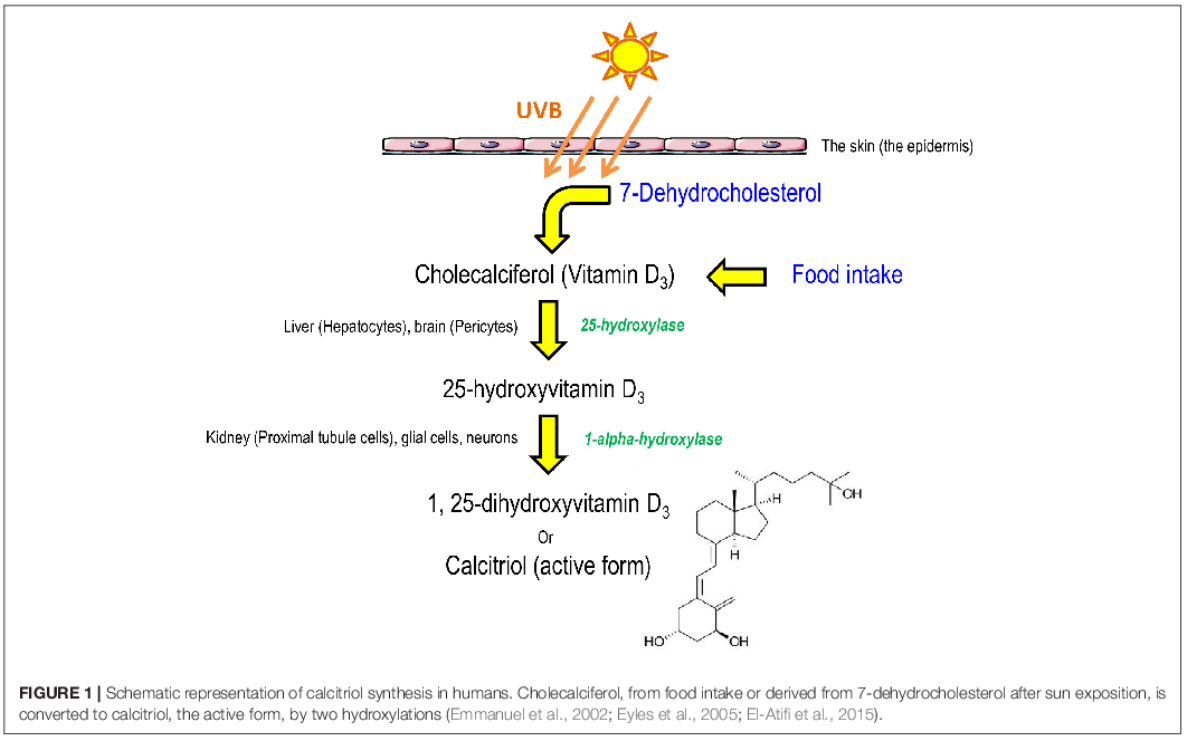

FIGURE 1 | Schematic representation of calcitriol synthesis in humans. Cholecalciferol, from food intake or derived from 7-dehydrocholesterol after sun exposition, is converted to calcitriol, the active form, by two hydroxylations (Emmanuel et al., 2002; Eyles et al., 2005; El-Atifi et al., 2015).

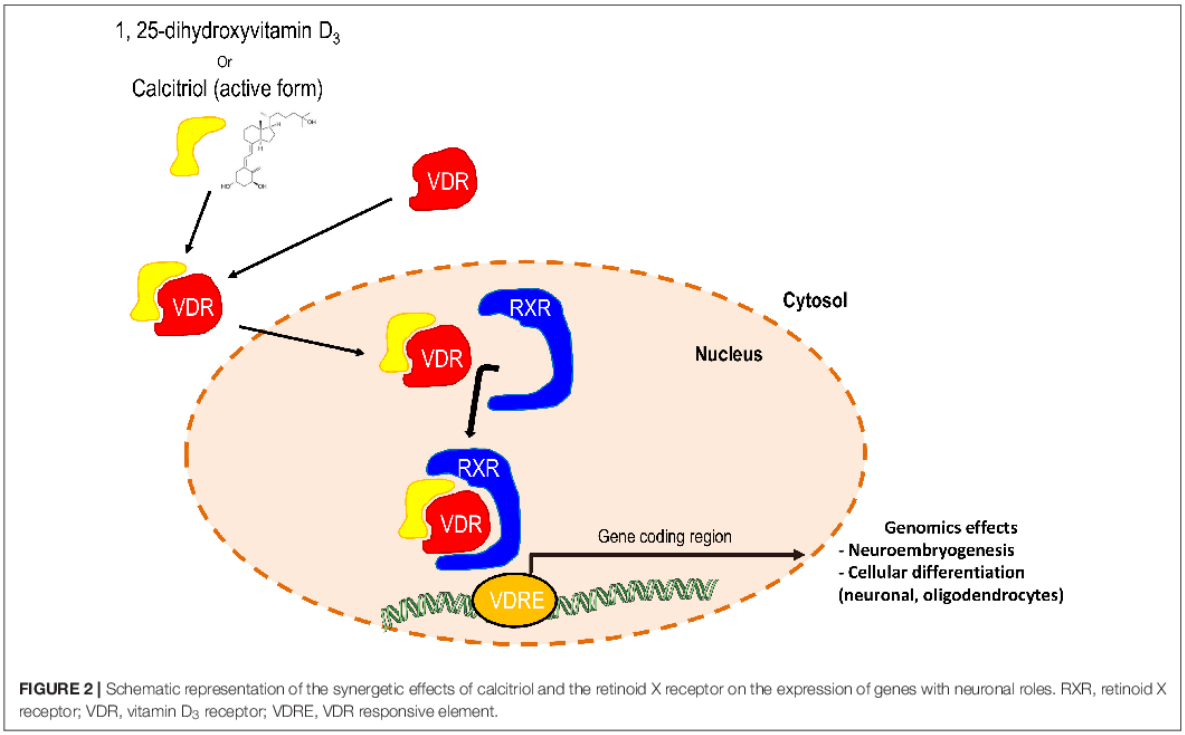

FIGURE 2 | Schematic representation of the synergetic effects of calcitriol and the retinoid X receptor on the expression of genes with neuronal roles. RXR, retinoid X receptor; VDR, vitamin D_3 receptor; VDRE, VDR responsive element.

diffuses across the plasma membrane, binds to the VDR, and the formed complex migrates to the nucleus. The activated VDR dimerizes with another nuclear receptor, the retinoic acid receptor (RXR). This RXR/VDR/calcitriol heterodimer binds to the vitamin D responsive element (VDRE), a specific sequence in the promoter region of target genes. Upon binding to the VDRE, the heterodimer activates or suppresses gene transcription. VDRs can also form homodimers but their functional significance is not known (VanAmerongen et al., 2004). In addition, efficient transcription requires co-activator or co-repressor proteins, such as Smad3, an effector of the TGF beta pathway (VanAmerongen et al., 2004). In the calcitriol pathway, Smad 3 acts as a coactivator and Smad 7 abrogates the Smad3-mediated VDR response. Cells of the central nervous system (microglia, neurons, and astrocytes) express VDR and can respond directly to calcitriol (Emmanuel et al., 2002).

Calcitriol has also been reported to modulate rapid non-genomic actions mediated through various mechanisms, such as the activation of G-protein coupled receptors and downstream protein kinase C (PKC), mitogen-activated protein kinase (MAPK) pathways, phospholipases A2 and C, and the opening of Ca^{2+} and Cl^{-} channels (Buitrago et al., 2013; Hii and Ferrante, 2016). However, these various effects have yet to be reported in cells of the nervous system.

Vitamin D3 and Synergistic Effects With Other Vitamins

The synergistic interactions between fat-soluble vitamins have been suggested since several decades and particularly between vitamin A and vitamin E in the field of lipid peroxidation (Tesoriere et al., 1996). However, the interaction of vitamin D3 with other fat-soluble vitamins is also suggested through different mechanisms and based on different responses induced by vitamin D3 *in vitro* or *in vivo*. Indeed, vitamin D3 has been shown to regulate the growth and differentiation of a number of various cell types *in vitro*, including bone, immune and hematopoietic cells, and keratinocytes, as well as cancer cells. However, *in vivo*, these responses are achieved at toxic doses that cause severe hypercalcemia (Issa et al., 1998). These observations suggest that the effects of calcitriol underline synergistic effects between other hormones or molecules at lower concentrations.

Firstly, vitamin D3 appears to have synergistic effects with other fat-soluble vitamins, such as vitamin K, particularly for bone and cardiovascular health (van Ballegooijen et al., 2017b). Regarding bone homeostasis, in an experimental study, Kerner et al. (1989) described that osteoblast-specific expression of osteocalcin, a vitamin K-dependent protein, is controlled at the transcriptional level by the calcitriol within the promoter of the osteocalcin gene. These results were supported by Sergeev et al. (1987), in a rat model, showing that VDR can undergo gamma-carboxylation in the presence of vitamin K, which putatively interferes with its nuclear functions through VDREs. In an experimental study investigating osteoporosis in ovariectomized rats, Matsunaga et al. (1999) reported that the combined treatment with vitamin D3 and K is more effective to prevent osteoporosis. In observational studies in humans, these interactions were also pointed out. In 387 hemodialyzed patients, vitamin D3 analog users present higher concentrations of bone Gla protein (BGD) indicating the role of vitamin D3 to stimulate this vitamin K-depend proteins (Fusaro et al., 2016). In the NOREPOS study among 1318 older adults, results underlined that a combination of vitamin D3 and K supplementations at low concentrations was linked with a greater hip fracture risk compared to supplementations at high concentrations or to the group supplemented with just one vitamin at low concentrations (Finnes et al., 2016). Several clinical trials support this synergetic interaction and particularly in postmenopausal osteoporosis (van Ballegooijen et al., 2017b). For instance, in an interventional, randomized and placebo-controlled study led in 172 Japanese post-menopausal women with osteopenia and osteoporosis, results showed that only vitamin K plus vitamin D3 increased bone mineral density (Ushiroyama et al., 2002). In 78 Korean post-menopausal women over 60 years of age, vitamin K treatment associated to vitamin D and calcium increased bone mineral density (Je et al., 2011). Regarding cardiovascular health, the synergy between vitamin D3 and K was also reported. Similarly, this synergy could be linked to vitamin D3-induced stimulation of vitamin K-dependent proteins, such as matrix Gla protein (MGP), which needs gamma-glutamate carboxylation to inhibit the vascular calcification (Mayer et al., 2017). Indeed, in a rodent model, vitamin K deficiency caused by warfarin treatment, promotes arterial calcifications and this occurs earlier when high doses of vitamin D are associated (Price et al., 2000). A prospective study indicates that the combined treatment of low dose of vitamin D and a low status of vitamin K promoted systolic and diastolic blood pressures increase and hypertension after 6 years of follow up (van Ballegooijen et al., 2017a). These results were supported by another study showing that this association induces a significantly higher aortic pulse wave than in subjects with isolated vitamin D3 or vitamin K deficiency, reflecting a higher aortic resistance (Mayer et al., 2017). In addition, a randomized and double-blind trial on 42 non-dialyzed patients with chronic kidney disease showed that vitamin D3 associated with vitamin K has an additive or a synergistic effect on the decrease of intima-media thickness (Kurnatowska et al., 2015). However, synergistic effect between vitamin D3 and K may only exist at optimal concentrations. Indeed, an observational single-center cohort study showed that vitamin D3 supplementation on renal-transplanted patients with vitamin K deficiency induced increased mortality and graft failures (van Ballegooijen et al., 2019). Many more trials are currently being led as one can see on web sites for registered trials[1,2].

Similarly, interactions between calcitriol and vitamin E were observed and particularly to mediate cellular antiproliferative effects. The association of low doses of calcitriol and vitamin E succinate has been reported to have additive effects on the inhibition of human prostatic cancer cells LNCaP proliferation through the stimulation of VDR expression, without adverse effect on calcemia (Yin et al., 2009). An another study led on a rat model showed that vitamin D and E deficiencies have synergistic

[1]www.clinicaltrials.gov

[2]www.clinicaltrialsregister.eu

effects on rickets development (Sergeev et al., 1987). However, the additive or synergistic mechanism of this association is still unclear and requires further study.

In addition, a synergistic effect of vitamin D3 and A, which is a retinoic acid precursor, has been reported in various cellular models (breast, prostate, colon, and leukemia) but also in mycobacteria (Guilland, 2011; Greenstein et al., 2012). These effects could be linked to the dimerization between the VDR and RXR, which creates an interconnection between the calcitriol and retinoic acid cellular pathways. Indeed, retinoic acid could modulate the vitamin D3 effects. Several studies pointed out an antagonism or additive/synergetic effects between both vitamins. For instance, Kane et al. (1996) showed an inhibition by retinoic acid of the antiproliferative effect of calcitriol on colon cancer cells. However, several studies reported a synergistic effect. *In vitro*, on human prostatic cancer cells LNCaP, Blutt et al. (1997) suggested that calcitriol and retinoic acid act synergistically to inhibit the growth of cancer cells and cause accumulation of cells in G1. Carlberg et al. (1993) showed that in drosophila SL-3 cells transfected with mouse VDR or RXR genes, the VDRE was synergistically activated by RXR and VDR, but only in the presence of both factors. Regarding the nervous system, the RXR has been shown to be involved in the differentiation of oligodendrocyte progenitors into mature oligodendrocytes (de la Fuente et al., 2015), and also in neuronal differentiation (Mounier et al., 2015). It is well known that retinoic acid plays a major role during the embryological development of the central nervous system, leading the neuroectoderm to caudalize itself. On the other hand, calcitriol also plays a role in neuro-embryogenesis (Shirazi et al., 2015). Thus, it is conceivable that a synergistic interconnection between retinoic acid and calcitriol exists during nervous system development. All of the interactions between vitamin D and other fat-soluble vitamins presented above show that this field is quite large and matter for further explorations in the nervous system.

Cardiovascular Effects and Systemic Interactions of Vitamin D3

Vitamin D3 has been suspected to play a role in cardioprotection. Indeed, VDR-deficient mice showed adverse cardiac remodeling and hypertension (Meems et al., 2011). However, in an observational, prospective and population-based cohort study, calcitriol or calcidiol plasmatic levels have failed in predicting higher risk of heart failure (Meems et al., 2016). Thus, further studies are required to investigate strong evidence-based relationship between Vitamin D3 and heart failure. On the other hand, 1,25-$(OH)_2$-vitamin D3 may also induce adverse effects in humans. Another observational, prospective and population-based cohort study demonstrated that plasma calcitriol levels are associated with an elevated risk of hypertension (van Ballegooijen et al., 2015). Intriguingly and unexpectedly, cholecalciferol plasma levels are inversely associated with hypertension. However, calcitriol supplementation was shown to cause renal calcification in an experimental laboratory study led on a suckling rat model (Dostal et al., 1984), which is confirmed by the fact that, in humans, cholecalciferol supplementation is associated with kidney-stone formation, linked to increased hypercalciuria (Letavernier and Daudon, 2018).

ROLES OF VITAMIN D3 IN THE NERVOUS SYSTEM

As reported above and in **Table 1**, data suggest that calcitriol has a role in the nervous system and that vitamin D3 acts as a neurosteroid (Emmanuel et al., 2002; Melcangi and Panzica, 2009). However, the role, if any, of the calcitriol in the peripheral nervous system needs to be more precisely defined.

Vitamin D3 and Cell Differentiation

We further investigate the role of calcitriol in nervous system development, particularly neuronal cell differentiation, by focusing on the various actors known to be regulated by calcitriol, such as the Wnt signaling pathway, Sonic hedgehog (Shh), and Klotho, as well as on the putative role of progesterone to stimulate the effect of calcitriol in differentiation.

Wnt Proteins

Wnt proteins are cysteine-rich glycosylated proteins that control multiple processes involving neuronal development, angiogenesis, immunity, tumorigenesis, fibrosis, and stem-cell proliferation (Maiese, 2015). Wnt is also involved in nervous system development, particularly as a positive regulator of the myelination process, by promoting myelin gene expression. Tawk et al. (2011) demonstrated that the inactivation of Wnt components *in vitro* in mouse Schwann cells leads to severe dysmyelination and the inhibition of myelin gene expression. Calcitriol has been shown to disrupt Wnt/β-catenin signaling through multiple mechanisms. Hlaing et al. (2014) reported that vitamin D promotes cardiac differentiation through the negative modulation of the canonical Wnt signaling pathway and upregulation of the expression of Wnt11, *in vitro* culture of H9c2 rat embryonic myocardium cells. Lim et al. (2014) found that decreased expression of the VDR is associated with decreased expression of Wnt/β-catenin signals in follicle dermal papilla cells, inhibiting the proliferation, and differentiation of hair follicles and epidermal cells.

The Shh Pathway

Sonic hedgehog signaling is involved in the induction of neuronal populations in the central and peripheral nervous systems and neural stem-cell proliferation (Choudhry et al., 2014). In a recent study in an embryonic carcinoma mice cell line (P19EC), Vuong et al. (2017) clearly showed that Shh signaling regulates neuronal differentiation and neurite growth. In an experimental study using VDR-deficient mice, Teichert et al. (2011) reported that VDR-null animals overexpress Shh in keratinocytes and that such overexpression is downregulated by 1,25-$(OH)_2$-vitamin D3. These results were supported by Dormoy et al. (2012) who showed that vitamin D decreases cell proliferation and increases cell death by inhibiting the Shh pathway in human renal carcinoma cells. Although the Wnt/β-catenin pathway and Shh

TABLE 1 | Different experimental models or human cohorts aimed to investigate the positive or negative role of Vitamin D3.

Level	Model	Sample size (*N* = x)	Study design	Variable	Outcome	References
Cellular	Astrocytes			Vitamin D3 supplementation	↑ GDNF, NT-3, NT-4	Neveu et al., 1994
	Primary cortical neurons (E18 rats)			Vitamin D3 + progesterone supplementation	Better neuroprotection (vs. progesterone alone)	Atif et al., 2009
	Embryonic hippocampal cells			Vitamin D3 supplementation	Delay proliferation Enhance neuronal differentiation	Marini et al., 2010
	Human renal carcinoma cells			Vitamin D3 supplementation	↑ Cell proliferation ↓ Apoptosis	Dormoy et al., 2012
	H9c2 rat embryonic myocardium cells			Vitamin D3 supplementation	Cardiac differentiation	Hlaing et al., 2014
	Follicle dermal papilla cells			VDR (KO)	Inhibition of proliferation and differentiation	Lim et al., 2014
	Human melanocytes			H2O2 + calcipotriol	↑ MFN2	Gong et al., 2015
	Rat primary Schwann cells			Vitamin D3 supplementation	↑ Synthesis of IGF-1, MBP	Sakai et al., 2015
	Pancreatic cell line INS-1 (rats)			Vitamin D3 supplementation	↑ GDAP1	Pepaj et al., 2015
	Glial cells			Vitamin D3 supplementation	↑ Synthesis of estrogen	Caccamo et al., 2018
Animal	Rats	112		Vitamin D3 supplementation	↓ Hippocampic iNOS synthesis	Garcion et al., 1998
		24		Vitamin D3 in utero deficiency	Cortical atrophy, Ventricular dilation, ↑ NGF and GDNF	Eyles et al., 2003
		26		Vitamin D3 supplementation + peripheral nerve trauma	↑ Axonogenesis and axon diameter	Chabas et al., 2008
		36		Vitamin D3 supplementation + Peripheral nerve trauma	↑ Neurite myelination Electro-clinical recovery	Chabas et al., 2013
		30		Vitamin D3 pre and post natal deficiency	↑ Synapses number cortical atrophy	Al-harbi et al., 2017
	Mice	15		VDR (KO)	Heterogeneity in axonal diameters and axonal partitioning (Sciatic nerve)	Sakai et al., 2015
Human	Parkinson's disease	114	Experimental (randomized, double-blind, placebo-controlled)	Vitamin D3 supplementation	Stabilization of symptoms severity (CT or TT genotypes)	Suzuki et al., 2013
		51	Experimental (pilot randomized, double-blind, placebo-controlled)	Vitamin D3 supplementation	↑ Balance (52–66 y.o)	Hiller et al., 2018
	Alzheimer's disease	43	Experimental (pre-post pilot, multivariate analyses)	Memantine + Vitamin D3	↑ Cognitive performance	Annweiler et al., 2012
	Multiple sclerosis	348	Experimental (phase II, multicenter, randomized, double-blind, placebo-controlled)	Vitamin D3 supplementation	Anti-inflammatory phenotype	Smolders et al., 2010
	Diabetic neuropathy	112	Experimental (non-randomized, double-blind, placebo-controlled)	Vitamin D3 supplementation	↓ Hyperesthesia and burning sensation	Shehab et al., 2015

y.o., years old.

signaling are well known to regulate the progression of spinal-cord progenitors and promote neurogenesis, particularly spinal motor-neuron development, the role of vitamin D in motor-neuron cell differentiation needs to be investigated. Further studies are necessary to clearly elucidate the role of vitamin D in neuronal cell differentiation through this pathway (Appel and Eisen, 2003; Andersson et al., 2013).

The Klotho Pathway

Several studies have reported a complex interaction between calcitriol activity and the Klotho gene. The Klotho gene was discovered in 1997 when mice in which this gene was silenced developed pre-mature aging syndrome (Kuro-o et al., 1997). It is highly expressed in the brain and, to a lesser extent, in other organs (Kuro-o et al., 1997). The choroid plexus is a site of abundant Klotho expression. It is well known that several factors, including phosphate and vitamin D, can regulate the production of Klotho, as well as fibroblast growth factor 23 (FGF23). Kalueff and Tuohimaa (2007) suggested that Klotho expression is upregulated by calcitriol in a murine model. FGF23 was identified as a phosphaturic hormone which is produced in the bone and controls mineral homeostasis by the regulation of calcitriol (White et al., 2000). FGF23 is known to suppress vitamin D hormone production in the kidney by downregulating renal 1α hydroxylase expression, thereby suppressing the production of calcitriol (Erben, 2016). However, little is known about the functional role of Klotho and FGF23 in the central nervous system. Although Anour et al. (2012) reported that Klotho/VDR complex mutant mice do not show obvious behavioral abnormalities, mice with a non-functioning vitamin D receptor fully restored the premature aging phenotype in Klotho deficient mice. These mice produce excessive amounts of calcitriol due to the lack of the suppressive effect of FGF23 on 1α hydroxylase expression. Thus, the premature aging phenotype in Klotho deficient mice could be caused by intoxication with the vitamin D hormone, leading to severe hypercalcemia and hyperphosphatemia and subsequent organ damage (Erben, 2016). Anamizu et al. (2005) reported that Klotho insufficiency causes atrophy and dysfunction of spinal large anterior horn cells in a mouse model deficient for Klotho, suggesting its putative role in neuronal-cell differentiation, potentially promoted by vitamin D.

Progesterone

Marini et al. (2010) reported that vitamin D delays cell proliferation and induces cell differentiation, with modification of soma lengthening and the formation of axons and dendrites in a study using embryonic hippocampal cells. Various observations have also shown that progesterone treatment may be beneficial in several brain-injury models (Sayeed and Stein, 2009). Although progesterone treatment of animals submitted to traumatic brain injury was shown ineffective, treatment with this steroid was effective if calcitriol was simultaneously given (Cekic et al., 2009). In addition, results show that progesterone combined with vitamin D promotes better neuroprotection against excitotoxicity than progesterone alone in an E18 rat primary cortical neurons pretreated with various concentrations of progesterone and vitamin D separately or in combination for 24 h (Atif et al., 2009). Moreover, given the role of progesterone in myelin formation in the peripheral nervous system, it could be informative to further study whether calcitriol can synergize with progesterone activity in the myelination process in the peripheral nervous system (Zárate et al., 2017). Finally, calcitriol has been shown to increase local estrogen production in glial cells through the upregulation of the aromatase enzyme (Caccamo et al., 2018). Given the role of estrogens on neuroprotection and neuronal DNA repair enzymes in rodents (Zárate et al., 2017), we suggest that calcitriol can exert a neuroprotective effect through the estrogen pathway.

Neuronal Cell Differentiation

Calcitriol could be used to potentiate neuronal-cell differentiation in progenitor cell lines. Indeed, Agholme et al. (2010) reported that *in vitro* pre-treatment of SH-SY5Y cells, human neuroblastoma cells, with retinoic acid, followed by culturing on an extracellular matrix in combination with a cocktail of neurotrophic factors associated with vitamin D3 treatment, generated sustainable cells with an unambiguous resemblance to adult neurons. Preliminary experiments conducted in our lab on neuronal cells with various concentrations of calcitriol suggest that calcitriol can induce motor-neuron differentiation but without any effect on proliferation. Confirmatory studies are under way.

Axonal Homogeneity

As mentioned, vitamin D3 and its metabolites also play a role in neurites integrity. The VDR KO mouse model described by Sakai et al. (2015) underlined the involvement of calcitriol and the VDR in axonal homogeneity, integrity, and maintenance of neuromuscular junctions. Indeed, the analysis of transversal sections of sciatic nerves from VDR-deficient mice showed heterogeneity of the axonal diameters and axonal repartitioning among the nerves (Sakai et al., 2015). In addition, they showed in a rat primary Schwann cells model, that calcitriol upregulates the expression of IGF-1, a myelin basic protein which is a myotrophic and neurotrophic factor. Gao et al. (1999) showed that IGF-I deficient mice exhibit reduced peripheral nerve conduction velocities and smaller axonal diameters. They also demonstrated that IGF-1 plays a key role in the growth and development of the peripheral nervous system and that systemic IGF-1 treatment can enhance nerve function in these adults deficient mice (Gao et al., 1999).

Anti-oxidative Activity

Anti-oxidative stress activity has been reported for calcitriol in the central nervous system (Garcion et al., 1998). Injections of lipopolysaccharide were performed *in vivo* in rat hippocampus to induce the synthesis of induced nitric oxide synthase (iNOS), which is partially involved in oxidative stress in the brain and vasodilation through nitrogen monoxide (NO) generation. This study showed significant inhibition of iNOS synthesis in the group with calcitriol treatment, suggesting a putative role of calcitriol against oxidative stress and vasodilation in the brain. Furthermore, the authors also showed that vitamin D increased the intracellular levels of glutathione, the major

intracellular redox buffer, in primary cultures of newborn-rat astrocytes (Garcion et al., 1999). Although oxidative stress and inflammatory processes appear to promote calcium dysregulation with age, several endogenous steroid hormones, including vitamin D, estrogen, and insulin may counteract, at least partially, these effects (Frazier et al., 2017).

Renin-Angiotensin System and Vitamin D

Several studies have shown an interaction between the renin-angiotensin system (RAS) and calcitriol regulation. Rammos et al. (2008) showed that vitamin D downregulates renin and vitamin D deficiency upregulates the RAS in a murine model. These results have been supported by several studies showing that renin expression and plasma angiotensin II production are elevated in VDR-null mice, leading to hypertension and cardiac hypertrophy, whereas 1,25-$(OH)_2$-vitamin D3 treatment suppresses renin expression (Li et al., 2002; Yang et al., 2018). In addition, 1,25-$(OH)_2$-vitamin D3 administration corrects hypertension induced by activation of the RAS in a model of 1-alpha-hydroxylase-deficient mice (Zhang et al., 2015). These renal abnormalities were also observed in a rat model of diabetes in which calcitriol blocks RAS activation (Deng et al., 2016). These interactions have also been observed in humans. In a large cohort, Tomaschitz et al. (2010) reported that serum 1,25-$(OH)_2$-vitamin D3 concentrations were inversely correlated with plasma renin activity and angiotensin II levels. Calcitriol can also regulate the RAS in organs other than the kidney and perhaps in peripheral nerves, where angiotensin receptors have already been described. Indeed, Bessaguet et al. (2017) in a recent study showed that candesartan, a blocker of AT1 and AT2 receptors, prevents this type of neuropathy by acting on the RAS, in mice exhibiting sensory small fiber injury induced by resiniferatoxin treatment. They concluded that the AT2R may have neuroprotective effects (Bessaguet et al., 2017). Given the previous observation in kidney, the role of vitamin D in this pathway needs to be investigated to clarify its role in the regulation of the RAS, particularly its interaction with oxidative stress, well known to interact with the RAS (Luo et al., 2015). RAS hyperactivity associated with progression to renal damage and the modulation of calcitriol production is found in chronic kidney diseases (Santos et al., 2012).

Relationships between Vitamin D3, both cholecalciferol and calcitriol, and renal function have been extensively studied. First, renal injuries induce a decline in the glomerular filtration rate (eGFR), often associated with a reduction of 1-alpha-hydroxylase enzyme activity in kidney, inducing a decrease of plasma 1,25-$(OH)_2$-vitamin D3 levels. Such low levels in the blood result in several downstream effects, such as secondary hyperparathyroidism and the modification of bone homeostasis, requiring treatment with 1,25-$(OH)_2$-vitamin D3 or one of its analogs in human patients with chronic kidney diseases (Bhan, 2014). As shown by a cross-sectional study integrating results of 5 cohort studies and clinical trials, it seems that low eGFR is also associated with important decrease in Vitamin D3 catabolism (de Boer et al., 2014). Second, Vitamin D deficiency impacts in a different manner the general population and renal transplanted patients. Indeed, as shown by a prospective population-based cohort study, it seems that low calcitriol and low cholecalciferol plasma levels are not associated with decreased eGFR in the general population (Keyzer et al., 2015a). On the contrary, a prospective observational single-center cohort study in stable renal transplanted patients, showed that low 25-OH-vitamin D3 (<12 ng/mL) is associated with a rapid decline in eGFR (Keyzer et al., 2015b). Interestingly, it seems that vitamin D3 might be not "useful" to normal persons but might have an important positive effect in kidney transplanted persons. This might also be the case for people with peripheral neuropathies.

VITAMIN D3 IN NEUROLOGICAL DISORDERS

It is commonly accepted that a large proportion of the population in developed countries exhibit insufficient 25-OH-vitamin D3 concentrations in the blood (Singh and Bonham, 2014). Low levels of 25-OH-vitamin D3 are associated with an increased risk of all-cause mortality (Gröber et al., 2015). Although the major sites of action of calcitriol in calcium homeostasis are the bones, kidneys, intestine, and parathyroid gland (Issa et al., 1998), the nervous system may also be involved, particularly in myelinating areas. Various associations have been reported between vitamin D status and brain diseases, such as epilepsy. 25-OH-vitamin D3 supplementation results in improved seizure control in patients with pharmaco-resistant epilepsy (Holló et al., 2012; Miratashi et al., 2017). In 2013, Zhao et al. reported a correlation between 25-OH-vitamin D3 deficiency and the prevalence of Alzheimer's and Parkinson's diseases (Oudshoorn et al., 2008; Zhao et al., 2013). In addition, a study in the United States reported a higher prevalence of dementia among participants with 25-OH-vitamin D3 deficiency (Buell et al., 2010). Kalueff and Tuohimaa (2007) reported the importance of vitamin D/VDR bioactivation in brain neurons, glial cells, brain macrophages, the spinal cord, and the peripheral nervous system, with putative autocrine or paracrine activity.

Brain and Central Nervous-System Disorders

In the nervous system, vitamin D is involved in calcium trafficking, the redox status, and induction of the synthesis of synaptic structural proteins, neurotrophic factors, and deficient neurotransmitters (Mpandzou et al., 2016). Several results underline the impact of 25-OH-vitamin D3 deficiency as a promoting factor in various neurodegenerative diseases, such as amyotrophic lateral sclerosis and Parkinson's and Alzheimer's diseases (Evatt, 2010; Knekt et al., 2010; Mpandzou et al., 2016). The role of calcium in neurodegenerative disorders has been further studied over the last several years (Frazier et al., 2017). In humans, vitamin D deficiency has long been known to be accompanied by irritability, anxiety, depression, psychoses, and defects in mental development (Kalueff and Tuohimaa, 2007). Calcitriol deficiency is also associated with poor cognitive function in human adults, as well as in children, and could also affect brain development (Wilkins et al., 2006; Lee et al., 2009; Llewellyn et al., 2011). Eyles et al. (2003) demonstrated that rats

born to vitamin D3-deficient mothers had profound alterations of the brain at birth. Changes in brain structure and a reduction in brain content of nerve-growth factor (NGF) and glial cell-derived neurotrophic factor (GDNF) suggest that low maternal vitamin D3 levels affect the developing brain (Eyles et al., 2003). These results were supported by an experimental study in a rat model with a combined prenatal and postnatal vitamin D3-deficiency (Al-harbi et al., 2017). Al-harbi et al. (2017) reported that this deficiency promoted a decrease in the number of synapses in the molecular layer of the hippocampus, associated with a reduction of cortical thickness.

Astrocytes, which are VDR expressing cells, are important immune cells and contribute to inflammation during neurological disorders. Jiao et al. (2017) reported that lipopolysaccharide-stimulated neuroinflammation in astrocytes could enhance the expression of the VDR and Cyp27B1. In contrast, vitamin D suppressed the expression of proinflammatory cytokines, such as tumor necrosis factor-α, interleukin-1β, and TLR4 *in vivo*. These results support a function of reactive astrocytes in stimulating the inflammatory response in neurodegeneration and brain injury and a putative role of vitamin D (Jiao et al., 2017).

Mascarenhas et al. reported an association between severe hypovitaminosis D and persistent, non-specific musculoskeletal pain in humans (Plotnikoff and Quigley, 2003; Mascarenhas and Mobarhan, 2004). Serum vitamin D levels have been inversely correlated with painful manifestations and associated with neuromuscular disorders, which can lead to increased pain sensitivity. Thus, vitamin D3 may also be involved in nociceptive sensitivity (de Oliveira et al., 2017). 1,25-$(OH)_2$-vitamin D3 may also upregulate the expression of neurotrophic factors, such as GDNF in C6 glioma cells (Naveilhan et al., 1996), NT-3, or NT-4 in rat astrocytes (Neveu et al., 1994), TGFβ in neuroblastoma cells (Veenstra et al., 1997), and NGF in the central (Brown et al., 2003; Gezen-Ak et al., 2011) and peripheral nervous systems (Cornet et al., 1998).

Interventional studies of vitamin D3 supplementation for various central nervous system (CNS) diseases have shown promising results. In a randomized double-blind placebo-controlled trial in patients with Parkinson FokI CT and TT genotypes, 12 months of 1,200 UI/day vitamin D3 supplementation resulted in stabilization of the severity (Suzuki et al., 2013). Another randomized double-blind controlled study that assessed 4 months of vitamin D3 supplementation (10.000 UI/day) also showed improvements in balance only in 52- to 66-year-old patients with Parkinson's disease (Hiller et al., 2018). In a single-center trial in patients with Alzheimer's disease, co-administration of memantine with vitamin D3 (400–1000 UI/day or 100,000–200,000 UI/month) for 6 months resulted in a significant and synergistic effect on global cognitive performance (Annweiler et al., 2012). A similar protocol with memantine and vitamin D3 (100,000 UI/month) for 6 months is currently being tested in a single-center double-blind randomized placebo-controlled superiority trial to study its impact on the cognitive performance of patients with Alzheimer's disease and similar disorders (Annweiler et al., 2011). Finally, in an observational retrospective study, 2,000 UI/day vitamin D3 supplementation for 9 months showed no significant adverse events and appeared to have beneficial effects for patients with amyotrophic lateral sclerosis. However, given the low number of patients included (37), further studies are necessary (Karam et al., 2013).

Demyelinating Diseases

In multiple sclerosis, a demyelinating disease of the central nervous system, environmental factors may contribute to the onset of the disease, in addition to a genetic component. Poor exposure to sun light, resulting in reduced production of vitamin D3 in the skin, is thought to be a risk factor for multiple sclerosis. An association of vitamin D levels with multiple sclerosis was determined in a case control study, which showed an inverse relationship between serum 25-OH-vitamin D3 levels and the prevalence of multiple sclerosis (Pandit et al., 2013). Moreover, low 25-OH-vitamin D3 levels at birth could increase the risk of developing multiple sclerosis, as shown in a recent case-control study (Munger et al., 2016). In addition, vitamin D3 supplementation is increasingly recommended to patients with multiple sclerosis (Nystad et al., 2014). Interventional studies have also been conducted on patients with multiple sclerosis to study the impact of vitamin D3 supplementation. In an interventional single group trial, high doses of vitamin D3 (20,000 UI/day) given to patients with relapsing remitting multiple sclerosis for 12 weeks showed a shift from a pro-inflammatory to an anti-inflammatory profile (higher proportion of IL-10^+ $CD4^+$ and fewer TH1/TH2 cells) without hypercalcemia or hypercalciuria (Smolders et al., 2010). A phase I/II dose-escalation trial studying the safety of high-dose vitamin D3 supplementation (40,000 UI/day for 28 weeks, then 10,000 UI/day for 12 weeks and no supplementation for 12 weeks), associated with calcium supplementation (1,200 mg/day for 42 weeks), confirmed no significant adverse events (Burton et al., 2010). Other interventional studies for vitamin D3 supplementation in patients with multiple sclerosis are currently ongoing (Smolders et al., 2011; Dörr et al., 2012; Bhargava et al., 2014).

In a rodent model of experimental autoimmune encephalomyelitis (EAE), animals immunized against central nervous system proteins, such as myelin-basic protein, develop a paralytic disease that mimics multiple sclerosis. High doses of calcitriol have been shown to prolong survival and improve demyelination scores in the central nervous system relative to those of untreated rodents (Issa et al., 1998; Shirazi et al., 2017). Sakai et al. (2015) showed that calcitriol is essential for the synthesis of myelin basic protein, which is a main component of myelin. Indeed, rat primary Schwann cells treated with calcitriol showed increased production of myelin basic protein, suggesting calcitriol involvement in protein remyelination. Moreover, the effect of high doses of calcitriol on remyelination was investigated in C57B1/6 mice, previously treated with cuprizone, which induces oligodendrocyte apoptosis and subsequent myelin disruption. Calcitriol was able to promote the regenerative process by stimulating oligodendrocyte maturation and astrocyte activation, with a significant increase in

myelination (Nystad et al., 2014). Both studies suggest an active role of calcitriol in myelination in the central and peripheral nervous systems.

Peripheral Neuropathies

Calcitriol coordinates the biosynthesis of neurotransmitters in the central nervous system, which regulate cardiovascular autonomic function and may explain its putative role in the development of cardiovascular autonomic neuropathy (Dimova et al., 2017). In addition, Chabas et al. (2008) showed that vitamin D2 (ergocalciferol: a compound produced by yeast with effects similar to those of vitamin D3) has positive effects *in vivo* at a dose of 100 IU/kg/day in a rat model of peripheral nerve trauma. At the end of treatment, they observed a significant increase in axonogenesis and axon diameter, improving the response of sensory neurons (Chabas et al., 2008). In 2013, the same authors showed that vitamin D3 is beneficial at a dose of 500 IU/kg/day in a rat model of peripheral nerve trauma, inducing significant locomotor and electrophysiological recovery. The authors also demonstrated that 25-OH-vitamin D3 increases the number of preserved or newly formed axons in the proximal end, the mean axon diameter in the distal end, and neurite myelination in both the distal and proximal ends (Chabas et al., 2013). In an observational prospective open case-control study with 70 patients undergoing paclitaxel chemotherapy, Grim et al. (2017) reported that estimated vitamin D levels in the group without chemotherapy-induced peripheral neuropathy (CIPN) were 38.2 (24.95, 47.63) nmol/L, whereas it was 25.6 (19.7, 32.55) nmol/L in the group with CIPN. Numerous reports have linked vitamin D deficiency to an increased risk of diabetes mellitus and complications, such as neuropathy (Putz et al., 2013). Indeed, in a prospective clinical cohort study of 69 diabetic patients, Celikbilek et al. (2015) reported, that serum vitamin D levels were significantly lower in patients with diabetic peripheral neuropathy than in those without. These results were supported by an observational study showing that 25-OH-vitamin D3 levels were significantly lower in the neuropathy patient group of a 96-patient cohort with type 1 diabetes (Ozuguz et al., 2016). In addition, in a case-control study, Alamdari et al. (2015) reported that lower levels of circulating 25-OH-vitamin D3 may contribute to the risk of large-fiber neuropathy in type 2 diabetic subjects, even after adjustment for demographic variables, comorbidities, and diabetes treatment. They suggested that each 1 ng/mL increase in the concentration of seric 25-OH-vitamin D3 correlates with a 2.2 and 3.4% decrease in the presence and severity of nerve conduction velocity (NCV) impairment, respectively (Alamdari et al., 2015). Putz et al. (2014) suggested that vitamin D supplementation could have beneficial effects on neuropathic pain and may block the progression of neuronal degeneration. These authors also suggested that vitamin D deficiency could promote diabetic plantar ulcers (Putz et al., 2014). In a prospective placebo-controlled trial that included 112 type 2 diabetic patients with diabetic peripheral neuropathy and vitamin D deficiency, Shehab et al. (2015) showed that short-term oral vitamin D supplementation (50,000 UI/week for 8 weeks) improved hyperesthesia and the burning sensation, assessed by the neuropathy symptom score (NSS). However, this supplementation had no effect on the neuropathy disability score (NDS) nor nerve conduction study (NCS) (Shehab et al., 2015).

Diabetic neuropathy is associated with decreased NGF expression in human diabetic nerves (Anand et al., 1996) and vitamin D3 is also known to induce NGF synthesis in human cell lines (Fukuoka et al., 2001; Shehab et al., 2015). Thus, the observed improvement in diabetic neuropathy may be mediated

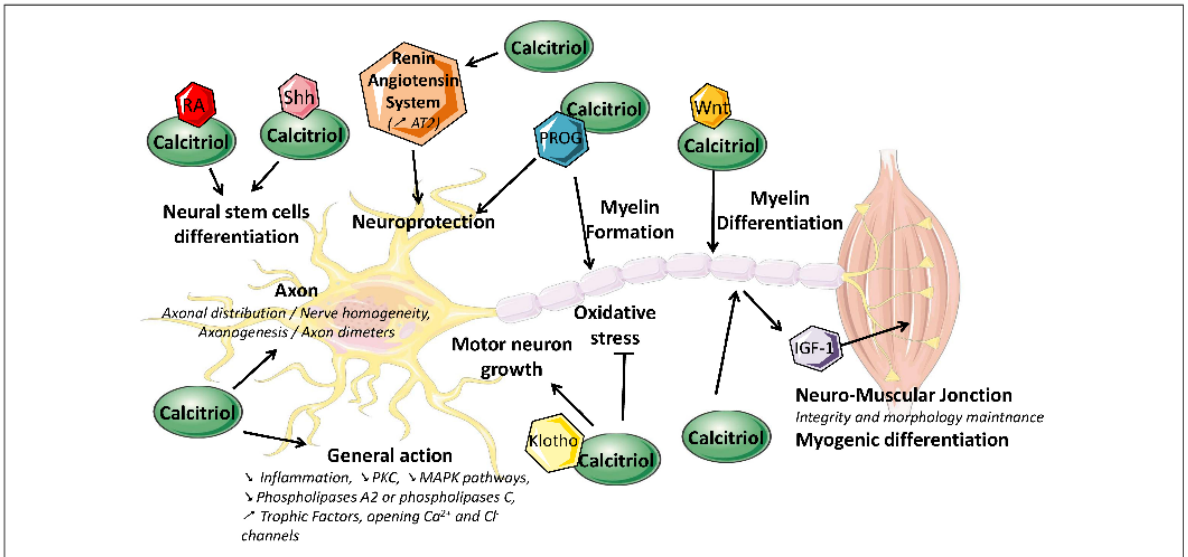

FIGURE 3 | Schematic representation of the putative roles of calcitriol in the peripheral nervous system. IGF-1, insulin-like growth factor-1; MAPK, mitogen-activated protein kinase; PKC, protein kinase C; PROG, progesterone; RA, retinoic acid; Shh, Sonic hedgehog.

through the upregulation of NGF. Recently, in an experimental randomized clinical trial on 81 women suffering from diabetic neuropathy, Nadi et al. (2017) showed that exercise combined with vitamin D supplementation decreases the complications of diabetic neuropathy. In addition, a case-report study with one Type-1 patient suffering from diabetic neuropathy, mentioned an improvement after correction of his vitamin D3 deficiency following supplementation of 50,000 UI/week for 4 weeks (Bell, 2012). On the other hand, an interventional randomized double-blind placebo-controlled trial in non-vitamin D-deficient patients with Type 2 diabetes, showed that vitamin D3 supplementation of 50,000 UI/week for 6 months provided no improvement of diabetic neuropathy (Westra et al., 2016). Placebo-controlled multi-centric studies are required to assess the role of vitamin D3 supplementation on diabetic neuropathies (Valensi et al., 2005). As previously reported, the number of studies that have investigated the role of vitamin D in the treatment of neuropathies is still limited, mostly to diabetic neuropathy.

Charcot-Marie-Tooth Disease

Charcot-Marie-Tooth (CMT) disease is the most common form of hereditary motor and sensory neuropathy. Caused by either axonal or demyelinating alterations. More than 90 mutated genes are involved in the development of this neuropathic disease. The observed phenotype is variable but often consists of a progressive distal motor deficiency, foot deformities, or muscular atrophy (Vallat et al., 2007).

Mutations of the ganglioside-induced differentiation-associated protein 1 (*GDAP1*) gene cause autosomal dominant and autosomal recessive CMT diseases, with more than 40 different pathogenic mutations. Pepaj et al. (2015) used a proteomic approach to show that 1,25-dihydroxyvitamin D3 treatment induces overexpression of GDAP1 in a rat pancreatic beta-1 cell line. Thus, 1,25-vitamin D3 could potentially play a role in CMT, through the up-regulation of the *GDAP1* gene. Further studies are required to assess the impact of 1,25-dihydroxyvitamin D3 supplementation on the expression of the *GDAP1* gene in CMT patients and its clinical impact.

Moreover, another form of CMT disease, type 2A, is caused by mutations in the mitofusin-2 (*MFN2*) gene, which is physiologically involved in the fusion/fission of mitochondria. Preclinical studies conducted on neurons from a CMT2A mouse model showed that an MFN2 agonist could normalize mitochondrial trafficking and mobility along axons (Gezen-Ak et al., 2011). Furthermore, Gong et al. (2015) showed that treatment of human melanocytes with 0.05% H_2O_2 and calcipotriol (which is a structural analog of calcitriol) at doses varying from 20 to 80 nM upregulated the expression of MFN2. Thus, calcitriol could be an promising candidate in further studies on CMT2A disease.

Calcitriol has been reported to exhibit gene-dependent synergistic or antagonistic effects when co-administered with inhibitors of histone deacetylase (HDAC) (Malinen et al., 2008; Seuter et al., 2013). Interestingly, HDAC6 inhibition has been reported to restore nerve conduction and motor capacity in glycyl-tRNA synthetase (GARS)-mutated murine neuroblastoma cells, a model for CMT Type 2D (Benoy et al., 2018). Thus, if HDAC inhibitors succeed in showing a therapeutic effect in CMT2D, it would be interesting to further study if calcitriol could potentialize therapeutic effects of HDAC inhibitors in CMT2D diseases. To our knowledge, no study has been conducted yet on the impact of vitamin D3 on the progression of CMT disease. This could represent a new field of therapeutic research in CMT disease.

A New Field of Research

Several questions should be raised to clearly assess the role of calcitriol in the peripheral nervous system. Does calcitriol have an impact on neuronal differentiation (and on axonal trophicity), or does calcitriol act more on Schwann cells myelination, or does calcitriol improve cellular communications between axons and Schwann cells thus improving myelination and nerve conduction velocities? This would imply a cellular, an animal and a human level of experiments.

For instance, at cellular level, neuronal differentiation comparing standard to calcitriol-supplemented cell cultures, may help assess if calcitriol induces or speeds-up neuronal differentiation. This could be performed on cell lines such as SH-SY5Y or on induced pluripotent stem cells (iPSc). Several techniques such as qRT-PCR, Western-blot and immunostaining on PGP9.5, islet, tuj1, HB9 expression, which are markers of neuronal differentiation, could assess an additive or a synergistic effect of vitamin D3 and other fat-soluble vitamins. Moreover, as micro-glial cells can synthetize calcitriol, 3D-cell culture including neuronal and glial cells could be relevant to study micro-environmental regulation of calcitriol synthesis.

At animal level, experiments could also be led on mice or rats with sciatic nerves injuries, physically or chemically induced, to determine if calcitriol has a positive impact on recovery. Numerous animal models exist for both acquired (toxic, diabetic, crush) and hereditary neuropathies (Sereda et al., 1996). Calcitriol would be administered orally or by a local long term delivery mean as done for curcumin for instance (Caillaud et al., 2018). Effects of calcitriol supplementation could be assessed by functional (skillful walking, grip strength, rotarod), histological (g-ratio) and electrophysiological (NCVs) tests. In these conditions, it would be important to check if calcitriol plays a role in the remyelination process and has synergistic effects with another factor as previously reported.

At a human level, as vitamin D3 is frequently given to elders, a prospective interventional study should be planned to monitor the incidence of peripheral neuropathies. Alternatively, as patients receiving a chemotherapy frequently develop neuropathies, a prospective interventional study could be envisioned to prevent those to occur, provided positive results to investigate in animal models.

CONCLUSION

Basic science data suggest that current knowledge of calcitriol may still be incomplete and that it may play a more important role in peripheral nerve trophicity than previously thought (**Figure 3**).

Several preliminary clinical studies tend to show that calcitriol, indeed, plays such a role. Future molecular and cellular studies may show calcitriol supplementation to be a beneficial means to positively influence peripheral nervous system homeostasis by regulating several processes, such as myelin genesis and axonal maintenance.

AUTHOR CONTRIBUTIONS

PAF and FP wrote a large proportion of the manuscript and searched for references. FM wrote some parts of the manuscript and inserted the references. ASL and CD proofread the sections concerning gene regulation and pharmacology. LM, as a neurologist, proofread the clinical part of the manuscript. FF wrote some parts of the manuscript and modified the general structure to make it more readable. FS initiated the work on vitamin D and proofread the manuscript several times.

FUNDING

This work was supported by the University of Limoges, Limoges, France and CHU de Limoges, France.

REFERENCES

Agholme, L., Lindström, T., Kgedal, K., Marcusson, J., and Hallbeck, M. (2010). An in vitro model for neuroscience: differentiation of SH-SY5Y cells into cells with morphological and biochemical characteristics of mature neurons. *J. Alzheimers Dis.* 20, 1069–1082. doi: 10.3233/JAD-2010-091363

Alamdari, A., Mozafari, R., Tafakhori, A., Faghihi-Kashani, S., Hafezi-Nejad, N., Sheikhbahaei, S., et al. (2015). An inverse association between serum vitamin D levels with the presence and severity of impaired nerve conduction velocity and large fiber peripheral neuropathy in diabetic subjects. *Neurol. Sci.* 36, 1121–1126. doi: 10.1007/s10072-015-2207-0

Al-harbi, A.-N., Khan, K. M., and Rahman, A. (2017). Developmental vitamin D deficiency affects spatial learning in wistar rats. *J. Nutr.* 147, 1795–1805. doi: 10.3945/jn.117.249953

Anamizu, Y., Kawaguchi, H., Seichi, A., Yamaguchi, S., Kawakami, E., Kanda, N., et al. (2005). Klotho insufficiency causes decrease of ribosomal RNA gene transcription activity, cytoplasmic RNA and rough ER in the spinal anterior horn cells. *Acta Neuropathol.* 109, 457–466. doi: 10.1007/s00401-004-0971-7

Anand, P., Terenghi, G., Warner, G., Kopelman, P., Williams-Chestnut, R. E., and Sinicropi, D. V. (1996). The role of endogenous nerve growth factor in human diabetic neuropathy. *Nat. Med.* 2, 703–707. doi: 10.1038/nm0696-703

Andersson, E. R., Salto, C., Villaescusa, J. C., Cajanek, L., Yang, S., Bryjova, L., et al. (2013). Wnt5a cooperates with canonical wnts to generate midbrain dopaminergic neurons in vivo and in stem cells. *Proc. Natl. Acad. Sci. U.S.A.* 110, E602–E610. doi: 10.1073/pnas.1208524110

Annweiler, C., Fantino, B., Parot-Schinkel, E., Thiery, S., Gautier, J., and Beauchet, O. (2011). Alzheimer's disease - input of vitamin D with memantine assay (AD-IDEA Trial): study protocol for a randomized controlled trial. *Trials* 12:230. doi: 10.1186/1745-6215-12-230

Annweiler, C., Herrmann, F. R., Fantino, B., Brugg, B., and Beauchet, O. (2012). Effectiveness of the combination of memantine plus vitamin D on cognition in patients with alzheimer disease: a pre-post pilot study. *Cogn. Behav. Neurol.* 25, 121–127. doi: 10.1097/WNN.0b013e31826df647

Anour, R., Andrukhova, O., Ritter, E., Zeitz, U., and Erben, R. G. (2012). Klotho lacks a vitamin D independent physiological role in glucose homeostasis, bone turnover, and steady-state PTH secretion in vivo. *PLoS One* 7:e31376. doi: 10.1371/journal.pone.0031376

Appel, B., and Eisen, J. S. (2003). Retinoids run rampant: multiple roles during spinal cord and motor neuron development. *Neuron* 40, 461–464. doi: 10.1016/S0896-6273(03)00688-3

Atif, F., Sayeed, I., Ishrat, T., and Stein, D. G. (2009). Progesterone with vitamin D affords better neuroprotection against excitotoxicity in cultured cortical neurons than progesterone alone. *Mol. Med.* 15, 328–336. doi: 10.2119/molmed.2009.00016

Baeke, F., Takiishi, T., Korf, H., Gysemans, C., and Mathieu, C. (2010). Vitamin D: modulator of the immune system. *Curr. Opin. Pharmacol.* 10, 482–496. doi: 10.1016/j.coph.2010.04.001

Bell, D. S. H. (2012). Reversal of the symptoms of diabetic neuropathy through correction of vitamin D deficiency in a type 1 diabetic patient. *Case Rep. Endocrinol.* 2012:165056. doi: 10.1155/2012/165056

Benoy, V., Van Helleputte, L., Prior, R., D'Ydewalle, C., Haeck, W., Geens, N., et al. (2018). HDAC6 is a therapeutic target in mutant GARS-induced charcot-marie-tooth disease. *Brain* 141, 673–687. doi: 10.1093/brain/awx375

Bessaguet, F., Danigo, A., Magy, L., Sturtz, F., Desmoulière, A., and Demiot, C. (2017). Candesartan prevents resiniferatoxin-induced sensory small-fiber neuropathy in mice by promoting angiotensin II-mediated AT2 receptor stimulation. *Neuropharmacology* 126, 142–150. doi: 10.1016/J.NEUROPHARM.2017.08.039

Bhan, I. (2014). Breaking down the Vitamin D-GFR relationship. *Am. J. Kidney Dis.* 64, 168–170. doi: 10.1053/j.ajkd.2014.05.004

Bhargava, P., Cassard, S., Steele, S. U., Azevedo, C., Pelletier, D., Sugar, E. A., et al. (2014). The vitamin D to ameliorate multiple sclerosis (VIDAMS) trial: study design for a multicenter, randomized, double-blind controlled trial of vitamin D in multiple sclerosis. *Contemp. Clin. Trials* 39, 288–293. doi: 10.1016/j.cct.2014.10.004

Blutt, S. E., Allegretto, E. A., Pike, J. W., and Weigel, N. L. (1997). 1,25-Dihydroxyvitamin D3 and 9-Cis-retinoic acid act synergistically to inhibit the growth of LNCaP prostate cells and cause accumulation of cells in G1. *Endocrinology* 138, 1491–1497. doi: 10.1210/endo.138.4.5063

Brown, J., Bianco, J. I., McGrath, J. J., and Eyles, D. W. (2003). 1,25-Dihydroxyvitamin D3 induces nerve growth factor, promotes neurite outgrowth and inhibits mitosis in embryonic rat hippocampal neurons. *Neurosci. Lett.* 343, 139–143. doi: 10.1016/S0304-3940(03)00303-3

Buell, J. S., Dawson-Hughes, B., Scott, T. M., Weiner, D. E., Dallal, G. E., Qui, W. Q., et al. (2010). 25-Hydroxyvitamin D, dementia, and cerebrovascular pathology in elders receiving home services. *Neurology* 74, 18–26. doi: 10.1212/WNL.0b013e3181beecb7

Buitrago, C., Gonzalez Pardo, V., and Boland, R. (2013). Role of VDR in 1α,25-dihydroxyvitamin D3-dependent non-genomic activation of MAPKs, Src and Akt in skeletal muscle cells. *J. Steroid Biochem. Mol. Biol.* 136, 125–130. doi: 10.1016/j.jsbmb.2013.02.013

Burton, J. M., Kimball, S., Vieth, R., Bar-Or, A., Dosch, H.-M., Cheung, R., et al. (2010). A phase I/II dose-escalation trial of vitamin D3 and calcium in multiple sclerosis. *Neurology* 74, 1852–1859. doi: 10.1212/WNL.0b013e3181e1cec2

Caccamo, D., Ricca, S., Currò, M., and Ientile, R. (2018). Health risks of hypovitaminosis D: a review of new molecular insights. *Int. J. Mol. Sci.* 19:E892. doi: 10.3390/ijms19030892

Caillaud, M., Chantemargue, B., Richard, L., Vignaud, L., Frédéric, F., Faye, P.-A., et al. (2018). Local low dose curcumin treatment improves functional recovery and remyelination in a rat model of sciatic nerve crush through inhibition of oxidative stress. *Neuropharmacology* 139, 98–116. doi: 10.1016/j.neuropharm.2018.07.001

Carlberg, C., Bendik, I., Wyss, A., Meier, E., Sturzenbecker, L. J., Grippo, J. F., et al. (1993). Two nuclear signalling pathways for vitamin D. *Nature* 361, 657–660. doi: 10.1038/361657a0

Cekic, M., Sayeed, I., and Stein, G. D. (2009). Hormone may be more effective than monotherapy for nervous. *Front. Neuroendocrinol.* 30, 158–172. doi: 10.1016/j.yfrne.2009.04.002

Celikbilek, A., Yesim Gocmen, A., Tanik, N., Borekci, E., Adam, M., Celikbilek, M., et al. (2015). Decreased serum vitamin D levels are associated with diabetic peripheral neuropathy in a rural area of turkey. *Acta Neurol. Belg.* 115, 47–52. doi: 10.1007/s13760-014-0304-0

Chabas, D. S., Marqueste, T., Garcia, S., Lavaut, M.-N., Nguyen, C., Legre, R., et al. (2013). Cholecalciferol (Vitamin D3) improves myelination and recovery after nerve injury. *PLoS One* 8:e65034. doi: 10.1371/journal.pone.0065034

Chabas, O. A., Rao, G., Garcia, S., Lavaut, M.-N., Risso, J.-J., Legre, R., et al. (2008). Vitamin D2 potentiates axon regeneration. *J. Neurotrauma* 25, 1247–1256. doi: 10.1089/neu.2008.0593

Choudhry, Z., Rikani, A. A., Choudhry, A. M., Tariq, S., Zakaria, F., Asghar, M. W., et al. (2014). Sonic hedgehog signalling pathway: a complex network. *Ann. Neurosci.* 21, 28–31. doi: 10.5214/ans.0972.7531.210109

Christakos, S., Dhawan, P., Verstuyf, A., Verlinden, L., and Carmeliet, G. (2016). Vitamin D: metabolism, molecular mechanism of action, and pleiotropic effects. *Physiol. Rev.* 96, 365–408. doi: 10.1152/physrev.00014.2015

Cornet, A., Baudet, C., Neveu, I., Baron-Van Evercooren, A., Brachet, P., and Naveilhan, P. (1998). 1,25-Dihydroxyvitamin D3 regulates the expression of VDR and NGF gene in schwann cells in vitro. *J. Neurosci. Res.* 53, 742–746. doi: 10.1002/(sici)1097-4547(19980915)53%3A6%3C742%3A%3Aaid-jnr11%3E3.0.co%3B2-%23

de Boer, I., Sachs, M. C., Chonchol, M., Himmelfarb, J., Hoofnagle, N. A., Ix, J. H., et al. (2014). Estimated GFR and circulating 24,25-dihydroxyvitamin D3 concentration: a participant-level analysis of 5 cohort studies and clinical trials. *Am. J. Kidney Dis.* 64, 187–197. doi: 10.1053/j.ajkd.2014.02.015

de la Fuente, A. G., Errea, O., van Wijngaarden, P., Gonzalez, G. A., Kerninon, C., Jarjour, A. A., et al. (2015). Vitamin D receptor–retinoid X receptor heterodimer signaling regulates oligodendrocyte progenitor cell differentiation. *J. Cell Biol.* 211, 975–985. doi: 10.1083/jcb.201505119

de Oliveira, D. L., Hirotsu, C., Tufik, S., and Levy Andersen, M. (2017). The interfaces between vitamin D, sleep and pain. *J. Endocrinol.* 234, R23–R36. doi: 10.1530/JOE-16-0514

Deng, X., Cheng, J., and Shen, M. (2016). Vitamin D improves diabetic nephropathy in rats by inhibiting renin and relieving oxidative stress. *J. Endocrinol. Investig.* 39, 657–666. doi: 10.1007/s40618-015-0414-4

Dimova, R., Tankova, T., and Chakarova, N. (2017). Vitamin D in the spectrum of prediabetes and cardiovascular autonomic dysfunction. *J. Nutr.* 147, 1607–1615. doi: 10.3945/jn.117.250209

Dormoy, V., Béraud, C., Lindner, V., Coquard, C., Barthelmebs, M., Brasse, D., et al. (2012). Vitamin D3 triggers antitumor activity through targeting hedgehog signaling in human renal cell carcinoma. *Carcinogenesis* 33, 2084–2093. doi: 10.1093/carcin/bgs255

Dörr, J., Ohlraun, S., Skarabis, H., and Paul, F. (2012). Efficacy of vitamin D supplementation in multiple sclerosis (EVIDIMS Trial): study protocol for a randomized controlled trial. *Trials* 13:15. doi: 10.1186/1745-6215-13-15

Dostal, L. A., Toverud, S. U., and Peach, R. (1984). Renal calcification in suckling rats after high doses of calcitriol (1,25-Dihydroxycholecalciferol). *Arch. Pathol. Lab. Med.* 108, 410–415.

El-Atifi, M., Dreyfus, M., Berger, F., and Wion, D. (2015). Expression of CYP2R1 and VDR in human brain pericytes: the neurovascular vitamin D autocrine/paracrine model. *Neuroreport* 26, 245–248. doi: 10.1097/WNR.0000000000000328

Emmanuel, G., Wion-Barbot, N., Montero-Menei, C. N., Berger, F., and Wion, F. (2002). New clues about vitamin D functions in the nervous system. *Trends Endocrinol. Metab.* 13, 100–105. doi: 10.1016/S1043-2760(01)00547-1

Erben, R. G. (2016). Update on FGF23 and klotho signaling. *Mol. Cell. Endocrinol.* 432, 56–65. doi: 10.1016/j.mce.2016.05.008

Evatt, M. L. (2010). Beyond vitamin status. *Arch. Neurol.* 67, 795–797. doi: 10.1001/archneurol.2010.123

Eyles, D., Brown, J., Mackay-Sim, A., McGrath, J., and Feron, F. (2003). Vitamin D3 and brain development. *Neuroscience* 118, 641–653. doi: 10.1016/S0306-4522(03)00040-X

Eyles, D. W., Smith, S., Kinobe, R., Hewison, M., and McGrath, J. J. (2005). Distribution of the vitamin D receptor and 1 alpha-hydroxylase in human brain. *J. Chem. Neuroanat.* 29, 21–30. doi: 10.1016/j.jchemneu.2004.08.006

Finnes, T. E., Lofthus, C. M., Meyer, H. E., Søgaard, A. J., Tell, G. S., Apalset, E. M., et al. (2016). A combination of low serum concentrations of vitamins K1 and D is associated with increased risk of hip fractures in elderly norwegians: a NOREPOS study. *Osteoporos. Int.* 27, 1645–1652. doi: 10.1007/s00198-015-3435-0

Frazier, H. N., Maimaiti, S., Anderson, K. L., Brewer, L. D., Gant, J. C., Porter, N. M., et al. (2017). Calcium's role as nuanced modulator of cellular physiology in the brain. *Biochem. Biophys. Res. Commun.* 483, 981–987. doi: 10.1016/j.bbrc.2016.08.105

Fukuoka, M., Sakurai, K., Ohta, T., Kiyoki, M., and Katayama, I. (2001). Tacalcitol, an active vitamin D3, induces nerve growth factor production in human epidermal keratinocytes. *Skin Pharmacol. Appl. Skin Physiol.* 14, 226–233. doi: 10.1159/000056351

Fusaro, M., Giannini, S., Gallieni, M., Noale, M., Tripepi, G., Rossini, M., et al. (2016). Calcimimetic and vitamin D analog use in hemodialyzed patients is associated with increased levels of vitamin K dependent proteins. *Endocrine* 51, 333–341. doi: 10.1007/s12020-015-0673-z

Gao, W. Q., Shinsky, N., Ingle, G., Beck, K., Elias, K. A., and Powell-Braxton, L. (1999). IGF-I deficient mice show reduced peripheral nerve conduction velocities and decreased axonal diameters and respond to exogenous IGF-I treatment. *J. Neurobiol.* 39, 142–152. doi: 10.1002/(sici)1097-4695(199904)39%3A1%3C142%3A%3Aaid-neu11%3E3.0.co%3B2-h

Garabédian, M. (2000). La vitamine D: les nouvelles fonctions d'une ancienne vitamine. *Oleagineux Corps Gras Lipides* 7, 271–275. doi: 10.1051/ocl.2000.0271

Garcion, E., Sindji, L., Leblondel, G., Brachet, P., and Darcy, F. (1999). 1,25-Dihydroxyvitamin D3 regulates the synthesis of gamma-glutamyl transpeptidase and glutathione levels in rat primary astrocytes. *J. Neurochem.* 73, 859–866. doi: 10.1046/j.1471-4159.1999.0730859.x

Garcion, E., Sindji, L., Montero-Menei, C., Andre, C., Brachet, P., and Darcy, F. (1998). Expression of inducible nitric oxide synthase during rat brain inflammation: regulation by 1,25-dihydroxyvitamin D3. *Glia* 22, 282–294. doi: 10.1002/(sici)1098-1136(199803)22%3A3%3C282%3A%3Aaid-glia7%3E3.0.co%3B2-7

Gezen-Ak, D., Dursun, E., and Yilmazer, S. (2011). The effects of vitamin D receptor silencing on the expression of LVSCC-A1C and LVSCC-A1D and the release of NGF in cortical neurons. *PLoS One* 6:e17553. doi: 10.1371/journal.pone.0017553

Ginde, A. A., Liu, M. C., and Camargo, C. A. (2009). Demographic differences and trends of vitamin D insufficiency in the US population, 1988-2004. *Arch. Intern. Med.* 169, 626–632. doi: 10.1001/archinternmed.2008.604

Gong, Q., Li, X., Sun, J., Ding, G., Zhou, M., Zhao, W., et al. (2015). The effects of calcipotriol on the dendritic morphology of human melanocytes under oxidative stress and a possible mechanism: is it a mitochondrial protector? *J. Dermatol. Sci.* 77, 117–124. doi: 10.1016/j.jdermsci.2014.12.006

Greenstein, R. J., Su, L., and Brown, S. T. (2012). Vitamins A & D inhibit the growth of mycobacteria in radiometric culture. *PLoS One* 7:e29631. doi: 10.1371/journal.pone.0029631

Grim, J., Ticha, A., Hyspler, R., Valis, M., and Zadak, Z. (2017). Selected risk nutritional factors for chemotherapy-induced polyneuropathy. *Nutrients* 9:535. doi: 10.3390/nu9060535

Gröber, U., Reichrath, J., and Holick, M. F. (2015). Live longer with vitamin D? *Nutrients* 7, 1871–1880. doi: 10.3390/nu7031871

Guilland, J.-C. (2011). Les interactions entre les vitamines A, D, E et K: synergie et/ou compétition. *Oléagineux Corps Gras Lipides* 18, 59–67. doi: 10.1051/ocl.2011.0376

Hii, C. S., and Ferrante, A. (2016). The Non-Genomic Actions of Vitamin D. *Nutrients* 8:135. doi: 10.3390/nu8030135

Hiller, A. L., Murchison, C. F., Lobb, M. B., O'Connor, S., O'Connor, M., and Quinn, J. F. (2018). A randomized, controlled pilot study of the effects of vitamin D supplementation on balance in Parkinson's disease: does age matter? *PLoS One* 13:e0203637. doi: 10.1371/journal.pone.0203637

Hlaing, S. M., Garcia, L. A., Contreras, J. R., Norris, K. C., Ferrini, M. G., and Artaza, J. N. (2014). 1,25-Vitamin D3 promotes cardiac differentiation through modulation of the WNT signaling pathway. *J. Mol. Endocrinol.* 53, 303–317. doi: 10.1530/JME-14-0168

Holick, M. F. (2006). High prevalence of vitamin D inadequacy and implications for health. *Mayo Clin. Proc.* 81, 353–373. doi: 10.4065/81.3.353

Holló, A., Clemens, Z., Kamondi, A., Lakatos, P., and Szucs, A. (2012). Correction of vitamin D deficiency improves seizure control in epilepsy: a pilot study. *Epilepsy Behav.* 24, 131–133. doi: 10.1016/j.yebeh.2012.03.011

Issa, L. L., Leong, G. M., and Eisman, J. A. (1998). Molecular mechanism of vitamin D receptor action. *Inflamm. Res.* 47, 451–475. doi: 10.1007/s000110050360

Je, S. H., Joo, N. S., Choi, B. H., Kim, K. M., Kim, B. T., Park, S. B., et al. (2011). Vitamin K supplement along with vitamin D and calcium reduced serum

concentration of undercarboxylated osteocalcin while increasing bone mineral density in Korean postmenopausal women over sixty-years-old. *J. Korean Med. Sci.* 26, 1093–1098. doi: 10.3346/jkms.2011.26.8.1093

Jiao, K. P., Li, S. M., Lv, W. Y., Jv, M. L., and He, H. Y. (2017). Vitamin D3 repressed astrocyte activation following lipopolysaccharide stimulation in vitro and in neonatal rats. *Neuroreport* 28, 492–497. doi: 10.1097/WNR.0000000000000782

Kalueff, A.-V., and Tuohimaa, P. (2007). Neurosteroid hormone vitamin D and its utility in clinical nutrition. *Curr. Opin. Clin. Nutr. Metab. Care* 10, 12–19. doi: 10.1097/MCO.0b013e328010ca18

Kane, K. F., Langman, M. J., and Williams, G. R. (1996). Antiproliferative responses to two human colon cancer cell lines to vitamin D3 are differently modified by 9-cis-retinoic acid. *Cancer Res.* 56, 623–632.

Karam, C., Barrett, M. J., Imperato, T., MacGowan, D. J., and Scelsa, S. (2013). Vitamin D deficiency and its supplementation in patients with amyotrophic lateral sclerosis. *J. Clin. Neurosci.* 20, 1550–1553. doi: 10.1016/j.jocn.2013.01.011

Kerner, S. A., Scott, R. A., and Pike, J. W. (1989). Sequence elements in the human osteocalcin gene confer basal activation and inducible response to hormonal vitamin D3. *Proc. Natl. Acad. Sci. U.S.A.* 86, 4455–4459. doi: 10.1073/pnas.86.12.4455

Keyzer, C. A., Lambers-Heerspink, H. J., Joosten, M. M., Deetman, P. E., Gansevoort, R. T., Navis, G., et al. (2015a). Plasma vitamin D level and change in albuminuria and EGFR according to sodium intake. *Clin. J. Am. Soc. Nephrol.* 10, 2119–2127. doi: 10.2215/CJN.03830415

Keyzer, C. A., Riphagen, I. J., Joosten, M. M., Navis, G., Muller Kobold, A. C., Kema, I. P., et al. (2015b). Associations of 25(OH) and 1,25(OH)2 Vitamin D with long-term outcomes in stable renal transplant recipients. *J. Clin. Endocrinol. Metab.* 100, 81–89. doi: 10.1210/jc.2014-3012

Knekt, P., Kilkkinen, A., Rissanen, H., Marniemi, J., Sääksjärvi, K., and Heliövaara, M. (2010). Serum vitamin D and the risk of Parkinson disease. *Arch. Neurol.* 67, 808–811. doi: 10.1001/archneurol.2010.120

Kumar, R. (1986). The metabolism and mechanism of action of 1,25-dihydroxyvitamin D3. *Kidney Int.* 30, 793–803. doi: 10.1038/ki.1986.258

Kurnatowska, I., Grzelak, P., Masajtis-Zagajewska, A., Kaczmarska, M., Stefańczyk, L., Vermeer, C., et al. (2015). Effect of vitamin K2 on progression of atherosclerosis and vascular calcification in nondialyzed patients with chronic kidney disease stages 3-5. *Pol. Arch. Med. Wewn.* 125, 631–640. doi: 10.20452/pamw.3041

Kuro-o, M., Nabeshima, Y. I., Matsumura, Y., Aizawa, H., Kawaguchi, H., Suga, T., et al. (1997). Mutation of the mouse *Klotho* gene leads to a syndrome resembling ageing. *Nature* 390, 45–51. doi: 10.1038/36285

Lee, D. M., Tajar, A., Ulubaev, A., Pendleton, N., O'Neill, W. T., O'Connor, B. D., et al. (2009). Association between 25-Hydroxyvitamin D levels and cognitive performance in middle-aged and older European men. *J. Neurol. Neurosurg. Psychiatry* 80, 722–729. doi: 10.1136/jnnp.2008.165720

Letavernier, E., and Daudon, M. (2018). Vitamin D, hypercalciuria and kidney stones. *Nutrients* 10:E366. doi: 10.3390/nu10030366

Li, Y. C., Kong, J., Wei, M., Chen, Z.-F., Liu, S. Q., and Cao, L.-P. (2002). 1,25-Dihydroxyvitamin D(3) is a negative endocrine regulator of the renin-angiotensin system. *J. Clin. Investig.* 110, 229–238. doi: 10.1172/JCI15219

Lim, Y. Y., Kim, S. Y., Kim, H. M., Li, K. S., Kim, M. N., Park, K. C., et al. (2014). Potential relationship between the canonical wnt signalling pathway and expression of the vitamin D receptor in alopecia. *Clin. Exp. Dermatol.* 39, 368–375. doi: 10.1111/ced.12241

Llewellyn, D. J., Lang, I. A., Langa, K. M., Muniz-Terrera, G., Phillips, C. L., Cherubini, A., et al. (2011). Vitamin D and risk of cognitive decline in elderly persons. *Obstet. Gynecol. Surv.* 66, 354–355. doi: 10.1097/OGX.0b013e31822c1957

Luo, H., Wang, X., Chen, C., Wang, J., Zou, X., Li, C., et al. (2015). Oxidative stress causes imbalance of renal renin angiotensin system (RAS) components and hypertension in obese zucker rats. *J. Am. Heart Assoc.* 4:e001559. doi: 10.1161/JAHA.114.001559

Maiese, K. (2015). Novel applications of trophic factors, wnt and wisp for neuronal repair and regeneration in metabolic disease. *Neural Regen. Res.* 10, 518–528. doi: 10.4103/1673-5374.155427

Malinen, M., Saramäki, A., Ropponen, A., Degenhardt, T., Väisänen, S., and Carlberg, C. (2008). Distinct HDACs regulate the transcriptional response of human cyclin-dependent kinase inhibitor genes to trichostatin A and 1α,25-dihydroxyvitamin D3. *Nucleic Acids Res.* 36, 121–132. doi: 10.1093/nar/gkm913

Marini, F., Bartoccini, E., Cascianelli, G., Voccoli, V., Gioia Baviglia, M., Viola Magni, M., et al. (2010). Effect of 1alpha, 25-dihydroxyvitamin D3 in embryonic hippocampal cells. *Hippocampus* 20, 696–705. doi: 10.1002/hipo.20670

Mascarenhas, R., and Mobarhan, S. (2004). Hypovitaminosis D-induced pain. *Nutr. Rev.* 62, 354–359. doi: 10.1111/j.1753-4887.2004.tb00061.x

Matsunaga, S., Ito, H., and Sakou, T. (1999). The effect of vitamin K and D supplementation on ovariectomy-induced bone loss. *Calcif. Tissue Int.* 65, 285–289. doi: 10.1007/s002239900700

Mayer, O., Seidlerová, J., Wohlfahrt, P., Filipovský, J., Cífková, R., Černá, V., et al. (2017). Synergistic effect of low K and D vitamin status on arterial stiffness in a general population. *J. Nutr. Biochem.* 46, 83–89. doi: 10.1016/j.jnutbio.2017.04.010

Meems, L. M., van der Harst, P., van Gilst, W. H., and de Boer, R. A. (2011). Vitamin D biology in heart failure: molecular mechanisms and systematic review. *Curr. Drug Targets* 12, 29–41. doi: 10.2174/138945011793591554

Meems, L. M. G., Brouwers, F. P., Joosten, M. M., Lambers Heerspink, H. J., de Zeeuw, D., Bakker, S. J., et al. (2016). Plasma calcidiol, calcitriol, and parathyroid hormone and risk of new onset heart failure in a population-based cohort study. *ESC Heart Fail.* 3, 189–197. doi: 10.1002/ehf2.12089

Melcangi, R. C., and Panzica, G. (2009). Neuroactive steroids: an update of their roles in central and peripheral nervous system. *Psychoneuroendocrinology* 34(Suppl. 1), S1–S8. doi: 10.1016/j.psyneuen.2009.11.001

Miratashi, Y., Amir, S., Abbasi, M., Masoud, S., and Yazdi, M. (2017). Epilepsy and vitamin D: a comprehensive review of current knowledge. *Rev. Neurosci.* 28, 185–201. doi: 10.1515/revneuro-2016-0044

Mounier, A., Georgiev, D., Nam, K. N., Fitz, N. F., Castranio, E. L., Wolfe, C. M., et al. (2015). Bexarotene-activated retinoid X receptors regulate neuronal differentiation and dendritic complexity. *J. Neurosci.* 35, 11862–11876. doi: 10.1523/JNEUROSCI.1001-15.2015

Mpandzou, G., Aït Ben Haddou, E., Regragui, W., Benomar, A., and Yahyaoui, M. (2016). Vitamin D deficiency and its role in neurological conditions: a review. *Rev. Neurol.* 172, 109–122. doi: 10.1016/j.neurol.2015.11.005

Munger, K. L., Åivo, J., Hongell, K., Soilu-Hänninen, M., Surcel, H.-M., and Ascherio, A. (2016). Vitamin D status during pregnancy and risk of multiple sclerosis in offspring of women in the Finnish maternity cohort. *JAMA Neurol.* 73, 515–519. doi: 10.1001/jamaneurol.2015.4800

Nadi, M., Marandi, S. M., Esfarjani, F., Saleki, M., and Mohammadi, M. (2017). The comparison between effects of 12 weeks combined training and vitamin D supplement on improvement of sensory-motor neuropathy in type 2 diabetic women. *Adv. Biomed. Res.* 6:55. doi: 10.4103/2277-9175.205528

Naveilhan, P., Neveu, I., Wion, D., and Brachet, P. (1996). 1,25-Dihydroxyvitamin D3, an inducer of glial cell line-derived neurotrophic factor. *Neuroreport* 7, 2171–2175. doi: 10.1097/00001756-199609020-00023

Neveu, I., Naveilhan, P., Baudet, C., Brachet, P., and Metsis, M. (1994). 1,25-Dihydroxyvitamin D3 regulates NT-3, NT-4 but not BDNF MRNA in astrocytes. *Neuroreport* 6, 124–126. doi: 10.1097/00001756-199412300-00032

Nystad, A. E., Wergeland, S., Aksnes, L., Myhr, K. M., Lars, B., and Torkildsen, O. (2014). Effect of high-dose 1.25 dihydroxyvitamin d3 on remyelination in the cuprizone model. *APMIS* 122, 1178–1186. doi: 10.1111/apm.12281

Oudshoorn, C., Mattace-Raso, F. U., Van Der Velde, N., Colin, E. M., and Van Der Cammen, T. J. (2008). Higher serum vitamin D3 levels are associated with better cognitive test performance in patients with Alzheimer's disease. *Demen. Geriatr. Cogn. Disord.* 25, 539–543. doi: 10.1159/000134382

Ozuguz, U., Oruc, S., Ulu, M. S., Demirbas, H., Acay, A., Coker, B., et al. (2016). Does vitamin D have any role in the improvement of diabetic peripheral neuropathy in type 1 diabetic patients? *J. Endocrinol. Investig.* 39, 1411–1417. doi: 10.1007/s40618-016-0509-6

Pandit, L., Ramagopalan, S. V., Malli, C., D'Cunha, A., Kunder, R., and Shetty, R. (2013). Association of vitamin D and multiple sclerosis in India. *Mult. Scler. J.* 19, 1592–1596. doi: 10.1177/1352458513482375

Pepaj, M., Bredahl, M. K., Gjerlaugsen, N., Bornstedt, M. E., and Thorsby, P. M. (2015). Discovery of novel vitamin D-regulated proteins in INS-1 cells: a proteomic approach. *Diabetes Metab. Res. Rev.* 31, 481–491. doi: 10.1002/dmrr.2629

Plotnikoff, G. A., and Quigley, J. M. (2003). Prevalence of severe hypovitaminosis D in patients with persistent, nonspecific musculoskeletal pain. *Mayo Clin. Proc.* 78, 1463–1470. doi: 10.4065/78.12.1463

Price, P. A., Faus, S. A., and Williamson, M. K. (2000). Warfarin-induced artery calcification is accelerated by growth and vitamin D. *Arterioscler. Thromb. Vasc. Biol.* 20, 317–327. doi: 10.1161/01.atv.20.2.317

Putz, Z., Martos, T., Németh, N., Erzsébet Körei, A., Erzsébet Vági, O., Soma Kempler, M., et al. (2014). Is there an association between diabetic neuropathy and low vitamin D levels? *Curr. Diab. Rep.* 14:537. doi: 10.1007/s11892-014-0537-6

Putz, Z., Martos, T., Németh, N., Erzsébet Körei, A., Szabó, M., Erzsébet Vági, O., et al. (2013). Vitamin D and neuropathy. *Orv. Hetil.* 154, 2012–2015. doi: 10.1556/OH.2013.29769

Rammos, G., Tseke, P., and Ziakka, S. (2008). Vitamin D, the renin-angiotensin system, and insulin resistance. *Int. Urol. Nephrol.* 40, 419–426. doi: 10.1007/s11255-007-9244-4

Rosen, C. J. (2011). Clinical practice. Vitamin D insufficiency. *N. Engl. J. Med.* 364, 248–254.

Ross, A. C., Manson, J. E., Abrams, S. A., Aloia, J. F., Brannon, P. M., Clinton, S. K., et al. (2011). The 2011 report on dietary reference intakes for calcium and vitamin d from the institute of medicine: what clinicians need to know. *J. Clin. Endocrinol. Metab.* 96, 53–58. doi: 10.1210/jc.2010-2704

Sakai, S., Suzuki, M., Tashiro, Y., Tanaka, K., Takeda, S., Aizawa, K., et al. (2015). Vitamin D receptor signaling enhances locomotive ability in mice. *J. Bone Miner. Res.* 30, 128–136. doi: 10.1002/jbmr.2317

Santos, P. C., Krieger, J. E., and Costa Pereira, A. (2012). Renin-angiotensin system, hypertension, and chronic kidney disease: pharmacogenetic implications. *J. Pharmacol. Sci.* 120, 77–88. doi: 10.1254/jphs.12r03cr

Sayeed, I., and Stein, D. G. (2009). Progesterone as a neuroprotective factor in traumatic and ischemic brain injury. *Prog. Brain Res.* 175, 219–237. doi: 10.1016/S0079-6123(09)17515-5

Sereda, M., Griffiths, I., Pühlhofer, A., Stewart, H., Rossner, M. J., Zimmerman, F., et al. (1996). A transgenic rat model of charcot-marie-tooth disease. *Neuron* 16, 1049–1060.

Sergeev, I. N., Kha, K. P., Blazheevich, N. V., and Spirichev, V. B. (1987). [Effect of combined vitamin D and E deficiencies on calcium metabolism and bone tissue of the rat]. *Vopr. Pitan.* 1, 39–43.

Seuter, S., Heikkinen, S., and Carlberg, C. (2013). Chromatin acetylation at transcription start sites and vitamin D receptor binding regions relates to effects of 1α,25-dihydroxyvitamin D3 and histone deacetylase inhibitors on gene expression. *Nucleic Acids Res.* 41, 110–124. doi: 10.1093/nar/gks959

Shehab, D., Al-Jarallah, K., Abdella, N., Mojiminiyi, O. A., and Al Mohamedy, H. (2015). Prospective evaluation of the effect of short-term oral vitamin D supplementation on peripheral neuropathy in type 2 diabetes mellitus. *Med. Princ. Pract.* 24, 250–256. doi: 10.1159/000375304

Shirazi, H. A., Rasouli, J., Ciric, B., Rostami, A., and Xian Zhang, G. (2015). 1,25-Dihydroxyvitamin D3 enhances neural stem cell proliferation and oligodendrocyte differentiation. *Exp. Mol. Pathol.* 98, 240–245. doi: 10.1016/j.yexmp.2015.02.004

Shirazi, H. A., Rasouli, J., Ciric, B., Wei, D., Rostami, A., and Xian Zhang, G. (2017). 1,25-Dihydroxyvitamin D3 suppressed experimental autoimmune encephalomyelitis through both immunomodulation and oligodendrocyte maturation. *Exp. Mol. Pathol.* 102, 515–521. doi: 10.1016/j.yexmp.2017.05.015

Singh, G., and Bonham, A. J. (2014). A predictive equation to guide vitamin D replacement dose in patients. *J. Am. Board Fam. Med.* 27, 495–509. doi: 10.3122/jabfm.2014.04.130306

Smolders, J., Hupperts, R., Barkhof, F., Grimaldi, L. M., Holmoy, T., Killestein, J., et al. (2011). Efficacy of vitamin D3 as add-on therapy in patients with relapsing-remitting multiple sclerosis receiving subcutaneous interferon β-1a: a phase II, multicenter, double-blind, randomized, placebo-controlled trial. *J. Neurol. Sci.* 311, 44–49. doi: 10.1016/j.jns.2011.04.013

Smolders, J., Peelen, E., Thewissen, M., Cohen Tervaert, J. W., Menheere, P., Hupperts, R., et al. (2010). Safety and T cell modulating effects of high dose vitamin D3 supplementation in multiple sclerosis. *PLoS One* 5:e15235. doi: 10.1371/journal.pone.0015235

Spanaus, K., and von Eckardstein, A. (2017). Evaluation of two fully automated immunoassay based tests for the measurement of 1α,25-dihydroxyvitamin D in human serum and comparison with LC-MS/MS. *Clin. Chem. Lab. Med.* 55, 1305–1314. doi: 10.1515/cclm-2016-1074

Stumpf, W. E. (2012). Drugs in the brain - cellular imaging with receptor microscopic autoradiography. *Prog. Histochem. Cytochem.* 47, 1–26. doi: 10.1016/j.proghi.2011.12.001

Suzuki, M., Yoshioka, M., Hashimoto, M., Murakami, M., Noya, M., Takahashi, D., et al. (2013). Randomized, double-blind, placebo-controlled trial of vitamin D supplementation in Parkinson disease. *Am. J. Clin. Nutr.* 97, 1004–1013. doi: 10.3945/ajcn.112.051664

Tawk, M., Makoukji, J., Belle, M., Fonte, C., Trousson, A., Hawkins, T., et al. (2011). Wnt/ -catenin signaling is an essential and direct driver of myelin gene expression and myelinogenesis. *J. Neurosci.* 31, 3729–3742. doi: 10.1523/JNEUROSCI.4270-10.2011

Teichert, A. E., Elalieh, H., Elias, P. M., Welsh, J., and Bikle, D. D. A. (2011). Overexpression of hedgehog signaling is associated with epidermal tumor formation in vitamin D receptor null mice arnaud. *J. Investig. Dermatol.* 131, 2289–2297. doi: 10.1038/jid.2011.196

Tesoriere, L., Bongiorno, A., Pintaudi, A. M., D'Anna, R., D'Arpa, D., and Livrea, M. A. (1996). Synergistic Interactions between Vitamin A and Vitamin E against lipid peroxidation in phosphatidylcholine liposomes. *Arch. Biochem. Biophys.* 326, 57–63. doi: 10.1006/abbi.1996.0046

Tomaschitz, A., Pilz, S., Ritz, E., Grammer, T., Drechsler, C., Boehm, B. O., et al. (2010). Independent association between 1,25-dihydroxyvitamin D, 25-hydroxyvitamin D and the renin-angiotensin system: the Ludwigshafen risk and cardiovascular health (LURIC) study. *Clin. Chim. Acta Int. J. Clin. Chem.* 411, 1354–1360. doi: 10.1016/j.cca.2010.05.037

Ushiroyama, T., Ikeda, A., and Ueki, M. (2002). Effect of continuous combined therapy with vitamin K(2) and vitamin D(3) on bone mineral density and coagulofibrinolysis function in postmenopausal women. *Maturitas* 41, 211–221. doi: 10.1016/s0378-5122(01)00275-4

Valensi, P., Le Devehat, C., Richard, J.-L., Farez, C., Khodabandehlou, T., Rosenbloom, R. A., et al. (2005). A multicenter, double-blind, safety study of QR-333 for the treatment of symptomatic diabetic peripheral neuropathy. A preliminary report. *J. Diabetes Complications* 19, 247–253. doi: 10.1016/j.jdiacomp.2005.05.011

Vallat, J.-M., Magy, L., Lagrange, E., Sturtz, F., Magdelaine, C., Grid, D., et al. (2007). Diagnostic value of ultrastructural nerve examination in charcot-marie-tooth disease: two CMT 1B cases with pseudo-recessive inheritance. *Acta Neuropathol.* 113, 443–449. doi: 10.1007/s00401-007-0196-7

van Ballegooijen, A. J., Beulens, J. W. J., Keyzer, C. A., Navis, G. J., Berger, S. P., de Borst, M. H., et al. (2019). Joint association of vitamins D and K status with long-term outcomes in stable kidney transplant recipients. *Nephrol. Dial. Transplantat.*

van Ballegooijen, A. J., Cepelis, A., Visser, M., Brouwer, I. A., van Schoor, N. M., and Beulens, J. W. (2017a). Joint association of low vitamin D and vitamin K status with blood pressure and hypertension. *Hypertension* 69, 1165–1172. doi: 10.1161/HYPERTENSIONAHA.116.08869

van Ballegooijen, A. J., Pilz, S., Tomaschitz, A., Grübler, M. R., and Verheyen, N. (2017b). The synergistic interplay between vitamins D and K for bone and cardiovascular health: a narrative review. *Int. J. Endocrinol.* 2017:7454376. doi: 10.1155/2017/7454376

van Ballegooijen, A. J., Gansevoort, R. T., Lambers-Heerspink, H. J., de Zeeuw, D., Visser, M., Brouwer, I. A., et al. (2015). Plasma 1,25-dihydroxyvitamin D and the risk of developing hypertension: the prevention of renal and vascular end-stage disease study. *Hypertension* 66, 563–570. doi: 10.1161/HYPERTENSIONAHA.115.05837

VanAmerongen, B. M., Dijkstra, C. D., Lips, P., and Polman, C. H. (2004). Multiple sclerosis and vitamin D: an update. *Eur. J. Clin. Nutr.* 58, 1095–1109. doi: 10.1038/sj.ejcn.1601952

Veenstra, T. D., Windebank, A. J., and Kumar, R. (1997). 1,25-Dihydroxyvitamin D3 regulates the expression of N-Myc, c-Myc, protein kinase C, and transforming growth factor-beta2 in neuroblastoma cells. *Biochem. Biophys. Res. Commun.* 235, 15–18. doi: 10.1006/bbrc.1997.6718

Vuong, T. A., Leem, Y. E., Kim, B. G., Cho, H., Lee, S. J., Un Bae, G., et al. (2017). A sonic hedgehog coreceptor, BOC regulates neuronal differentiation and neurite

outgrowth via interaction with ABL and JNK activation. *Cell. Signal.* 30, 30–40. doi: 10.1016/j.cellsig.2016.11.013

Westra, S., Krul-Poel, Y. H., van Wijland, H. J., ter Wee, M. M., Stam, F., Lips, P., et al. (2016). Effect of vitamin D supplementation on health status in non-vitamin D deficient people with type 2 diabetes mellitus. *Endocr. Connect.* 5, 61–69. doi: 10.1530/EC-16-0070

White, K. E., Evans, W. E., O'Riordan, J. L. H., Speer, M. C., Econs, M., Lorenz-Depiereux, B., et al. (2000). Autosomal dominant hypophosphataemic rickets is associated with mutations in FGF23. *Nat. Genet.* 26, 345–348. doi: 10.1038/81664

Wilkins, C. H., Sheline, Y. I., Roe, C. M., Birge, S. J., and Morris, J. C. (2006). Vitamin D deficiency is associated with low mood and worse cognitive performance in older adults. *Am. J. Geriatr. Psychiatry* 14, 1032–1040. doi: 10.1097/01.JGP.0000240986.74642.7c

Yang, S., Li, A., Wang, J. W., Liu, J., Han, Y., Zhang, W., et al. (2018). Vitamin D receptor: a novel therapeutic target for kidney diseases. *Curr. Med. Chem.* 25, 3256–3271. doi: 10.2174/0929867325666180214122352

Yin, Y., Ni, J., Chen, M., Guo, Y., and Yeh, S. (2009). RRR-alpha-vitamin E succinate potentiates the antitumor effect of calcitriol in prostate cancer without overt side effects. *Clin. Cancer Res.* 15, 190–200. doi: 10.1158/1078-0432.CCR-08-0910

Zárate, S., Stevnsner, T., and Gredilla, R. (2017). Role of estrogen and other sex hormones in brain aging. Neuroprotection and DNA repair. *Front. Aging Neurosci.* 9:430. doi: 10.3389/fnagi.2017.00430

Zhang, W., Chen, L., Zhang, L., Xiao, M., Ding, J., Goltzman, D., et al. (2015). Administration of exogenous 1,25(OH)2D3 normalizes overactivation of the central renin-angiotensin system in 1α(OH)ase knockout mice. *Neurosci. Lett.* 588, 184–189. doi: 10.1016/j.neulet.2015.01.013

Zhao, Y., Sun, Y., Ji, H. F., and Shen, L. (2013). Vitamin D levels in Alzheimer's and Parkinson's diseases: a meta-analysis. *Nutrition* 29, 828–832. doi: 10.1016/j.nut.2012.11.018

Conflict of Interest Statement: The authors declare that the research was conducted in the absence of any commercial or financial relationships that could be construed as a potential conflict of interest.

Conclusion

As shown in this review, calcitriol seems to actively participate in nervous system development and neural cells differentiation. The aim of this study was, therefore, to elucidate calcitriol role in PNS, but also to evaluate if its supplementation could be applied to improve neural cell culture. Indeed, positive results have already been observed in SH-SY5Y cells' morphology and features, after treatment with vitamin D3 and other neurotrophic factors (Agholme et al. 2010). In the case of our cellular model, it could be interesting to test calcitriol in our differentiation protocol to generate MN from hiPSC. In particular, we have envisaged to supplement cells with calcitriol from induction of rosettes formation, until MN generation. We would like to evaluate if its supplementation could have a synergistic action with the already employed differentiation factors, in increasing neural cells viability and MN proportion, and in promoting neurites' formation and maintenance. Given the promising role of calcitriol, we hope to start these tests in the next future.

<u>Article 6</u> - GDAP1 defect promotes mitochondrial dysfunction and oxidative stress in a Charcot-Marie-Tooth model of hiPSC-derived motor neurons

Article in preparation

The previously described method, to generate MN from hiPSC, has been thus used to obtain and analyze a cellular model of *GDAP1*-associated CMT disease. Specifically, in this study, we focused on molecular mechanisms related to the *GDAP1* nonsense c.581C>G (p.Ser194*) mutation, to elucidate *GDAP1* role in physiological and pathological conditions. This is the first *GDAP1* functional analysis on a human model of MN.

First, dermal fibroblasts were obtained from a CMT2H patient (patient 3-A), with the homozygous *GDAP1* p.Ser194*mutation, and two unaffected controls. After amplification, fibroblasts were reprogrammed in hiPSC, which were then differentiated in neural progenitors (NP), and, at the end, in MN. Once we get the four cellular types (fibroblasts, hiPSC, NP and MN) for each subject, we could perform expression, morphological, and functional studies, on all, or some, of them. To begin, we evaluated *GDAP1* mRNA and protein expression in the four models, revealing its predominant neural expression, but also its absence in patient 3-A cells. Secondly, with ultrastructural analysis, we detected cytoplasmic vacuoles (maybe lipid droplets) accumulation, and mitochondrial morphology's abnormalities in patient's MN. Lastly, in these cells, we observed also increased death rate and oxidative stress.

In our study, we assessed a human cellular model to better investigate molecular mechanisms impaired in this axonal form of CMT disease. Basing on our preliminary findings, we could suppose that metabolism alterations and oxidative stress may play a key role in determine the cellular dysfunction and death in patient's MN, where GDAP1 protein is very weakly expressed.

GDAP1 defect promotes mitochondrial dysfunction and oxidative stress in a Charcot-Marie-Tooth model of hiPSC-derived motor neurons.

Federica Miressi[1], Nesrine Benslimane[1], Frédéric Favreau[1,2], Laurence Richard[1,3], Sylvie Bourthoumieu[1,4], Marion Rassat[1], Cécile Laroche[5,6], Laurent Magy[1,3], Corinne Magdelaine[1,2], Franck Sturtz[1,2], Pierre-Antoine Faye[1,2§] and Anne-Sophie Lia[1,2,7,*§].

[1] Univ. Limoges, MMNP, EA6309, F-87000 Limoges, France

[2] CHU Limoges, Service de Biochimie et Génétique Moléculaire, F-87000 Limoges, France

[3] CHU Limoges, Service de Neurologie, F-87000 Limoges, France

[4] CHU Limoges, Service de Cytogénétique, F-87000 Limoges, France

[5] CHU Limoges, Service de Pédiatrie, F-87000 Limoges, France

[6] CHU Limoges, Centre de Compétence des Maladies Héréditaires du Métabolisme, F-87000 Limoges, France.

[7] CHU Limoges, Service de Bioinformatique, F-87000 Limoges, France

* Corresponding author

Anne-Sophie LIA

anne-sophie.lia@unilim.fr

EA6309, Faculté de Médecine, Université de Limoges

2 rue Dr Marcland

87025 Limoges Cedex

FRANCE

.

[§] These authors have equally contributed to this work

Key words

CMT disease, GDAP1, hiPSC, motor neurons, mitochondria

Abstract

Mutations in the ganglioside-induced differentiation associated protein 1 (*GDAP1*) gene have been associated with demyelinating and axonal forms of Charcot-Marie-Tooth disease (CMT), the most frequent hereditary peripheral neuropathy in humans. Previous studies reported the prevalent *GDAP1* expression in neural tissues and cells, from animal models. Here, we described the first GDAP1 functional study on human induced-pluripotent stem cells (hiPSC)-derived motor neurons, obtained from normal subjects and from a CMT2H patient, carrying the *GDAP1* homozygous p.S194* mutation. At mRNA level, we observed that, in normal subjects, *GDAP1* is mainly expressed in motor neurons, while it is drastically decreased in patient's cells containing a premature termination codon (PTC), probably degraded by the nonsense-mediated mRNA decay (NMD) system. Morphological and functional investigations revealed, in CMT patient's motor neurons, a decrease of cell viability associated to lipid metabolism dysfunction and oxidative stress development. Mitochondrion is a key organelle in oxidative stress generation but it is also mainly involved in energetic metabolism. Thus, in CMT patient's motor neurons, mitochondrial cristae defects were observed, even if no deficit in ATP production emerged. This cellular model of hiPSC-derived motor neurons underlines the role of mitochondrion and oxidative stress in CMT disease and paves the way for new treatment evaluation.

1 Introduction

Charcot-Marie-Tooth (CMT) disease is a heterogeneous group of sensory-motor disorders, belonging to the larger class of genetic neuropathies. With an estimated prevalence of 1/2,500, it is considered as the most frequent inherited pathology of the peripheral nervous system. It indifferently affects both sexes, of any geographical origin and age, and it is clinically defined by muscular weakness and atrophy, foot deformities, like pes cavus, sometimes sensory loss and balance issues (Bird 2020). Traditionally, basing on electrophysiological studies, demyelinating forms, characterized by reduced nerve conduction velocity (NCV), can be distinguished from axonal CMT forms, with preserved NCV values. More recently, a third group, identified as intermediate CMT, has been described, ranking between demyelinating and axonal forms in its clinical aspects. According to the associated mode of inheritance of the disease, CMT is further classified in autosomal, dominant or recessive forms, and X-linked, dominant or recessive

forms. More than 80 genes have been identified to be mutated in these different CMT subgroups (Bird 2020), although the complete duplication of *PMP22* gene, responsible of the so-called CMT1A, remains the main genetic cause of this pathology.

Mutations in *GDAP1* (ganglioside-induced differentiation protein 1) gene have been reported for the first time in 2001 (Baxter et al. 2002; Cuesta et al. 2002), and are well known to induce multiple types of Charcot-Marie-Tooth disease. Autosomal recessive mode of inheritance has been observed in demyelinating (CMT4A or AR-CMTde-GDAP1), intermediate (RI-CMTA or AR-CMTin-GDAP1) and axonal (CMT2H or AR-CMTax-GDAP1) forms, while autosomal dominant mutations seem to lead exclusively to axonal CMT (CMT2K or AD-CMTax-GDAP1) (Mathis et al. 2015; Sivera et al. 2017). *GDAP1*, located on chromosome 8 of the human genome, encodes a 358 aa protein, expressed on the outer mitochondrial membrane of neurons and, at lower levels, of myelinating Schwann cells (Niemann et al. 2005; Pedrola et al. 2005; 2008). Even if GDAP1 CMT-inducing mutations have been largely described in their clinical aspects and associated phenotypes, fewer studies have deeply investigated the molecular mechanisms altered in motor neurons and responsible of the neural degeneration.

Three main animal models have been developed to elucidate GDAP1 role in cellular physiology, through its up- or down- regulation, in Drosophila malanogaster (López Del Amo et al. 2015; López del Amo et al. 2017) its depletion, in mice (Niemann et al. 2014; Barneo-Muñoz et al. 2015), or its mutation, in yeasts (Rzepnikowska et al. 2020). Concerning the cellular models, given the inaccessibility of human neurons, all functional studies employed a large amount of alternative strategies, such as primary cultures of murine neurons (Pedrola et al. 2008; Huber et al. 2013), rat Schwann cells (Niemann et al. 2005), and human fibroblasts (Cassereau et al. 2009; 2020), but also transfected, or non-transfected, cell lines, like Cos7, HeLa, SH-SY5Y, N1E-115, HT22 (Niemann et al. 2005; Pedrola et al. 2005; 2008; Niemann et al. 2009; Wagner et al. 2009; Kabzińska et al. 2011; Noack et al. 2012; Huber et al. 2013; Pla-Martín et al. 2013; González-Sánchez et al. 2017). These existing models have allowed highlighting some GDAP1 functions. GDAP1involvement in mitochondria fission and fusion events has been observed in N1E-115 cells and in a model of transfected Cos7 cells (Niemann et al. 2005; 2009; Wagner et al. 2009; Huber et al. 2013), while HT22 cells and human fibroblasts have been fundamental to reveal GDAP1 implication in protection from oxidative stress (Noack et al. 2012; Cassereau et al. 2020). In addition, it seems that GDAP1 takes part, also, in regulating Ca^{2+} homeostasis, as shown in SH-SY5Y and transfected HeLa cells (Pla-Martín et al. 2013; González-Sánchez et al. 2017). However, the lack of motor neurons of human origin failed to demonstrate the potential extrapolation of these investigations in CMT patients.

Human induced-pluripotent stem cells (hiPSC), created for the first time in 2006 (Takahashi e Yamanaka 2006), have become a powerful tool in the exploration of neurological and neuromuscular diseases. The main advantage of hiPSC is that they can be obtained from an easy-to-take cell type, like fibroblasts, and they can be potentially differentiated in any kind of cell of human body, like neurons or glial cells. Moreover, it has been shown that they can be generated from unaffected individuals, but also from affected patients (Faye et al. 2020). In the case of Charcot-Marie-Tooth disease, models of hiPSC-derived motor neurons have been established for different forms associated to different genes, like *NELF*, *MFN2* (Saporta et al. 2015), *HSPB1* (Kim et al. 2016), but also hiPSC-derived Schwann cells presenting the *PMP22* duplication (Shi et al. 2018). hiPSC for GDAP1 are reported in three studies (Saporta et al. 2015; Martí et al. 2017; Faye et al. 2020), and only once they were finally differentiated into motor neurons (Faye et al. 2020).

Here, we report the first functional study on human hiPSC-derived motor neurons from CMT patient, carrying the homozygous p.S194* mutation in *GDAP1*, underlining the role of mitochondrion and oxidative stress in this human GDAP1-defect of CMT disease.

2 Materials and Methods

Subjects

All subjects gave their informed consent for inclusion before participating in the study. The study was conducted in accordance with the Declaration of Helsinki. The family of the CMT-patient presented two cases (Figure 1). The propositus, here reported as "patient", presented early his first symptoms. This young boy was characterized by a severe axonal neuropathy, with subacute progression and polyvisceral disorders leading to an early death at the age of three. His younger brother developed motor impairment in feet, distal atrophy and abolished deep tendon reflexes associated to mental retardation. Parents, with a first degree of consanguinity, were asymptomatic, as well as the elder brother. Genetic analyses detected, in *GDAP1* gene, the c.581C>G (p.Ser194*) mutation, homozygous in the patient and his affected brother, and heterozygous in the other family members. Two control subjects, without any clinical neurological signs, were enrolled in this study: Ctrl-1, a 24 year-old man, and Ctrl-2, a 30-year old woman.

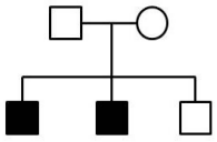

Figure 1 Pedigree of patient's family. Affected members are marked with black symbols.

Skin biopsies and fibroblasts cell culture

Skin biopsies were obtained from patient, Ctrl-1, and Ctrl-2, and incubated in CHANG Medium® D (Irvine Scientific), with 10% Fetal Bovine Serum (FBS) (Gibco, Thermo Fisher SCIENTIFIC). After two weeks, once fibroblasts have migrated from the skin fragment and grew in the culture dish, they were isolated using trypsin. In the first 3 days, fibroblasts were cultivated combining the Chang Medium® D (25%) with the RPMI 1640 medium (75%) (Gibco, Thermo Fisher SCIENTIFIC), supplemented with 10% FBS. Then, Chang medium D was completely replaced by RPMI medium and FBS.

hiPSC generation and characterization

hiPSC were generated following the iStem (INSERM/UEVE UMR861, AFM, Genopole, Evry, France) protocol. First day, CF-1 Mouse Embryonic Fibroblasts (MEF), Mitomycin-C treated (TebuBio), were seeded on gelatin coating (Sigma-Aldrich, Merck), at 25,000 cells/cm2 density. The second day, 600,000 fibroblasts, from patient and controls, were reprogrammed with three plasmids (Plasmid #6 pCXLE-hOCT3/4 shp53-F Addgene, Plasmid #7 pCXLE-hSK Addgene, Plasmid #8 pCXLE-hUL Addgene), through the Nucleofector II device (Amaxa, Lonza). Reprogrammed cells were cultured in DMEM+GlutaMAX medium (Gibco, Thermo Fisher SCIENTIFIC), supplemented with 10% FBS, 1% MEM non-essential amino acids (Thermo Fisher SCIENTIFIC), 1% Sodium Pyruvate (Thermo Fisher SCIENTIFIC), and, at day 1, with 0.1% gentamycin (Thermo Fisher SCIENTIFIC). Culture medium was replaced every day. After 14-21 days, colonies were selected, using a needle, and transferred in new gelatin/MEF coated dishes. HiPSC colonies grew in a KO-DMEM medium (Gibco, Thermo Fisher SCIENTIFIC), with 20% KnockOut Serum Replacement (Gibco, Thermo Fisher SCIENTIFIC), 1% MEM non-essential amino acids, 1% Glutamine (Gibco, Thermo Fisher SCIENTIFIC), 0.1% β-mercaptoethanol (Gibco, Thermo Fisher SCIENTIFIC), and 0.1% gentamycin. It was replaced every day, extemporaneously supplemented with 20 ng/mL Fibroblast Growth Factor (FGF2) (PeproTech). After hiPSC amplification, all quality controls were performed (Supplementary Data and Figures).

Motor neurons generation and culture

Differentiation protocol was applied as previously described by Faye *et al* (Faye, 2020). After neural progenitors (NP) were obtained, they were seeded on poly-L-ornithine/laminine-coated dishes, and cultured in neural media, adding 100 ng/ml Sonic Hedgehog (Shh) (PeproTech), 5 µM RA (Sigma-Aldrich, Merck), 10 ng/mL BDNF (brain-derived

neurotrophic factor) (PeproTech Inc.), 10 ng/mL GDNF (glial cell line-derived neurotrophic factor) (PeproTech Inc.), and 10 ng/mL IGF-1 (insulin-like growth factor-1) (PeproTech Inc.). Then, they were passed every 3 to 4 days, maintaining at high density. In order to generate completely differentiated motor neurons (MN), NP were seeded at a density of 20,000 to 30,000 cells/cm2, using the same coating and the same culture medium.

RNA analysis

Total RNA was extracted from fibroblasts, hiPSC, NP and MN, of Ctrl-1 and patient, using the miRNeasy Mini kit (QIAGEN®). After verifying RNA integrity with the Bioanalyzer 2100 system (Agilent Technologies), it was converted in cDNA with the QuantiTect® Reverse Transcription kit (QIAGEN ®). For the quantitative PCR (qPCR, or Real-Time PCR), primers were designed between the 5th and the 6th exons of *GDAP1*, and between the 5th and the 6th exons of *TBP* (TATA-Box Binding Protein), chosen as reference gene. The reaction was performed on the Corbett Rotor-Gene 6000 Machine (© QIAGEN), prepared with the Rotor-Gene SYBR-Green PCR Kit (400) (©QIAGEN).

Immunocytochemistry

Cells were fixed in 4% paraformaldehyde (PFA) (Sigma-Aldrich, Merck) for 10 minutes and permeabilized with 0.1% Triton X-100 (Sigma-Aldrich, Merck) for 1 hour. They were incubated overnight at 4°C with the primary antibody, prepared in 3% BSA, and, the next day, with the secondary antibody for 1 hour at room temperature. All antibodies' dilutions and references are reported in Supplementary Table 1. Nuclei were stained with 2 µg/mL 4',6'-diamidino-2-phénylindole dihydrochloride (DAPI) (Sigma-Aldrich, Merck). Images captures were performed using a fluorescence microscope (Leica Microsystems) or a confocal microscope (Zeiss), while their processing and analysis were made with NIS Element BR software, Zen Black and Zen Bleu software, and Image J software. For the 3,3′-Diaminobenzidine (DAB) staining, MN were fixed, permeabilized and incubated with the GDAP1 primary antibody overnight. Next day, the VECTASTAIN® Elite ABC kit (Vector Laboratories) was used for the avidin-biotin/peroxidase detection. The DAB+ chromogen, i.e. the peroxidase substrate solution, was added to induce the formation of the brown precipitate, visualized with a light microscope.

Electron microscopy

All manipulations for the electron microscopy were performed in Neurology and Anatomic Pathology departments at University Hospital of Limoges. Cells were fixed in 2.5% glutaraldehyde, then incubated 30 minutes, at RT, in 2% OsO_4 (Euromedex). After washing them with distilled water, they were dehydrated 10 minutes in a series of ethanol dilutions (30%, 50%, 70%, 95%) and three times in 100% ethanol. At the end, they were embedded overnight in Epon 812. Thin blocks were selected and stained with uranyl acetate and lead citrate, and examine using a Jeol 1011 electron microscope.

Adenosine Triphosphate (ATP) quantification

ATP was dosed using CellTiter-Glo® Luminescent Cell Vaibility Assay kit (Promega), and the luminescent signal was recorded with the Fluoroskan Ascent®FL (Thermo Fisher SCIENTIFIC,) following manufacturer instructions. DAPI staining was used to normalize luminescence's values to the number of cells.

Succinate dehydrogenase (Complex II) activity

Succinate dehydrogenase activity was measured using the Cell Proliferation Kit I (Roche), following manufacturer conditions. Absorbance of formazan crystals, at 595 nm, was recorded with the Multiskan™ FC Microplate Photometer (Thermo Fisher SCIENTIFIC), and normalized to the number of cells, measured with DAPI staining.

Mitochondrial Superoxide quantification

Fibroblasts and MN were analyzed in basal conditions as well as in stressed conditions. Stressed wells were treated 2 hours with 1mM H2O2,

prepared in culture medium. After the treatment, 5 µM MitoSOX™ Red mitochondrial superoxide marker (Molecular Probes, Thermo Fisher SCIENTIFIC) was added to the whole of plate, incubated for 10 minutes at 37˚C. Fluorescent signal was detected using the Leica DM IRB microscope, and normalized to the number of cells, measured with DAPI staining.

Statistical analysis

All statistical analyses were performed using the Graphpad Prism 5 software (GraphPad Software, Inc.). Data were expressed as mean ± SEM (Standard Error of the Mean). They were compared using the nonparametric Mann–Whitney U test. P< 0.05 was considered significant.

3 Results

GDAP1 sequencing

We obtained and cultured fibroblasts of two unaffected controls (Ctrl-1 and Ctrl-2), and the CMT-patient, for which NGS analysis had revealed the *GDAP1* homozygous mutation p.S194*. No difference between the three subjects was observed in fibroblast's culture. Genomic DNA was extracted from fibroblasts and Sanger sequencing was performed for all *GDAP1* exons (Figure 2). It confirmed, in patient's DNA, the presence of the homozygous c.581C>G mutation in exon 5 of *GDAP1*, responsible for the amino acidic substitution of the Serine 194 (TCA) with a stop codon (TGA), in GDAP1 protein. No GDAP1 mutation was detected in Ctrl-1 and Ctrl-2.

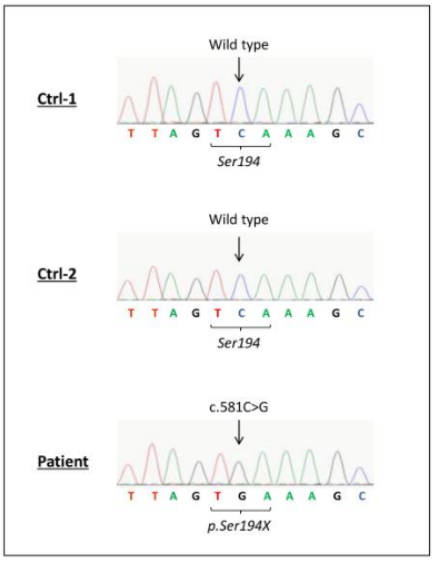

Figure 2 Sanger Sequencing confirmed the *GDAP1* homozygous c.581C>G mutation in patient's fibroblasts, not observed in controls

MN characterization

MN's characterization was carried out five days after plating NP at 30,000 cells/cm2 density. PGP9.5, the ubiquitin carboxyl-terminal hydrolase highly expressed in nerves, and Tuj-1, the neural-specific β-tubulin III, were chosen as neural markers and examined by ICC. All cells were PGP9.5-positive (red) and Tuj-positive (green), as shown in Figure 3A. Cells expressed also the cholyne acetyltransferase (ChAT) enzyme (green), confirming the cholinergic function of these hiPSC-derived motor neurons (Figure 3B).

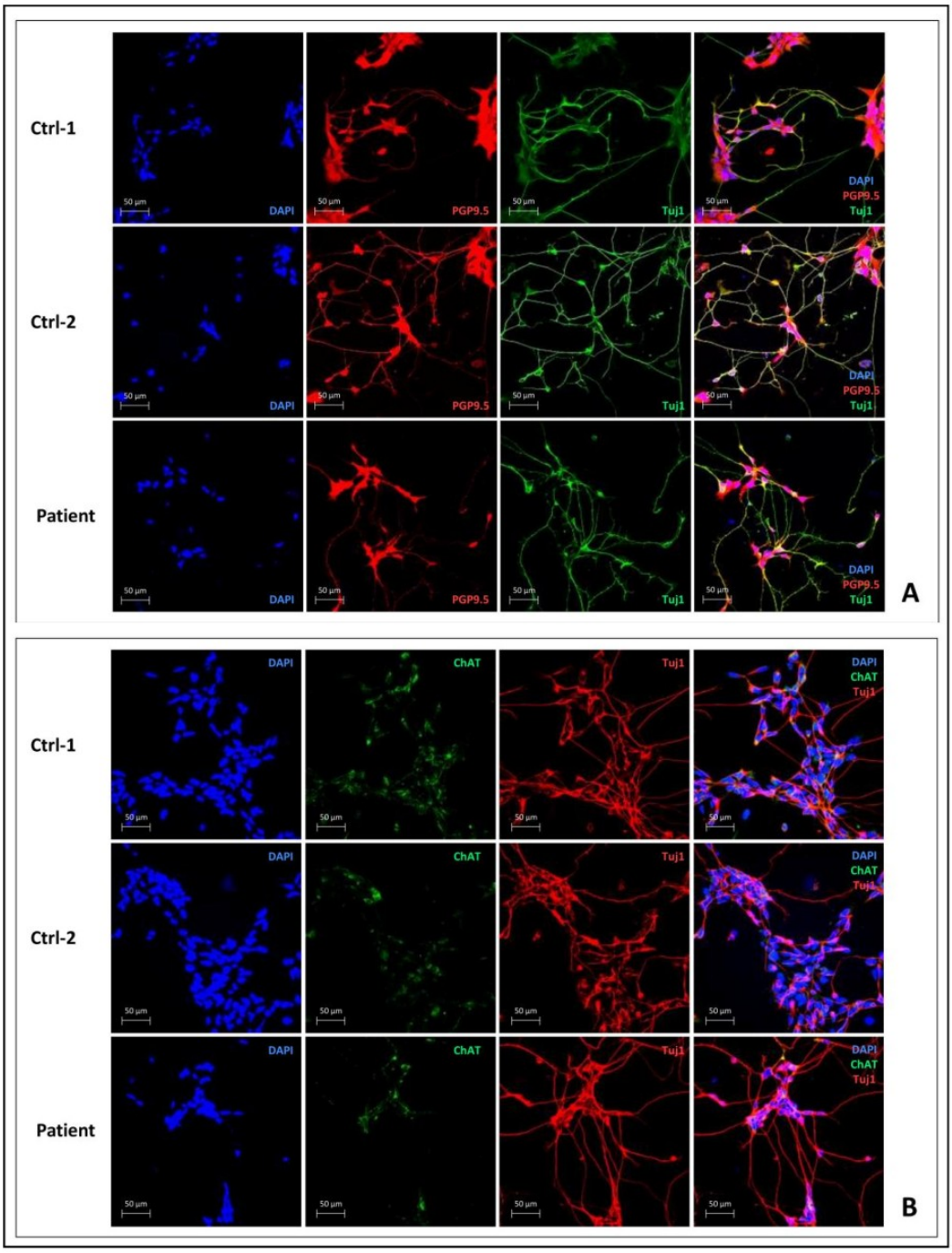

Figure 3 Characterization of hiPSC-derived motor neurons for Ctrl-1, Ctrl-2 and patient. (A): DAPI (blue) for nuclei staining, PGP9.5 (red), and β-tubulin III (Tuj1) (green); (B): DAPI (blue) for nuclei staining , choline acetyltransferase (ChAT) (green), and β-tubulin III (Tuj1) (red).

GDAP1 mRNA expression

In order to investigate GDAP1 functions and GDAP1-associated mechanisms, we evaluated the expression of *GDAP1* mRNA and protein, from fibroblasts to hiPSC, NP, and MN, of patient and Ctrl-1 subject. After checking RNA integrity and gDNA contamination (data not shown), qPCR on mRNA was performed, revealing, for Ctrl-1, that *GDAP1* is differently expressed in the four cell types (Figure 4A). It was evident that *GDAP1* is weakly expressed in fibroblasts and in hiPSC. In contrast, *GDAP1* mRNA levels significantly increased in neural cell types, associated with the progression of neural differentiation. *GDAP1* expression was around 33-fold higher in NP, and 56-fold higher in MN, compared to fibroblast levels. In patient's cells, even if the same expression trend was observed in the four cell types (FB, hiPSC, NP, and MN), the global amount of *GDAP1* mRNA was significantly reduced. Indeed, *GDAP1* mRNA was nearly absent in patient's fibroblasts and hiPSC, and remained weak in NP and MN (Figure 4B).

GDAP1 protein expression

To complete mRNA analysis, we evaluated GDAP1 protein expression on MN, the cellular type known to express GDAP1, in contrast to fibroblasts, where GDAP1 seemed lacking (Figure 5).

Fibroblasts were stained with GDAP1 antibody (red), and Prolyl 4-hydroxylase subunit-β antibody (P4HB) (green), chosen as fibroblasts' marker. As expected, no GDAP1 signal was observed, both in controls' and patient's fibroblasts (Figure 5A).

In MN, GDAP1 staining (red) was associated to Tuj-1 staining (green), specific of neural cells. As shown in Figure 5B, GDAP1 protein was detected in MN of Ctrl-1 and Ctrl-2, located in neurons' cell body. In contrast, no fluorescent red signal was observed in patient's MN, suggesting the absence, or weak expression of GDAP1 protein (Figure 5B). These results were supported by the DAB staining showing a high expression of GDAP1 in MN of Ctrl-1 compared to patient (Figure 6).

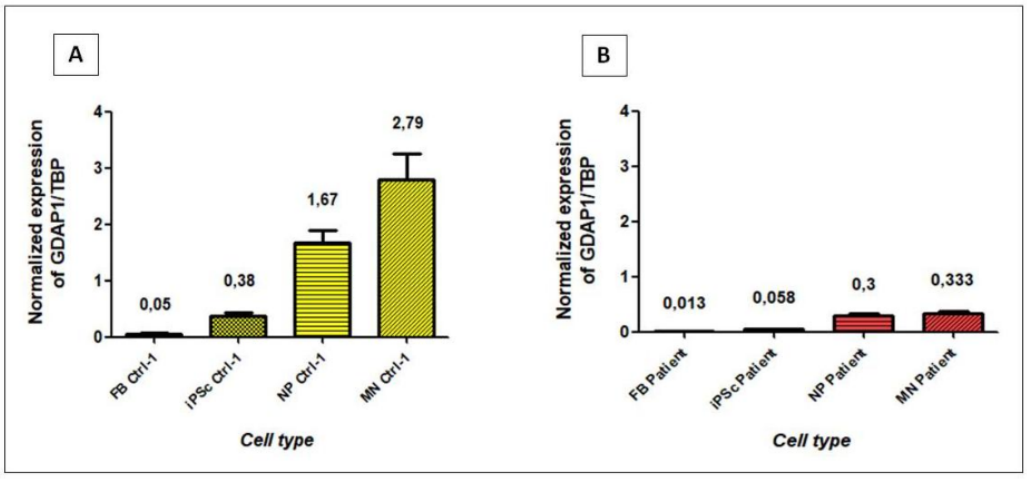

Figure 4 Normalized *GDAP1* expression in fibroblasts (FB), induced-pluripotent stem cells (hiPSC), neural progenitors (NP), and motor neurons (MN), from Ctrl-1 subject (A) or CMT patient (B). Compared to Ctrl-1, medians from patient results were significantly different in hiPSC, NP and MN ($p < 0.05$, Mann-Whitney test). TBP was chosen as reference gene.

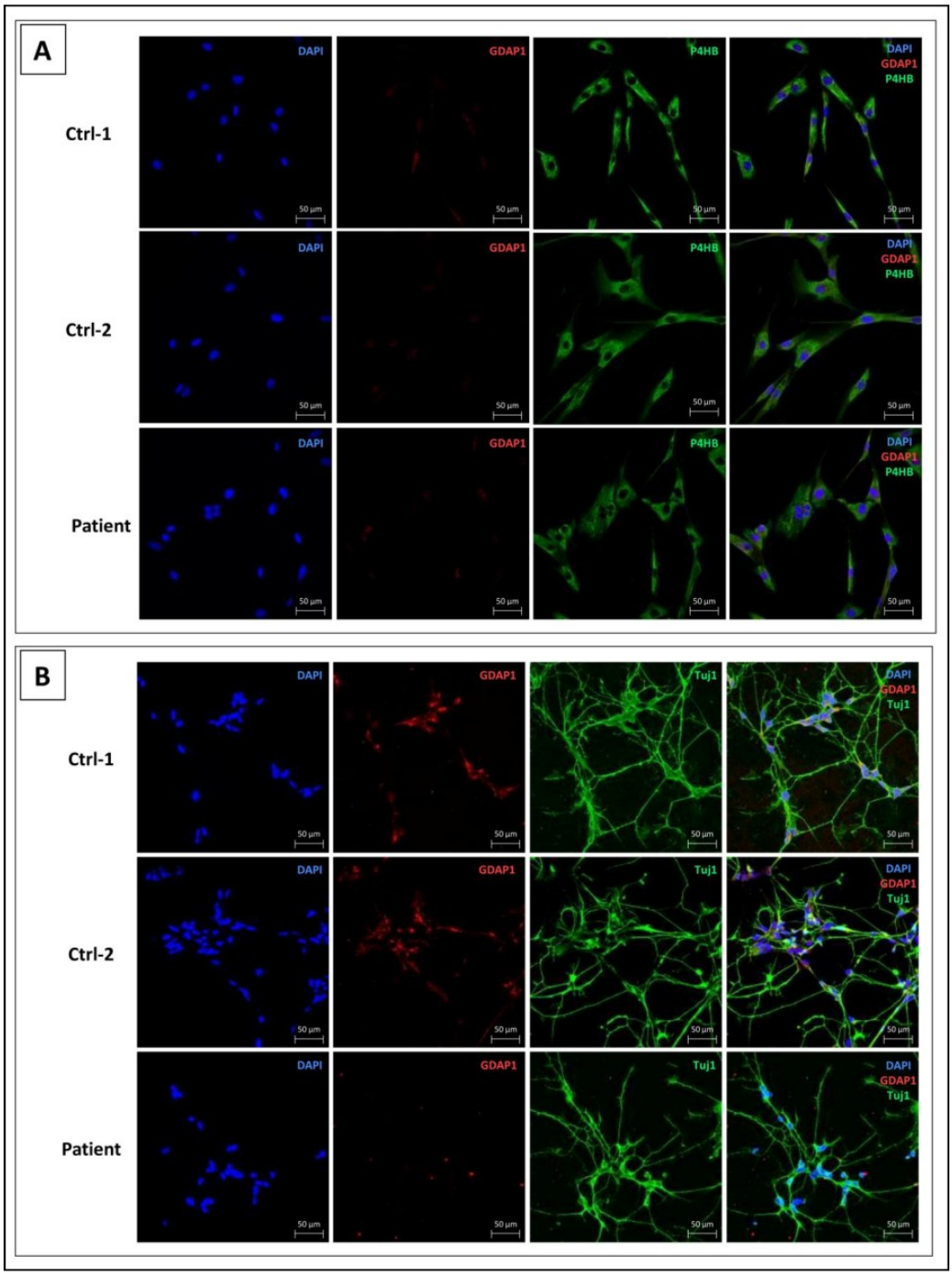

Figure 5 GDAP1 protein expression in fibroblasts (A) and MN (B). (A) DAPI (blue) for nuclei staining, GDAP1 (red), and Prolyl 4-hydroxylase subunit-β antibody (P4HB) (green), as fibroblast marker; (B): DAPI (blue) for nuclei staining, GDAP1 (red), and β-tubulin III (green), as neural marker. As expected, GDAP1 signal was not observed in fibroblasts of both controls and patient, and in patient's MN.

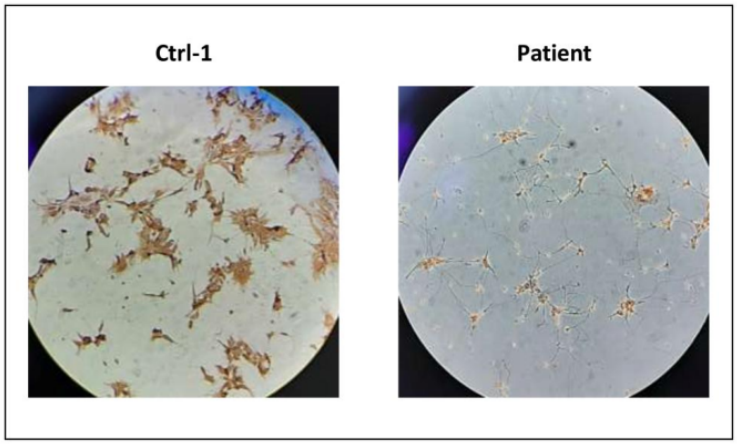

Figure 6 DAB staining for GDAP1, in motor neurons from Ctrl-1 and patient. Control's cells presented a strong brown staining, above all cells in soma region, compared to the background noise detected in patient's cells.

Proliferation and viability of neural cells

Neural progenitors are known to rapidly proliferate. However, this proliferation decreases throughout their final differentiation into motor neurons. Among all existing markers, we analyzed proliferation rate of NP with the Ki-67 staining. It was evaluated at day 1, right after NP seeding, and at day 4, when neurons have started their differentiation process. As shown in Figure 7A, at d1, about 70% of NP of Ctrl-1 and Ctrl-2 were Ki-67-positive, whereas only 60% of patient's NP expressed Ki-67.

At d4, proliferating cells were reduced to 60% in controls, and considerably reduced to 40% in patient's cells (Figure 7B). These results were supported by motor neurons viability. Throughout the NP differentiation, we observed, for patient, a high number of dead cells, and, at day 7, we performed a DAPI staining to evaluate the number of survived cells. A significant 60% reduction of patient's MN viability was revealed, compared to Ctrl-1 or Ctrl-2 ($p < 0.0001$) (Figure 8).

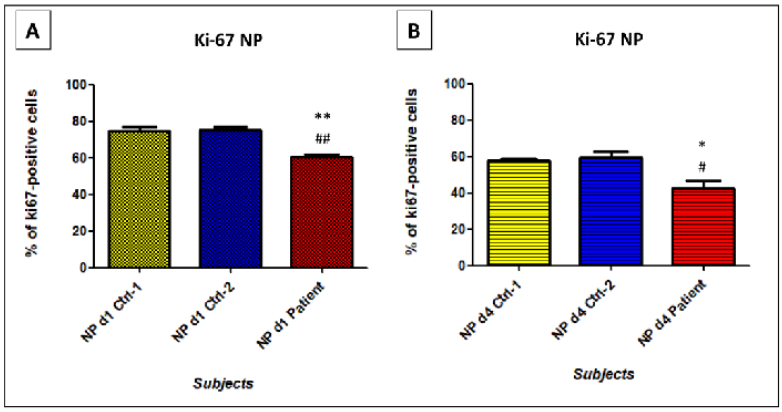

Figure 7 Percentage of Ki-67 expressing-NP of Ctrl-1, Ctrl-2, and patient, at day 1 (A) and day 4 (B) after the beginning of the differentiation process. Lower growth rate in patient's neural cells carrying the p.Ser194* mutation in GDAP1, was observed. ** $p < 0.01$ Ctrl-1 *vs* Patient; ## $p < 0.01$ Ctrl-2 *vs* Patient; * $p < 0.05$ Ctrl-1 *vs* Patient; # $p < 0.05$ Ctrl-2 *vs* Patient

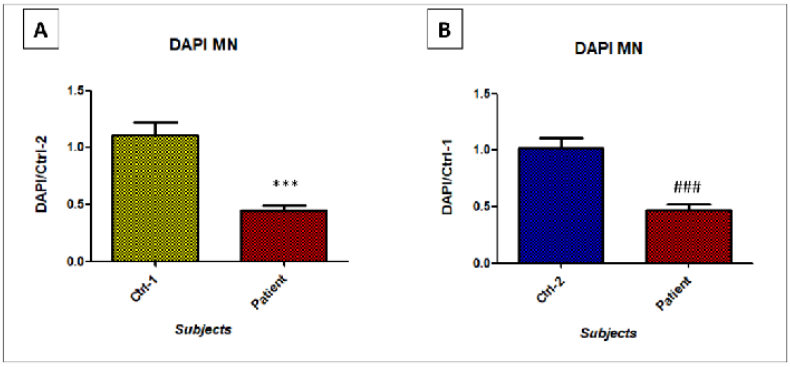

Figure 8 DAPI staining on MN from Ctrl-1, Ctrl-2, and patient, at day 7 after the beginning of the differentiation. *** p <0.001 Ctrl-1 *vs* Patient; ### p <0.001 Ctrl-2 *vs* Patient.

Ultrastructure of motor neurons and its mitochondrial morphology

HiPSC-derived motor neurons of controls and patient were analyzed by electron microscopy. Surprisingly, in cytoplasm of multiple patient's MN, we observed the emergence of several round structures, of various sizes, suspected to be lipid droplets (Figure 9). These vacuoles appeared as electron-dense structures with a homogeneous content, surrounded by a more electron-dense line. They were not observed in control's MN, and in fibroblasts of the three subjects.

Given the mitochondrial localization of GDAP1 protein, we investigated mitochondrial morphology and structure.

Looking at MN's ultrastructure, any difference in mitochondrial size and shape was remarked between controls and patient. Moreover, MN of both subjects presented elongated and fragmented mitochondria. However, focusing on mitochondrial cristae, we observed that their organization was altered in mitochondria of patient's MN. In particular, cristae's regular distribution and thickness were perturbed, preventing to discriminate their structure in mitochondrial compartment. Swollen cristae were also observed. This disorganization of mitochondrial cristae was not present in Ctrl-1 and Ctr-2 MN, as well as in fibroblasts of the three subjects (Figure 10).

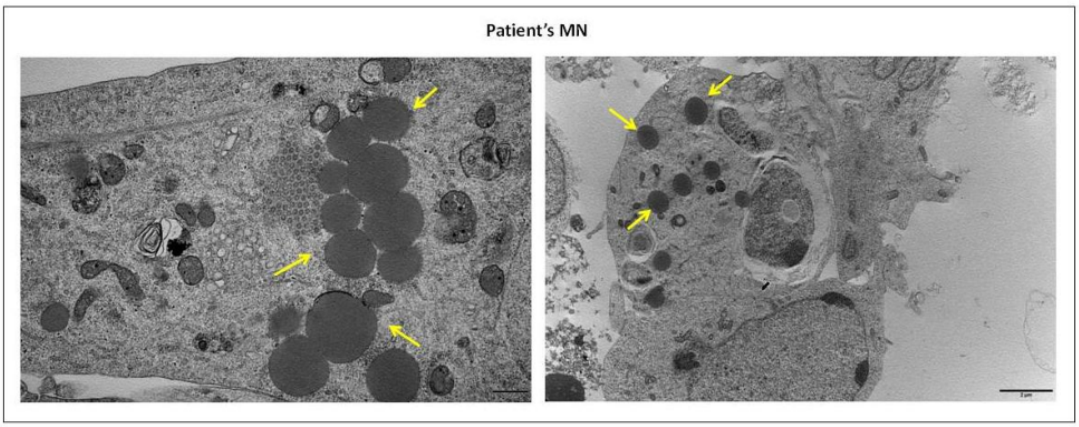

Figure 5 Ultrastructure analysis, by EM, on patient's MN. Suggested lipid droplets (LD) are indicated by yellow arrows and only observed in patient cells.

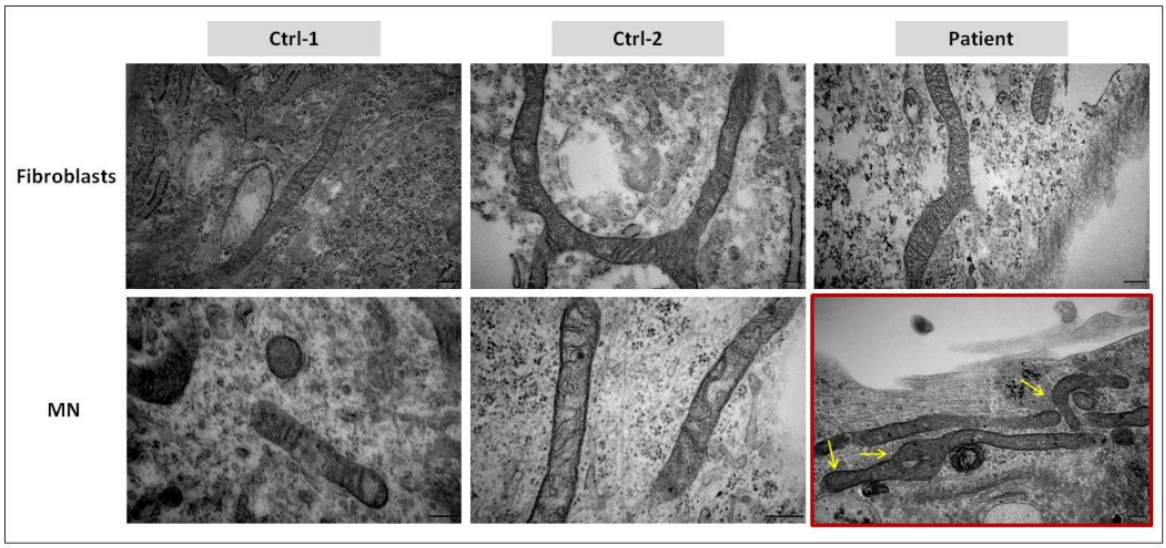

Figure 6 Ultrastructure analysis, by EM on ultrathin sections, of mitochondria in Ctrl-1, Ctrl-2, and patient's fibroblasts and motor neurons. As indicated by yellow arrows, mitochondrial cristae was altered in patient's MN exhibiting a perturbation of cristae distribution and thickness.

Mitochondrial functions and oxidative stress measurement

The alteration of cristae organization in mitochondria of patient's MN, led us to investigate the oxidative phosphorylation through the activity of electron transport chain (ETC) complexes and ATP production. Given the limited availability of hiPSC-derived MN, we performed the MTT test to evaluate the activity of the succinate dehydrogenase (complex II). In both fibroblasts and MN, Succinate dehydrogenase activity seemed to be slightly increased in patient's cells, compared to Ctrl-1 and Ctrl-2, and it reached significant difference ($p = 0.0106$) in fibroblasts (Figure 11). In contrast, ATP levels were not significantly different between patient's and controls' fibroblasts and motor neurons (Figure 12).

Mitochondrion is also the main producer of reactive oxygen species, such as superoxide anion, inducing oxidative stress. A perturbation of mitochondrial cristae could promote redox imbalance. As expected, and shown in Figure 13, in patient's MN, Superoxide anion levels were significantly higher ($p = 0.04$) than in Ctrl-1. This significant difference was even observed with fibroblasts ($p = 0.0188$). The same trend emerged in the comparison with Ctrl-2 cells, but significant difference was not reached.

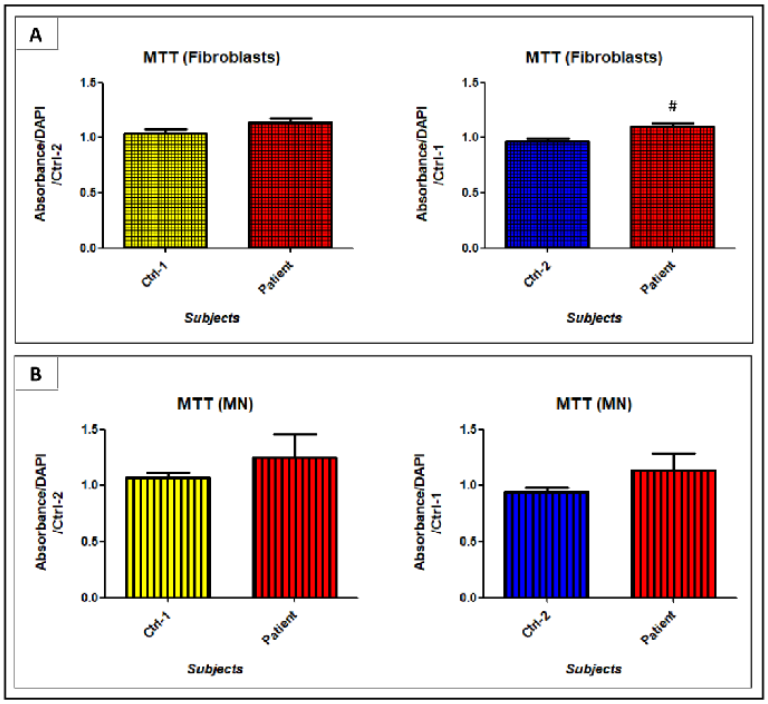

Figure 7 Succinate dehydrogenase activity evaluated in fibroblasts (A) and MN (B) of Ctrl-1, Ctrl-2, and patient. # $p < 0.05$ Ctrl-2 *vs* Patient.

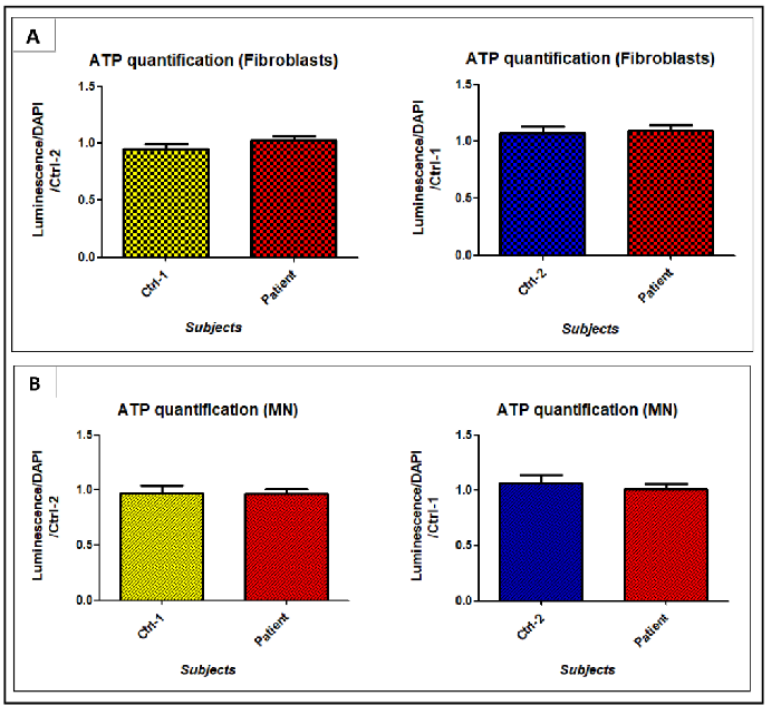

Figure 8 ATP production evaluated in fibroblasts (A) and MN (B) of Ctrl-1, Ctrl-2, and patient.

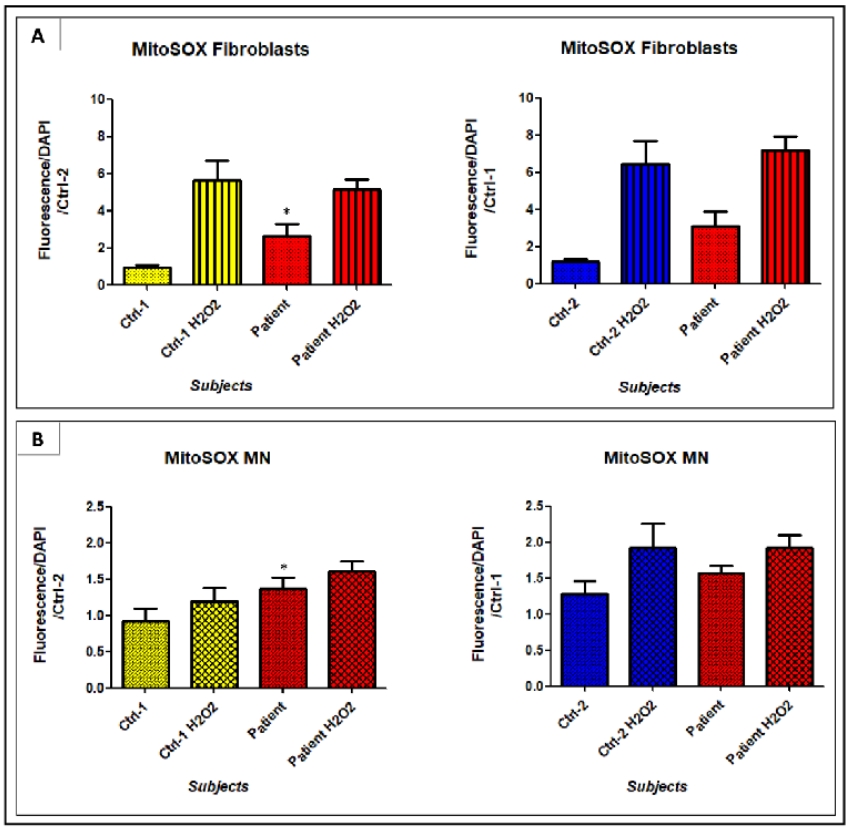

Figure 9 Superoxide anion quantification in fibroblasts (A) and MN (B) of Ctrl-1, Ctrl-2, and patient, using the MitoSOX™ Red mitochondrial superoxide indicator. Cells treated with 1 mM H_2O_2, 2h at 37°C (fibroblasts and MN) were used as positive controls.* $p < 0.05$ Ctrl-1 *vs* Patient.

4 Discussion

More than 80 mutations in *GDAP1* gene have been already reported to be responsible for demyelinating, axonal, and intermediate forms of Charcot-Marie-Tooth disease, and associated to heterogeneous phenotypic manifestations (Rzepnikowska e Kochański 2018). However, GDAP1 role in cellular functions and processes has not been clearly elucidated whereas several well construct studies have been performed (Niemann et al. 2005; Cassereau et al. 2009; Noack et al. 2012; Barneo-Muñoz et al. 2015). Thus, the pathological role of GDAP1 in this disease development remains to understand. Cellular and animal models expressing *GDAP1* mutations surely represent the most accessible and easier models to mimic GDAP1-induced pathophysiology. Murine and human GDAP1 proteins share 94% of amino acid homology supporting the relevance of this rodent model from expression and localization studies (Niemann et al. 2005; Pedrola et al. 2008), to structural studies

(Googins et al. 2020), upgraded by two existing *GDAP1* knock-out animal models (Niemann et al. 2014; Barneo-Muñoz et al. 2015). Further analyses were conducted using Drosophila, and its *GDAP1*-ortholog gene (CG4623) (López Del Amo et al. 2015; López del Amo et al. 2017), or yeast models, transfected with the human *GDAP1* (Estela et al. 2011; Rzepnikowska et al. 2020). Anyway, the high intra-species and inter-species variability, together with the complexity of GDAP1 molecular mechanisms involved in Charcot-Marie-Tooth disease, may limit the animal models' reliability. Concerning the cellular models developed for GDAP1, most of them have animal origin (mice, rats) (Niemann et al. 2005, 20; Pedrola et al. 2008; Huber et al. 2013), or are immortalized cell lines, naturally expressing *GDAP1* (SH-SY5Y, N1E-115, HT22) (Niemann et al. 2005; Pedrola et al. 2005; Noack et al. 2012; González-Sánchez et al. 2017), or by transfection (HeLa, Cos7) (Pedrola et al. 2008; Wagner et al. 2009; Kabzińska et al. 2011; Huber et al. 2013). Indeed, a limited number of cell types express *GDAP1*, notably neurons and Schwann cells. These cell types cannot be obtained from humans, and used, in vitro, as cellular models. Given the inability to culture human neural cells, the only model available in these conditions was represented by human fibroblasts (Cassereau et al. 2009; Noack et al. 2012; Cassereau et al. 2020), which, unfortunately, poorly express *GDAP1* (Noack et al. 2012). The aim of this study was to go beyond limits imposed by existing animal and cellular models, developing a new solid model of human motor neurons carrying the homozygous p.Ser194* mutation in *GDAP1* to investigate GDAP1 functions and extrapolate data from previous studies.

In animal models, like mice and rats, GDAP1 has been shown to be largely expressed in neurons. In particular, the higher expression was detected in cerebellum, cerebral cortex, hippocampus, olfactory bulb, spinal nerve, but also in sciatic nerve, and motor and sensory neurons (Niemann et al. 2005; Pedrola et al. 2005; 2008). *GDAP1* expression in Schwann cells was controversial, whereas, in non-neural tissues, it was poorly explored (Niemann et al. 2005; Pedrola et al. 2005; 2008). Here, we compared, for the first time, *GDAP1* mRNA and protein expression in four cell types of the same control subject (Ctrl-1): fibroblasts, hiPSC, NP, and MN. mRNA expression revealed, on Ctrl-1 cells, that GDAP1 is weakly expressed in fibroblasts and hiPSC, while its expression was significantly higher in NP, and, above all, in MN. It is interesting to note that *GDAP1* mRNA in fibroblasts represented only 3% of NP-*GDAP1* mRNA, and 1.8% of MN-*GDAP1* mRNA. This is in agreement with Noack et al. work, who showed that control human fibroblasts expressed only 2.6% of *GDAP1* mRNA compared to embryonic stem cells-derived motor neurons (Noack et al. 2012). Interestingly, in patient's cells, presenting the homozygous codon-stop mutation c.581C>G in exon 5, *GDAP1* mRNA was only 10-20% of mRNA estimated in each cell types of Ctrl-1, reaching 6- and 8-fold smaller than those assessed in Ctrl-1 NP and Ctrl-1 MN. Our data seem to suggest that *GDAP1* mRNA is degraded in patient's cells. Since mutated *GDAP1* mRNA contains a premature termination codon (PTC), the Nonsense-mediated mRNA decay (NMD) system could be activated and induce its degradation, preventing the synthesis of a truncated, and maybe non-functional, protein (Auer-Grumbach et al. 2008). In any case, the NMD system is not always 100% efficient and some PTC-mRNA can escape NMD, and be detected by qPCR, as shown here. Real time qPCR results were also supported by GDAP1 protein expression. Indeed, GDAP1 was not express in fibroblasts, both in controls and patient, while the GDAP1 staining was present in Ctrl's MN, and, as expected, lacked in patient's MN. Given the high GDAP1 neural expression, we chose MN and NP, as cellular models to investigate its functions, and evaluate its role in Charcot-Marie-Tooth disease development. However, the weak GDAP1 expression detected in fibroblasts do not exclude a GDAP1 role in this cell type, and the possibility of conducting functional studies of them (Cassereau et al. 2009; 2020). Based on our results, GDAP1 seems also to be weakly expressed in hiPSC. We think that the higher spontaneous differentiation, and the reduced maintenance of stemness, observed in patient's hiPSC, may be the consequence of GDAP1 lacking. Indeed, as demonstrated by Prieto et al., *GDAP1*

knock-out impairs cell reprogramming, and it alters cell cycle progression, in murine hiPSC (Prieto et al. 2016).

Morphological and functional analyses, conducted on human MN, allowed highlighting two main mechanisms, the energetic metabolism dysfunction and the oxidative stress, as key components in CMT disease progression. First, we investigated the mitochondrial morphology and oxidative phosphorylation. Electron microscopy revealed, exclusively in patient's MN, a general disorganization of mitochondrial cristae, which could affect the inner mitochondrial space and subsequent metabolism. The disruption of cristae structure has already been associated to other diseases characterized by a mutation or a lack of proteins involved in mitochondrial functions, such as Optic atrophy 1 (OPA1) protein (Perkins, Bossy-Wetzel, e Ellisman 2009), or Mitofusin 2 (Mfn2) protein (Vallat et al. 2008). Cristae abnormalities were also reported in nerves' axonal mitochondria of a CMT2 patient, carrying the c.174_176delGCCinsTGTG mutation in *GDAP1* (Benedetti et al. 2010). We investigated, therefore, if mitochondria morphological alterations resulted in an electron transport chain's (ETC) impairment. However, only a slight increase in succinate dehydrogenase activity was observed, but not reached significant levels, and ATP production was preserved in patient's fibroblasts and MN. However, the markers used to evaluate oxidative phosphorylation could not be pertinent, thus the measurement of each complex activity, by oxygraphy, could be useful to investigate ETC function. Based on these preliminary results and previous studies, GDAP1 can play a key role in controlling mitochondrial morphology and dynamics (Niemann et al. 2005; 2009; Huber et al. 2013). Anyway, the morphological disturbance, induced by the GDAP1 p.Ser194* mutation in our conditions seems to not impact the ETC activity and the cellular respiration process.

Moreover, in cytoplasm of patient MN, vacuoles, suspected to be lipid droplets (LD), were observed and could be considered as an accumulation of energetic substrate, such as triglycerides, linked to a defect of mitochondrial beta oxidation or a hallmark of cellular stress, previously observed in nutrient imbalance, inflammation and oxidative stress (Jarc e Petan 2019). Moreover, several studies have demonstrated that their accumulation is one of earliest events following the induction of cellular apoptosis (Boren e Brindle 2012). Thus, the accumulation of LD could be also considered as an early signal of apoptotic pathways' activation, explaining the significant reduction of patient's MN observed in last steps of neural differentiation. The synthesis of lipid droplets, in neurons, has been observed in pathogenesis of several neurodegenerative diseases, like amyotrophic lateral sclerosis (ALS), Huntington's disease, Alzheimer's disease, Parkinson's disease and Hereditary spastic paraplegia (Farmer et al. 2020). LD were also described in the ultrastructural analysis of motor neurons obtained from *GDAP1* knock-out mice (Barneo-Muñoz et al. 2015) in accordance with our results and supporting this relevant cellular model. In stress conditions, a cytoprotective role against reactive oxygen species (ROS) is also given to LD since they sequester fatty acids, a potential target of ROS, which save other vital cell targets of ROS to detrimental injury, such as membrane lipids, amino acids, and nucleic acids. This phenomenon is probably responsible for the LD formation in our cellular model of CMT-motor neurons carrying the *GDAP1* Ser194* mutation. In fact, GDAP1 has been also suggested to have an antioxidant role in cellular homeostasis (Noack et al. 2012; López Del Amo et al. 2015). Consequently, in patient's MN, the lack of GDAP1 protein increases the amount of generated ROS, supported, in our study, by the MitoSOX™ Red mitochondrial superoxide indicator analysis. However, in our study, a significant increase of ROS has also been detected in patient's fibroblasts, where GDAP1 is weakly expressed and lipid droplets lacking. The overproduction of superoxide anion, in *GDAP1*-mutated fibroblasts, has also been reported in a recent work (Cassereau et al. 2020). These data could support that, even if at lower levels, GDAP1 protein could be also present in cell types other than neural cells. In this case, nevertheless, other molecular mechanisms and proteins would take part to the cellular antioxidant defense, counterbalancing the GDAP1 deficiency.

In conclusion, the role of GDAP1 impairment in Charcot-Marie-Tooth pathophysiology through mitochondrial dysfunction and oxidative stress development was underlined in an original human model of motor neuron from patient's fibroblasts, carrying the homozygous codon-stop c.581C>G mutation. The results underlined that GDAP1 is mostly expressed in neural cell types such as MN and PN, but also, at lower levels, in fibroblasts and hiPSC cells. In patient's cells, 80-90% of *GDAP1* mRNA would be degraded by the NMD system, leading to the considerable reduction of GDAP1 protein. Taken together, these results demonstrated that hiPSC cells can be a powerful tool to recreate any suitable cellular model from patients carrying mutations, essential in understanding the pathophysiological role of the altered protein, but also necessary to develop new therapeutic strategies.

Acknowledgements

The authors thank the "Région Limousin", "Club 41", "Lions Club", "Mairie de St Yrieix La Perche", and the University Hospital of Limoges for their support. We thank the I-Stem institute (INSERM/UEVE UMR 861, AFM, Genopole, Evry, France) and the AFM-Téléthon institute for the training they offered to help us to generate hiPSC, and Claire Carrion of University of Limoges for the help in ICC acquisitions.

.

Funding

This research received no external funding.

Conflicts of Interest

The authors declare no conflict of interest.

Ethics approval and consent to participate

Ethical approval was obtained for the work described in this manuscript from the ethics committee of Limoges University Hospital: N°384-2020-40, as well as the consent of both parents to diffuse this human data. This study was performed in accordance with the Declaration of Helsinki.

References

Auer-Grumbach, M., C. Fischer, L. Papić, E. John, B. Plecko, R. Bittner, G. Bernert, et al. 2008. «Two Novel Mutations in the GDAP1 and PRX Genes in Early Onset Charcot-Marie-Tooth Syndrome». *Neuropediatrics* 39 (1): 33–38. https://doi.org/10.1055/s-2008-1077085.

Barneo-Muñoz, Manuela, Paula Juárez, Azahara Civera-Tregón, Laura Yndriago, David Pla-Martin, Jennifer Zenker, Carmen Cuevas-Martín, et al. 2015. «Lack of GDAP1 Induces Neuronal Calcium and Mitochondrial Defects in a Knockout Mouse Model of Charcot-Marie-Tooth Neuropathy». A cura di Gregory A. Cox. *PLOS Genetics* 11 (4): e1005115. https://doi.org/10.1371/journal.pgen.1005115.

Baxter, Rachel V., Kamel Ben Othmane, Julie M. Rochelle, Jason E. Stajich, Christine Hulette, Susan Dew-Knight, Faycal Hentati, et al. 2002. «Ganglioside-Induced Differentiation-Associated Protein-1 Is Mutant in Charcot-Marie-Tooth Disease Type 4A/8q21». *Nature Genetics* 30 (1): 21–22. https://doi.org/10.1038/ng796.

Benedetti, Sara, Stefano Carlo Previtali, Silvia Coviello, Marina Scarlato, Federica Cerri, Emanuela Di Pierri, Lara Piantoni, et al. 2010. «Analyzing Histopathological Features of Rare Charcot-Marie-Tooth Neuropathies to Unravel Their Pathogenesis». *Archives of Neurology* 67 (12). https://doi.org/10.1001/archneurol.2010.303.

Bird, Thomas D. 2020. «Charcot-Marie-Tooth (CMT) Hereditary Neuropathy Overview». In *GeneReviews®*, a cura di Margaret P. Adam, Holly H. Ardinger, Roberta A. Pagon, Stephanie E. Wallace, Lora JH Bean, Karen Stephens, e Anne Amemiya. Seattle (WA): University of Washington, Seattle. http://www.ncbi.nlm.nih.gov/books/NBK1358/.

Boren, J, e K M Brindle. 2012. «Apoptosis-Induced Mitochondrial Dysfunction Causes Cytoplasmic Lipid Droplet Formation». *Cell Death & Differentiation* 19 (9): 1561–70. https://doi.org/10.1038/cdd.2012.34.

Cassereau, Julien, Arnaud Chevrollier, Philippe Codron, Cyril Goizet, Naïg Gueguen, Christophe Verny, Pascal Reynier, Dominique Bonneau, Guy Lenaers, e Vincent Procaccio. 2020. «Oxidative Stress Contributes Differentially to the Pathophysiology of Charcot-Marie-Tooth Disease Type 2K». *Experimental Neurology* 323 (gennaio): 113069. https://doi.org/10.1016/j.expneurol.2019.113069.

Cassereau, Julien, Arnaud Chevrollier, Naïg Gueguen, Marie-Claire Malinge, Franck Letournel, Guillaume Nicolas, Laurence Richard, et al. 2009. «Mitochondrial Complex I Deficiency in

GDAP1-Related Autosomal Dominant Charcot-Marie-Tooth Disease (CMT2K)». *Neurogenetics* 10 (2): 145–50. https://doi.org/10.1007/s10048-008-0166-9.

Cuesta, Ana, Laia Pedrola, Teresa Sevilla, Javier García-Planells, María José Chumillas, Fernando Mayordomo, Eric LeGuern, Ignacio Marín, Juan J. Vílchez, e Francesc Palau. 2002. «The Gene Encoding Ganglioside-Induced Differentiation-Associated Protein 1 Is Mutated in Axonal Charcot-Marie-Tooth Type 4A Disease». *Nature Genetics* 30 (1): 22–25. https://doi.org/10.1038/ng798.

Estela, Anna, David Pla-Martín, Maribel Sánchez-Piris, Hiromi Sesaki, e Francesc Palau. 2011. «Charcot-Marie-Tooth-Related Gene *GDAP1* Complements Cell Cycle Delay at G_2/M Phase in *Saccharomyces Cerevisiae Fis1* Gene-Defective Cells». *Journal of Biological Chemistry* 286 (42): 36777–86. https://doi.org/10.1074/jbc.M111.260042.

Farmer, Brandon C., Adeline E. Walsh, Jude C. Kluemper, e Lance A. Johnson. 2020. «Lipid Droplets in Neurodegenerative Disorders». *Frontiers in Neuroscience* 14 (luglio): 742. https://doi.org/10.3389/fnins.2020.00742.

Faye, Pierre-Antoine, Nicolas Vedrenne, Federica Miressi, Marion Rassat, Sergii Romanenko, Laurence Richard, Sylvie Bourthoumieu, et al. 2020. «Optimized Protocol to Generate Spinal Motor Neuron Cells from Induced Pluripotent Stem Cells from Charcot Marie Tooth Patients». *Brain Sciences* 10 (7): 407. https://doi.org/10.3390/brainsci10070407.

González-Sánchez, Paloma, David Pla-Martín, Paula Martínez-Valero, Carlos B. Rueda, Eduardo Calpena, Araceli del Arco, Francesc Palau, e Jorgina Satrústegui. 2017. «CMT-Linked Loss-of-Function Mutations in GDAP1 Impair Store-Operated Ca2+ Entry-Stimulated Respiration». *Scientific Reports* 7 (1): 42993. https://doi.org/10.1038/srep42993.

Googins, Matthew R., Aigbirhemwen O. Woghiren-Afegbua, Michael Calderon, Claudette M. St. Croix, Kirill I. Kiselyov, e Andrew P. VanDemark. 2020. «Structural and Functional Divergence of GDAP1 from the Glutathione S-transferase Superfamily». *The FASEB Journal* 34 (5): 7192–7207. https://doi.org/10.1096/fj.202000110R.

Huber, Nina, Sofia Guimaraes, Michael Schrader, Ueli Suter, e Axel Niemann. 2013. «Charcot-Marie-Tooth Disease-associated Mutants of GDAP1 Dissociate Its Roles in Peroxisomal and Mitochondrial Fission». *EMBO Reports* 14 (6): 545–52. https://doi.org/10.1038/embor.2013.56.

Jarc, Eva, e Toni Petan. 2019. «Lipid Droplets and the Management of Cellular Stress», 18.

Kabzińska, Dagmara, Axel Niemann, Hanna Drac, Nina Huber, Anna Potulska-Chromik, Irena Hausmanowa-Petrusewicz, Ueli Suter, e Andrzej Kochański. 2011. «A New Missense GDAP1 Mutation Disturbing Targeting to the Mitochondrial Membrane Causes a Severe Form of AR-CMT2C Disease». *Neurogenetics* 12 (2): 145–53. https://doi.org/10.1007/s10048-011-0276-7.

Kim, Ji-Yon, So-Youn Woo, Young Bin Hong, Heesun Choi, Jisoo Kim, Hyunjung Choi, Inhee Mook-Jung, et al. 2016. «HDAC6 Inhibitors Rescued the Defective Axonal Mitochondrial Movement in Motor Neurons Derived from the Induced Pluripotent Stem Cells of Peripheral Neuropathy Patients with *HSPB1* Mutation». *Stem Cells International* 2016: 1–14. https://doi.org/10.1155/2016/9475981.

López del Amo, Víctor, Martina Palomino-Schätzlein, Marta Seco-Cervera, José Luis García-Giménez, Federico Vicente Pallardó, Antonio Pineda-Lucena, e Máximo Ibo Galindo. 2017. «A Drosophila Model of GDAP1 Function Reveals the Involvement of Insulin Signalling in the Mitochondria-Dependent Neuromuscular Degeneration». *Biochimica et Biophysica Acta (BBA) - Molecular Basis of Disease* 1863 (3): 801–9. https://doi.org/10.1016/j.bbadis.2017.01.003.

López Del Amo, Víctor, Marta Seco-Cervera, José Luís García-Giménez, Alexander J. Whitworth, Federico V. Pallardó, e Máximo Ibo Galindo. 2015. «Mitochondrial Defects and Neuromuscular Degeneration Caused by Altered Expression of Drosophila Gdap1: Implications for the Charcot–Marie–Tooth Neuropathy». *Human Molecular Genetics* 24 (1): 21–36. https://doi.org/10.1093/hmg/ddu416.

Martí, Salvador, Marian León, Carmen Orellana, Javier Prieto, Xavier Ponsoda, Carlos López-García, Juan Jesús Vílchez, Teresa Sevilla, e Josema Torres. 2017. «Generation of a Disease-Specific IPS Cell Line Derived from a Patient with Charcot-Marie-Tooth Type 2K Lacking Functional GDAP1 Gene». *Stem Cell Research* 18 (gennaio): 1–4. https://doi.org/10.1016/j.scr.2016.11.017.

Mathis, Stéphane, Cyril Goizet, Meriem Tazir, Corinne Magdelaine, Anne-Sophie Lia, Laurent Magy, e Jean-Michel Vallat. 2015. «Charcot–Marie–Tooth Diseases: An Update and Some New Proposals for the Classification». *Journal of Medical Genetics* 52 (10): 681–90. https://doi.org/10.1136/jmedgenet-2015-103272.

Niemann, Axel, Nina Huber, Konstanze M. Wagner, Christian Somandin, Michael Horn, Frédéric Lebrun-Julien, Brigitte Angst, et al. 2014. «The Gdap1 Knockout Mouse Mechanistically Links Redox Control to Charcot–Marie–Tooth Disease». *Brain* 137 (3): 668–82. https://doi.org/10.1093/brain/awt371.

Niemann, Axel, Marcel Ruegg, Veronica La Padula, Angelo Schenone, e Ueli Suter. 2005. «Ganglioside-Induced Differentiation Associated Protein 1 Is a Regulator of the Mitochondrial Network». *Journal of Cell Biology* 170 (7): 1067–78. https://doi.org/10.1083/jcb.200507087.

Niemann, Axel, Konstanze Marion Wagner, Marcel Ruegg, e Ueli Suter. 2009. «GDAP1 Mutations Differ in Their Effects on Mitochondrial Dynamics and Apoptosis Depending on the Mode of Inheritance». *Neurobiology of Disease* 36 (3): 509–20. https://doi.org/10.1016/j.nbd.2009.09.011.

Noack, Rebecca, Svenja Frede, Philipp Albrecht, Nadine Henke, Annika Pfeiffer, Katrin Knoll, Thomas Dehmel, et al. 2012. «Charcot–Marie–Tooth Disease CMT4A: GDAP1 Increases Cellular Glutathione and the Mitochondrial Membrane Potential». *Human Molecular Genetics* 21 (1): 150–62. https://doi.org/10.1093/hmg/ddr450.

Pedrola, Laia, Antonio Espert, Teresa Valdés-Sánchez, Maribel Sánchez-Piris, Erich E. Sirkowski, Steven S. Scherer, Isabel Fariñas, e Francesc Palau. 2008. «Cell Expression of GDAP1 in the Nervous System and Pathogenesis of Charcot-Marie-Tooth Type 4A Disease». *Journal of Cellular and Molecular Medicine* 12 (2): 679–89. https://doi.org/10.1111/j.1582-4934.2007.00158.x.

Pedrola, Laia, Antonio Espert, Xingyao Wu, Reyes Claramunt, Michael E. Shy, e Francesc Palau. 2005. «GDAP1, the Protein Causing Charcot–Marie–Tooth Disease Type 4A, Is Expressed in Neurons and Is Associated with Mitochondria». *Human Molecular Genetics* 14 (8): 1087–94. https://doi.org/10.1093/hmg/ddi121.

Perkins, Guy, Ella Bossy-Wetzel, e Mark H. Ellisman. 2009. «New Insights into Mitochondrial Structure during Cell Death». *Experimental Neurology* 218 (2): 183–92. https://doi.org/10.1016/j.expneurol.2009.05.021.

Pla-Martín, David, Carlos B. Rueda, Anna Estela, Maribel Sánchez-Piris, Paloma González-Sánchez, Javier Traba, Sergio de la Fuente, et al. 2013. «Silencing of the Charcot–Marie–Tooth Disease-Associated Gene GDAP1 Induces Abnormal Mitochondrial Distribution and Affects Ca2+ Homeostasis by Reducing Store-Operated Ca2+ Entry». *Neurobiology of Disease* 55 (luglio): 140–51. https://doi.org/10.1016/j.nbd.2013.03.010.

Prieto, Javier, Marian León, Xavier Ponsoda, Francisco García-García, Roque Bort, Eva Serna, Manuela Barneo-Muñoz, et al. 2016. «Dysfunctional Mitochondrial Fission Impairs Cell Reprogramming». *Cell Cycle* 15 (23): 3240–50. https://doi.org/10.1080/15384101.2016.1241930.

Rzepnikowska, Weronika, Joanna Kaminska, Dagmara Kabzińska, e Andrzej Kochański. 2020. «Pathogenic Effect of GDAP1 Gene Mutations in a Yeast Model». *Genes* 11 (3): 310. https://doi.org/10.3390/genes11030310.

Rzepnikowska, Weronika, e Andrzej Kochański. 2018. «A Role for the GDAP1 Gene in the Molecular Pathogenesis of Charcot-Marie-Tooth Disease». *Acta Neurobiologiae Experimentalis* 78 (1): 1–13. https://doi.org/10.21307/ane-2018-002.

Saporta, Mario A., Vu Dang, Dmitri Volfson, Bende Zou, Xinmin (Simon) Xie, Adijat Adebola, Ronald K. Liem, Michael Shy, e John T. Dimos. 2015. «Axonal Charcot–Marie–Tooth Disease Patient-Derived Motor Neurons Demonstrate Disease-Specific Phenotypes Including Abnormal Electrophysiological Properties». *Experimental Neurology* 263 (gennaio): 190–99. https://doi.org/10.1016/j.expneurol.2014.10.005.

Shi, Lei, Lihua Huang, Ruojie He, Weijun Huang, Huiyan Wang, Xingqiang Lai, Zhengwei Zou, et al. 2018. «Modeling the Pathogenesis of Charcot-Marie-Tooth Disease Type 1A Using Patient-Specific IPSCs». *Stem Cell Reports* 10 (1): 120–33. https://doi.org/10.1016/j.stemcr.2017.11.013.

Sivera, Rafael, Marina Frasquet, Vincenzo Lupo, Tania García-Sobrino, Patricia Blanco-Arias, Julio Pardo, Roberto Fernández-Torrón, et al. 2017. «Distribution and Genotype-Phenotype Correlation of GDAP1 Mutations in Spain». *Scientific Reports* 7 (1): 6677. https://doi.org/10.1038/s41598-017-06894-6.

Takahashi, Kazutoshi, e Shinya Yamanaka. 2006. «Induction of Pluripotent Stem Cells from Mouse Embryonic and Adult Fibroblast Cultures by Defined Factors». *Cell* 126 (4): 663–76. https://doi.org/10.1016/j.cell.2006.07.024.

Vallat, Jean-Michel, Robert A. Ouvrier, John D. Pollard, Corinne Magdelaine, Danqing Zhu, Garth A. Nicholson, Simon Grew, Monique M. Ryan, e Benoît Funalot. 2008. «Histopathological Findings in Hereditary Motor and Sensory Neuropathy of Axonal Type With Onset in Early Childhood Associated With *Mitofusin 2* Mutations». *Journal of Neuropathology & Experimental Neurology* 67 (11): 1097–1102. https://doi.org/10.1097/NEN.0b013e31818b6cbc.

Wagner, Konstanze M., Marcel Rüegg, Axel Niemann, e Ueli Suter. 2009. «Targeting and Function of the Mitochondrial Fission Factor GDAP1 Are Dependent on Its Tail-Anchor». A cura di Mark R. Cookson. *PLoS ONE* 4 (4): e5160. https://doi.org/10.1371/journal.pone.0005160.

Supplementary data

Supplementary materials:

DNA extraction

DNA was extracted from fibroblasts and hiPSC of Ctrl-1, Ctrl-2, and patient, using the Puregene Tissu kit (©QIAGEN), and following manufacturer's instructions.

Sanger Sequencing

Primers, for each *GDAP1* exon, were designed on the Human GHCh37/hg19 genome (Supplementary data). Extracted DNA was amplified, and sequenced on the Applied Biosystems 3130 xl Genetic Analyzer (Applied Biosystems). Sequences were aligned using the Sequencher 4.7 software.

Supplementary tables:

Supplementary table 1 Primary antibodies used for characterization of hiPSC and neural cells.

Antibody	Company	Cat. Number	Species	Dilution
		Pluripotency markers		
Sox2	Biolegend	630802	Rabbit	1:200
Oct3/4	Santa Cruz Biotech	sc-5779	Mouse	1:50
Nanog	DSHB	PCRP-NANOGP1-2D8-s	Mouse	1:5
		Germinal Layers markers		
α-SMA	DAKO	M0851	Mouse	1:500
Sox17	R&D	AF1924	Goat	1:100
MAP2	Merck	M-4403	Mouse	1:500
		Neural markers		
PGP9.5	Abcam	ab108986	Rabbit	1:100
Tuj1	R&D	MAB1195	Mouse	1:1000
Chat	Chemicon	AB144P	Goat	1:50
		Other		
GDAP1	Proteintech	13152-1-AP	Rabbit	1:100
P4HB	OriGene	AF0910-1	Mouse	1:100
Ki-67	Leica	NCL-L-Ki67-MM1	Mouse	1:100

Supplementary results:

hiPSC generation, maintaining and validation

Following the iStem (INSERM/UEVE UMR861, AFM, Genopole, Evry, France) procedure, hiPSC cells were generated from fibroblasts of Ctrl-1 (A), Ctrl-2 (B), and the CMT-patient (C). Two weeks after fibroblasts' nucleofection, hiPSC colonies were selected for each subject. One clone for each subject was amplified and, at passage 15, validated with all quality controls. Colonies' morphology was checked. Pluripotency was established by the alkaline phosphatase test, the EB formation, the spontaneous differentiation in the three germ layers, and immunocytochemistry analysis for pluripotency markers (Supplementary figure 1). We verified also, by array Comparative Genomic Hybridization (aCGH), the lack of large genomic copy number variations (CNV) in hiPSC genome. Thus, for Ctrl-1, Ctr-2, and the patient, aCGH allowed comparing the genome of hiPSC with the genome of own fibroblasts. It demonstrated the absence of novel Copy Number Variations (CNV), as large deletions or duplications, supporting that hiPSCc and fibroblasts have the same genetic background (data not shown).

Motor neurons generation and validation

For each subject, hiPSC were led to neural differentiation, following the protocol described by Faye et al (Faye et al. 2020) (Supplementari figure 2). Briefly, hiPSC colonies were cut to obtain EB, which were first cultured in suspension, and secondly seeded to generate rosettes. The selection of rosettes allowed isolating neural progenitors (NP), which were amplified and, after 5-6 passages, seeded at low density, to generate motor neurons (MN). The same protocol was successfully performed for Ctrl-1, Ctrl-2 and the CMT-patient.

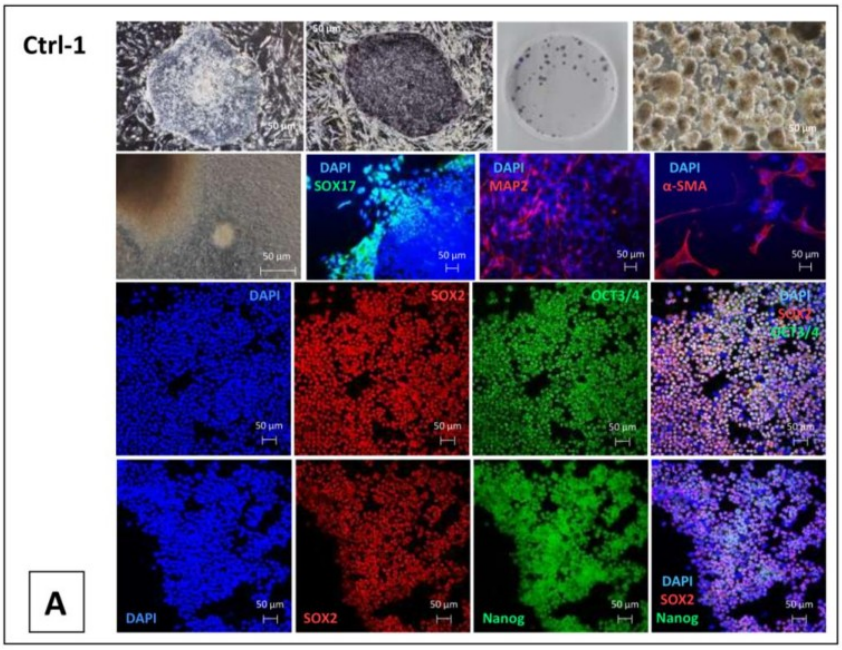
Ctrl-1
DAPI
SOX17
DAPI
MAP2
DAPI
α-SMA
DAPI
SOX2
OCT3/4
DAPI
SOX2
OCT3/4
DAPI
SOX2
Nanog
DAPI
SOX2
Nanog
A

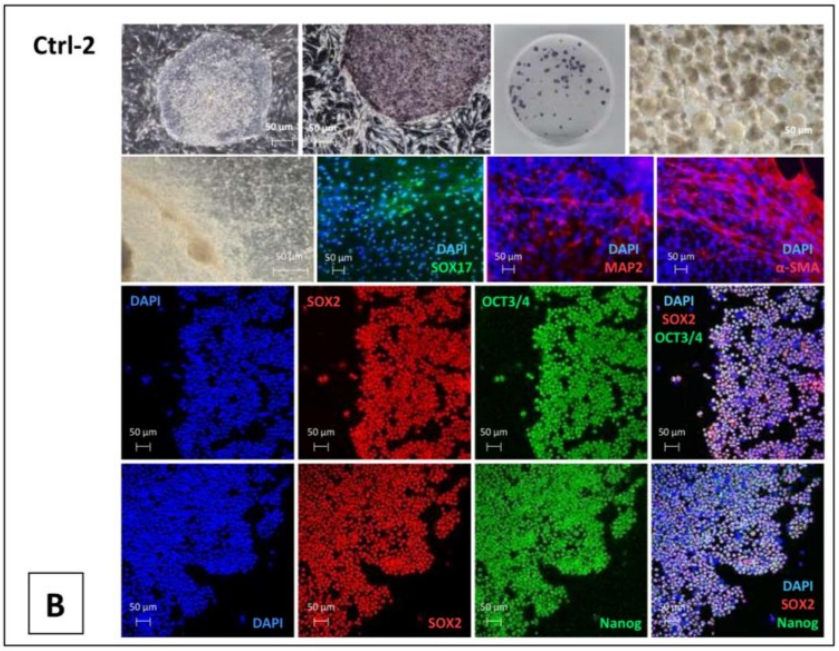
Ctrl-2
DAPI
SOX17
DAPI
MAP2
DAPI
α-SMA
DAPI
SOX2
OCT3/4
DAPI
SOX2
OCT3/4
DAPI
SOX2
Nanog
DAPI
SOX2
Nanog
B

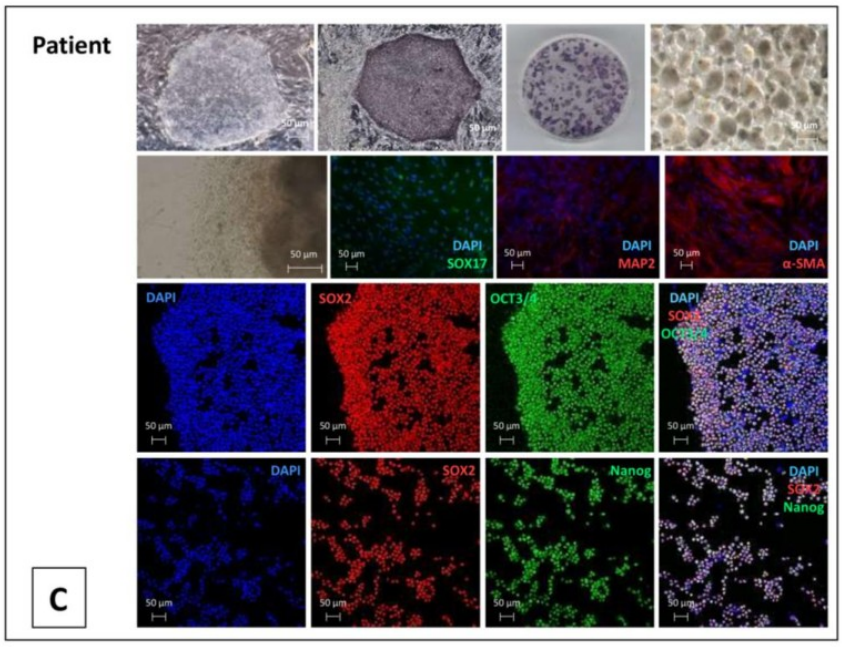

Supplementary figure 1 HiPSC quality controls for Ctrl-1 (A), Ctrl-2 (B), and patient (C). hiPSC colonies had a typical morphology, expressed alkaline phosphatase, could originate EB and spontaneous differentiate in the three embryonic germ layers [Sox17 (green): endoderm, α-SMA(red): mesoderm, MAP2 (red): ectoderm]. hiPSC expressed also pluripotency markers: Oct3/4 (green), Sox2 (red), Nanog (green).

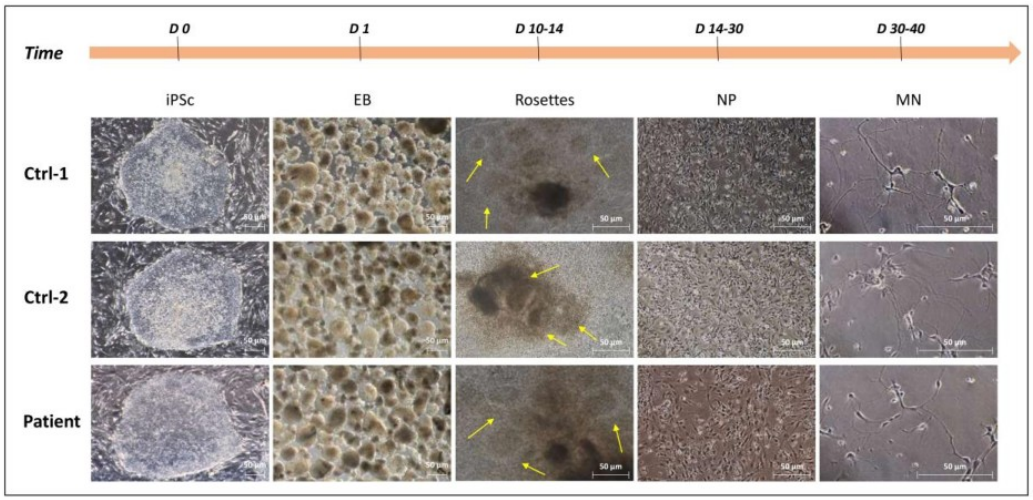

Supplementary figure 2 hiPSC differentiation into motor neurons, for Ctrl-1, Ctrl-2 and patient from D0 to D30-40.

Article 6: Complementary results

Additional functional studies, on fibroblasts and hiPSC-derived PN and MN, were performed, on patient 3-A and controls, to investigate other important aspects potentially connected to *GDAP1*. Specifically, we evaluated cellular levels of total glutathione (GSH) and oxidized glutathione (GSSG), and the mitochondrial membrane potential. Given technical issues encountered, and difficulties in results' interpretation, we present them here, in a separate section.

- **Glutathione quantification**

Cellular levels of total GSH were estimated in fibroblasts, PN, and MN, of the two control subjects, and the CMT-patient presenting the homozygous GDAP1 p.Ser194* mutation.

In fibroblasts, it seemed that total GSH was higher in patient's cells, compared to Ctrl-1 and Ctrl-2. Anyway, in both cases, difference was not significant (Complementary Figure 1A).

In NP, we did not observe any difference between controls and patient (Complementary Figure 1B).

In MN, total GSH was apparently reduced in patient's cells, compared to controls, even if difference was not statistically significant (Complementary Figure 1C). In this case, GSH quantification was performed at day 7 of NP final differentiation into MN. As shown in the Article 6, at d7, the number of patient's MN was significantly lower than controls' MN. Since the GHS test does not take into account this cells death rate, we cannot directly compare raw values. We can only consider that patient's MN were ~41% of Ctrl-1 MN, and their GSH concentration was ~33% of GSH concentration in Ctrl-1 MN. Compared to Ctrl-2 MN, patients' MN were ~46%, and their GSH concentration was 36% of theirs. Calculating the ratios, we can suppose that GSH could be slightly lower in patient's MN than in controls' MN, but with current results, we cannot draw conclusions from this analysis.

On the other hand, given the limited availability of cells, GSSG levels were not detectable. We were not, thus, able to quantify oxidized glutathione.

Overall, this test was not suitable for total and oxidized glutathione quantification in our cellular models. Alternative tests, which allow also cell counting, could be more appropriate for this type of analysis.

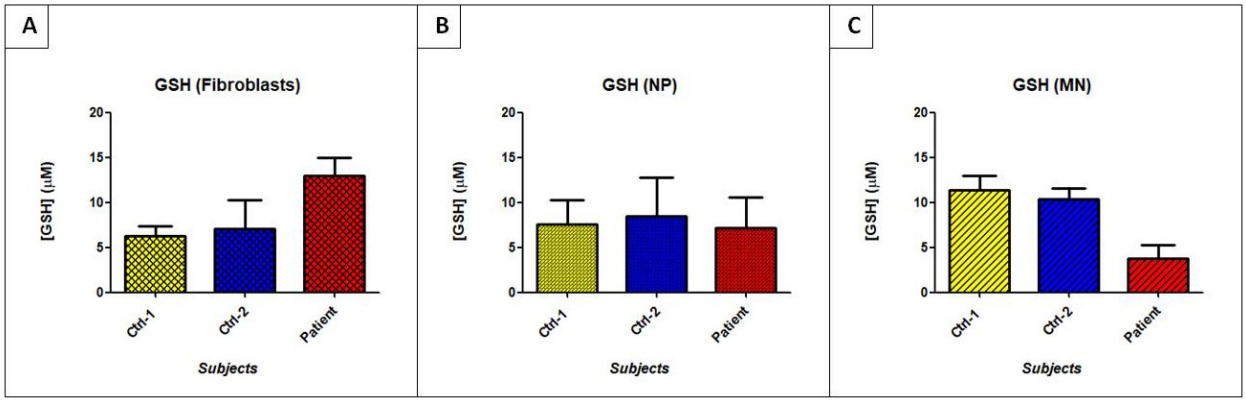

Complementary Figure 1: Measurement of GSH in fibroblasts, NP, and MN, of patient, Ctrl-1 and Ctrl-2.

- **Mitochondrial membrane potential (ΔΨ) measurement**

Mitochondrial membrane potential was evaluated, on MN of patient and controls, with the JC-1 probe, analyzed by flow cytometry. Anyway, technical problems occurred in MN labeling, and obtained results were not conclusive. Preliminary tests would be necessary before this analysis can be performed again.

Conclusion

Two models of hiPSC for *GDAP1* have already been proposed (Saporta et al. 2015; Martí et al. 2017). However, no work has reported the creation of hiPSC-derived MN for *GDAP1*, and, to date, functional studies on human MN have never been described. In the present study, thanks to hiPSC strategy, we could obtain a cellular model of human MN, to investigate pathological mechanisms associated with a codon-stop mutation in *GDAP1*. In CMT-patients' MN, we could detect new features and abnormalities, like altered mitochondrial structure and vacuoles (LD?) accumulation, but also confirm already suggested *GDAP1* functions, in protection from ROS. Further in-depth analyses, on this cellular model, will be needed to clarify *GDAP1* implication in cellular respiration and metabolism, as well as in mitochondrial dynamics. Specifically, oxygraphy, lipidomics analysis, and mitochondrial tracking, have been already envisaged, even if limited, so far, by the restricted number of cells. Glutathione and mitochondrial membrane potential will be also revaluated, after modification of current protocols.

Discussion and Perspectives

This project entirely focused on hereditary peripheral neuropathies, considering two main aspects of this group of diseases: their genetics and molecular analysis, and their functional analysis, through a specific cellular model. Here, we argue about our new findings and emerged results, discussing whether and how they can actually be relevant for existing, and future, procedures and research. At the same time, we evaluate the main practical limits of our study, and the possible improvements to introduce, with the purpose of better exploring and characterizing hereditary peripheral neuropathies.

Part I - Genetic analysis of hereditary peripheral neuropathies

In last years, the introduction of NGS technology, in routine analyses of hereditary peripheral neuropathies, has surely improved and simplified the diagnosis procedure. Targeted NGS is widely used to directly screen the more than 90 genes involved in Charcot-Marie-Tooth disease and sensory and motor neuropathies. At Biochemistry and Molecular Genetics Department of University Hospital of Limoges, a 93-gene panel is currently employed, whose libraries are prepared with an amplicon-based strategy, and sequenced on Ion Proton sequencer. Previously, data derived from target NGS were exclusively exploited to search for point mutations and small indels, given the lack of bioinformatic tools for CNV detection. Cov'Cop and CovCopCan software were conceived and designed, at University Hospital of Limoges, to extend the potential of NGS analysis to CNV.

CMT and CNV

The lack of a systematic exploration of CNV, in all CMT- and peripheral neuropathies-genes, is due to the poor and insufficient knowledge about the role of these large (>1 kb) deletions and duplications in the pathology. If we exclude *PMP22* duplication, which is the genetic cause of ~15% of all CMT diagnosed cases, CNV in other genes have been occasionally described. In 2010, a first study was conducted in a cohort of 97 CMT-patients, to evaluate CNV in 34 CMT genes, by comparative

genomic hybridization (CGH) microarrays. They detected CNV in three CMT-genes (*ARHGEF10, MTMR2, SPTLC1),* but none of them were considered disease-causing, suggesting the rare implication of CNV in CMT pathology (Huang et al. 2010). After few months, another work described, for the first time, two different large deletions which entirely eliminated *GJB1* coding sequence, in CMT1X patients (Gonzaga-Jauregui et al. 2010). Then, CNV occurrence in CMT was also reported in *MPZ* gene, first described as simple duplication (Høyer et al. 2011), then as multiplication and increased gene dosage, with the identification of five *MPZ* copies (Maeda et al. 2012). Further analyses highlighted CNV in seven genes already associated with CMT disease (*NDRG1*, *PRX*, *FGD4*, *INF2*, *GAN*, *GDAP1*, *LRSAM1*) (Okamoto et al. 2014; Dohrn et al. 2017; Mortreux et al. 2020). Most of CNV reported for CMT were deletions, less often duplications.

Since, in last years, few studies have explored and identified occurrence of CNV to be responsible for CMT pathology, favoring the investigation of point mutations and small indels, this phenomenon is still considered rare. In previous studies, CNV frequency in CMT has been estimated between 1% and 2.5% (Høyer et al. 2011; Pehlivan et al. 2016; Mortreux et al. 2020). In Limoges, the analysis of target NGS data, by Cov'Cop and CovCopCan software, has allowed us to detect CNV in 15.4% of CMT patients (Miressi et al. 2020) – Article 3), even if their pathogenicity is still under investigation. In any case, our findings seem to suggest that CNV could be more frequent than reported in literature. For instance, in the two clinical cases (Article 2 and Article 3) presented in this study, we described two novel CNV, one deletion, and one duplication, in *SACS* and *AARS1*.

Since 2018, at Biochemistry and Molecular Genetics Department of University Hospital of Limoges, the CNV systematic analysis, by bioinformatic approach, has been included in the routine diagnostic procedure. Given the emerging role of CNV in CMT disease, the current molecular examination is now regularly combined with investigation of genomic deletions and duplications, in CMT-panel genes. In some cases, detected CNV are, then, more thoroughly explored by the EA6309 research team, at University of Limoges. Other CNV are currently under analysis and several articles are in preparation.

Between diagnosis and research

Bioinformatic software, as Cov'Cop and CovCopCan, have been conceived with a dual function. First, they are essential in detecting CNV, already described and already linked to CMT. On the other way, their main role is surely connected with the research field. Since few CNV have been reported for CMT and associated peripheral neuropathies, we can suppose, on the basis of our preliminary results, that a huge number of CNV rests to be discovered. The high frequency of *PMP22* duplication in some CMT1 forms, and the simultaneous subsistence of *PMP22* point mutations in other CMT forms, reinforces the idea that CNV may occur in genes for which pathological single nucleotide mutations have already been confirmed. The detection of new disease-causing CNV could also be important in revealing unknown molecular mechanisms, caused by the genomic imbalance (gain or loss), and responsible for specific pathological manifestations.

We think that a solid cooperation between diagnosis and research could help to reduce, at least in part, the present high rate of undiagnosed cases of peripheral neuropathies.

Is CMT a multilocus genetic pathology?

In inherited diseases, we tend to consider the unique correlation "one patient : one mutation", assuming that, in most of cases, only one genomic alteration is responsible for the observed disorder. The simultaneous presence of multiple point mutations or SV is generally reported in more complex pathologies, like cancers, characterized by high genomic instability (Whitworth et al. 2016). In 2016, an extensive analysis, on more than 7,000 patients requiring a molecular diagnosis, showed how 5% of diagnosed cases included two or more genomic loci (Posey et al. 2017). Furthermore, a more recent study has focused, in particular, on phenotypic expansions, i.e. on clinical cases characterized by a set of phenotypic features wider than those already described for the associated genomic locus. It revealed that ~32% of families with phenotypic expansions presented multilocus variations, a much higher proportion than that reported for the unselected cohort of patients (Karaca et al. 2018). All

these findings seem to suggest that complex and blended clinical manifestations could be, in most cases, the result of multiple genomic alterations, and, thus, reflect the combination of multiple impaired mechanisms. CMT pathology is known to be characterized by a high clinical and genetic heterogeneity, since various involved genes present different associated phenotypic features, and different modes of transmission (Morena, Gupta, and Hoyle 2019). In addition, in some cases, a moderate or striking intrafamilial variability has also been described (Bo et al. 2008; Kostera-Pruszczyk et al. 2014; Gogou et al. 2020). In CMT disease, various cases of digenic inheritance, which is the simultaneous occurrence of two disease-causing variations in two distinct genes, have been reported, for different associations of genes, as for example: *EGR2* and *GJB1* (Chung et al. 2005), *PMP22* (duplication) and *GJB1* (Hodapp et al. 2006), *GDAP1* and *MFN2* (Cassereau et al. 2011C; Vital et al. 2012), *LRSAM1* and *MARS*, *MFN2* and *PMP22* (point mutation) (Yoshimura et al. 2019). In some of these cases, within the same family, patients carrying both mutations showed a more severe phenotype, comparing to other family members carrying one single mutated gene (Chung et al. 2005; Hodapp et al. 2006; Cassereau et al. 2011C; Vital et al. 2012). We remarked this variable disease's severity in the case of Family 2 of our study. The daughter, who was more affected and with additional clinical signs (learning problems, mental retardation), presented the combination of three different CMT-mutated genes (*MORC2*, *MFN2*, *AARS1*), compared to her mother (*MORC2*, *AARS1*), who was less affected. Moreover, our findings are supported by the emerging role of modifier genes (or modifier alleles) in CMT pathogenesis, particularly investigated in recent years. Indeed, evidence from genetic studies suggest that the effect of one allele could be modified by a second allele, the so-called modifier gene (Kousi and Katsanis 2015). The primary mutated gene would be sufficient, by itself, to induce the phenotypic manifestation, while the second one would impact, for example, the disease severity or progression (Bis-Brewer, Fazal, and Züchner 2020). In the case of our Family 2, we cannot exclude that *MFN2* mutation and *AARS1* duplication can actually act like modifier alleles in the daughter, whereas the main CMT manifestation is due to the *MORC2* mutation (in mother and daughter).

Even if this is the first case of CMT disease reporting three variations in three different genes, we believe that the multilocus inheritance and the contribution of modifier genes are considerably underestimated in peripheral neuropathies, whose molecular diagnosis is often closed after the detection of one, or sometimes two, genomic mutations. The detailed assessment of the clinical history, as well as the accurate examination of the genotype/phenotype correlation, in all family members, are first crucial steps for a correct genetic analysis. The possibility of multiple genomic loci and a wilder genetic analysis should be envisaged in families with heterogenous phenotypes, as well as in sporadic complex cases.

Perspectives for diagnosis and research

As previously discussed, the molecular analysis at Biochemistry and Molecular Genetics Department of University Hospital of Limoges allows the routine diagnosis for CMT and associated peripheral neuropathies. On the other hand, in research, at University of Limoges, it is employed in discovery of novel mutations and mechanisms. This research purpose can be supported by more extensive NGS strategies, like WES, which has been tested for the complex genetic analysis reported in Article 3. WES could allow to go beyond the 93 genes of CMT-panel and reveal further pathogenic mutations in other exonic regions. The next step would then involve the examination of intronic regions, but also intergenic regions, through the WGS. Rare disease-causing intronic mutations have been detected in CMT genes, like *MPZ* or *GDAP1*, responsible for modifying splicing process (Sabet et al. 2006; Masingue et al. 2018). Furthermore, in some pathological conditions, more complex mechanisms can be induced by intronic alterations. For example, this is the case of the neurological disorder CANVAS (cerebellar ataxia, neuropathy, vestibular areflexia syndrome), which has been associated to the biallelic repeat expansion in an intronic region of *RFC1* gene (Cortese et al. 2019).

In diagnosis, the future systematic combination of the 93-genes panel with WES and WGS strategies will surely increase the chances of detecting multilocus genetic mutations in CMT disease. Currently, the main limit of these analyses is due to the high cost and the high number of data to interpret.

Part II - A cellular model for hereditary peripheral neuropathies

The genetic characterization is just the first step in the understanding of peripheral neuropathies. Even in case the genetic mutation has been well defined, it is necessary to evaluate its direct, or indirect, effects on cellular physiology. Cellular models are an essential tool to recreate pathological cellular contexts and explore impaired mechanisms induced by genomic mutations. For *GDAP1* gene, and, in particular, its axonal form of CMT2, we successfully developed a cellular model of human motor neurons, derived from human induced-pluripotent stem cells (hiPSC).

From hiPSC to motor neurons

Our cellular model of hiPSC-derived MN arose from the need to analyze pathophysiology of a specific CMT form, reproducing the same involved cellular type (MN), of the same affected species (humans). A considerable advantage of our strategy is the possibility to generate MN from dermal fibroblasts, an easy-to-obtain cell type. Skin biopsies were obtained thanks to the collaboration with the Neuropathies' Center of Reference of University Hospital of Limoges. Fibroblasts were reprogrammed in hiPSC applying the protocol proposed in 2006, by Pr Yamanaka, transfecting them with three plasmids expressing Oct4, Sox2, Klf4 et l-Myc genes (Takahashi and Yamanaka 2006). Despite the low reprogramming efficiency of plasmids, we opted for this strategy to avoid random integration and insertional mutagenesis events, occasionally occurring in virus transduction. We cultured reprogrammed hiPSC on feeder cells (MEF), with traditional culture media. With our protocol, we did not observe any technical problem, our hiPSC passed all quality controls, and they could easily generate embryonic bodies (EB) to be differentiated. We succeeded in created hiPSC for two CMT-patients carrying two different codon-stop mutations in *GDAP1* (p.Ser194* and p.Gln163*), and five unaffected subjects (three women, two men).

However, some aspects of our protocol can still be improved. Indeed, hiPSC culture on feeders has some drawbacks, since media preparation, MEF preparation, hiPSC cleaning and passage, are labor-intensive and very time-consuming, but also with a significant related cost. Additionally, culture on feeders uses animal-derived cells, which limits its use for eventual clinical application (Sasaki, Suzuki, and Takahashi 2015). We have, therefore, envisaged to approach the feeder-free (FF) culture. In order to organize this technical transition, a member of our research team has recently followed a technical training on FF hiPSC culture, in Regenerative Medicine and Skeleton (RMeS) INSERM U1229 of University of Nantes. This culture strategy could replace culture on feeders, as already shown in previous studies (Nakagawa et al. 2015; Colombier et al. 2020). We have already successfully cultured FF-hiPSC for two of the five controls, and for the p.Ser194* patient. The differentiation protocol from FF-hiPSC has to be tested in the next future.

In our study, after hiPSC amplification and validation, we could differentiate them into MN. In our laboratory team, we developed a new protocol to obtain MN from hiPSC in about 30 days. In last ten years, various differentiation protocols have been proposed. In most of them, stem cells were first detached to favor formation of EB, which were cultured in suspension, before being sedimented to obtain neural rosettes (Hu and Zhang 2009; Corti et al. 2012). Neural rosettes can be then easily selected to isolate neural progenitors, which can completely differentiate in MN (Lee et al. 2007; Lukovic et al. 2017). This procedure was followed in establishing our protocol. Then, we had to choose the most suitable differentiating factors, responsible for activation or inhibition of specific cellular pathways. Testing already described protocols, we obtained poor results. That is why we decided to focus on main mechanisms of embryonic development, and select main factors involved in MN-differentiation. With our new protocol, we obtained 100% cells expressing neuronal markers and 80% cells expressing spinal MN markers. MN were also ChAT-positive, and their electrical proprieties could be evaluated by patch clamp. The efficiency rate of our differentiation protocol was much higher compared to previous works (Dimos et al. 2008; Chambers et al. 2009; Hu and Zhang

2009), while the culture period (20-30 days) was on average of the others. More recently, some protocols reduced the differentiation time, and improved hiPSC-derived neurons' purity, through the stable expression of a transcription factor involved in neuronal differentiation (Ngn2) (Zhang et al. 2013; Wang et al. 2017). The hiPSC engineering has been obtained infecting them with lentivirus (Zhang et al. 2013) or adeno-associated virus (Wang et al. 2017), which implies all drawbacks of virus manipulation, already discussed above. Although our strategy takes, surely, more culture time, it does not require further manipulation on cells genome, and it rests a safer and fairly easy-to-achieve procedure.

Recently, we have considered additional factors which could improve our differentiation protocol. In a recent review, we explored the role of 1,25-Dihydroxyvitamin D3, or calcitriol, in the peripheral nervous system (Article 5). In pathological conditions, like nerve trauma, vitamin D3 administration seems to favor axonogenesis (Chabas et al. 2008; Chabas et al. 2013). On the other hand, its deficiency has been associated with diabetic peripheral neuropathy (Shehab et al. 2015; Alamdari et al. 2015). Calcitriol involvement in axon maintenance and regeneration rests to be investigated. Anyway, it could be interesting to evaluate if its supplementation, in hiPSC differentiation into MN, may have a synergistic effect with other differentiation factors, to favor the activation of neuronal pathways. In our differentiation protocol, Calcitriol could be supplemented after EB seeding, to promote rosettes formation, and maintained during all following steps, to help NP and MN growth.

A model for GDAP1 study

For the investigation of GDAP1 functions, many studies have already been conducted on animal and cellular models. Animal models (mice, *Drosophila melanogaster*, *Saccharomyces cerevisiae*) have been fundamental to evaluate the effects of *GDAP1* suppression/mutation/over- and under-expression, on the whole organism, so to reproduce, on them, a pathological condition comparable to the human CMT disease (Niemann et al. 2014; Barneo-Muñoz et al. 2015; López Del Amo et al.

2015; López del Amo et al. 2017; Estela et al. 2011; Rzepnikowska et al. 2020). Mice are definitely the animal model closer to humans, and their GDAP1 protein share 94% of amino acidic identity with the human GDAP1 (Googins et al. 2020). However, the two *GDAP1*-knockout murine models, proposed by two different research teams, presented some differences, in the age of onset of first symptoms (19 months *vs* 3 months), and, at histological level, in nerve structure and myelin aspect (hypomyelination *vs* normal myelin thickness) (Niemann et al. 2014; Barneo-Muñoz et al. 2015). These findings suggest that many parameters can vary, also in the same model, so it can be hard to evaluate if its features can be really compared to human condition. On the other hand, human cellular models are limited, since neurons and Schwann cells, which are the CMT-affected, and *GDAP1*-more expressing, cells, cannot be obtained from patients, and cultured *in vitro*. Also cellular models created by transfection of immortalized cell lines, turned out to be interesting in revealing unknown mechanisms associated to GDAP1. Anyway, we have to consider that the cellular context can mostly depend on the cell type. This means that, even if we induce *GDAP1* expression in a cell, we cannot be sure that all protein interactions, and all GDAP1-involving pathways, are conserved and activated in the same way as in neurons. The choice of cellular type could, thus, impact the observed results.

After evaluating all positive and negative aspects of existing GDAP1 models, we decided to develop a human cellular model of MN for *GDAP1*, exploiting the hiPSC technology. Our strategy presents multiple advantages. First, it is a human model, so there are not species-related inconveniences. Then, we recreated a model of MN, the cells directly involved in the CMT disease. Moreover, cells derive from dermal fibroblasts of CMT-patients. This means that all patient's genomic features are conserved, and *GDAP1* mutations are already present, and do not need to be introduced. MN, obtained with our differentiation protocol, can usually be cultured for 7-10 days after the final differentiation, enabling to perform all suitable studies, in this time period.

Our model of hiPSC-derived MN has allowed to obtain interesting results. However, it is not defect-free, and, in our study, two major drawbacks emerged: the time required for complete

differentiation (previously analyzed), and, above all, the number of cells. In fact, we had to face the limited availability of MN, mostly due to the high susceptibility of neural cell type. We noticed that, although NP are very proliferating cells, they could degenerate when cell passage is too elevated (>10), losing their ability to differentiate into MN. Therefore, some analyses, requiring a very high number of cells, have been excluded from the study. Specific functional tests will be discussed in the next section.

GDAP1 functional analyses

We successfully obtained MN from the five control subjects, and for the two CMT-patients, carrying two *GDAP1* homozygous mutations (p.Gln163*, p.Ser194*). Anyway, expression, morphological and functional studies were exclusively performed on cells belonging to patient 3-A, with the homozygous *GDAP1* p.Ser194* mutation, and cells of two controls (Ctrl-1 and Ctrl-2). First interesting results derived from expression studies. This was the first analysis that compared *GDAP1* mRNA expression in different cell types (fibroblasts, hiPSC, NP, MN), which were all human, and all derived from the same subject. The expression study has been also fundamental to validate our models, since our results, in each cell type, were in agreement with previous expression studies, conducted on animal cells and tissues, and human fibroblasts (Niemann et al. 2005; Pedrola et al. 2005; 2008; Noack et al. 2012). The confirmation of the higher *GDAP1* expression in neural cells supported the choice of MN as the more suitable cellular model to investigate *GDAP1* functions and its involvement in CMT disease. In patient MN, in addition, we demonstrated that *GDAP1* mRNA was degraded, and its protein quite absent.

Morphological examination, by EM, concerned the global structure of cells, to focus, then, on mitochondria morphology and internal organization, since GDAP1 protein is known to be located in the OMM (Niemann et al. 2005). For functional analyses, we selected preliminary tests that, a priori, did not require a too high number of cells. In particular, we decided to evaluate two main cellular

processes: the energy production (Succinate dehydrogenase activity and ATP quantification), and the oxidative stress (MitoSOX and Glutathione quantification).

First, in patient's MN we observed a general disorganization of mitochondrial inner space, and alteration of mitochondrial cristae structure. This could support the hypothesis that GDAP1 protein plays a role in regulating mitochondrial morphology and dynamics. GDAP1 involvement in mitochondrial fission and, maybe, fusion events had already been reported in previous works (Niemann et al. 2005; 2009; Wagner et al. 2009). However, the structural impairment, observed in inner mitochondrial space, seemed to not disturb Succinate dehydrogenase activity and ATP production, suggesting that GDAP1 could not be involved in energetic metabolism. Our findings appeared in contrast with analyses conducted by Cassereau *et al.*, in 2008 and 2019. In these cases, in CMT-patient's fibroblasts, carrying specific *GDAP1* mutations, they detected a deficiency of ETC Complex I activity, decreased respiration rate, and decreased ATP production (Cassereau et al. 2009; 2020). Given the low *GDAP1* expression level in fibroblasts, they may not be the most appropriate cellular model to detect GDAP1-induced impairment. Anyway, if the metabolic alteration has been detected in this cell type, it could be also present, and maybe in more significant way, in MN. That is why, a more deepened functional analysis of all ETC complexes, by oxygraphy, has been envisaged for future studies, thanks to the collaboration with the MitoLab, UMR CNRS 6015-INSERM 1083 of University of Angers. It might be necessary to perform oxygraphy on NP cells, more available than MN.

Secondly, we detected, in patient's MN, increased levels of oxidative stress, and, in particular, of mitochondrial superoxide anion. GDAP1 role in protection from ROS had been suggested in multiple studies, on different cellular and animal models (Noack et al. 2012; López Del Amo et al. 2015; Cassereau et al. 2020), and we confirmed it with the MitoSOX analysis.

In cytoplasm of the same cells, ultrastructural analysis revealed accumulation of spherical structures, that we supposed to be lipid droplets. This phenomenon has been described in some pathological conditions of the CNS, like Amyotrophic Lateral Sclerosis, Huntington's disease, Parkinson's disease,

even if their role is not completely known (Farmer et al. 2020). In CMT disease, only one recent work has described the formation of LD in human cells (Giudetti et al. 2020). This study was conducted on CMT2B fibroblasts carrying the p.Val162Met mutation in *RAB7* gene. In this case, the alteration of lipid metabolism and the LD accumulation have been associated with RAB7 role in controlling lipid signaling and lipophagy (Giudetti et al. 2020). In animal models, LD have been observed in embryonic motor neurons obtained from GDAP1 knock-out mice (Barneo-Muñoz et al. 2015). In our MN model, we suggested that LD formation could be associated with increased oxidative stress state, as shown in other cellular and animal models (Bailey et al. 2015; Jin et al. 2018). LD would act as a cellular defense system, to sequester and protect lipids from ROS action, when GDAP1 is suppressed. Another hypothesis could be that lipids accumulation is the consequence of a dysregulated lipid metabolism in MN, as a defect in the carnitine carrier system, which would induce accumulation of lipids in cytoplasm, or in the mitochondrial β-oxidation, responsible for lipids catabolism. In fact, in a cellular model of primary human muscle cells, it has been observed that GDAP1 silencing reduced lipid oxidation, without affecting glucose metabolism (Lassiter et al. 2018).

A lipidomic analysis could be interesting in establishing the complete lipid profile, for patient's and controls' MN (or NP), and evaluate which lipid class is more perturbed by *GDAP1* mutation. This would also help us to identify the origin of LD. The collaboration with the University of Angers will be essential for our purpose.

The measurement of total and oxidized glutathione could provide an additional proof about GDAP1 participation in antioxidant cellular defenses, as shown in previous studies (López Del Amo et al. 2015). Anyway, as reported in "Complementary results" section, total glutathione quantification, in NP and MN, cannot be compared between patient's and controls' cells, since number of cells was too much variable and not quantifiable. Furthermore, levels of oxidized glutathione were too low to be detected. Another Glutathione quantification test has to be evaluated, to make the experiment suitable for all cell types.

Taken together, functional analyses allowed to discover some altered mechanisms induced, in MN, by the homozygous p.Ser194* mutation in *GDAP1*. Our preliminary results will be deepened through additional analyses, to better characterized the pathological state. This study confirmed how it can be important to chose the good cellular model in this kind of investigation, and how hiPSC could be a fundamental tool to obtain it.

Our project has focused on a *GDAP1* mutation, p.Ser194*, associated with a recessive axonal form of CMT disease (CMT2H). The same protocol can also be employed for alternative pathological CMT axonal forms. Given the remarkable clinical difference observed between GDAP1-autosomal dominant and GDAP1-autosomal recessive forms, functional analyses on human MN, obtained from AD- and AR-patients, could reveal independent impaired mechanisms in these two different conditions. Moreover, *GDAP1* mutations have also be described in demyelinating CMT. In fact, previous studies revealed that *GDAP1* is not only expressed in neuronal cells, but also in Schwann cells (Cuesta et al. 2002; Niemann et al. 2005). This strategy, therefore, can reveal impaired mechanisms in both cell types. Exactly as for MN, SC can be generated from hiPSC, for patients and controls, and some differentiation protocols have already been proposed (Shi et al. 2018; Muller et al. 2018). Moreover, it could be interesting to evaluate if the interaction of these two cell types can further impact the pathogenic process. To recreate*, in vitro*, a cellular model that reflects, as much as possible, the *in vivo* condition, we can envisage to establish a MN/SC co-culture. In this way, we could first consider if some molecular mechanisms are impaired when cells are separately cultured, then, we could analyze if MN/SC co-culture alters the observed features.

CMT treatment and further applications for our hiPSC-derived motor neurons

The prevalence of Charcot-Marie-Tooth disease is estimated to be 1/2500. Many mutations in many genes have been detected, and functional analyses, on animal and cellular models, have revealed multiple molecular mechanisms, differentially impaired in CMT forms. In any case, despite the current wide knowledge about this pathology and its causes, a treatment for CMT diseases is not yet available. A recent study identified three main obstacles in the discovery of a valid CMT treatment: the genetic and clinical heterogeneity of Charcot-Marie-Tooth disease, which is often considered as a motley group of motor-sensory neuropathies; a relatively small number of patients for each CMT form, which can limit the interest of pharmaceutical companies; the mismatch between results observed in preclinical studies, on animal and cellular models, and the clinical trials, on human subjects (Juneja et al. 2019). Most of existing clinical trials have been proposed for CMT1A, the most frequent form. A first interesting study concerned a treatment with ascorbic acid (vitamin C) and progesterone antagonists (Wayne State University), but, although promising results on mice, it failed in clinical trials (Passage et al. 2004; Pareyson et al. 2011; Lewis 2013). Another advanced study is based on PXT3003 (Pharnext), a low-dose combination of baclofen, naltrexone, and sorbitol. Positive preclinical outcomes in rodent models (mice and rats), led PXT3003 to be accepted for an exploratory, randomised, double-blind and placebo-controlled phase II study (Chumakov et al. 2014; Attarian et al. 2014; 2016). Since, in phase II, clinical effectiveness was demonstrated, PXT3003 is currently undergoing a multicenter, randomised, placebo controlled phase III study (Prukop et al. 2020). More recently, a new targeted strategy has been proposed. It is based on use of antisense oligonucleotides (ASO) (Ionis Pharmaceuticals Inc.), to suppress *PMP22* mRNA, and, in preclinical studies, it showed first promising results on rodent models (Zhao et al. 2017). Alternative therapeutic approaches were also proposed for CMT subtypes, other than CMT1A. For example, IFB-088 (InFlectis BioScience) has been successfully tested on mice models of CMT1B (mutated *MPZ* gene) (Guédat and Miniou 2016), while MFN2 agonists (Washington University) have been shown to restore mitochondrial defects in CMT2A murine neurons (Rocha et al. 2018). IFB-088 recently completed the phase I of clinical trial.

In the complex context of CMT disease, most of proposed therapeutic strategies seem to target specific gene-related mechanisms. Given the high number of involved genes, we can suppose that a considerable number of potential therapeutic molecules will need to be tested on specific models. As already discussed, even if it is a mandatory step of preclinical trials, the employment of animal models presents limitations and drawbacks, often related to physiological differences between animals and humans. Moreover, their exploitation must always take into account ethical rules and restrictions. The advantage of iPSC technology is that it allows to recreate any required human cell type, like, in the case of peripheral neuropathies, motor neurons and Schwann cells. In addition, patients' samples, as blood and skin biopsies, are more and more frequently collected by clinicians, providing the "raw matter" to establishing new hiPSC lines (Juneja et al. 2019). hiPSC role is, therefore, important, not only in investigation of pathological mechanisms, but also in providing diversified cellular models, adaptable to the candidate therapeutic strategy. Since they are not primary cultures, hiPSC-derived MN and SC can be generated whenever necessary, from hiPSC, favoring, in this way, a large-scale drug screen. Definitely, hiPSC will not replace, for now, animal models, but they can constitute a valid tool for preliminary analysis.

As discussed above, treatments are often designed on the basis of pathological mechanisms responsible for the specific CMT form. For *GDAP1*, no preclinical and clinical studies were reported, maybe because its functions rest partially unclear, and cellular and animal models are limited. Our hiPSC-derived MN, carrying nonsense mutations in *GDAP1*, may be employed as cellular tool to test new therapeutic molecules. Our analysis has revealed that, in MN of patient with the homozygous p.Ser194* mutation, *GDAP1* mRNA was ~8 fold lower than in Ctrl-1 MN. We supposed that its mRNA, presenting a premature termination codon (PTC), is probably degraded by the cellular quality-control mechanism known as nonsense-mediated mRNA decay (NMD). Consequentially, a good proportion of GDAP1 protein is not formed, as we have shown by ICC. We can, therefore, consider to inactivate the NMD system, and enable the translation of *GDAP1* mRNA in a truncated protein, using NMD inhibitors. Their action can be combined to that of read-through molecules. In basal translational

read-through, the ribosome goes past the stop-codon and continues the mRNA translation in the UTR region (Li and Zhang 2019). This is a rare natural mechanism of the cell, but, in pathological conditions, it can be induced by pharmaceutical compounds (Dabrowski, Bukowy-Bieryllo, and Zietkiewicz 2018). Examples of read-through molecules are the aminoglycosides, which can be associated with nephrotoxicity and ototoxicity, and the Ataluren or PTC124 (Translarna^{TM}), safer and suitable for administration (Hirawat et al. 2007). Ataluren has been approved for the treatment of nonsense mutation Duchenne muscular dystrophy (nmDMD) (Landfeldt, Sejersen, and Tulinius 2019). An example of NMD inhibitors is the Amlexanox, a non-toxic molecule which also acts as read-through compound (Gonzalez-Hilarion et al. 2012). Furthermore, it has been shown that some fungi extracts, like the so-called H7, present the same dual function of Amlexanox (NMD-inhibition and read-through) (Benhabiles et al. 2017). We thought that it could be interesting to test this kind of molecules on our cellular model of CMT hiPSC-MN, to evaluate if the restoration of GDAP1 protein can prevent the occurrence of the pathological condition. It is for this reason that, in our team, thanks to the collaboration with the UMR9020 CNRS - UMR-S1277 Inserm of Lille, a new project has been initiated to start the exploration of alterative therapeutic strategies for CMT disease. Indeed, positive results from these preliminary studies, on GDAP1-CMT MN, could pave the way, for read-through molecules, to other CMT forms, or other neuropathies, induced by codon-stop mutations.

Lastly, to validate and improve our analysis on peripheral neuropathies and *GDAP1*, but also to test potential therapeutic strategies, an animal model seems to be necessary. That is why, a collaboration with The Jackson Laboratory of Bar Harbor (USA) has been created, with the aim of obtaining a murine model for GDAP1.

Conclusion

The complete understanding of hereditary peripheral neuropathies, and Charcot-Marie-Tooth disease, still remains a challenge, at genetic and mechanistic level. Moreover, a valid therapy for CMT forms has not been found yet. The first aim of this study was to highlight genetic aspects which are often underestimated in diagnostic procedure. We showed that multiple genes can collaborate, in some cases, to induce CMT pathology, but we also highlighted the importance of looking for CNV. This would be important, not only to reduce the rate of undiagnosed cases for hereditary peripheral neuropathies, but also to discover unknown CMT pathological mechanisms. Secondly, to help the examination of these pathological mechanisms, we presented a differentiation protocol to generate motor neurons (the affected cells in CMT), from hiPSC. Once obtained MN, these cells were used to compared functional data, between cells of unaffected control subjects, and cells of a CMT2H-patient, carrying, in particular, a homozygous codon-stop mutation in *GDAP1* gene. Our analysis revealed that oxidative stress and mitochondrial impairment can be responsible for the pathological condition in this CMT form.

Our study, therefore, ranged from molecular to functional analysis. Further investigations will be conducted on our MN cellular model to clarify the involvement of some pathological mechanisms. Moreover, we hope to use it, in the near future, to test new potential therapeutic strategies for CMT disease, before proceeding on animal models.

References

Acloque, Hervé, Meghan S. Adams, Katherine Fishwick, Marianne Bronner-Fraser, and M. Angela Nieto. 2009. “Epithelial-Mesenchymal Transitions: The Importance of Changing Cell State in Development and Disease.” *Journal of Clinical Investigation* 119 (6): 1438–49. https://doi.org/10.1172/JCI38019.

Agholme, Lotta, Tobias Lindström, Katarina Kågedal, Jan Marcusson, and Martin Hallbeck. 2010. “An In Vitro Model for Neuroscience: Differentiation of SH-SY5Y Cells into Cells with Morphological and Biochemical Characteristics of Mature Neurons.” *Journal of Alzheimer’s Disease* 20 (4): 1069–82. https://doi.org/10.3233/JAD-2010-091363.

Aguilar, Tomás Alejandro Fregoso, Brenda Carolina Hernández Navarro, and Jorge Alberto Mendoza Pérez. 2016. “Endogenous Antioxidants: A Review of Their Role in Oxidative Stress.” In *A Master Regulator of Oxidative Stress - The Transcription Factor Nrf2*, edited by Jose Antonio Morales-Gonzalez, Angel Morales-Gonzalez, and Eduardo Osiris Madrigal-Santillan. InTech. https://doi.org/10.5772/65715.

Alamdari, Azam, Rambod Mozafari, Abbas Tafakhori, Sara Faghihi-Kashani, Nima Hafezi-Nejad, Sara Sheikhbahaei, Neda Naderi, Maryam Ebadi, and Alireza Esteghamati. 2015. “An Inverse Association between Serum Vitamin D Levels with the Presence and Severity of Impaired Nerve Conduction Velocity and Large Fiber Peripheral Neuropathy in Diabetic Subjects.” *Neurological Sciences* 36 (7): 1121–26. https://doi.org/10.1007/s10072-015-2207-0.

Alberts, Bruce, ed. 2002. *Molecular Biology of the Cell*. 4th ed. New York: Garland Science.

Alfadda, Assim A., and Reem M. Sallam. 2012. “Reactive Oxygen Species in Health and Disease.” *Journal of Biomedicine and Biotechnology* 2012: 1–14. https://doi.org/10.1155/2012/936486.

Amati-Bonneau, Patrizia, Dan Milea, Dominique Bonneau, Arnaud Chevrollier, Marc Ferré, Virginie Guillet, Naïg Gueguen, et al. 2009. “OPA1-Associated Disorders: Phenotypes and Pathophysiology.” *The International Journal of Biochemistry & Cell Biology* 41 (10): 1855–65. https://doi.org/10.1016/j.biocel.2009.04.012.

Aoyama, T., S. Hata, T. Nakao, Y. Tanigawa, C. Oka, and M. Kawaichi. 2009. “Cayman Ataxia Protein Caytaxin Is Transported by Kinesin along Neurites through Binding to Kinesin Light Chains.” *Journal of Cell Science* 122 (22): 4177–85. https://doi.org/10.1242/jcs.048579.

Arancibia-Carcamo, I Lorena, and David Attwell. 2014. “The Node of Ranvier in CNS Pathology.” *Acta Neuropathol*, 15.

Arnold, Ria, Tushar Issar, Arun V Krishnan, and Bruce A Pussell. 2016. “Neurological Complications in Chronic Kidney Disease.” *JRSM Cardiovascular Disease* 5 (March): 204800401667768. https://doi.org/10.1177/2048004016677687.

Ashrafi, Ghazaleh, Julia S. Schlehe, Matthew J. LaVoie, and Thomas L. Schwarz. 2014. “Mitophagy of Damaged Mitochondria Occurs Locally in Distal Neuronal Axons and Requires PINK1 and Parkin.” *Journal of Cell Biology* 206 (5): 655–70. https://doi.org/10.1083/jcb.201401070.

Attarian, Shahram, Jean-Michel Vallat, Laurent Magy, Benoît Funalot, Pierre-Marie Gonnaud, Arnaud Lacour, Yann Péréon, et al. 2014. “An Exploratory Randomised Double-Blind and Placebo-Controlled Phase 2 Study of a Combination of Baclofen, Naltrexone and Sorbitol (PXT3003) in Patients with Charcot-Marie-Tooth Disease Type 1A.” *Orphanet Journal of Rare Diseases* 9 (1): 199. https://doi.org/10.1186/s13023-014-0199-0.

———. 2016. “Erratum to: An Exploratory Randomised Double-Blind and Placebo-Controlled Phase 2 Study of a Combination of Baclofen, Naltrexone and Sorbitol (PXT3003) in

Patients with Charcot-Marie-Tooth Disease Type 1A." *Orphanet Journal of Rare Diseases* 11 (1): 92. https://doi.org/10.1186/s13023-016-0463-6.

Azzedine, H, M Ruberg, D Ente, C Gilardeau, S Périé, B Wechsler, A Brice, E LeGuern, and O Dubourg. 2003. "Variability of Disease Progression in a Family with Autosomal Recessive CMT Associated with a S194X and New R310Q Mutation in the GDAP1 Gene." *Neuromuscular Disorders* 13 (4): 341–46. https://doi.org/10.1016/S0960-8966(02)00281-X.

Bailey, Andrew P., Grielof Koster, Christelle Guillermier, Elizabeth M.A. Hirst, James I. MacRae, Claude P. Lechene, Anthony D. Postle, and Alex P. Gould. 2015. "Antioxidant Role for Lipid Droplets in a Stem Cell Niche of Drosophila." *Cell* 163 (2): 340–53. https://doi.org/10.1016/j.cell.2015.09.020.

Ban, Tadato, Takaya Ishihara, Hiroto Kohno, Shotaro Saita, Ayaka Ichimura, Katsumi Maenaka, Toshihiko Oka, Katsuyoshi Mihara, and Naotada Ishihara. 2017. "Molecular Basis of Selective Mitochondrial Fusion by Heterotypic Action between OPA1 and Cardiolipin." *Nature Cell Biology* 19 (7): 856–63. https://doi.org/10.1038/ncb3560.

Bansagi, Boglarka, Thalia Antoniadi, Sarah Burton-Jones, Sinead M. Murphy, John McHugh, Michael Alexander, Richard Wells, et al. 2015. "Genotype/Phenotype Correlations in AARS-Related Neuropathy in a Cohort of Patients from the United Kingdom and Ireland." *Journal of Neurology* 262 (8): 1899–1908. https://doi.org/10.1007/s00415-015-7778-4.

Bansagi, Boglarka, Helen Griffin, Roger G. Whittaker, Thalia Antoniadi, Teresinha Evangelista, James Miller, Mark Greenslade, et al. 2017. "Genetic Heterogeneity of Motor Neuropathies." *Neurology* 88 (13): 1226–34. https://doi.org/10.1212/WNL.0000000000003772.

Barneo-Muñoz, Manuela, Paula Juárez, Azahara Civera-Tregón, Laura Yndriago, David Pla-Martin, Jennifer Zenker, Carmen Cuevas-Martín, et al. 2015. "Lack of GDAP1 Induces Neuronal Calcium and Mitochondrial Defects in a Knockout Mouse Model of Charcot-Marie-Tooth Neuropathy." Edited by Gregory A. Cox. *PLOS Genetics* 11 (4): e1005115. https://doi.org/10.1371/journal.pgen.1005115.

Barohn, Richard J., and Anthony A. Amato. 2013. "Pattern-Recognition Approach to Neuropathy and Neuronopathy." *Neurologic Clinics* 31 (2): 343–61. https://doi.org/10.1016/j.ncl.2013.02.001.

Barreto, Lidiane Carine Lima Santos, Fernanda Santos Oliveira, Paula Santos Nunes, Iandra Maria Pinheiro de França Costa, Catarina Andrade Garcez, Gabriel Mattos Goes, Eduardo Luis Aquino Neves, Jullyana de Souza Siqueira Quintans, and Adriano Antunes de Souza Araújo. 2016. "Epidemiologic Study of Charcot-Marie-Tooth Disease: A Systematic Review." *Neuroepidemiology* 46 (3): 157–65. https://doi.org/10.1159/000443706.

Baxter, Rachel V., Kamel Ben Othmane, Julie M. Rochelle, Jason E. Stajich, Christine Hulette, Susan Dew-Knight, Faycal Hentati, et al. 2002. "Ganglioside-Induced Differentiation-Associated Protein-1 Is Mutant in Charcot-Marie-Tooth Disease Type 4A/8q21." *Nature Genetics* 30 (1): 21–22. https://doi.org/10.1038/ng796.

Beijer, Danique, Angela Sisto, Jonas Van Lent, Jonathan Baets, and Vincent Timmerman. 2019. "Defects in Axonal Transport in Inherited Neuropathies." *Journal of Neuromuscular Diseases* 6 (4): 401–19. https://doi.org/10.3233/JND-190427.

Belikov, Aleksey V., Burkhart Schraven, and Luca Simeoni. 2015. "T Cells and Reactive Oxygen Species." *Journal of Biomedical Science* 22 (1): 85. https://doi.org/10.1186/s12929-015-0194-3.

Belin, Sophie, Kristen L. Zuloaga, and Yannick Poitelon. 2017. “Influence of Mechanical Stimuli on Schwann Cell Biology.” *Frontiers in Cellular Neuroscience* 11 (November): 347. https://doi.org/10.3389/fncel.2017.00347.

Benhabiles, Hana, Sara Gonzalez-Hilarion, Séverine Amand, Christine Bailly, Anne Prévotat, Philippe Reix, Dominique Hubert, et al. 2017. “Optimized Approach for the Identification of Highly Efficient Correctors of Nonsense Mutations in Human Diseases.” Edited by Georg Stoecklin. *PLOS ONE* 12 (11): e0187930. https://doi.org/10.1371/journal.pone.0187930.

Bennett, D L H, M Groves, J Blake, J L Holton, R H M King, R W Orrell, L Ginsberg, and M M Reilly. 2008. “The Use of Nerve and Muscle Biopsy in the Diagnosis of Vasculitis: A 5 Year Retrospective Study.” *J Neurol Neurosurg Psychiatry*, 6.

Berciano, José, Antonio García, Elena Gallardo, Kristien Peeters, Ana L. Pelayo-Negro, Silvia Álvarez-Paradelo, José Gazulla, Miriam Martínez-Tames, Jon Infante, and Albena Jordanova. 2017. “Intermediate Charcot–Marie–Tooth Disease: An Electrophysiological Reappraisal and Systematic Review.” *Journal of Neurology* 264 (8): 1655–77. https://doi.org/10.1007/s00415-017-8474-3.

Bessaguet, Flavien, Aurore Danigo, Hichem Bouchenaki, Mathilde Duchesne, Laurent Magy, Laurence Richard, and Franck Sturtz. 2018. “Neuroprotective Effect of Angiotensin II Type 2 Receptor Stimulation in Vincristine-Induced Mechanical Allodynia” 159 (12): 9.

Bhattacharyya, Asima, Ranajoy Chattopadhyay, Sankar Mitra, and Sheila E. Crowe. 2014. “Oxidative Stress: An Essential Factor in the Pathogenesis of Gastrointestinal Mucosal Diseases.” *Physiological Reviews* 94 (2): 329–54. https://doi.org/10.1152/physrev.00040.2012.

Bird, T. D., J. Ott, and E. R. Giblett. 1982. “Evidence for Linkage of Charcot-Marie-Tooth Neuropathy to the Duffy Locus on Chromosome 1.” *American Journal of Human Genetics* 34 (3): 388–94.

Bird, Thomas D. 1993. “Hereditary Ataxia Overview.” In *GeneReviews®*, edited by Margaret P. Adam, Holly H. Ardinger, Roberta A. Pagon, Stephanie E. Wallace, Lora JH Bean, Karen Stephens, and Anne Amemiya. Seattle (WA): University of Washington, Seattle. http://www.ncbi.nlm.nih.gov/books/NBK1138/.

———. 2020. “Charcot-Marie-Tooth (CMT) Hereditary Neuropathy Overview.” In *GeneReviews®*, edited by Margaret P. Adam, Holly H. Ardinger, Roberta A. Pagon, Stephanie E. Wallace, Lora JH Bean, Karen Stephens, and Anne Amemiya. Seattle (WA): University of Washington, Seattle. http://www.ncbi.nlm.nih.gov/books/NBK1358/.

Bis-Brewer, Dana M., Sarah Fazal, and Stephan Züchner. 2020. “Genetic Modifiers and Non-Mendelian Aspects of CMT.” *Brain Research* 1726 (January): 146459. https://doi.org/10.1016/j.brainres.2019.146459.

Bo, R. D., M. Moggio, M. Rango, S. Bonato, M. G. D’Angelo, S. Ghezzi, G. Airoldi, et al. 2008. “Mutated Mitofusin 2 Presents with Intrafamilial Variability and Brain Mitochondrial Dysfunction.” *Neurology* 71 (24): 1959–66. https://doi.org/10.1212/01.wnl.0000327095.32005.a4.

Boczonadi, Veronika, Matthew J. Jennings, and Rita Horvath. 2018. “The Role of TRNA Synthetases in Neurological and Neuromuscular Disorders.” *FEBS Letters* 592 (5): 703–17. https://doi.org/10.1002/1873-3468.12962.

Boggs, J. M. 2006. “Myelin Basic Protein: A Multifunctional Protein.” *Cellular and Molecular Life Sciences* 63 (17): 1945–61. https://doi.org/10.1007/s00018-006-6094-7.

Bond, Allison M., Oneil G. Bhalala, and John A. Kessler. 2012. “The Dynamic Role of Bone Morphogenetic Proteins in Neural Stem Cell Fate and Maturation.” *Developmental Neurobiology* 72 (7): 1068–84. https://doi.org/10.1002/dneu.22022.

Bouillot, S., M.L. Martin-Negrier, A. Vital, X. Ferrer, A. Lagueny, D. Vincent, M. Coquet, J.M. Orgogozo, B. Bloch, and C. Vital. 2002. “Peripheral Neuropathy Associated with Mitochondrial Disorders: 8 Cases and Review of the Literature.” *Journal of the Peripheral Nervous System* 7 (4): 213–20. https://doi.org/10.1046/j.1529-8027.2002.02027.x.

Bourque, Pierre R., Jodi Warman Chardon, and Rami Massie. 2015. “Autoimmune Peripheral Neuropathies.” *Clinica Chimica Acta* 449 (September): 37–42. https://doi.org/10.1016/j.cca.2015.02.039.

Brand, Martin D. 2010. “The Sites and Topology of Mitochondrial Superoxide Production.” *Experimental Gerontology* 45 (7–8): 466–72. https://doi.org/10.1016/j.exger.2010.01.003.

Brieger, K, S Schiavone, Jr. Miller, and Kh Krause. 2012. “Reactive Oxygen Species: From Health to Disease.” *Swiss Medical Weekly*, August. https://doi.org/10.4414/smw.2012.13659.

Brito, Olga Martins de, and Luca Scorrano. 2008. “Mitofusin 2 Tethers Endoplasmic Reticulum to Mitochondria.” *Nature* 456 (7222): 605–10. https://doi.org/10.1038/nature07534.

Brizzi, Kate T., and Jennifer L. Lyons. 2014. “Peripheral Nervous System Manifestations of Infectious Diseases.” *The Neurohospitalist* 4 (4): 230–40. https://doi.org/10.1177/1941874414535215.

Brückmann, Christof, Adriana Di Santo, Kathrin Nora Karle, Anil Batra, and Vanessa Nieratschker. 2016. “Validation of Differential *GDAP1* DNA Methylation in Alcohol Dependence and Its Potential Function as a Biomarker for Disease Severity and Therapy Outcome.” *Epigenetics* 11 (6): 456–63. https://doi.org/10.1080/15592294.2016.1179411.

Burgess, Robert W. 2018. “Editorial: Axonopathy in Neurodegenerative Disease.” *Frontiers in Neuroscience* 12: 3.

Cadet, J., and J. R. Wagner. 2013. “DNA Base Damage by Reactive Oxygen Species, Oxidizing Agents, and UV Radiation.” *Cold Spring Harbor Perspectives in Biology* 5 (2): a012559–a012559. https://doi.org/10.1101/cshperspect.a012559.

Caillaud, Martial, Benjamin Chantemargue, Laurence Richard, Laetitia Vignaud, Frédéric Favreau, Pierre-Antoine Faye, Philippe Vignoles, et al. 2018. “Local Low Dose Curcumin Treatment Improves Functional Recovery and Remyelination in a Rat Model of Sciatic Nerve Crush through Inhibition of Oxidative Stress.” *Neuropharmacology* 139 (September): 98–116. https://doi.org/10.1016/j.neuropharm.2018.07.001.

Callaghan, Brian C., Raymond S. Price, and Eva L. Feldman. 2015. “Distal Symmetric Polyneuropathy: A Review.” *JAMA* 314 (20): 2172. https://doi.org/10.1001/jama.2015.13611.

Campello, Silvia, and Luca Scorrano. 2010. “Mitochondrial Shape Changes: Orchestrating Cell Pathophysiology.” *EMBO Reports* 11 (9): 678–84. https://doi.org/10.1038/embor.2010.115.

Carod-Artal, Francisco Javier. 2018. “Infectious Diseases Causing Autonomic Dysfunction.” *Clinical Autonomic Research*, 15.

Cartoni, Romain, and Jean-Claude Martinou. 2009. “Role of Mitofusin 2 Mutations in the Physiopathology of Charcot–Marie–Tooth Disease Type 2A.” *Experimental Neurology* 218 (2): 268–73. https://doi.org/10.1016/j.expneurol.2009.05.003.

Cassereau, J., C. Casasnovas, N. Gueguen, M.- C. Malinge, V. Guillet, P. Reynier, D. Bonneau, et al. 2011C. “Simultaneous MFN2 and GDAP1 Mutations Cause Major Mitochondrial Defects in a Patient with CMT.” *Neurology* 76 (17): 1524–26. https://doi.org/10.1212/WNL.0b013e318217e77d.

Cassereau, Julien, Arnaud Chevrollier, Dominique Bonneau, Christophe Verny, Vincent Procaccio, Pascal Reynier, and Marc Ferré. 2011B. “A Locus-Specific Database for Mutations in GDAP1 Allows Analysis of Genotype-Phenotype Correlations in Charcot-Marie-Tooth Diseases Type 4A and 2K.” *Orphanet Journal of Rare Diseases* 6 (1): 87. https://doi.org/10.1186/1750-1172-6-87.

Cassereau, Julien, Arnaud Chevrollier, Philippe Codron, Cyril Goizet, Naïg Gueguen, Christophe Verny, Pascal Reynier, Dominique Bonneau, Guy Lenaers, and Vincent Procaccio. 2020. “Oxidative Stress Contributes Differentially to the Pathophysiology of Charcot-Marie-Tooth Disease Type 2K.” *Experimental Neurology* 323 (January): 113069. https://doi.org/10.1016/j.expneurol.2019.113069.

Cassereau, Julien, Arnaud Chevrollier, Naïg Gueguen, Valérie Desquiret, Christophe Verny, Guillaume Nicolas, Frédéric Dubas, et al. 2011A. “Mitochondrial Dysfunction and Pathophysiology of Charcot–Marie–Tooth Disease Involving GDAP1 Mutations.” *Experimental Neurology* 227 (1): 31–41. https://doi.org/10.1016/j.expneurol.2010.09.006.

Cassereau, Julien, Arnaud Chevrollier, Naïg Gueguen, Marie-Claire Malinge, Franck Letournel, Guillaume Nicolas, Laurence Richard, et al. 2009. “Mitochondrial Complex I Deficiency in GDAP1-Related Autosomal Dominant Charcot-Marie-Tooth Disease (CMT2K).” *Neurogenetics* 10 (2): 145–50. https://doi.org/10.1007/s10048-008-0166-9.

Chabas, Jean-François, Olivier Alluin, Guillaume Rao, Stéphane Garcia, Marie-Noëlle Lavaut, Jean Jacques Risso, Régis Legre, et al. 2008. “Vitamin D $_2$ Potentiates Axon Regeneration.” *Journal of Neurotrauma* 25 (10): 1247–56. https://doi.org/10.1089/neu.2008.0593.

Chabas, Jean-Francois, Delphine Stephan, Tanguy Marqueste, Stephane Garcia, Marie-Noelle Lavaut, Catherine Nguyen, Regis Legre, Michel Khrestchatisky, Patrick Decherchi, and Francois Feron. 2013. “Cholecalciferol (Vitamin D3) Improves Myelination and Recovery after Nerve Injury.” Edited by Eliana Scemes. *PLoS ONE* 8 (5): e65034. https://doi.org/10.1371/journal.pone.0065034.

Chada, Sonita R, and Peter J Hollenbeck. 2004. “Nerve Growth Factor Signaling Regulates Motility and Docking of Axonal Mitochondria.” *Current Biology* 14 (14): 1272–76. https://doi.org/10.1016/j.cub.2004.07.027.

Chambers, Stuart M, Christopher A Fasano, Eirini P Papapetrou, Mark Tomishima, Michel Sadelain, and Lorenz Studer. 2009. “Highly Efficient Neural Conversion of Human ES and IPS Cells by Dual Inhibition of SMAD Signaling.” *Nature Biotechnology* 27 (3): 275–80. https://doi.org/10.1038/nbt.1529.

Chan, David C. 2020. “Mitochondrial Dynamics and Its Involvement in Disease.” *Annual Review of Pathology: Mechanisms of Disease* 15 (1): 235–59. https://doi.org/10.1146/annurev-pathmechdis-012419-032711.

Chandrasekhar, Anand. 2004. “Turning Heads: Development of Vertebrate Branchiomotor Neurons.” *Developmental Dynamics* 229 (1): 143–61. https://doi.org/10.1002/dvdy.10444.

Chang, Eun, Won Mo, Hyun Doo, Ji-Su Lee, Hwan Park, Byung-Ok Choi, and Young Hong. 2019. “Aminosalicylic Acid Reduces ER Stress and Schwann Cell Death Induced by MPZ Mutations.” *International Journal of Molecular Medicine*, May. https://doi.org/10.3892/ijmm.2019.4178.

Chaudhry, Vinay, Andrea M. Corse, Richard O’Brian, David R. Cornblath, Andrew S. Klein, and Paul J. Thuluvath. 1999. “Autonomic and Peripheral (Sensorimotor) Neuropathy in Chronic Liver Disease: A Clinical and Electrophysiologic Study.” *Hepatology* 29 (6): 1698–1703. https://doi.org/10.1002/hep.510290630.

Chen, Hsiuchen, Scott A. Detmer, Andrew J. Ewald, Erik E. Griffin, Scott E. Fraser, and David C. Chan. 2003. “Mitofusins Mfn1 and Mfn2 Coordinately Regulate Mitochondrial Fusion and Are Essential for Embryonic Development.” *Journal of Cell Biology* 160 (2): 189–200. https://doi.org/10.1083/jcb.200211046.

Chen, Hsiuchen, J. Michael McCaffery, and David C. Chan. 2007. “Mitochondrial Fusion Protects against Neurodegeneration in the Cerebellum.” *Cell* 130 (3): 548–62. https://doi.org/10.1016/j.cell.2007.06.026.

Chernousov, Michael, and David Carey. 2000. “Schwann Cell Extracellular Matrix Molecules and Their Receptors.” *Histology and Histopathology*, no. 15 (April): 593–601. https://doi.org/10.14670/HH-15.593.

Chevalier-Larsen, Erica, and Erika L.F. Holzbaur. 2006. “Axonal Transport and Neurodegenerative Disease.” *Biochimica et Biophysica Acta (BBA) - Molecular Basis of Disease* 1762 (11–12): 1094–1108. https://doi.org/10.1016/j.bbadis.2006.04.002.

Chinnery, P. F., and G. Hudson. 2013. “Mitochondrial Genetics.” *British Medical Bulletin* 106 (1): 135–59. https://doi.org/10.1093/bmb/ldt017.

Chumakov, Ilya, Aude Milet, Nathalie Cholet, Gwenaël Primas, Aurélie Boucard, Yannick Pereira, Esther Graudens, et al. 2014. “Polytherapy with a Combination of Three Repurposed Drugs (PXT3003) down-Regulates Pmp22 over-Expression and Improves Myelination, Axonal and Functional Parameters in Models of CMT1A Neuropathy.” *Orphanet Journal of Rare Diseases* 9 (1): 201. https://doi.org/10.1186/s13023-014-0201-x.

Chung, K. W., I. N. Sunwoo, S. M. Kim, K. D. Park, W.-K. Kim, T. S. Kim, H. Koo, M. Cho, J. Lee, and B. O. Choi. 2005. “Two Missense Mutations of EGR2 R359W and GJB1 V136A in a Charcot–Marie–Tooth Disease Family.” *Neurogenetics* 6 (3): 159–63. https://doi.org/10.1007/s10048-005-0217-4.

Ciaramitaro, Palma, Mauro Mondelli, Francesco Logullo, Serena Grimaldi, Bruno Battiston, Arman Sard, Cecilia Scarinzi, et al. 2010. “Traumatic Peripheral Nerve Injuries: Epidemiological Findings, Neuropathic Pain and Quality of Life in 158 Patients.” *Journal of the Peripheral Nervous System* 15 (2): 120–27. https://doi.org/10.1111/j.1529-8027.2010.00260.x.

Claramunt, R. 2005. “Genetics of Charcot-Marie-Tooth Disease Type 4A: Mutations, Inheritance, Phenotypic Variability, and Founder Effect.” *Journal of Medical Genetics* 42 (4): 358–65. https://doi.org/10.1136/jmg.2004.022178.

Colina-Tenorio, L., P. Horten, N. Pfanner, and H. Rampelt. 2020. “Shaping the Mitochondrial Inner Membrane in Health and Disease.” *Journal of Internal Medicine* 287 (6): 645–64. https://doi.org/10.1111/joim.13031.

Colombier, Pauline, Boris Halgand, Claire Chédeville, Caroline Chariau, Valentin François-Campion, Stéphanie Kilens, Nicolas Vedrenne, et al. 2020. “NOTO Transcription Factor Directs Human Induced Pluripotent Stem Cell-Derived Mesendoderm Progenitors to a Notochordal Fate.” *Cells* 9 (2): 509. https://doi.org/10.3390/cells9020509.

Colombini, Marco. 2012. “VDAC Structure, Selectivity, and Dynamics.” *Biochimica et Biophysica Acta (BBA) - Biomembranes* 1818 (6): 1457–65. https://doi.org/10.1016/j.bbamem.2011.12.026.

Compston, Alastair. 2019. “From the Archives.” *Brain* 142 (8): 2538–43. https://doi.org/10.1093/brain/awz200.

Cooper, Arthur JL, John T Pinto, and Patrick S Callery. 2011. “Reversible and Irreversible Protein Glutathionylation: Biological and Clinical Aspects.” *Expert Opinion on Drug Metabolism & Toxicology* 7 (7): 891–910. https://doi.org/10.1517/17425255.2011.577738.

Cortese, Andrea, Roberto Simone, Roisin Sullivan, Jana Vandrovcova, Huma Tariq, Wai Yan Yau, Jack Humphrey, et al. 2019. “Biallelic Expansion of an Intronic Repeat in RFC1 Is a Common Cause of Late-Onset Ataxia.” *Nature Genetics* 51 (4): 649–58. https://doi.org/10.1038/s41588-019-0372-4.

Corti, S., M. Nizzardo, C. Simone, M. Falcone, M. Nardini, D. Ronchi, C. Donadoni, et al. 2012. “Genetic Correction of Human Induced Pluripotent Stem Cells from Patients with Spinal Muscular Atrophy.” *Science Translational Medicine* 4 (165): 165ra162-165ra162. https://doi.org/10.1126/scitranslmed.3004108.

Course, Meredith M., and Xinnan Wang. 2016. “Transporting Mitochondria in Neurons.” *F1000Research* 5 (July): 1735. https://doi.org/10.12688/f1000research.7864.1.

Crimella, C., A. Tonelli, G. Airoldi, C. Baschirotto, M. G. D’Angelo, S. Bonato, L. Losito, A. Trabacca, N. Bresolin, and M. T. Bassi. 2010. “The GST Domain of GDAP1 Is a Frequent Target of Mutations in the Dominant Form of Axonal Charcot Marie Tooth Type 2K.” *Journal of Medical Genetics* 47 (10): 712–16. https://doi.org/10.1136/jmg.2010.077909.

Cuesta, Ana, Laia Pedrola, Teresa Sevilla, Javier García-Planells, María José Chumillas, Fernando Mayordomo, Eric LeGuern, Ignacio Marín, Juan J. Vílchez, and Francesc Palau. 2002. “The Gene Encoding Ganglioside-Induced Differentiation-Associated Protein 1 Is Mutated in Axonal Charcot-Marie-Tooth Type 4A Disease.” *Nature Genetics* 30 (1): 22–25. https://doi.org/10.1038/ng798.

Dabrowski, Maciej, Zuzanna Bukowy-Bieryllo, and Ewa Zietkiewicz. 2018. “Advances in Therapeutic Use of a Drug-Stimulated Translational Readthrough of Premature Termination Codons.” *Molecular Medicine* 24 (1): 25. https://doi.org/10.1186/s10020-018-0024-7.

Davies, Michael J. 2016. “Protein Oxidation and Peroxidation.” *Biochemical Journal* 473 (7): 805–25. https://doi.org/10.1042/BJ20151227.

Degli Esposti, Davide, Jocelyne Hamelin, Nelly Bosselut, Raphaël Saffroy, Mylène Sebagh, Alban Pommier, Cécile Martel, and Antoinette Lemoine. 2012. “Mitochondrial Roles and Cytoprotection in Chronic Liver Injury.” *Biochemistry Research International* 2012: 1–16. https://doi.org/10.1155/2012/387626.

Derouault, P., B. Parfait, R. Moulinas, C-C. Barrot, F. Sturtz, S. Merillou, and A-S Lia. 2017. “‘ COV’COP’ Allows to Detect CNVs Responsible for Inherited Diseases among Amplicons Sequencing Data.” *Bioinformatics* 33 (10): 1586–88. https://doi.org/10.1093/bioinformatics/btx017.

Derouault, Paco, Jasmine Chauzeix, David Rizzo, Federica Miressi, Corinne Magdelaine, Sylvie Bourthoumieu, Karine Durand, et al. 2020. “CovCopCan: An Efficient Tool to Detect Copy Number Variation from Amplicon Sequencing Data in Inherited Diseases and Cancer.” Edited by Aaron E. Darling. *PLOS Computational Biology* 16 (2): e1007503. https://doi.org/10.1371/journal.pcbi.1007503.

Derrickson, Bryan H, and Gerard J Tortora. 2017. *Tortora's Principles of Anatomy & Physiology*.

Dharani, Krishnagopal. 2015. "Dendrites and Primary Thoughts." In *The Biology of Thought*, 109–22. Elsevier. https://doi.org/10.1016/B978-0-12-800900-0.00006-3.

Dimos, J. T., K. T. Rodolfa, K. K. Niakan, L. M. Weisenthal, H. Mitsumoto, W. Chung, G. F. Croft, et al. 2008. "Induced Pluripotent Stem Cells Generated from Patients with ALS Can Be Differentiated into Motor Neurons." *Science* 321 (5893): 1218–21. https://doi.org/10.1126/science.1158799.

Ding, Wen-Xing, and Xiao-Ming Yin. 2012. "Mitophagy: Mechanisms, Pathophysiological Roles, and Analysis." *Biological Chemistry* 393 (7): 547–64. https://doi.org/10.1515/hsz-2012-0119.

Dohrn, Maike F., Nicola Glöckle, Lejla Mulahasanovic, Corina Heller, Julia Mohr, Christine Bauer, Erik Riesch, et al. 2017. "Frequent Genes in Rare Diseases: Panel-Based next Generation Sequencing to Disclose Causal Mutations in Hereditary Neuropathies." *Journal of Neurochemistry* 143 (5): 507–22. https://doi.org/10.1111/jnc.14217.

Dyck, Peter James, and Edward Lambert. 1968. "Lower Motor and Primary Sensory Neuron Diseases With Peroneal Muscular Atrophy: I. Neurologic, Genetic, and Electrophysiologic Findings in Hereditary Polyneuropathies." *Archives of Neurology* 18 (6): 603. https://doi.org/10.1001/archneur.1968.00470360025002.

Erdem, Sevim, Jerry R. Mendell, and Zarife Sahenk. 1998. "Fate of Schwann Cells in CMT1A and HNPP: Evidence for Apoptosis." *Journal of Neuropathology & Experimental Neurology* 57 (6): 635–42. https://doi.org/10.1097/00005072-199806000-00009.

Estela, Anna, David Pla-Martín, Maribel Sánchez-Piris, Hiromi Sesaki, and Francesc Palau. 2011. "Charcot-Marie-Tooth-Related Gene *GDAP1* Complements Cell Cycle Delay at G_2 /M Phase in *Saccharomyces Cerevisiae Fis1* Gene-Defective Cells." *Journal of Biological Chemistry* 286 (42): 36777–86. https://doi.org/10.1074/jbc.M111.260042.

Fabrini, Raffaele, Anastasia De Luca, Lorenzo Stella, Giampiero Mei, Barbara Orioni, Sarah Ciccone, Giorgio Federici, Mario Lo Bello, and Giorgio Ricci. 2009. "Monomer−Dimer Equilibrium in Glutathione Transferases: A Critical Re-Examination." *Biochemistry* 48 (43): 10473–82. https://doi.org/10.1021/bi901238t.

Fahrner, Jill A., Raymond Liu, Michael Scott Perry, Jessica Klein, and David C. Chan. 2016. "A Novel de Novo Dominant Negative Mutation in *DNM1L* Impairs Mitochondrial Fission and Presents as Childhood Epileptic Encephalopathy." *American Journal of Medical Genetics Part A* 170 (8): 2002–11. https://doi.org/10.1002/ajmg.a.37721.

Farmer, Brandon C., Adeline E. Walsh, Jude C. Kluemper, and Lance A. Johnson. 2020. "Lipid Droplets in Neurodegenerative Disorders." *Frontiers in Neuroscience* 14 (July): 742. https://doi.org/10.3389/fnins.2020.00742.

Faye, Pierre Antoine, François Poumeaud, Federica Miressi, Anne Sophie Lia, Claire Demiot, Laurent Magy, Frédéric Favreau, and Franck G. Sturtz. 2019. "Focus on 1,25-Dihydroxyvitamin D3 in the Peripheral Nervous System." *Frontiers in Neuroscience* 13 (April): 348. https://doi.org/10.3389/fnins.2019.00348.

Faye, Pierre-Antoine, Nicolas Vedrenne, Federica Miressi, Marion Rassat, Sergii Romanenko, Laurence Richard, Sylvie Bourthoumieu, et al. 2020. "Optimized Protocol to Generate Spinal Motor Neuron Cells from Induced Pluripotent Stem Cells from Charcot Marie Tooth Patients." *Brain Sciences* 10 (7): 407. https://doi.org/10.3390/brainsci10070407.

Feely, S. M. E., M. Laura, C. E. Siskind, S. Sottile, M. Davis, V. S. Gibbons, M. M. Reilly, and M. E. Shy. 2011. “MFN2 Mutations Cause Severe Phenotypes in Most Patients with CMT2A.” *Neurology* 76 (20): 1690–96. https://doi.org/10.1212/WNL.0b013e31821a441e.

Fehrenbacher, Kammy L, Hyeong-Cheol Yang, Anna Card Gay, Thomas M Huckaba, and Liza A. Pon. 2004. “Live Cell Imaging of Mitochondrial Movement along Actin Cables in Budding Yeast.” *Current Biology*, 9.

Filadi, Riccardo, Diana Pendin, and Paola Pizzo. 2018. “Mitofusin 2: From Functions to Disease.” *Cell Death & Disease* 9 (3): 330. https://doi.org/10.1038/s41419-017-0023-6.

Friedman, J. R., L. L. Lackner, M. West, J. R. DiBenedetto, J. Nunnari, and G. K. Voeltz. 2011. “ER Tubules Mark Sites of Mitochondrial Division.” *Science* 334 (6054): 358–62. https://doi.org/10.1126/science.1207385.

Fröb, Franziska, and Michael Wegner. 2020. “The Role of Chromatin Remodeling Complexes in Schwann Cell Development.” *Glia* 68 (8): 1596–1603. https://doi.org/10.1002/glia.23766.

Fu, Jun, Shixu Dai, Yuanyuan Lu, Rui Wu, Zhaoxia Wang, Yun Yuan, and He Lv. 2017. “Similar Clinical, Pathological, and Genetic Features in Chinese Patients with Autosomal Recessive and Dominant Charcot–Marie–Tooth Disease Type 2K.” *Neuromuscular Disorders* 27 (8): 760–65. https://doi.org/10.1016/j.nmd.2017.04.001.

Furness, John B. 2012. “The Enteric Nervous System and Neurogastroenterology.” *Nature Reviews Gastroenterology & Hepatology* 9 (5): 286–94. https://doi.org/10.1038/nrgastro.2012.32.

García-Sobrino, Tania, Patricia Blanco-Arias, Francesc Palau, Carmen Espinós, Laura Ramirez, Anna Estela, Beatriz San Millán, Manuel Arias, María-Jesús Sobrido, and Julio Pardo. 2017. “Phenotypical Features of a New Dominant GDAP1 Pathogenic Variant (p.R226del) in Axonal Charcot-Marie-Tooth Disease.” *Neuromuscular Disorders* 27 (7): 667–72. https://doi.org/10.1016/j.nmd.2017.01.008.

Gemignani, Franco, Giorgia Melli, Sara Alfieri, Cristina Inglese, and Adriana Marbini. 2004. “Sensory Manifestations in Charcot-Marie-Tooth Disease.” *Journal of the Peripheral Nervous System* 9 (1): 7–14. https://doi.org/10.1111/j.1085-9489.2004.09103.x.

Ghosh, Nandini, Amitava Das, Scott Chaffee, Sashwati Roy, and Chandan K. Sen. 2018. “Reactive Oxygen Species, Oxidative Damage and Cell Death.” In *Immunity and Inflammation in Health and Disease*, 45–55. Elsevier. https://doi.org/10.1016/B978-0-12-805417-8.00004-4.

Gilbert, Scott Frederick. 2000. “The Neural Crest.” In *Developmental Biology*, 6th ed. Sunderland (MA): Sinauer Associates.

Giudetti, Anna Maria, Flora Guerra, Serena Longo, Raffaella Beli, Roberta Romano, Fiore Manganelli, Maria Nolano, Vincenzo Mangini, Lucio Santoro, and Cecilia Bucci. 2020. “An Altered Lipid Metabolism Characterizes Charcot-Marie-Tooth Type 2B Peripheral Neuropathy.” *Biochimica et Biophysica Acta (BBA) - Molecular and Cell Biology of Lipids* 1865 (12): 158805. https://doi.org/10.1016/j.bbalip.2020.158805.

Glick, Danielle, Sandra Barth, and Kay F. Macleod. 2010. “Autophagy: Cellular and Molecular Mechanisms.” *The Journal of Pathology* 221 (1): 3–12. https://doi.org/10.1002/path.2697.

Gogou, Maria, Evangelos Pavlou, Vasilios Kimiskidis, Konstantinos Kouskouras, Efterpi Pavlidou, Theophanis Papadopoulos, Katerina Haidopoulou, and Liana Fidani. 2020. “Novel Mutations Involved in Charcot-Marie-Tooth 4C and Intrafamilial Variability:

Let's Not Miss the Forest for the Trees." *Journal of Pediatric Genetics*, April, s-0040-1709695. https://doi.org/10.1055/s-0040-1709695.

Gonçalves, Nádia Pereira, Christian Bjerggaard Vægter, and Lone Tjener Pallesen. 2018. "Peripheral Glial Cells in the Development of Diabetic Neuropathy." *Frontiers in Neurology* 9 (May): 268. https://doi.org/10.3389/fneur.2018.00268.

Gonzaga-Jauregui, Claudia, Feng Zhang, Charles F. Towne, Sat Dev Batish, and James R. Lupski. 2010. "GJB1/Connexin 32 Whole Gene Deletions in Patients with X-Linked Charcot–Marie–Tooth Disease." *Neurogenetics* 11 (4): 465–70. https://doi.org/10.1007/s10048-010-0247-4.

Gonzalez-Hilarion, Sara, Terence Beghyn, Jieshuang Jia, Nadège Debreuck, Gonzague Berte, Kamel Mamchaoui, Vincent Mouly, Dieter C Gruenert, Benoit Déprez, and Fabrice Lejeune. 2012. "Rescue of Nonsense Mutations by Amlexanox in Human Cells." *Orphanet Journal of Rare Diseases* 7 (1): 58. https://doi.org/10.1186/1750-1172-7-58.

González-Sánchez, Paloma, David Pla-Martín, Paula Martínez-Valero, Carlos B. Rueda, Eduardo Calpena, Araceli del Arco, Francesc Palau, and Jorgina Satrústegui. 2017. "CMT-Linked Loss-of-Function Mutations in GDAP1 Impair Store-Operated Ca2+ Entry-Stimulated Respiration." *Scientific Reports* 7 (1): 42993. https://doi.org/10.1038/srep42993.

Googins, Matthew R., Aigbirhemwen O. Woghiren-Afegbua, Michael Calderon, Claudette M. St. Croix, Kirill I. Kiselyov, and Andrew P. VanDemark. 2020. "Structural and Functional Divergence of GDAP1 from the Glutathione S-transferase Superfamily." *The FASEB Journal* 34 (5): 7192–7207. https://doi.org/10.1096/fj.202000110R.

Guédat, Philippe, and Pierre Miniou. 2016. "INFLECTIS BIOSCIENCE SAS," 2.

Guillemot, F. 2007. "Spatial and Temporal Specification of Neural Fates by Transcription Factor Codes." *Development* 134 (21): 3771–80. https://doi.org/10.1242/dev.006379.

Hammond, C. 2015. *Cellular and Molecular Neurophysiology*. Fourth edition. Amsterdam ; Boston: Elsevier/AP, Academic Press is an imprint of Elsevier.

Harding, A. E., and P. K. Thomas. 1980. "THE CLINICAL FEATURES OF HEREDITARY MOTOR AND SENSORY NEUROPATHY TYPES I AND II." *Brain* 103 (2): 259–80. https://doi.org/10.1093/brain/103.2.259.

Hayasaka, Kiyoshi, Masato Himoro, Wataru Sato, Goro Takada, Keiichi Uyemura, Nobuyoshi Shimizu, Thomas D. Bird, P. Michael Conneally, and Phillip F. Chance. 1993. "Charcot–Marie–Tooth Neuropathy Type 1B Is Associated with Mutations of the Myelin P0 Gene." *Nature Genetics* 5 (1): 31–34. https://doi.org/10.1038/ng0993-31.

Heggeness, M. H., M. Simon, and S. J. Singer. 1978. "Association of Mitochondria with Microtubules in Cultured Cells." *Proceedings of the National Academy of Sciences* 75 (8): 3863–66. https://doi.org/10.1073/pnas.75.8.3863.

Hicks, Caitlin W., and Elizabeth Selvin. 2019. "Epidemiology of Peripheral Neuropathy and Lower Extremity Disease in Diabetes." *Current Diabetes Reports* 19 (10): 86. https://doi.org/10.1007/s11892-019-1212-8.

Hirawat, Samit, Ellen M. Welch, Gary L. Elfring, Valerie J. Northcutt, Sergey Paushkin, Seongwoo Hwang, Eileen M. Leonard, et al. 2007. "Safety, Tolerability, and Pharmacokinetics of PTC124, a Nonaminoglycoside Nonsense Mutation Suppressor, Following Single- and Multiple-Dose Administration to Healthy Male and Female Adult Volunteers." *The Journal of Clinical Pharmacology* 47 (4): 430–44. https://doi.org/10.1177/0091270006297140.

Hodapp, Julie A., Gregory T. Carter, Hillary P. Lipe, Sara J. Michelson, George H. Kraft, and Thomas D. Bird. 2006. “Double Trouble in Hereditary Neuropathy: Concomitant Mutations in the *PMP-22* Gene and Another Gene Produce Novel Phenotypes.” *Archives of Neurology* 63 (1): 112. https://doi.org/10.1001/archneur.63.1.112.

Hogan, Patrick G., and Anjana Rao. 2015. “Store-Operated Calcium Entry: Mechanisms and Modulation.” *Biochemical and Biophysical Research Communications* 460 (1): 40–49. https://doi.org/10.1016/j.bbrc.2015.02.110.

Hoppins, Suzanne, and Jodi Nunnari. 2009. “The Molecular Mechanism of Mitochondrial Fusion.” *Biochimica et Biophysica Acta (BBA) - Molecular Cell Research* 1793 (1): 20–26. https://doi.org/10.1016/j.bbamcr.2008.07.005.

Høyer, Helle, Geir J. Braathen, Anette K. Eek, Camilla F. Skjelbred, and Michael B. Russell. 2011. “Charcot-Marie-Tooth Caused by a Copy Number Variation in Myelin Protein Zero.” *European Journal of Medical Genetics* 54 (6): e580–83. https://doi.org/10.1016/j.ejmg.2011.06.006.

Hu, Bao-Yang, and Su-Chun Zhang. 2009. “Differentiation of Spinal Motor Neurons from Pluripotent Human Stem Cells.” *Nature Protocols* 4 (9): 1295–1304. https://doi.org/10.1038/nprot.2009.127.

Huang, Jia, Xingyao Wu, Gladys Montenegro, Justin Price, Gaofeng Wang, Jeffery M. Vance, Michael E. Shy, and Stephan Züchner. 2010. “Copy Number Variations Are a Rare Cause of Non-CMT1A Charcot-Marie-Tooth Disease.” *Journal of Neurology* 257 (5): 735–41. https://doi.org/10.1007/s00415-009-5401-2.

Huber, Nina, Christoph Bieniossek, Konstanze Marion Wagner, Hans-Peter Elsässer, Ueli Suter, Imre Berger, and Axel Niemann. 2016. “Glutathione-Conjugating and Membrane-Remodeling Activity of GDAP1 Relies on Amphipathic C-Terminal Domain.” *Scientific Reports* 6 (1): 36930. https://doi.org/10.1038/srep36930.

Huber, Nina, Sofia Guimaraes, Michael Schrader, Ueli Suter, and Axel Niemann. 2013. “Charcot-Marie-Tooth Disease-associated Mutants of GDAP1 Dissociate Its Roles in Peroxisomal and Mitochondrial Fission.” *EMBO Reports* 14 (6): 545–52. https://doi.org/10.1038/embor.2013.56.

Hurd, Thomas Ryan, Matthew DeGennaro, and Ruth Lehmann. 2012. “Redox Regulation of Cell Migration and Adhesion.” *Trends in Cell Biology* 22 (2): 107–15. https://doi.org/10.1016/j.tcb.2011.11.002.

Ishihara, N. 2004. “Mitofusin 1 and 2 Play Distinct Roles in Mitochondrial Fusion Reactions via GTPase Activity.” *Journal of Cell Science* 117 (26): 6535–46. https://doi.org/10.1242/jcs.01565.

Isose, Sagiri, Satoshi Kuwabara, Norito Kokubun, Yasunori Sato, Masahiro Mori, Kazumoto Shibuya, Yukari Sekiguchi, et al. 2009. “Utility of the Distal Compound Muscle Action Potential Duration for Diagnosis of Demyelinating Neuropathies.” *Journal of the Peripheral Nervous System* 14 (3): 151–58. https://doi.org/10.1111/j.1529-8027.2009.00226.x.

Jessen, K R, and R Mirsky. 2016. “The Repair Schwann Cell and Its Function in Regenerating Nerves.” *J Physiol*, 11.

Jin, Yi, Yanjie Tan, Lupeng Chen, Yan Liu, and Zhuqing Ren. 2018. “Reactive Oxygen Species Induces Lipid Droplet Accumulation in HepG2 Cells by Increasing Perilipin 2 Expression.” *International Journal of Molecular Sciences* 19 (11): 3445. https://doi.org/10.3390/ijms19113445.

Jonckheere, An I., Jan A. M. Smeitink, and Richard J. T. Rodenburg. 2012. “Mitochondrial ATP Synthase: Architecture, Function and Pathology.” *Journal of Inherited Metabolic Disease* 35 (2): 211–25. https://doi.org/10.1007/s10545-011-9382-9.

Ju, Ming-Shaung, Chou-Ching K. Lin, and Cheng-Tao Chang. 2017. “Researches on Biomechanical Properties and Models of Peripheral Nerves - a Review.” *Journal of Biomechanical Science and Engineering* 12 (1): 16-00678-16–00678. https://doi.org/10.1299/jbse.16-00678.

Juneja, Manisha, Joshua Burns, Mario A Saporta, and Vincent Timmerman. 2019. “Challenges in Modelling the Charcot-Marie-Tooth Neuropathies for Therapy Development.” *Journal of Neurology, Neurosurgery & Psychiatry* 90 (1): 58–67. https://doi.org/10.1136/jnnp-2018-318834.

Kabzińska, Dagmara, Axel Niemann, Hanna Drac, Nina Huber, Anna Potulska-Chromik, Irena Hausmanowa-Petrusewicz, Ueli Suter, and Andrzej Kochański. 2011. “A New Missense GDAP1 Mutation Disturbing Targeting to the Mitochondrial Membrane Causes a Severe Form of AR-CMT2C Disease.” *Neurogenetics* 12 (2): 145–53. https://doi.org/10.1007/s10048-011-0276-7.

Kang, Jian-Sheng, Jin-Hua Tian, Ping-Yue Pan, Philip Zald, Cuiling Li, Chuxia Deng, and Zu-Hang Sheng. 2008. “Docking of Axonal Mitochondria by Syntaphilin Controls Their Mobility and Affects Short-Term Facilitation.” *Cell* 132 (1): 137–48. https://doi.org/10.1016/j.cell.2007.11.024.

Karaca, Ender, Jennifer E Posey, Zeynep Coban Akdemir, Davut Pehlivan, Tamar Harel, Shalini N Jhangiani, Yavuz Bayram, et al. 2018. “Phenotypic Expansion Illuminates Multilocus Pathogenic Variation.” *Genetics in Medicine* 20 (12): 1528–37. https://doi.org/10.1038/gim.2018.33.

Kelner, Michael J., and Mark A. Montoya. 2000. “Structural Organization of the Human Glutathione Reductase Gene: Determination of Correct CDNA Sequence and Identification of a Mitochondrial Leader Sequence.” *Biochemical and Biophysical Research Communications* 269 (2): 366–68. https://doi.org/10.1006/bbrc.2000.2267.

Kostera-Pruszczyk, Anna, Joanna Kosinska, Agnieszka Pollak, Piotr Stawinski, Anna Walczak, Krystyna Wasilewska, Anna Potulska-Chromik, Piotr Szczudlik, Anna Kaminska, and Rafal Ploski. 2014. “Exome Sequencing Reveals Mutations in *MFN2* and *GDAP1* in Severe Charcot-Marie-Tooth Disease: Kostera-Pruszczyk.” *Journal of the Peripheral Nervous System* 19 (3): 242–45. https://doi.org/10.1111/jns.12088.

Kousi, M., and N. Katsanis. 2015. “Genetic Modifiers and Oligogenic Inheritance.” *Cold Spring Harbor Perspectives in Medicine* 5 (6): a017145–a017145. https://doi.org/10.1101/cshperspect.a017145.

Kouyoumdjian, João Aris. 2006. “Peripheral Nerve Injuries: A Retrospective Survey of 456 Cases.” *Muscle & Nerve* 34 (6): 785–88. https://doi.org/10.1002/mus.20624.

Kraus, Felix, and Michael T. Ryan. 2017. “The Constriction and Scission Machineries Involved in Mitochondrial Fission.” *Journal of Cell Science* 130 (18): 2953–60. https://doi.org/10.1242/jcs.199562.

Krumova, Katerina, and Gonzalo Cosa. 2016. “Chapter 1. Overview of Reactive Oxygen Species.” In *Comprehensive Series in Photochemical & Photobiological Sciences*, edited by Santi Nonell and Cristina Flors, 1:1–21. Cambridge: Royal Society of Chemistry. https://doi.org/10.1039/9781782622208-00001.

Kubli, Dieter A., and Åsa B. Gustafsson. 2012. “Mitochondria and Mitophagy: The Yin and Yang of Cell Death Control.” *Circulation Research* 111 (9): 1208–21. https://doi.org/10.1161/CIRCRESAHA.112.265819.

Kudoh, Tetsuhiro, Stephen W. Wilson, and Igor B. Dawid. 2002. “Distinct Roles for Fgf, Wnt and Retinoic Acid in Posteriorizing the Neural Ectoderm.” *Development (Cambridge, England)* 129 (18): 4335–46.

Kühlbrandt, Werner. 2015. “Structure and Function of Mitochondrial Membrane Protein Complexes.” *BMC Biology* 13 (1): 89. https://doi.org/10.1186/s12915-015-0201-x.

Kulawiak, Bogusz, Jan Höpker, Michael Gebert, Bernard Guiard, Nils Wiedemann, and Natalia Gebert. 2013. “The Mitochondrial Protein Import Machinery Has Multiple Connections to the Respiratory Chain.” *Biochimica et Biophysica Acta (BBA) - Bioenergetics* 1827 (5): 612–26. https://doi.org/10.1016/j.bbabio.2012.12.004.

Landfeldt, Erik, Thomas Sejersen, and Már Tulinius. 2019. “A Mini-Review and Implementation Model for Using Ataluren to Treat Nonsense Mutation Duchenne Muscular Dystrophy.” *Acta Paediatrica* 108 (2): 224–30. https://doi.org/10.1111/apa.14568.

Landowski, Lila M., P. James B. Dyck, JaNean Engelstad, and Bruce V. Taylor. 2016. “Axonopathy in Peripheral Neuropathies: Mechanisms and Therapeutic Approaches for Regeneration.” *Journal of Chemical Neuroanatomy* 76 (October): 19–27. https://doi.org/10.1016/j.jchemneu.2016.04.006.

Lassiter, David G., Rasmus J.O. Sjögren, Brendan M. Gabriel, Anna Krook, and Juleen R. Zierath. 2018. “AMPK Activation Negatively Regulates GDAP1, Which Influences Metabolic Processes and Circadian Gene Expression in Skeletal Muscle.” *Molecular Metabolism* 16 (October): 12–23. https://doi.org/10.1016/j.molmet.2018.07.004.

Latour, Philippe, Christel Thauvin-Robinet, Chantal Baudelet-Méry, Pierre Soichot, Veronica Cusin, Laurence Faivre, Marie-Claire Locatelli, et al. 2010. “A Major Determinant for Binding and Aminoacylation of TRNAAla in Cytoplasmic Alanyl-TRNA Synthetase Is Mutated in Dominant Axonal Charcot-Marie-Tooth Disease.” *The American Journal of Human Genetics* 86 (1): 77–82. https://doi.org/10.1016/j.ajhg.2009.12.005.

Le Dréau, Gwenvael, and Elisa Martí. 2012. “Dorsal-Ventral Patterning of the Neural Tube: A Tale of Three Signals.” *Developmental Neurobiology* 72 (12): 1471–81. https://doi.org/10.1002/dneu.22015.

Lee, Hyojin, George Al Shamy, Yechiel Elkabetz, Claude M. Schofield, Neil L. Harrsion, Georgia Panagiotakos, Nicholas D. Socci, Viviane Tabar, and Lorenz Studer. 2007. “Directed Differentiation and Transplantation of Human Embryonic Stem Cell-Derived Motoneurons: DIRECTED DIFFERENTIATION AND TRANSPLANTATION OF HUMAN EMBRYONIC STEM CELL-DERIVED MOTONEURONS.” *STEM CELLS* 25 (8): 1931–39. https://doi.org/10.1634/stemcells.2007-0097.

Levine, Todd D. 2018. “Small Fiber Neuropathy: Disease Classification Beyond Pain and Burning.” *Journal of Central Nervous System Disease* 10 (January): 117957351877170. https://doi.org/10.1177/1179573518771703.

Lewis, Richard A. 2013. “High-Dosage Ascorbic Acid Treatment in Charcot-Marie-Tooth Disease Type 1A: Results of a Randomized, Double-Masked, Controlled Trial.” *JAMA Neurology* 70 (8): 981. https://doi.org/10.1001/jamaneurol.2013.3178.

Li, Chuan, and Jianzhi Zhang. 2019. “Stop-Codon Read-through Arises Largely from Molecular Errors and Is Generally Nonadaptive.” Edited by Laurent Duret. *PLOS Genetics* 15 (5): e1008141. https://doi.org/10.1371/journal.pgen.1008141.

Li, Xinyuan, Pu Fang, Jietang Mai, Eric T Choi, Hong Wang, and Xiao-feng Yang. 2013. “Targeting Mitochondrial Reactive Oxygen Species as Novel Therapy for Inflammatory Diseases and Cancers.” *Journal of Hematology & Oncology* 6 (1): 19. https://doi.org/10.1186/1756-8722-6-19.

Li, Yu-Jie, Yu-Lu Cao, Jian-Xiong Feng, Yuanbo Qi, Shuxia Meng, Jie-Feng Yang, Ya-Ting Zhong, et al. 2019. “Structural Insights of Human Mitofusin-2 into Mitochondrial Fusion and CMT2A Onset.” *Nature Communications* 10 (1): 4914. https://doi.org/10.1038/s41467-019-12912-0.

Lindström, Lisa, Tongbin Li, Darina Malycheva, Arun Kancharla, Helén Nilsson, Neelanjan Vishnu, Hindrik Mulder, Martin Johansson, Catalina Ana Rosselló, and Maria Alvarado-Kristensson. 2018. “The GTPase Domain of Gamma-Tubulin Is Required for Normal Mitochondrial Function and Spatial Organization.” *Communications Biology* 1 (1): 37. https://doi.org/10.1038/s42003-018-0037-3.

Liu, Hong, Takatoshi Nakagawa, Tae Kanematsu, Takafumi Uchida, and Shuichi Tsuji. 2008. “Isolation of 10 Differentially Expressed CDNAs in Differentiated Neuro2a Cells Induced Through Controlled Expression of the GD3 Synthase Gene.” *Journal of Neurochemistry* 72 (5): 1781–90. https://doi.org/10.1046/j.1471-4159.1999.0721781.x.

Liu, Lei, and Ruxu Zhang. 2014. “Intermediate Charcot-Marie-Tooth Disease.” *Neuroscience Bulletin* 30 (6): 999–1009. https://doi.org/10.1007/s12264-014-1475-7.

Liu, Zewen, Tingyang Zhou, Alexander C. Ziegler, Peter Dimitrion, and Li Zuo. 2017. “Oxidative Stress in Neurodegenerative Diseases: From Molecular Mechanisms to Clinical Applications.” *Oxidative Medicine and Cellular Longevity* 2017: 1–11. https://doi.org/10.1155/2017/2525967.

Longo, Nicola, Marta Frigeni, and Marzia Pasquali. 2016. “Carnitine Transport and Fatty Acid Oxidation.” *Biochimica et Biophysica Acta (BBA) - Molecular Cell Research* 1863 (10): 2422–35. https://doi.org/10.1016/j.bbamcr.2016.01.023.

López del Amo, Víctor, Martina Palomino-Schätzlein, Marta Seco-Cervera, José Luis García-Giménez, Federico Vicente Pallardó, Antonio Pineda-Lucena, and Máximo Ibo Galindo. 2017. “A Drosophila Model of GDAP1 Function Reveals the Involvement of Insulin Signalling in the Mitochondria-Dependent Neuromuscular Degeneration.” *Biochimica et Biophysica Acta (BBA) - Molecular Basis of Disease* 1863 (3): 801–9. https://doi.org/10.1016/j.bbadis.2017.01.003.

López Del Amo, Víctor, Marta Seco-Cervera, José Luís García-Giménez, Alexander J. Whitworth, Federico V. Pallardó, and Máximo Ibo Galindo. 2015. “Mitochondrial Defects and Neuromuscular Degeneration Caused by Altered Expression of Drosophila Gdap1: Implications for the Charcot–Marie–Tooth Neuropathy.” *Human Molecular Genetics* 24 (1): 21–36. https://doi.org/10.1093/hmg/ddu416.

Lozeron, Pierre, Jean-Marc Trocello, and Nathalie Kubis. 2013. “Acquired Neuropathies.” *Journal of Neurology* 260 (9): 2433–40. https://doi.org/10.1007/s00415-013-6994-z.

Lukovic, Dunja, Andrea Diez Lloret, Petra Stojkovic, Daniel Rodríguez-Martínez, Maria Amparo Perez Arago, Francisco Javier Rodriguez-Jimenez, Patricia González-Rodríguez, et al. 2017. “Highly Efficient Neural Conversion of Human Pluripotent Stem Cells in Adherent and Animal-Free Conditions: Pluripotent Stem Cell Derived Neural Progenitors.” *STEM CELLS Translational Medicine* 6 (4): 1217–26. https://doi.org/10.1002/sctm.16-0371.

Lyons, David A., and William S. Talbot. 2008. “Axonal Domains: Role for Paranodal Junction in Node of Ranvier Assembly.” *Current Biology* 18 (18): R876–79. https://doi.org/10.1016/j.cub.2008.07.070.

MacVicar, Thomas, and Thomas Langer. 2016. “OPA1 Processing in Cell Death and Disease – the Long and Short of It.” *Journal of Cell Science* 129 (12): 2297–2306. https://doi.org/10.1242/jcs.159186.

Maday, Sandra, Karen E. Wallace, and Erika L.F. Holzbaur. 2012. “Autophagosomes Initiate Distally and Mature during Transport toward the Cell Soma in Primary Neurons.” *Journal of Cell Biology* 196 (4): 407–17. https://doi.org/10.1083/jcb.201106120.

Maeda, Meiko Hashimoto, Jun Mitsui, Bing-Wen Soong, Yuji Takahashi, Hiroyuki Ishiura, Shin Hayashi, Yuichiro Shirota, et al. 2012. “Increased Gene Dosage of Myelin Protein Zero Causes Charcot-Marie-Tooth Disease.” *Annals of Neurology* 71 (1): 84–92. https://doi.org/10.1002/ana.22658.

Magy, Laurent, and Jean-Michel Vallat. 2009. “Peripheral neuropathies.” *La Revue Du Praticien* 59 (6): 839–40.

Malli, Roland, and Wolfgang F. Graier. 2017. “The Role of Mitochondria in the Activation/Maintenance of SOCE: The Contribution of Mitochondrial Ca2+ Uptake, Mitochondrial Motility, and Location to Store-Operated Ca2+ Entry.” In *Store-Operated Ca^{2+} Entry (SOCE) Pathways*, edited by Klaus Groschner, Wolfgang F. Graier, and Christoph Romanin, 993:297–319. Advances in Experimental Medicine and Biology. Cham: Springer International Publishing. https://doi.org/10.1007/978-3-319-57732-6_16.

Mallik, A. 2005. “Nerve Conduction Studies: Essentials and Pitfalls in Practice.” *Journal of Neurology, Neurosurgery & Psychiatry* 76 (suppl_2): ii23–31. https://doi.org/10.1136/jnnp.2005.069138.

Mandal, Amrita, and Catherine M. Drerup. 2019. “Axonal Transport and Mitochondrial Function in Neurons.” *Frontiers in Cellular Neuroscience* 13 (August): 373. https://doi.org/10.3389/fncel.2019.00373.

Manivannan, Muniyandi, and Pawan Kumar Suresh. 2012. “On the Somatosensation of Vision.” *Annals of Neurosciences* 19 (1). https://doi.org/10.5214/ans.0972.7531.180409.

Marco, A. 2003. “Evolutionary and Structural Analyses of GDAP1, Involved in Charcot-Marie-Tooth Disease, Characterize a Novel Class of Glutathione Transferase-Related Genes.” *Molecular Biology and Evolution* 21 (1): 176–87. https://doi.org/10.1093/molbev/msh013.

Marí, Montserrat, Albert Morales, Anna Colell, Carmen García-Ruiz, and José C. Fernández-Checa. 2009. “Mitochondrial Glutathione, a Key Survival Antioxidant.” *Antioxidants & Redox Signaling* 11 (11): 2685–2700. https://doi.org/10.1089/ars.2009.2695.

Martí, Salvador, Marian León, Carmen Orellana, Javier Prieto, Xavier Ponsoda, Carlos López-García, Juan Jesús Vílchez, Teresa Sevilla, and Josema Torres. 2017. “Generation of a Disease-Specific IPS Cell Line Derived from a Patient with Charcot-Marie-Tooth Type 2K Lacking Functional GDAP1 Gene.” *Stem Cell Research* 18 (January): 1–4. https://doi.org/10.1016/j.scr.2016.11.017.

Martin, John Harry, Howard J Radzyner, and Michael E Leonard. 2012. *Neuroanatomy Text and Atlas*. New York; Chicago; San Francisco: McGraw-Hill Medical.

Martinez-Vicente, Marta. 2017. “Neuronal Mitophagy in Neurodegenerative Diseases.” *Frontiers in Molecular Neuroscience* 10 (March). https://doi.org/10.3389/fnmol.2017.00064.

Masingue, Marion, Jimmy Perrot, Robert-Yves Carlier, Guenaelle Piguet-Lacroix, Philippe Latour, and Tanya Stojkovic. 2018. “WES Homozygosity Mapping in a Recessive Form of Charcot-Marie-Tooth Neuropathy Reveals Intronic GDAP1 Variant Leading to a Premature Stop Codon.” *Neurogenetics* 19 (2): 67–76. https://doi.org/10.1007/s10048-018-0539-7.

Mastroeni, Diego, Omar M. Khdour, Elaine Delvaux, Jennifer Nolz, Gary Olsen, Nicole Berchtold, Carl Cotman, Sidney M. Hecht, and Paul D. Coleman. 2017. “Nuclear but Not Mitochondrial-Encoded Oxidative Phosphorylation Genes Are Altered in Aging, Mild Cognitive Impairment, and Alzheimer’s Disease.” *Alzheimer’s & Dementia* 13 (5): 510–19. https://doi.org/10.1016/j.jalz.2016.09.003.

Mathis, Stéphane, Cyril Goizet, Meriem Tazir, Corinne Magdelaine, Anne-Sophie Lia, Laurent Magy, and Jean-Michel Vallat. 2015. “Charcot–Marie–Tooth Diseases: An Update and Some New Proposals for the Classification.” *Journal of Medical Genetics* 52 (10): 681–90. https://doi.org/10.1136/jmedgenet-2015-103272.

Mazunin, I. O., S. A. Levitskii, M. V. Patrushev, and P. A. Kamenski. 2015. “Mitochondrial Matrix Processes.” *Biochemistry (Moscow)* 80 (11): 1418–28. https://doi.org/10.1134/S0006297915110036.

Mbemba Fundu, Théophile, Paulin Mutwale Kapepula, Justin Mboloko Esimo, José Remacle, and Nadege Kabamba Ngombe. 2020. “Subcellular Localization of Glutathione Peroxidase, Change in Glutathione System during Ageing and Effects on Cardiometabolic Risks and Associated Diseases.” In *Glutathione System and Oxidative Stress in Health and Disease*, edited by Margarete Dulce Bagatini. IntechOpen. https://doi.org/10.5772/intechopen.89384.

McCommis, Kyle S., and Brian N. Finck. 2015. “Mitochondrial Pyruvate Transport: A Historical Perspective and Future Research Directions.” *Biochemical Journal* 466 (3): 443–54. https://doi.org/10.1042/BJ20141171.

Menorca, Ron M.G., Theron S. Fussell, and John C. Elfar. 2013. “Peripheral Nerve Trauma: Mechanisms of Injury and Recovery.” *Hand Clinics* 29 (3): 317–30. https://doi.org/10.1016/j.hcl.2013.04.002.

Miressi, Federica, Pierre-Antoine Faye, Ioanna Pyromali, Sylvie Bourthoumieux, Paco Derouault, Marie Husson, Frédéric Favreau, Franck Sturtz, Corinne Magdelaine, and Anne-Sophie Lia. 2020. “A Mutation Can Hide Another One: Think Structural Variants!” *Computational and Structural Biotechnology Journal* 18: 2095–99. https://doi.org/10.1016/j.csbj.2020.07.021.

Mirończuk-Chodakowska, Iwona, Anna Maria Witkowska, and Małgorzata Elżbieta Zujko. 2018. “Endogenous Non-Enzymatic Antioxidants in the Human Body.” *Advances in Medical Sciences* 63 (1): 68–78. https://doi.org/10.1016/j.advms.2017.05.005.

Misra, UshaKant, Jayantee Kalita, and PradeepP Nair. 2008. “Diagnostic Approach to Peripheral Neuropathy.” *Annals of Indian Academy of Neurology* 11 (2): 89. https://doi.org/10.4103/0972-2327.41875.

Moattari, Mehrnaz, Farahnaz Moattari, Gholamreza Kaka, and Homa Mohseni Kouchesfahani. 2018. “A Review on Nerve Conduction Studies.” *Scholarly Journal of Psychology and Behavioral Sciences* 1 (3). https://doi.org/10.32474/SJPBS.2018.01.000115.

Morena, Jonathan, Anirudh Gupta, and J. Chad Hoyle. 2019. “Charcot-Marie-Tooth: From Molecules to Therapy.” *International Journal of Molecular Sciences* 20 (14): 3419. https://doi.org/10.3390/ijms20143419.

Morris, J R, and R J Lasek. 1982. “Stable Polymers of the Axonal Cytoskeleton: The Axoplasmic Ghost.” *Journal of Cell Biology* 92 (1): 192–98. https://doi.org/10.1083/jcb.92.1.192.

Mortreux, J., J. Bacquet, A. Boyer, E. Alazard, R. Bellance, A. G. Giguet-Valard, M. Cerino, et al. 2020. “Identification of Novel Pathogenic Copy Number Variations in Charcot-Marie-Tooth Disease.” *Journal of Human Genetics* 65 (3): 313–23. https://doi.org/10.1038/s10038-019-0710-5.

Motley, William W., Kevin Talbot, and Kenneth H. Fischbeck. 2010. “GARS Axonopathy: Not Every Neuron’s Cup of TRNA.” *Trends in Neurosciences* 33 (2): 59–66. https://doi.org/10.1016/j.tins.2009.11.001.

Muller, Quentin, Marie-Josée Beaudet, Thiéry De Serres-Bérard, Sabrina Bellenfant, Vincent Flacher, and François Berthod. 2018. “Development of an Innervated Tissue-Engineered Skin with Human Sensory Neurons and Schwann Cells Differentiated from IPS Cells.” *Acta Biomaterialia* 82 (December): 93–101. https://doi.org/10.1016/j.actbio.2018.10.011.

Mundorf, Annakarina, Stefanie Rommel, Malte Verheyen, Evanthia Mergia, Marcus Peters, and Nadja Freund. 2020. “Cigarette Smoke Exposure Has Region-Specific Effects on GDAP1 Expression in Mouse Hippocampus.” *Psychiatry Research* 289 (July): 112979. https://doi.org/10.1016/j.psychres.2020.112979.

Muroyama, Yuko, Motoyuki Fujihara, Makoto Ikeya, Hisato Kondoh, and Shinji Takada. 2002. “Wnt Signaling Plays an Essential Role in Neuronal Specification of the Dorsal Spinal Cord.” *Genes & Development* 16 (5): 548–53. https://doi.org/10.1101/gad.937102.

Murphy, Sinead M, Matilde Laura, Katherine Fawcett, Amelie Pandraud, Yo-Tsen Liu, Gabrielle L Davidson, Alexander M Rossor, et al. 2012. “Charcot–Marie–Tooth Disease: Frequency of Genetic Subtypes and Guidelines for Genetic Testing.” *Journal of Neurology, Neurosurgery & Psychiatry* 83 (7): 706–10. https://doi.org/10.1136/jnnp-2012-302451.

Nakagawa, Masato, Yukimasa Taniguchi, Sho Senda, Nanako Takizawa, Tomoko Ichisaka, Kanako Asano, Asuka Morizane, et al. 2015. “A Novel Efficient Feeder-Free Culture System for the Derivation of Human Induced Pluripotent Stem Cells.” *Scientific Reports* 4 (1): 3594. https://doi.org/10.1038/srep03594.

Nelis, E., S. Erdem, P. Y.K. Van den Bergh, M.-C. Belpaire-Dethiou, C. Ceuterick, V. Van Gerwen, A. Cuesta, et al. 2002. “Mutations in GDAP1: Autosomal Recessive CMT with Demyelination and Axonopathy.” *Neurology* 59 (12): 1865–72. https://doi.org/10.1212/01.WNL.0000036272.36047.54.

Niemann, Axel, Nina Huber, Konstanze M. Wagner, Christian Somandin, Michael Horn, Frédéric Lebrun-Julien, Brigitte Angst, et al. 2014. “The Gdap1 Knockout Mouse Mechanistically Links Redox Control to Charcot–Marie–Tooth Disease.” *Brain* 137 (3): 668–82. https://doi.org/10.1093/brain/awt371.

Niemann, Axel, Marcel Ruegg, Veronica La Padula, Angelo Schenone, and Ueli Suter. 2005. “Ganglioside-Induced Differentiation Associated Protein 1 Is a Regulator of the Mitochondrial Network.” *Journal of Cell Biology* 170 (7): 1067–78. https://doi.org/10.1083/jcb.200507087.

Niemann, Axel, Konstanze Marion Wagner, Marcel Ruegg, and Ueli Suter. 2009. “GDAP1 Mutations Differ in Their Effects on Mitochondrial Dynamics and Apoptosis Depending on the Mode of Inheritance.” *Neurobiology of Disease* 36 (3): 509–20. https://doi.org/10.1016/j.nbd.2009.09.011.

Noack, Rebecca, Svenja Frede, Philipp Albrecht, Nadine Henke, Annika Pfeiffer, Katrin Knoll, Thomas Dehmel, et al. 2012. “Charcot–Marie–Tooth Disease CMT4A: GDAP1 Increases Cellular Glutathione and the Mitochondrial Membrane Potential.” *Human Molecular Genetics* 21 (1): 150–62. https://doi.org/10.1093/hmg/ddr450.

Nochez, Yannick, Sophie Arsene, Naig Gueguen, Arnaud Chevrollier, Marc Ferré, Virginie Guillet, Valérie Desquiret, et al. 2009. “Acute and Late-Onset Optic Atrophy Due to a Novel OPA1 Mutation Leading to a Mitochondrial Coupling Defect.” *Molecular Vision* 15: 598–608.

Notterpek, Lucia, Mary C. Ryan, Andreas R. Tobler, and Eric M. Shooter. 1999. “PMP22 Accumulation in Aggresomes: Implications for CMT1A Pathology.” *Neurobiology of Disease* 6 (5): 450–60. https://doi.org/10.1006/nbdi.1999.0274.

Okamoto, Yuji, Meryem Tuba Goksungur, Davut Pehlivan, Christine R. Beck, Claudia Gonzaga-Jauregui, Donna M. Muzny, Mehmed M. Atik, et al. 2014. “Exonic Duplication CNV of NDRG1 Associated with Autosomal-Recessive HMSN-Lom/CMT4D.” *Genetics in Medicine* 16 (5): 386–94. https://doi.org/10.1038/gim.2013.155.

OpenStax College. 2013. *Anatomy and Physiology*. Houston, Texas: Rice University. https://openstaxcollege.org/files/textbook_version/hi_res_pdf/13/col11496-op.pdf.

Owen, Joshua B., and D. Allan Butterfield. 2010. “Measurement of Oxidized/Reduced Glutathione Ratio.” In *Protein Misfolding and Cellular Stress in Disease and Aging*, edited by Peter Bross and Niels Gregersen, 648:269–77. Methods in Molecular Biology. Totowa, NJ: Humana Press. https://doi.org/10.1007/978-1-60761-756-3_18.

Pagliuso, Alessandro, Pascale Cossart, and Fabrizia Stavru. 2018. “The Ever-Growing Complexity of the Mitochondrial Fission Machinery.” *Cellular and Molecular Life Sciences* 75 (3): 355–74. https://doi.org/10.1007/s00018-017-2603-0.

Pakhrin, Pukar Singh, Yongzhi Xie, Zhengmao Hu, Xiaobo Li, Lei Liu, Shunxiang Huang, Binghao Wang, et al. 2018. “Genotype–Phenotype Correlation and Frequency of Distribution in a Cohort of Chinese Charcot–Marie–Tooth Patients Associated with GDAP1 Mutations.” *Journal of Neurology* 265 (3): 637–46. https://doi.org/10.1007/s00415-018-8743-9.

Palau, Francesc, Anna Estela, David Pla-Martín, and Maribel Sánchez-Piris. 2009. “The Role of Mitochondrial Network Dynamics in the Pathogenesis of Charcot-Marie-Tooth Disease.” In *Inherited Neuromuscular Diseases*, edited by Carmen Espinós, Vicente Felipo, and Francesc Palau, 652:129–37. Advances in Experimental Medicine and Biology. Dordrecht: Springer Netherlands. https://doi.org/10.1007/978-90-481-2813-6_9.

Palikaras, Konstantinos, Eirini Lionaki, and Nektarios Tavernarakis. 2018. “Mechanisms of Mitophagy in Cellular Homeostasis, Physiology and Pathology.” *Nature Cell Biology* 20 (9): 1013–22. https://doi.org/10.1038/s41556-018-0176-2.

Paradies, Giuseppe, Valeria Paradies, Francesca M. Ruggiero, and Giuseppe Petrosillo. 2019. “Role of Cardiolipin in Mitochondrial Function and Dynamics in Health and Disease: Molecular and Pharmacological Aspects.” *Cells* 8 (7): 728. https://doi.org/10.3390/cells8070728.

Pareyson, Davide, Mary M Reilly, Angelo Schenone, Gian Maria Fabrizi, Tiziana Cavallaro, Lucio Santoro, Giuseppe Vita, et al. 2011. “Ascorbic Acid in Charcot–Marie–Tooth Disease Type 1A (CMT-TRIAAL and CMT-TRAUK): A Double-Blind Randomised Trial.” *The Lancet Neurology* 10 (4): 320–28. https://doi.org/10.1016/S1474-4422(11)70025-4.

Pareyson, Davide, Paola Saveri, Anna Sagnelli, and Giuseppe Piscosquito. 2015. “Mitochondrial Dynamics and Inherited Peripheral Nerve Diseases.” *Neuroscience Letters* 596 (June): 66–77. https://doi.org/10.1016/j.neulet.2015.04.001.

Passage, Edith, Jean Chrétien Norreel, Pauline Noack-Fraissignes, Véronique Sanguedolce, Josette Pizant, Xavier Thirion, Andrée Robaglia-Schlupp, Jean François Pellissier, and Michel Fontés. 2004. “Ascorbic Acid Treatment Corrects the Phenotype of a Mouse Model of Charcot-Marie-Tooth Disease.” *Nature Medicine* 10 (4): 396–401. https://doi.org/10.1038/nm1023.

Pedrola, Laia, Antonio Espert, Teresa Valdés-Sánchez, Maribel Sánchez-Piris, Erich E. Sirkowski, Steven S. Scherer, Isabel Fariñas, and Francesc Palau. 2008. “Cell Expression of GDAP1 in the Nervous System and Pathogenesis of Charcot-Marie-Tooth Type 4A Disease.” *Journal of Cellular and Molecular Medicine* 12 (2): 679–89. https://doi.org/10.1111/j.1582-4934.2007.00158.x.

Pedrola, Laia, Antonio Espert, Xingyao Wu, Reyes Claramunt, Michael E. Shy, and Francesc Palau. 2005. “GDAP1, the Protein Causing Charcot–Marie–Tooth Disease Type 4A, Is Expressed in Neurons and Is Associated with Mitochondria.” *Human Molecular Genetics* 14 (8): 1087–94. https://doi.org/10.1093/hmg/ddi121.

Pehlivan, Davut, Christine R. Beck, Yuji Okamoto, Tamar Harel, Zeynep H. C. Akdemir, Shalini N. Jhangiani, Marjorie A. Withers, et al. 2016. “The Role of Combined SNV and CNV Burden in Patients with Distal Symmetric Polyneuropathy.” *Genetics in Medicine* 18 (5): 443–51. https://doi.org/10.1038/gim.2015.124.

Philibert, Robert A, Brandan Penaluna, Teresa White, Sarah Shires, Tracy Gunter, Jill Liesveld, Cheryl Erwin, Nancy Hollenbeck, and Terry Osborn. 2014. “A Pilot Examination of the Genome-Wide DNA Methylation Signatures of Subjects Entering and Exiting Short-Term Alcohol Dependence Treatment Programs.” *Epigenetics* 9 (9): 1212–19. https://doi.org/10.4161/epi.32252.

Piazza, S., G. Ricci, E. Caldarazzo Ienco, C. Carlesi, L. Volpi, G. Siciliano, and M. Mancuso. 2010. “Pes Cavus and Hereditary Neuropathies: When a Relationship Should Be Suspected.” *Journal of Orthopaedics and Traumatology* 11 (4): 195–201. https://doi.org/10.1007/s10195-010-0114-y.

Pizzorno, Joseph. 2014. “Mitochondria—Fundamental to Life and Health.” *Integrative Medicine* 13 (2): 8.

Pla-Martín, David, Carlos B. Rueda, Anna Estela, Maribel Sánchez-Piris, Paloma González-Sánchez, Javier Traba, Sergio de la Fuente, et al. 2013. “Silencing of the Charcot–Marie–Tooth Disease-Associated Gene GDAP1 Induces Abnormal Mitochondrial Distribution and Affects Ca2+ Homeostasis by Reducing Store-Operated Ca2+ Entry.” *Neurobiology of Disease* 55 (July): 140–51. https://doi.org/10.1016/j.nbd.2013.03.010.

Poian, Andrea T. Da, and Miguel A. R. B. Castanho. 2015. *Integrative Human Biochemistry: A Textbook for Medical Biochemistry*. New York: Springer.

Posey, Jennifer E., Tamar Harel, Pengfei Liu, Jill A. Rosenfeld, Regis A. James, Zeynep H. Coban Akdemir, Magdalena Walkiewicz, et al. 2017. “Resolution of Disease Phenotypes Resulting from Multilocus Genomic Variation.” *New England Journal of Medicine* 376 (1): 21–31. https://doi.org/10.1056/NEJMoa1516767.

Poston, Chloe N., Srinivasan C. Krishnan, and Carthene R. Bazemore-Walker. 2013. “In-Depth Proteomic Analysis of Mammalian Mitochondria-Associated Membranes (MAM).” *Journal of Proteomics* 79 (February): 219–30. https://doi.org/10.1016/j.jprot.2012.12.018.

Prieto, Javier, Marian León, Xavier Ponsoda, Francisco García-García, Roque Bort, Eva Serna, Manuela Barneo-Muñoz, et al. 2016. “Dysfunctional Mitochondrial Fission Impairs Cell Reprogramming.” *Cell Cycle* 15 (23): 3240–50. https://doi.org/10.1080/15384101.2016.1241930.

Prukop, Thomas, Stephanie Wernick, Lydie Boussicault, David Ewers, Karoline Jäger, Julia Adam, Lorenz Winter, et al. 2020. “Synergistic PXT3003 Therapy Uncouples Neuromuscular Function from Dysmyelination in Male Charcot–Marie–Tooth Disease Type 1A (CMT1A) Rats.” *Journal of Neuroscience Research* 98 (10): 1933–52. https://doi.org/10.1002/jnr.24679.

Purves, Dale, ed. 2004. *Neuroscience*. 3rd ed. Sunderland, Mass: Sinauer Associates, Publishers.

Puurand, Marju, Kersti Tepp, Natalja Timohhina, Jekaterina Aid, Igor Shevchuk, Vladimir Chekulayev, and Tuuli Kaambre. 2019. “Tubulin BII and BIII Isoforms as the Regulators of VDAC Channel Permeability in Health and Disease.” *Cells* 8 (3): 239. https://doi.org/10.3390/cells8030239.

Quarles, Richard H. 2007. “Myelin Lipids and Proteins: Structure, Function, and Roles in Neurological Disorders.” In *Handbook of Contemporary Neuropharmacology*, edited by David R. Sibley, Michael Kuhar, Israel Hanin, and Phil Skolnick, hcn065. Hoboken, NJ, USA: John Wiley & Sons, Inc. https://doi.org/10.1002/9780470101001.hcn065.

Quintero, Omar A., Melinda M. DiVito, Rebecca C. Adikes, Melisa B. Kortan, Lindsay B. Case, Audun J. Lier, Niki S. Panaretos, et al. 2009. “Human Myo19 Is a Novel Myosin That Associates with Mitochondria.” *Current Biology* 19 (23): 2008–13. https://doi.org/10.1016/j.cub.2009.10.026.

Ramesh, Tushar, Sai V Nagula, Gabrielle G Tardieu, Erfanul Saker, Mohammadali Shoja, Marios Loukas, Rod J Oskouian, and R Shane Tubbs. 2017. “Update on the Notochord Including Its Embryology, Molecular Development, and Pathology: A Primer for the Clinician,” 11.

Rehklau, Katharina, Lena Hoffmann, Christine B Gurniak, Martin Ott, Walter Witke, Luca Scorrano, Carsten Culmsee, and Marco B Rust. 2017. “Cofilin1-Dependent Actin Dynamics Control DRP1-Mediated Mitochondrial Fission.” *Cell Death & Disease* 8 (10): e3063–e3063. https://doi.org/10.1038/cddis.2017.448.

Reinhold, Ak, and Hl Rittner. 2017. “Barrier Function in the Peripheral and Central Nervous System—a Review.” *Pflügers Archiv - European Journal of Physiology* 469 (1): 123–34. https://doi.org/10.1007/s00424-016-1920-8.

Rizzo, Federica, Dario Ronchi, Sabrina Salani, Monica Nizzardo, Francesco Fortunato, Andreina Bordoni, Giulia Stuppia, et al. 2016. “Selective Mitochondrial Depletion, Apoptosis Resistance, and Increased Mitophagy in Human Charcot-Marie-Tooth 2A Motor Neurons.” *Human Molecular Genetics* 25 (19): 4266–81. https://doi.org/10.1093/hmg/ddw258.

Rocha, Agostinho G., Antonietta Franco, Andrzej M. Krezel, Jeanne M. Rumsey, Justin M. Alberti, William C. Knight, Nikolaos Biris, et al. 2018. “MFN2 Agonists Reverse Mitochondrial Defects in Preclinical Models of Charcot-Marie-Tooth Disease Type 2A.” *Science* 360 (6386): 336–41. https://doi.org/10.1126/science.aao1785.

Roger, Andrew J., Sergio A. Muñoz-Gómez, and Ryoma Kamikawa. 2017. “The Origin and Diversification of Mitochondria.” *Current Biology* 27 (21): R1177–92. https://doi.org/10.1016/j.cub.2017.09.015.

Rossor, Alexander M, Bernadett Kalmar, Linda Greensmith, and Mary M Reilly. 2012. “The Distal Hereditary Motor Neuropathies.” *Journal of Neurology, Neurosurgery & Psychiatry* 83 (1): 6–14. https://doi.org/10.1136/jnnp-2011-300952.

Rossor, Alexander M., James M. Polke, Henry Houlden, and Mary M. Reilly. 2013. “Clinical Implications of Genetic Advances in Charcot–Marie–Tooth Disease.” *Nature Reviews Neurology* 9 (10): 562–71. https://doi.org/10.1038/nrneurol.2013.179.

Rossor, Alexander M., Pedro J. Tomaselli, and Mary M. Reilly. 2016. “Recent Advances in the Genetic Neuropathies:” *Current Opinion in Neurology*, September, 1. https://doi.org/10.1097/WCO.0000000000000373.

Rotthier, Annelies, Jonathan Baets, Vincent Timmerman, and Katrien Janssens. 2012. “Mechanisms of Disease in Hereditary Sensory and Autonomic Neuropathies.” *Nature Reviews Neurology* 8 (2): 73–85. https://doi.org/10.1038/nrneurol.2011.227.

Rubin, Devon I. 2012. “Needle Electromyography: Basic Concepts and Patterns of Abnormalities.” *Neurologic Clinics* 30 (2): 429–56. https://doi.org/10.1016/j.ncl.2011.12.009.

Rudnik-Schöneborn, S., D. Tölle, J. Senderek, K. Eggermann, M. Elbracht, U. Kornak, M. von der Hagen, et al. 2016. “Diagnostic Algorithms in Charcot-Marie-Tooth Neuropathies: Experiences from a German Genetic Laboratory on the Basis of 1206 Index Patients: Diagnostic Algorithms in Charcot-Marie-Tooth Neuropathies.” *Clinical Genetics* 89 (1): 34–43. https://doi.org/10.1111/cge.12594.

Ryu, E. J., M. Yang, J. A. Gustin, L.-W. Chang, R. R. Freimuth, R. Nagarajan, and J. Milbrandt. 2008. “Analysis of Peripheral Nerve Expression Profiles Identifies a Novel Myelin Glycoprotein, MP11.” *Journal of Neuroscience* 28 (30): 7563–73. https://doi.org/10.1523/JNEUROSCI.1659-08.2008.

Rzepnikowska, Weronika, Joanna Kaminska, Dagmara Kabzińska, and Andrzej Kochański. 2020. “Pathogenic Effect of GDAP1 Gene Mutations in a Yeast Model.” *Genes* 11 (3): 310. https://doi.org/10.3390/genes11030310.

Rzepnikowska, Weronika, and Andrzej Kochański. 2018. “A Role for the GDAP1 Gene in the Molecular Pathogenesis of Charcot-Marie-Tooth Disease.” *Acta Neurobiologiae Experimentalis* 78 (1): 1–13. https://doi.org/10.21307/ane-2018-002.

Sabet, A., J. Li, K. Ghandour, Q. Pu, X. Wu, J. Kamholz, M. E. Shy, and F. Cambi. 2006. “Skin Biopsies Demonstrate MPZ Splicing Abnormalities in Charcot-Marie-Tooth Neuropathy 1B.” *Neurology* 67 (7): 1141–46. https://doi.org/10.1212/01.wnl.0000238499.37764.b1.

Said, Gerard. 2002. “Indications and Usefulness of Nerve Biopsy.” *ARCH NEUROL* 59: 4.

Saini, Rajiv. 2011. “Oral Sex and Oral Cancer: A Virus Link.” *Journal of Pharmacy and Bioallied Sciences* 3 (3): 467. https://doi.org/10.4103/0975-7406.84472.

Salomão, Rubens Paulo A., Maria Thereza Drumond Gama, Flávio Moura Rezende Filho, Fernanda Maggi, José Luiz Pedroso, and Orlando G. P. Barsottini. 2017. “Late-Onset Friedreich’s Ataxia (LOFA) Mimicking Charcot–Marie–Tooth Disease Type 2: What Is Similar and What Is Different?” *The Cerebellum* 16 (2): 599–601. https://doi.org/10.1007/s12311-016-0822-9.

Salzer, James L. 2008. “Switching Myelination on and Off.” *Journal of Cell Biology* 181 (4): 575–77. https://doi.org/10.1083/jcb.200804136.

Sancho, Sara, Peter Young, and Ueli Suter. 2001. “Regulation of Schwann Cell Proliferation and Apoptosis in PMP22-Deficient Mice and Mouse Models of Charcot-Marie-Tooth Disease Type 1A.” *Brain* 124 (11): 2177–87. https://doi.org/10.1093/brain/124.11.2177.

Saporta, Mario A., Vu Dang, Dmitri Volfson, Bende Zou, Xinmin (Simon) Xie, Adijat Adebola, Ronald K. Liem, Michael Shy, and John T. Dimos. 2015. “Axonal Charcot–Marie–Tooth Disease Patient-Derived Motor Neurons Demonstrate Disease-Specific Phenotypes Including Abnormal Electrophysiological Properties.” *Experimental Neurology* 263 (January): 190–99. https://doi.org/10.1016/j.expneurol.2014.10.005.

Sasaki, Keiichi, Osamu Suzuki, and Nobuhiro Takahashi, eds. 2015. *Interface Oral Health Science 2014*. Tokyo: Springer Japan. https://doi.org/10.1007/978-4-431-55192-8.

Schon, Eric A., Salvatore DiMauro, and Michio Hirano. 2012. “Human Mitochondrial DNA: Roles of Inherited and Somatic Mutations.” *Nature Reviews Genetics* 13 (12): 878–90. https://doi.org/10.1038/nrg3275.

Schwarz, Nicole, and Rudolf Leube. 2016. “Intermediate Filaments as Organizers of Cellular Space: How They Affect Mitochondrial Structure and Function.” *Cells* 5 (3): 30. https://doi.org/10.3390/cells5030030.

Scott, Iain, and Richard J. Youle. 2010. “Mitochondrial Fission and Fusion.” Edited by Guy C. Brown and Michael P. Murphy. *Essays in Biochemistry* 47 (June): 85–98. https://doi.org/10.1042/bse0470085.

Senderek, J. 2003. “Mutations in the Ganglioside-Induced Differentiation-Associated Protein-1 (GDAP1) Gene in Intermediate Type Autosomal Recessive Charcot-Marie-Tooth Neuropathy.” *Brain* 126 (3): 642–49. https://doi.org/10.1093/brain/awg068.

Sevilla, T., T. Jaijo, D. Nauffal, D. Collado, M. J. Chumillas, J. J. Vilchez, N. Muelas, et al. 2008. “Vocal Cord Paresis and Diaphragmatic Dysfunction Are Severe and Frequent Symptoms of GDAP1-Associated Neuropathy.” *Brain* 131 (11): 3051–61. https://doi.org/10.1093/brain/awn228.

Shehab, D., Khaled Al-Jarallah, Nabila Abdella, Olusegun A. Mojiminiyi, and Hisham Al Mohamedy. 2015. “Prospective Evaluation of the Effect of Short-Term Oral Vitamin D Supplementation on Peripheral Neuropathy in Type 2 Diabetes Mellitus.” *Medical Principles and Practice* 24 (3): 250–56. https://doi.org/10.1159/000375304.

Shi, Lei, Lihua Huang, Ruojie He, Weijun Huang, Huiyan Wang, Xingqiang Lai, Zhengwei Zou, et al. 2018. “Modeling the Pathogenesis of Charcot-Marie-Tooth Disease Type 1A Using Patient-Specific IPSCs.” *Stem Cell Reports* 10 (1): 120–33. https://doi.org/10.1016/j.stemcr.2017.11.013.

Shield, Alison J., Tracy P. Murray, and Philip G. Board. 2006. “Functional Characterisation of Ganglioside-Induced Differentiation-Associated Protein 1 as a Glutathione Transferase.” *Biochemical and Biophysical Research Communications* 347 (4): 859–66. https://doi.org/10.1016/j.bbrc.2006.06.189.

Simões-Costa, Marcos, and Marianne E Bronner. 2015. “Establishing Neural Crest Identity: A Gene Regulatory Recipe,” 16.

Sivera, Rafael, Marina Frasquet, Vincenzo Lupo, Tania García-Sobrino, Patricia Blanco-Arias, Julio Pardo, Roberto Fernández-Torrón, et al. 2017. “Distribution and Genotype-Phenotype Correlation of GDAP1 Mutations in Spain.” *Scientific Reports* 7 (1): 6677. https://doi.org/10.1038/s41598-017-06894-6.

Spinazzi, Marco, Silvia Cazzola, Mario Bortolozzi, Alessandra Baracca, Emanuele Loro, Alberto Casarin, Giancarlo Solaini, et al. 2008. “A Novel Deletion in the GTPase Domain of OPA1 Causes Defects in Mitochondrial Morphology and Distribution, but Not in Function.” *Human Molecular Genetics* 17 (21): 3291–3302. https://doi.org/10.1093/hmg/ddn225.

Staff, Nathan P., and Anthony J. Windebank. 2014. “Peripheral Neuropathy Due to Vitamin Deficiency, Toxins, and Medications:” *CONTINUUM: Lifelong Learning in Neurology* 20 (October): 1293–1306. https://doi.org/10.1212/01.CON.0000455880.06675.5a.

Starkov, Anatoly A., and Gary Fiskum. 2003. “Regulation of Brain Mitochondrial H2O2 Production by Membrane Potential and NAD(P)H Redox State: ROS Production by Brain Mitochondria.” *Journal of Neurochemistry* 86 (5): 1101–7. https://doi.org/10.1046/j.1471-4159.2003.01908.x.

Stifani, Nicolas. 2014. “Motor Neurons and the Generation of Spinal Motor Neuron Diversity.” *Frontiers in Cellular Neuroscience* 8 (October). https://doi.org/10.3389/fncel.2014.00293.

Stiles, Joan, and Terry L. Jernigan. 2010. “The Basics of Brain Development.” *Neuropsychology Review* 20 (4): 327–48. https://doi.org/10.1007/s11065-010-9148-4.

Stolinski, C. 1995. “Structure and Composition of the Outer Connective Tissue Sheaths of Peripheral Nerve.” *Journal of Anatomy* 186 (Pt 1) (February): 123–30.

Sturtz, F.G., G. Chazot, and A.J.C. Vandenberghe. 1992. “Charcot-Marie-Tooth Disease from First Description to Genetic Localization of Mutations.” *Journal of the History of the Neurosciences* 1 (1): 47–58. https://doi.org/10.1080/09647049209525514.

Su, Bo, Xinglong Wang, Ling Zheng, George Perry, Mark A Smith, and Xiongwei Zhu. 2010. “Abnormal Mitochondrial Dynamics and Neurodegenerative Diseases.” *Biochimica et Biophysica Acta*, 8.

Su, Lian-Jiu, Jia-Hao Zhang, Hernando Gomez, Raghavan Murugan, Xing Hong, Dongxue Xu, Fan Jiang, and Zhi-Yong Peng. 2019. “Reactive Oxygen Species-Induced Lipid Peroxidation in Apoptosis, Autophagy, and Ferroptosis.” *Oxidative Medicine and Cellular Longevity* 2019 (October): 1–13. https://doi.org/10.1155/2019/5080843.

Suski, Jan M., Magdalena Lebiedzinska, Massimo Bonora, Paolo Pinton, Jerzy Duszynski, and Mariusz R. Wieckowski. 2012. “Relation Between Mitochondrial Membrane Potential and ROS Formation.” In *Mitochondrial Bioenergetics*, edited by Carlos M. Palmeira and António J. Moreno, 810:183–205. Methods in Molecular Biology. Totowa, NJ: Humana Press. https://doi.org/10.1007/978-1-61779-382-0_12.

Szigeti, Kinga, and James R Lupski. 2009. “Charcot–Marie–Tooth Disease.” *European Journal of Human Genetics* 17 (6): 703–10. https://doi.org/10.1038/ejhg.2009.31.

Takahashi, Kazutoshi, Koji Tanabe, Mari Ohnuki, Megumi Narita, Tomoko Ichisaka, Kiichiro Tomoda, and Shinya Yamanaka. 2007. “Induction of Pluripotent Stem Cells from Adult Human Fibroblasts by Defined Factors.” *Cell* 131 (5): 861–72. https://doi.org/10.1016/j.cell.2007.11.019.

Takahashi, Kazutoshi, and Shinya Yamanaka. 2006. “Induction of Pluripotent Stem Cells from Mouse Embryonic and Adult Fibroblast Cultures by Defined Factors.” *Cell* 126 (4): 663–76. https://doi.org/10.1016/j.cell.2006.07.024.

Tankisi, Hatice, Marit Otto, Kirsten Pugdahl, Birger Johnsen, and Anders Fuglsang-Frederiksen. 2012. “Correlation between Compound Muscle Action Potential Amplitude and Duration in Axonal and Demyelinating Polyneuropathy.” *Clinical Neurophysiology* 123 (10): 2099–2105. https://doi.org/10.1016/j.clinph.2012.04.002.

Tazir, Meriem, Tarik Hamadouche, Sonia Nouioua, Stephane Mathis, and Jean-Michel Vallat. 2014. “Hereditary Motor and Sensory Neuropathies or Charcot–Marie–Tooth Diseases: An Update.” *Journal of the Neurological Sciences* 347 (1–2): 14–22. https://doi.org/10.1016/j.jns.2014.10.013.

Tilokani, Lisa, Shun Nagashima, Vincent Paupe, and Julien Prudent. 2018. “Mitochondrial Dynamics: Overview of Molecular Mechanisms.” Edited by Caterina Garone and Michal Minczuk. *Essays in Biochemistry* 62 (3): 341–60. https://doi.org/10.1042/EBC20170104.

Timmer, John R., Charlotte Wang, and Lee Niswander. 2002. “BMP Signaling Patterns the Dorsal and Intermediate Neural Tube via Regulation of Homeobox and Helix-Loop-Helix Transcription Factors.” *Development (Cambridge, England)* 129 (10): 2459–72.

Timmerman, V., E. Nelis, W. Van Hul, B.W. Nieuwenhuijsen, K.L. Chen, S. Wang, K. Ben Othman, et al. 1992. “The Peripheral Myelin Protein Gene PMP–22 Is Contained

within the Charcot–Marie–Tooth Disease Type 1A Duplication." *Nature Genetics* 1 (3): 171–75. https://doi.org/10.1038/ng0692-171.

Timmerman, Vincent, Alleene Strickland, and Stephan Züchner. 2014. "Genetics of Charcot-Marie-Tooth (CMT) Disease within the Frame of the Human Genome Project Success." *Genes* 5 (1): 13–32. https://doi.org/10.3390/genes5010013.

Trushina, Eugenia. 2016. "A Shape Shifting Organelle: Unusual Mitochondrial Phenotype Determined with Three-Dimensional Electron Microscopy Reconstruction." *Neural Regeneration Research* 11 (6): 0. https://doi.org/10.4103/1673-5374.184477.

Turrens, J. F. 2003. "Mitochondrial Formation of Reactive Oxygen Species." *The Journal of Physiology* 552 (2): 335–44. https://doi.org/10.1113/jphysiol.2003.049478.

Uncini, Antonino, Keiichiro Susuki, and Nobuhiro Yuki. 2013. "Nodo-Paranodopathy: Beyond the Demyelinating and Axonal Classification in Anti-Ganglioside Antibody-Mediated Neuropathies." *Clinical Neurophysiology* 124 (10): 1928–34. https://doi.org/10.1016/j.clinph.2013.03.025.

Vallat, Jean-Michel, Robert A. Ouvrier, John D. Pollard, Corinne Magdelaine, Danqing Zhu, Garth A. Nicholson, Simon Grew, Monique M. Ryan, and Benoît Funalot. 2008. "Histopathological Findings in Hereditary Motor and Sensory Neuropathy of Axonal Type With Onset in Early Childhood Associated With *Mitofusin 2* Mutations." *Journal of Neuropathology & Experimental Neurology* 67 (11): 1097–1102. https://doi.org/10.1097/NEN.0b013e31818b6cbc.

van Spronsen, Myrrhe, Marina Mikhaylova, Joanna Lipka, Max A. Schlager, Dave J. van den Heuvel, Marijn Kuijpers, Phebe S. Wulf, et al. 2013. "TRAK/Milton Motor-Adaptor Proteins Steer Mitochondrial Trafficking to Axons and Dendrites." *Neuron* 77 (3): 485–502. https://doi.org/10.1016/j.neuron.2012.11.027.

Vital, Anne, Philippe Latour, Guilhem Sole, Xavier Ferrer, Marie Rouanet, François Tison, Claude Vital, and Cyril Goizet. 2012. "A French Family with Charcot–Marie–Tooth Disease Related to Simultaneous Heterozygous MFN2 and GDAP1 Mutations." *Neuromuscular Disorders* 22 (8): 735–41. https://doi.org/10.1016/j.nmd.2012.04.001.

Wagner, Konstanze M., Marcel Rüegg, Axel Niemann, and Ueli Suter. 2009. "Targeting and Function of the Mitochondrial Fission Factor GDAP1 Are Dependent on Its Tail-Anchor." Edited by Mark R. Cookson. *PLoS ONE* 4 (4): e5160. https://doi.org/10.1371/journal.pone.0005160.

Wagner, O. I., J. Lifshitz, P. A. Janmey, M. Linden, T. K. McIntosh, and J.-F. Leterrier. 2003. "Mechanisms of Mitochondria-Neurofilament Interactions." *The Journal of Neuroscience* 23 (27): 9046–58. https://doi.org/10.1523/JNEUROSCI.23-27-09046.2003.

Wakabayashi, Junko, Zhongyan Zhang, Nobunao Wakabayashi, Yasushi Tamura, Masahiro Fukaya, Thomas W. Kensler, Miho Iijima, and Hiromi Sesaki. 2009. "The Dynamin-Related GTPase Drp1 Is Required for Embryonic and Brain Development in Mice." *Journal of Cell Biology* 186 (6): 805–16. https://doi.org/10.1083/jcb.200903065.

Wang, Chao, Michael E. Ward, Robert Chen, Kai Liu, Tara E. Tracy, Xu Chen, Min Xie, et al. 2017. "Scalable Production of IPSC-Derived Human Neurons to Identify Tau-Lowering Compounds by High-Content Screening." *Stem Cell Reports* 9 (4): 1221–33. https://doi.org/10.1016/j.stemcr.2017.08.019.

Wang, Ying, and Fei Yin. 2016. "A Review of X-Linked Charcot-Marie-Tooth Disease." *Journal of Child Neurology* 31 (6): 761–72. https://doi.org/10.1177/0883073815604227.

Wanschers, Bas F.J., Rinske van de Vorstenbosch, Max A. Schlager, Daniël Splinter, Anna Akhmanova, Casper C. Hoogenraad, Bé Wieringa, and Jack A.M. Fransen. 2007. “A Role for the Rab6B Bicaudal–D1 Interaction in Retrograde Transport in Neuronal Cells.” *Experimental Cell Research* 313 (16): 3408–20. https://doi.org/10.1016/j.yexcr.2007.05.032.

Westermann, Benedikt. 2010. “Mitochondrial Dynamics in Model Organisms: What Yeasts, Worms and Flies Have Taught Us about Fusion and Fission of Mitochondria.” *Seminars in Cell & Developmental Biology* 21 (6): 542–49. https://doi.org/10.1016/j.semcdb.2009.12.003.

Whitworth, James, Anne-Bine Skytte, Lone Sunde, Derek H. Lim, Mark J. Arends, Lisa Happerfield, Ian M. Frayling, et al. 2016. “Multilocus Inherited Neoplasia Alleles Syndrome: A Case Series and Review.” *JAMA Oncology* 2 (3): 373. https://doi.org/10.1001/jamaoncol.2015.4771.

Wojsiat, Joanna, Katarzyna Marta Zoltowska, Katarzyna Laskowska-Kaszub, and Urszula Wojda. 2018. “Oxidant/Antioxidant Imbalance in Alzheimer’s Disease: Therapeutic and Diagnostic Prospects.” *Oxidative Medicine and Cellular Longevity* 2018: 1–16. https://doi.org/10.1155/2018/6435861.

Yatsuzuka, Atsuki, Akiko Hori, Minori Kadoya, Mami Matsuo-Takasaki, Toru Kondo, and Noriaki Sasai. 2019. “GPR17 Is an Essential Regulator for the Temporal Adaptation of Sonic Hedgehog Signalling in Neural Tube Development.” *Development* 146 (17): dev176784. https://doi.org/10.1242/dev.176784.

Yoshimura, Akiko, Jun-Hui Yuan, Akihiro Hashiguchi, Masahiro Ando, Yujiro Higuchi, Tomonori Nakamura, Yuji Okamoto, Masanori Nakagawa, and Hiroshi Takashima. 2019. “Genetic Profile and Onset Features of 1005 Patients with Charcot-Marie-Tooth Disease in Japan.” *Journal of Neurology, Neurosurgery & Psychiatry* 90 (2): 195–202. https://doi.org/10.1136/jnnp-2018-318839.

You, Jun, and Zhulong Chan. 2015. “ROS Regulation During Abiotic Stress Responses in Crop Plants.” *Frontiers in Plant Science* 6 (December). https://doi.org/10.3389/fpls.2015.01092.

Youle, Richard J., and Derek P. Narendra. 2011. “Mechanisms of Mitophagy.” *Nature Reviews Molecular Cell Biology* 12 (1): 9–14. https://doi.org/10.1038/nrm3028.

Zajączkowska, Renata, Magdalena Kocot-Kępska, Wojciech Leppert, Anna Wrzosek, Joanna Mika, and Jerzy Wordliczek. 2019. “Mechanisms of Chemotherapy-Induced Peripheral Neuropathy.” *International Journal of Molecular Sciences* 20 (6): 1451. https://doi.org/10.3390/ijms20061451.

Zhang, Juanjuan, Xiaoling Liu, Xiaoyang Liang, Yuanyuan Lu, Ling Zhu, Runing Fu, Yanchun Ji, et al. 2017. “A Novel ADOA-Associated OPA1 Mutation Alters the Mitochondrial Function, Membrane Potential, ROS Production and Apoptosis.” *Scientific Reports* 7 (1): 5704. https://doi.org/10.1038/s41598-017-05571-y.

Zhang, Yingsha, ChangHui Pak, Yan Han, Henrik Ahlenius, Zhenjie Zhang, Soham Chanda, Samuele Marro, et al. 2013. “Rapid Single-Step Induction of Functional Neurons from Human Pluripotent Stem Cells.” *Neuron* 78 (5): 785–98. https://doi.org/10.1016/j.neuron.2013.05.029.

Zhao, Hien Tran, Sagar Damle, Karli Ikeda-Lee, Steven Kuntz, Jian Li, Apoorva Mohan, Aneeza Kim, et al. 2017. “PMP22 Antisense Oligonucleotides Reverse Charcot-Marie-Tooth Disease Type 1A Features in Rodent Models.” *Journal of Clinical Investigation* 128 (1): 359–68. https://doi.org/10.1172/JCI96499.

Zimon, M., J. Baets, G. M. Fabrizi, E. Jaakkola, D. Kabzinska, J. Pilch, A. B. Schindler, et al. 2011. “Dominant GDAP1 Mutations Cause Predominantly Mild CMT Phenotypes.” *Neurology* 77 (6): 540–48. https://doi.org/10.1212/WNL.0b013e318228fc70.

Zis, Panagiotis, and Giustino Varrassi. 2017. “Painful Peripheral Neuropathy and Cancer.” *Pain and Therapy* 6 (2): 115–16. https://doi.org/10.1007/s40122-017-0077-2.

Zorov, Dmitry B., Magdalena Juhaszova, and Steven J. Sollott. 2014. “Mitochondrial Reactive Oxygen Species (ROS) and ROS-Induced ROS Release.” *Physiological Reviews* 94 (3): 909–50. https://doi.org/10.1152/physrev.00026.2013.

Zorova, Ljubava D., Vasily A. Popkov, Egor Y. Plotnikov, Denis N. Silachev, Irina B. Pevzner, Stanislovas S. Jankauskas, Valentina A. Babenko, et al. 2018. “Mitochondrial Membrane Potential.” *Analytical Biochemistry* 552 (July): 50–59. https://doi.org/10.1016/j.ab.2017.07.009.

Zorova, Lyubava, V. A. Popkov, E. J. Plotnikov, D. N. Silachev, I. B. Pevzner, S. S. Jankauskas, S. D. Zorov, V. A. Babenko, and D. B. Zorov. 2018. “Functional Significance of the Mitochondrial Membrane Potential.” *Biochemistry (Moscow), Supplement Series A: Membrane and Cell Biology* 12 (1): 20–26. https://doi.org/10.1134/S1990747818010129.

Neuropathies Périphériques Héréditaires: de la Génétique Moléculaire au modèle cellulaire de motoneurones dérivé d'hiPSC

La maladie de Charcot-Marie-Tooth (CMT) est la neuropathie périphérique héréditaire la plus fréquente. Actuellement plus de 80 gènes ont été identifiées comme étant à l'origine des CMT, mais le diagnostic génétique est posé seulement dans 30 à 40% des cas. Cette étude avait deux objectifs principaux: dans un premier temps, nous nous sommes intéressés aux CMT et neuropathies périphériques associées via une approche moléculaire et bioinformatique, pour optimiser leur caractérisation génétique; dans un second temps, nous avons étudié les mécanismes altérés dans une forme axonale de CMT, par la création d'un modèle cellulaire humain de cellules souches humaines induites à la pluripotence (hiPSc) et leur différenciation en motoneurones (MN). Dans la première partie du projet, nous présentons un nouvel outil bioinformatique, CovCopCan, développé au sein de l'équipe pour détecter les Variations du Nombre de Copies (CNV), à partir des données de NGS. Grâce à CovCopCan, deux nouveaux CNV ont été identifiés et nous discutons leur implication dans deux cas complexes de neuropathie périphérique. Nos travaux ont également permis de mettre en évidence trois variations génétiques chez un patient CMT, soulignant que la CMT peut être une pathologie génétique multilocus. Dans la deuxième partie de ce travail, un modèle cellulaire de MN a été créé pour étudier le gène *GDAP1* et son implication dans le CMT2H. Nous avons reprogrammé des fibroblastes dermiques de cinq sujets contrôles et de deux patients CMT, portant deux mutations codon-stop homozygotes sur le gène *GDAP1*, en cellules souches pluripotentes induites humaines (hiPSC). Nous avons ensuite mis au point un protocole de différenciation pour générer des MN à partir d'hiPSC. Les MN avec la mutation p.Ser194* sur *GDAP1* ont été analysés par des tests fonctionnels, morphologiques et d'expression. Nous avons confirmé l'expression neuronale de GDAP1, et nous avons mis en évidence que le stress oxydant et la dysfonction mitochondriale étaient à l'origine de la pathologie dans les MN CMT2H. Nos résultats ont montré que les analyses génétique et fonctionnelle sont essentielles pour la caractérisation complète de la maladie de CMT.

Mots-clés : Charcot-Marie-Tooth, génétique, motoneurones, hiPSC, mitochondries

Hereditary Peripheral Neuropathies: from Molecular Genetics to a cellular model of hiPSC-derived motor neurons.

Charcot-Marie-Tooth (CMT) disease is the most common hereditary peripheral neuropathy. To date, more than 80 genes have been identified to be involved in CMT, but genetic diagnosis is achieved only in 30-40% of cases. This study presented two main objectives: first, we focused on CMT and associated peripheral neuropathies using molecular and bioinformatic approaches to optimize their genetic characterization; secondly, we investigated impaired mechanisms in an axonal CMT form, by creating a human cellular model of human induced pluripotency stem cells (hiPSC) and their differentiation into motor neurons (MN). In the first part of the project, we developed a new bioinformatic tool, CovCopCan, to detect Copy Number Variations (CNV), starting from NGS data. Thanks to CovCopCan, two new CNV have been identified and we discuss their involvement in two complex cases of peripheral neuropathy. We also identified three genetic variations in a CMT patient highlighting that CMT can be a multilocus genetic pathology. In the second part of the project, we successfully generated a cellular model of MN for the study of *GDAP1* gene and its associated CMT2H form. We reprogrammed dermal fibroblasts of five control subjects and two CMT patients, carrying two different homozygous codon-stop mutations in *GDAP1*, into human induced-pluripotent stem cells (hiPSC). Then, we established a differentiation protocol to generate MN from hiPSC. MN with the *GDAP1* p.Ser194* mutation were analyzed by expression, morphological, and functional tests. We confirmed the neural expression of GDAP1, and we suggested that oxidative stress and mitochondrial impairment could be responsible for the pathological condition in CMT2H MN. Taken together, our results highlighted that both genetic and functional analyses are essential in the complete characterization of CMT disease.

Keywords: Charcot-Marie-Tooth, genetics, motor neurons, hiPSC, mitochondria